

Republic of Iraq
Ministry of Higher Education and
Scientific Research
University of Baghdad
College of Education for Pure Science
(Ibn -Al-Haitham)



Calculation The Range and Stopping Power for Proton Interaction with Biological Materials

A Thesis Submitted to the Council College of Education for
Pure Science (Ibn AL-Haitham)/ University of Baghdad in
Partial Fulfillment of the Requirements for the Degree of Master
of Science In Physics

By

Shaima Mohsen Hadi

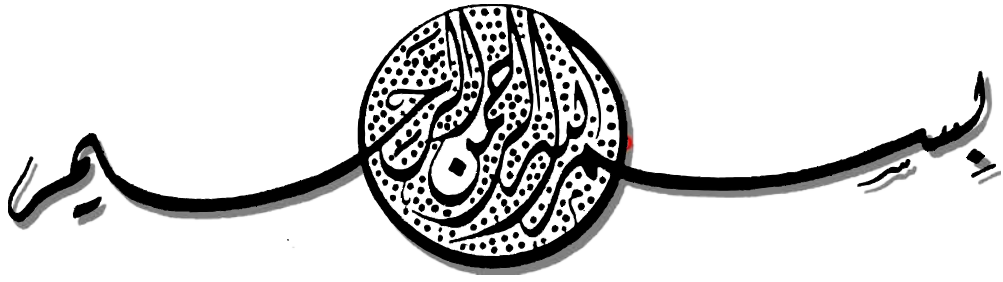
B.Sr c. 2006

Supervisor

Prof. Dr. Bashair Mohammed Saied

2018 A.D

1439 A.H



يُرَافِعُ لِلَّهِ الَّذِينَ يُؤْمِنُونَ بِمَنَابِقِ وَاللَّيْلِ
بِأَسْرَابٍ

أَوَانِمْ وَأَعْلَامٍ وَأَجْمَاعٍ وَاللَّهُ بِنَانِ
بِأَسْرَابٍ

بِعَمَلِنَا وَجَبِينَا
بِأَسْرَابٍ

صدق الله العظيم

سورة المجادلة: الآية (11)

Dedicated

To my supervisor 'prof. Bashair'

To my lovemy mother

To my brother and my father


To my sisters

To the martyrs of Iraq



Supervisor's Certification

I certify that this thesis titled " *Calculation The Range and Stopping Power for Proton Interaction with Biological Materials*" was prepared by (*Shaima Mohsen Hadi*), under my supervision at the Certification University of Baghdad/ Education College for Pure Science Ibn Al-Haitham / Department of Physics in partial fulfillment of the requirements for the degree of Master of Science in Physics.

Signature: 

Supervisor: Prof. Dr. Bashair Mohammed Saied

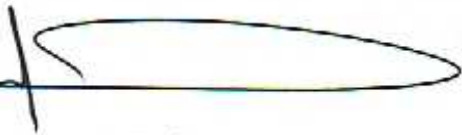
University of Baghdad/ College of Education for Pure Science (Ibn-Al-Haitham) /

Department of Physics

Date. 18 / 9 / 2017

PDF Reducer Demo

The Council of the Department of Physics has approved the examining committee

Signature: 

Name: Dr. Kareem A. Jasim

Titel: Professor.

University of Baghdad/ College of Education for Pure Science (Ibn-Al-Haitham) /

Department of Physics

Date: 18 / 9 / 2018

Certification of Examiners

We certify, that we have read the thesis titled " *Calculation The Range and Stopping Power for Proton Interaction with Biological Materials*" presented by *Shaima Mohsen Hadi* and as an examining committee, we examined the student on its contents, and in what is related to it, and that in our opinion it meets the standard of a thesis for the degree of Master of Science in Physics Science.

(Chairman)

Signature:

Name: Ass. Prof. Dr. Kareem K. Mohammad

Title: University of Nahrain

Address: Assistant Professor

Date: 7 / 13 / 2018

(Member)

Signature:

Name: Dr. Sameera Ahmed Ebrahiem

Title: University of Baghdad

Address: Assistant Professor

Date: 7 / 13 / 2018

(Member)

Signature:

Name: Ass. Prof. Dr. Naz Talab Jarallah

Title: Assistant Professor

Address: University of Baghdad

Date: 6 / 3 / 2018

(Supervisor)

Signature:

Name: Prof. Dr. Bashair Mohammed Saied

Title: Professor

Address: University of Baghdad

Date: 7 / 13 / 2018

Approved by the Dean of College of Education for Pure Science (Ibn Al-Haitham) / University of Bagdad

(The Dean)

Signature:

Name: Dr. Khalid Fahad Ali

Title: Professor

Date: / / 2018

Acknowledgements

I thank God, which has inspired me with strength, willingness and patience to establish this work.

I would like to express my sincere appreciation and gratitude to my supervisor, Dr. Bashair Mohammed, for her guidance, support and encouragement throughout my thesis work.

I offer thanks and appreciation to Physics Department and professors and Deanship of (College of Education for Pure Science - Ibn Al-Haitham - University of Baghdad).

Finally, I owe the greatest debt of gratitude to my family. I would like to thank my mother for a lifetime of support and encouragement.

Shaima

Abstract

One of the modern medical advances is the use of proton radiation in the treatment of tumors, where the proton beam is unique in the treatment because it deposits its energy deeply specific into the tissue therefore, in order to control the killing of cancer cells in tissues, an accurate description of the loss of ion energy and its range within the tissue should be provided.

In this study, the stopping power and range of proton have been calculated in thirteen tissue of the human body, namely (skin, eye lens, stomach, pancreas, liver, spleen, blood, ovary, testis, prostate, trachea, mammary gland and thyroid) tissue, using Bethe and Ziegler equations, Ziegler and Andreson (Vol.3) data. SRIM and SRIM (dictionary) program in energy range (1 KeV-200MeV). Using the Matlab program, the numerical calculations of the stopping power and range of each tissue were obtained. The results showed that the values of the stopping power and range of the proton in each tissue were different from the other tissues according to the different components of the tissue and its proportions and the stopping power of a single tissue varies according to the method used in the calculation.

We concluded that the largest amount of energy lost to the proton in the energy (0.07MeV) is in the mammary gland tissue. The largest proton range is also in this tissue (2.3939 cm at 180MeV) because mammary gland is less dense than the remaining tissue density, and we have produced semi-empirical formula for measuring the range that can be used to find the proton range in the tissue by knowledge of the energy of the proton, which helps the physician to determine the depth of the tumor and the energy that must be used in treatment of it without damaging in the other tissues surrounding.

List of contents

Title No.	Subject	Page
Chapter One: Introduction		
1-1	Intro daction	1
1-2	Stopping power	1
1-3	Bragg peak	2
1-4	Proton therapy	3
1-5	Types of tissues	3
1-6-1	Skin tissue	3
1-6-2	Eye lens	4
1-6-3	Stomach tissue	4
1-6-4	Pancreas tissue	5
1-6-5	Liver tissue	5
1-6-6	Spleen tissue	6
1-6-7	Blood tissue	6
1-6-8	Ovary tissue	7
1-6-9	Testis tissue	7
1-6-10	Prostate tissue	8
1-6-11	Trachea tissue	8
1-6-12	Mammary gland	9
1-6-13	Thyroid tissue	9
1-7	Previous study	11
1-8	The aim of this study	16
Chapter Two: Theory		
2-1	Interactions of radiation with matter	17
2-1-1	Proton interaction mechanisms	17
2-1-2	Interaction of proton with tissue	19
2-2	Mechanisms of energy loss of charged particles in matter	19
2-2-1	Electronic stopping	25
2-2-2	Nuclear stopping	26
2-2-3	Stopping power for compound or a mixture	27
2-3	Bragg rule additivity	27
2-4	Mean ionization potential (I)	28
2-5	Stopping power dependenc on particle energy	29
2-5-1	At low energies	29
2-5-2	At intermediate energies	29
2-5-3	At high energies	29
2-6	Range	30
2-6-1	Range of proton	31
2-7	Niels Bohr formula	31
2-8	Bethe theory	32
2-9	Bethe-Bloch formula	33
2-10	Ziegler formula	35
2-10-1	Review of theory	35
2-10-2	Fitting the high-energy region	37

Title No.	Subject	Page
2-10-3	Fitting at lower energies	38
2-10-4	Interpolation using 2-parameter fitting	38
2-11	SRIM programs	40
Chapter Three: Data Redaction & Analysis		
3-1	Stopping Power calculation	42
3-2	Chemical compositions of the human tissues	42
3-3 (a,b,c,d,e)	Stopping power for proton interaction with tissues	42
	a-Bethe formula	42
	b- Ziegler formula	43
	c- Ziegler and Andreson (Vol.3).[100]	44
	d- SRIM program	44
	e- SRIM program dictionary	45
3-4	Stopping power for proton interaction with tissues	45
3-5	Range calculation	62
Chapter Four: Result and discussion		
4-1 (a,b,c,d,e)	Stopping power for tissues	68
	a-Bethe formula	68
	b- Ziegler formula	68
	c- Ziegler and Andreson (Vol.3).[100]	68
	d- SRIM and SRIM (dictionary) program	68
	e-Present work	68
4-1-1	Stopping power for skin tissue	68
4-1-2	Stopping power for eye lens tissue	72
4-1-3	Stopping power for stomach tissue	74
4-1-4	Stopping power for pancreas tissue	77
4-1-5	Stopping power for liver tissue	80
4-1-6	Stopping power for spleen tissue	84
4-1-7	Stopping power for blood tissue	87
4-1-8	Stopping power for ovary tissue	90
4-1-9	Stopping power for testis tissue	94
4-1-10	Stopping power for prostate tissue	97
4-1-11	Stopping power for trachea tissue	100
4-1-12	Stopping power for mammary gland tissue	104
4-1-13	Stopping power for thyroid tissue	107
4-2	The range calculation	110
4-2-1	In skin tissue	111
4-2-2	In eye lens tissue	111
4-2-3	In stomach tissue	111
4-2-4	In pancreas tissue	111
4-2-5	In liver tissue	111
4-2-6	In spleen tissue	112
4-2-7	In boold tissue	112
4-2-8	In ovary tissue	112
4-2-9	In testis tissue	112
4-2-10	In prostate tissue	112
4-2-11	In trachea tissue	113
4-2-12	In mammary gland tissue	113
4-2-13	In thyroid tissue	113

Title No.	Subject	Page
Chapter Five: Conclusion&Future work		
5-1	Conclusion	114
5-2	Future work	121
	References	122

List of Tables

Table No.	Caption	Page
1-1	Chemical composition of various human tissues and fractional weight of the elements per tissue and density of tissues	10
3-1	Ionization potential and atomic numbers of elements considered for human tissue	43
3-2	Coefficient for stopping of hydrogen	44
3-3	The total stopping power for proton interacts with the composition of tissues.	46-47- 48-49
3-4	Stopping power for proton in skin tissues in (MeV-cm ² /g)	50
3-5	Stopping power for proton in eye lens tissues in (MeV-cm ² /g)	51
3-6	Stopping power for proton in stomach tissues in (MeV-cm ² /g)	52
3-7	Stopping power for proton in pancreas tissues in (MeV-cm ² /g)	53
3-8	Stopping power for proton in liver tissues in (MeV-cm ² /g)	54
3-9	Stopping power for proton in spleen tissues in (MeV-cm ² /g)	55
3-10	Stopping power for proton in blood tissues in (MeV-cm ² /g)	56
3-11	Stopping power for proton in ovary tissues in (MeV-cm ² /g)	57
3-12	Stopping power for proton in testis tissues in (MeV-cm ² /g)	58
3-13	Stopping power for proton in prostate tissues in (MeV-cm ² /g)	59
3-14	Stopping power for proton in trachea tissues in (MeV-cm ² /g)	60
3-15	Stopping power for proton in mammary gland tissues in (MeV-cm ² /g)	61
3-16	Stopping power for proton in thyroid tissues in (MeV-cm ² /g)	62
4-1	Percentage deviation (stopping power) in skin tissue in (MeV-cm ² /g)	71
4-2	Percentage deviation (stopping power) in eye lens tissue in (MeV-cm ² /g)	74
4-3	Percentage deviation (stopping power) in stomach tissue in (MeV-cm ² /g)	77
4-4	Percentage deviation (stopping power) in pancreas tissue in (MeV-cm ² /g)	80
4-5	Percentage deviation (stopping power) in liver tissue in (MeV-cm ² /g)	83
4-6	Percentage deviation (stopping power) in spleen tissue in (MeV-cm ² /g)	87
4-7	Percentage deviation (stopping power) in blood tissue in (MeV-cm ² /g)	90
4-8	Percentage deviation (stopping power) in ovary tissue in (MeV-cm ² /g)	93
4-9	Percentage deviation (stopping power) in testis tissue in	96
4-10	Percentage deviation (stopping power) in prostate tissue in (MeV-cm ² /g)	100
4-11	Percentage deviation (stopping power) in trachea tissue in (MeV-cm ² /g)	103
4-12	Percentage deviation (stopping power) in mammary gland tissue in (MeV-cm ² /g)	107
4-13	Percentage deviation (stopping power) in thyroid tissue in (MeV-cm ² /g)	110
5-1	Semi-empirical equation for human tissue	120

List of Figures

Figure No.	Caption	Page
1.1	Comparison of relative depth dose distributions of photons versus protons.	2
1-2	Components of the skin tissue	3
1-3	Eye human tissue	4
1-4	Part of the stomach	4
1-5	Pancreas tissue	5
1-6	Human liver anatomy	5
1-7	Spleen tissue	6
1-8	Blood tissue	6
1-9	Ovary tissue	7
1-10	Testis (testicular cancer)	7
1-11	Prostate tissue	8
1-12	Trachea tissue	8
1-13	Mammary gland tissue	9
1-14	Thyroid tissue	9
2-1	Schematic illustration of proton interaction mechanisms: (a) energy loss via coulombic interactions, (b) deflection of proton trajectory by repulsive coulomb scattering with nucleus, (c) removal of primary proton and creation of secondary particles via non-elastic nuclear interaction. (P: proton, e: electron, n: neutron, He: helium, and γ : gamma rays)	18
2-2	Encounter between a heavy charged particle of mass M_0 and a free electron of mass m_0 . The impact parameter b is indicated	20
2-3	The experimentally determined stopping power, ($-dE/dx$), for protons in air, low energy region where the Bethe formula applies down to $E \sim 0.3$ MeV with $I \sim 80$ eV. Below this range charge loss to electron capture causes the stopper power to reach a peak and start to decrease, and Fig (2.3b): High-energy region where a broad minimum occurs at $E \sim 1500$ MeV	25
2-4	Typical penetration curve for charged particles (solid line). The penetration depth x is in general presented in g/cm^2 , i.e. Length \times density N^0 : initial number of particles. R^0 : mean range and R_f : extrapolated range. For comparison a typical attenuation curve for electromagnetic radiation is added (dotted line).	30
2-5	The stopping number according to Bloch (1933) (solid line) approaches the Bohr and Bethe logarithms at low and high projectile speed, respectively. Also included is a curve consisting of the Bethe logarithm and the Z^4 correction which often, erroneously, is called the Bloch correction. $v_0 = c/137$ is the Bohr velocity	34
3-1	Range of proton in skin tissue	63
3-2	Range of proton in skin tissue in all methods	63
3-3	Range of proton in eye lens tissue	63
3-4	Range of proton in eye lens tissue in all methods	63
3-5	Range of proton in stomach tissue	63
3-6	Range of proton in stomach tissue in all methods	63
3-7	Range of proton in pancreas tissue	64

Figure No.	Caption	Page
3-8	Range of proton in pancreas tissue in all methods	64
3-9	Range of proton in liver tissue	64
3-10	Range of proton in liver tissue in all methods	64
3-11	Range of proton in spleen tissue	64
3-12	Range of proton in spleen tissue in all methods	64
3-13	Range of proton in blood tissue	65
3-14	Range of proton in blood tissue in all methods	65
3-15	Range of proton in ovary tissue	65
3-16	Range of proton in ovary tissue in all methods	65
3-17	Range of proton in testis tissue	65
3-18	Range of proton in testis tissue in all methods	65
3-19	Range of proton in prostate tissue	66
3-20	Range of proton in prostate tissue in all methods	66
3-21	Range of proton in trachea tissue	66
3-22	Range of proton in trachea tissue in all methods	66
3-23	Range of proton in mammary gland tissue	66
3-24	Range of proton in mammary gland tissue in all methods	66
3-25	Range of proton in thyroid tissue	67
3-26	Range of proton in thyroid tissue in all methods	67
4-1	Stopping power for proton in elements presented in skin tissue using Bethe equation	69
4-2	Stopping power for proton in elements presented in skin tissue using Ziegler equation	69
4-3	Stopping power for proton in elements presented in skin tissue using ref.[100]	69
4-4	Stopping power for proton in elements presented in skin tissue using SRIM and SRIM dictionary	69
4-5 (a,b,c)	Stopping power for skin tissue (present work)	69
	a- Stopping power for skin tissue from ($10^{-1.9}$ - $10^{-1.6}$ MeV-cm ² /g) (present work)	69
	b- Stopping power for skin tissue from (10^{-5} - 10^{-1} MeV-cm ² /g) (present work)	70
	c- Stopping power for skin tissue from ($10^{0.92}$ - $10^{0.96}$ MeV-cm ² /g) (present work)	70
4-6	Stopping power for proton in elements presented in eye lens tissue using Bethe equation	72
4-7	Stopping power for proton in elements presented in eye lens tissue using Ziegler equation	72
4-8	Stopping power for proton in elements presented in eye lens tissue using ref.[100]	72
4-9	Stopping power for proton in elements presented in eye lens tissue using SRIM program	72
4-10 (a,b,c)	Stopping power for eye lens tissue (present work)	72
	a- Stopping power for eye lens tissue from ($10^{-1.7}$ - $10^{-1.5}$ MeV-cm ² /g) (present work)	72

Figure No.	Caption	Page
4-10 (a,b,c)	b- Stopping power for eye lens tissue from (10^{-5} - 10^{-1} MeV-cm ² /g) (present work)	73
	c- Stopping power for eye lens tissue from ($10^{0.92}$ - $10^{0.96}$ MeV-cm ² /g) (present work)	73
4-11	Stopping power for proton in elements presented in stomach tissue using Bethe equation	74
4-12	Stopping power for proton in elements presented in stomach tissue using Ziegler equation	74
4-13	Stopping power for proton in elements presented in stomach tissue using ref.[100]	75
4-14	Stopping power for proton in elements presented in stomach tissue using SRIM program	75
4-15 (a,b,c)	Stopping power for stomach tissue (present work)	75
	a- Stopping power for stomach tissue from ($10^{-1.7}$ - $10^{-1.5}$ MeV-cm ² /g) (present work)	75
	b- Stopping power for stomach tissue from (10^{-5} - 10^{-1} MeV-cm ² /g) (present work)	76
	c- Stopping power for stomach tissue from ($10^{0.92}$ - $10^{0.96}$ MeV-cm ² /g) (present work)	76
4-16	Stopping power for proton in elements presented in pancreas tissue using Bethe equation	77
4-17	Stopping power for proton in elements presented in pancreas tissue using Ziegler equation	77
4-18	Stopping power for proton in elements presented in pancreas tissue using ref.[100]	78
4-19	Stopping power for proton in elements presented in pancreas tissue using SRIM and SRIM dictionary program	78
4-20 (a,b,c)	Stopping power for pancreas tissue (present work)	78
	a- Stopping power for pancreas tissue from ($10^{-1.7}$ - $10^{-1.5}$ MeV-cm ² /g) (present work)	78
	b- Stopping power for pancreas tissue from (10^{-5} - 10^{-1} MeV-cm ² /g) (present work)	79
	c- Stopping power for pancreas tissue from ($10^{0.92}$ - $10^{0.96}$ MeV-cm ² /g) (present work)	79
4-21	Stopping power for proton in elements presented in liver tissue using Bethe equation	80
4-22	Stopping power for proton in elements presented in liver tissue using Ziegler equation	80
4-23	Stopping power for proton in elements presented in liver tissue using ref.[100]	81
4-24	Stopping power for proton in elements presented in liver tissue using SRIM program	81
4-25 (a,b,c)	Stopping power for liver tissue (present work)	81

Figure No.	Caption	Page
4-25 (a,b,c)	a- Stopping power for liver tissue from ($10^{-1.7}$ - $10^{-1.5}$ MeV-cm ² /g) (present work)	81
	b- Stopping power for liver tissue from (10^{-5} - 10^{-1} MeV-cm ² /g) (present work)	82
	c- Stopping power for liver tissue from ($10^{0.92}$ - $10^{0.96}$ MeV-cm ² /g) (present work)	82
4-26	Stopping power for proton in elements presented in spleen tissue using Bethe equation	84
4-27	Stopping power for proton in elements presented in spleen tissue using Ziegler equation	86
4-28	Stopping power for proton in elements presented in spleen tissue using ref. [100]	87
4-29	Stopping power for proton in elements presented in spleen tissue using SRIM and SRIM dictionary program	84
4-30 (a,b,c)	Stopping power for spleen tissue (present work)	85
	a- Stopping power for spleen tissue from ($10^{-1.7}$ - $10^{-1.5}$ MeV-cm ² /g) (present work)	85
	b- Stopping power for spleen tissue from (10^{-5} - 10^{-1} MeV-cm ² /g) (present work)	85
	c- Stopping power for spleen tissue from ($10^{0.91}$ - $10^{0.94}$ MeV-cm ² /g) (present work)	85
4-31	Stopping power for proton in elements presented in blood tissue using Bethe equation	87
4-32	Stopping power for proton in elements presented in blood tissue using Ziegler equation	87
4-33	Stopping power for proton in elements presented in blood tissue using ref.[100]	88
4-34	Stopping power for proton in elements presented in blood tissue using SRIM and SRIM dictionary program	88
4-35 (a,b,c)	Stopping power for blood tissue (present work)	88
	a- Stopping power for blood tissue from ($10^{-1.7}$ - $10^{-1.5}$ MeV-cm ² /g) (present work)	88
	b- Stopping power for blood tissue from (10^{-5} - 10^{-1} MeV-cm ² /g) (present work)	89
	c- Stopping power for blood tissue from ($10^{0.91}$ - $10^{0.95}$ MeV-cm ² /g) (present work)	89
4-36	Stopping power for proton in elements presented in ovary tissue using Bethe equation	90
4-37	Stopping power for proton in elements presented in ovary tissue using Ziegler equation	90
4-38	Stopping power for proton in elements presented in ovary tissue using ref.[100]	91
4-39	Stopping power for proton in elements presented in ovary tissue using SRIM and SRIM dictionary program	91
4-40 (a,b,c)	Stopping power for ovary tissue (present work)	91
	a- Stopping power for ovary tissue from ($10^{-1.7}$ - $10^{-1.5}$ MeV-cm ² /g) (present work)	91

Figure No.	Caption	Page
	b- Stopping power for ovary tissue from (10^{-5} - 10^{-1} MeV-cm ² /g) (present work)	92
	c- Stopping power for ovary tissue from ($10^{0.92}$ - $10^{0.96}$ MeV-cm ² /g) (present work)	92
4-41	Stopping power for proton in elements presented in testis tissue using Bethe equation	94
4-42	Stopping power for proton in elements presented in testis tissue using Ziegler equation	94
4-43	Stopping power for proton in elements presented in testis tissue using ref.[100]	94
4-44	Stopping power for proton in elements presented in testis tissue using SRIM and SRIM dictionary program	94
	Stopping power for testis tissue (present work)	95
4-45 (a,b,c)	a- Stopping power for testis tissue from ($10^{-1.7}$ - $10^{-1.5}$ MeV-cm ² /g) (present work)	95
	b- Stopping power for testis tissue from (10^{-5} - 10^{-1} MeV-cm ² /g) (present work)	95
	c- Stopping power for testis tissue from ($10^{0.92}$ - $10^{0.96}$ MeV-cm ² /g) (present work)	95
4-46	Stopping power for proton in elements presented in prostate tissue using Bethe equation	97
4-47	Stopping power for proton in elements presented in prostate tissue using Ziegler equation	97
4-48	Stopping power for proton in elements presented in prostate tissue using ref.[100]	97
4-49	Stopping power for proton in elements presented in prostate tissue using SRIM and SRIM dictionary program	97
	Stopping power for prostate tissue (present work)	98
4-50 (a,b,c)	a- Stopping power for prostate tissue from ($10^{-1.7}$ - $10^{-1.5}$ MeV-cm ² /g) (present work)	98
	b- Stopping power for prostate tissue from (10^{-5} - 10^{-1} MeV-cm ² /g) (present work)	98
	c- Stopping power for prostate tissue from ($10^{0.92}$ - $10^{0.96}$ MeV-cm ² /g) (present work)	98
4-51	Stopping power for proton in elements presented in trachea tissue using Bethe equation	100
4-52	Stopping power for proton in elements presented in trachea tissue using Ziegler equation	100
4-53	Stopping power for proton in elements presented in trachea tissue using ref.[100]	101
4-54	Stopping power for proton in elements presented in trachea tissue using SRIM and SRIM dictionary program	101
	Stopping power for trachea tissue (present work)	101
4-55 (a,b,c)	a- Stopping power for trachea tissue from ($10^{-1.7}$ - $10^{-1.5}$ MeV-cm ² /g) (present work)	101
	b- Stopping power for trachea tissue from (10^{-5} - 10^{-1} MeV-cm ² /g) (present work)	102

Figure No.	Caption	Page
	c- Stopping power for trachea tissue from ($10^{0.92}$ - $10^{0.96}$ MeV-cm ² /g) (present work)	102
4-56	Stopping power for proton in elements presented in mammary gland tissue using Bethe equation	104
4-57	Stopping power for proton in elements presented in mammary gland tissue using Ziegler equation	104
4-58	Stopping power for proton in elements presented in mammary gland tissue using ref.[100]	104
4-59	Stopping power for proton in elements presented in mammary gland tissue using SRIM and SRIM dictionary program	104
	Stopping power for mammary gland tissue (present work)	105
4-60 (a,b,c)	a- Stopping power for mammary gland tissue from ($10^{-1.7}$ - $10^{-1.5}$ MeV-cm ² /g) (present work)	105
	b- Stopping power for mammary gland tissue from (10^{-5} - 10^{-1} MeV-cm ² /g) (present work)	105
	c- Stopping power for mammary gland tissue from ($10^{0.92}$ - $10^{0.96}$ MeV-cm ² /g) (present work)	105
4-61	Stopping power for proton in elements presented in thyroid tissue using Bethe equation	107
4-62	Stopping power for proton in elements presented in thyroid using Ziegler equation	107
4-63	Stopping power for proton in elements presented in thyroid tissue using ref.[100]	108
4-64	Stopping power for proton in elements presented in thyroid tissue using SRIM and SRIM dictionary program	108
	Stopping power for thyroid tissue (present work)	108
4-65 (a,b,c)	a- Stopping power for thyroid tissue from ($10^{-1.7}$ - $10^{-1.5}$ MeV-cm ² /g) (present work)	108
	b- Stopping power for thyroid tissue from (10^{-5} - 10^{-1} MeV-cm ² /g) (present work)	109
	c- Stopping power for thyroid tissue from ($10^{0.92}$ - $10^{0.96}$ MeV-cm ² /g) (present work)	109
5-1	Range of proton in skin tissue	120

List of Symbol

No.	Symbol	Definition
1	E	Proton energy (MeV)
2	S.P, -dE/dx	Stopping power (MeV-cm ² /g)
3	c	Velocity of light (m/sec)
4	v	Incident particle velocity= βc (m/sec)
5	β	=v/c
6	Z	Atomic number
7	m	Electron mass (g)
8	($\delta/2$)	Density effect correction
9	C/Z	Shell correction
10	b _{max} , b _{min}	Maximum and minimum impact parameters
11	Δt	Time interval of energy transfer (Sec)
12	ω	Orbital frequency. (radians per second)
13	r _o	The Bohr electron radius (cm)
14	K	Pre- factor constants = $4 \pi r_o^2 m_e c^2 = 0.0005099$
15	A ₁ ,A ₂ ,.....A ₁₂	Fitting constants
16	N _A	Avogadro's number (6.0221367(36)×10 ²³) mol ⁻¹
17	w _i	Weight fraction of i th element
18	ρ	Density of the stopping material
19	R	Range of proton in matter (cm)
20	SRIM	The Stopping and Range of Ion in Matter
21	F	Coulomb force= $k(ze^2/r^2)$
22	(KE) _e	Kinetic energy
23	γ	= $(T+Mc^2)/Mc^2 = 1/\sqrt{1 - \beta^2}$
24	p _e	Net momentum
25	$\Psi(Z_1)$	Bloch's error
26	a _o	Bohr radius
27	v _o	Bohr velocity
28	(-dE/dx) _e	Electronic stopping
29	(-dE/dx) _n	Nuclear stopping
30	RBE	relative biological effectiveness
31	n _i	Number of atoms of element <i>i</i> in the molecule
32	e	Electron charge
33	I	Mean ionization potential (MeV)
34	L _o	Born correction
35	L ₁	Barkas correction
36	L ₂	Bloch correction
37	L(B)	Stopping number

Chapter One

Introduction

1-1 Introduction

Nuclear science has contributed significantly to the development of tumor therapy with heavy charged particles. [1]. Radiation therapy uses the radiobiological effects of ionizing radiation (charged particles, neutrons, gamma rays or x-rays) to destroy tumor cells. The success of radiotherapy depends on the ability of the therapy system to concentrate the quantity (dose) of radiation on the target region (tumor). Ideally, a lethal while minimizing the irradiation of healthy adjacent tissues [2]. The motivation for the use of heavy particles in radiotherapy where their advantages compared to contemporary photon therapy in relative biological effectiveness (RBE) in tumor cells, compared to normal cells, better dose distributions or both [1], charged particles have a relatively well defined penetration range. The dominant mechanism by which charged particles lose their energies are inelastic interaction with the atomic electrons. They lose most of their energies near the end of their paths, at the so called Bragg Peak [3]. Proton radiotherapy is becoming popular because it can deliver a high radiation dose to the target while sparing adjacent healthy tissues or critical organs [4]. The Bragg peak is very narrow so if shifted from the desired target will cause healthy tissue to expose very high doses. The location where proton will stop, is closely related to the amount of stopping power of the medium through which it passes, which is a measure of how much energy is lost given to the medium. The magnitude of the stopping power depends on the proton energy and the type of the target medium [5] The range of proton is associated with the amount of stopping power [6]. In this study, we calculated total stopping power and range for proton in a number of organs and tissues of the human body to determine maximum energy loss for proton in that position of the tissue at the energy range selected. Results are presented in graphs and detailed discussions. Also, some views to the future work are presented.

1-2 Stopping power

The fast charged particles when passing through matter ionize the molecule or atom which they encounter, therefore fast particles lose energy gradually in many small steps. Stopping power means the average energy loss of the particle per unit path length [7]

$$S = -dE/dx \dots \dots \dots (1-1).$$

The minus means that the particles energy decreases along its path and therefore it is a negative quantity [8]. The stopping power depends on the type and the energy of the particle also on the properties of the material it passes [7]. The mass stopping power is a useful quantity because it expresses the rate of energy loss of the charged particle per g. cm⁻² of the traversed medium. The mass stopping power is the linear stopping power (MeV/cm) divided on the density, common units for mass stopping power, - dE/ρdx, are (MeV-cm²/ g) [8]. The total stopping power is the sum of the electronic stopping

power $(-dE/dx)_e$ (due to collisions with the target electrons), and the nuclear stopping power $(-dE/dx)_n$ (due to collisions with the target nucleus) [9].

$$(-dE/dx)_t = (-dE/dx)_e + (-dE/dx)_n \dots\dots\dots (1-2)$$

Production of an ion pair requires a fixed amount of energy, the density of ionization along the path is proportional to the stopping power of the material. Stopping power refers to the property of the material while energy loss per unit path length describes what happens to the particle. But numerical values and units are identical for both quantities [10].

1-3 Bragg peak

When an accelerator proton beams enter and travel through the tissue with minimal dose deposition along the path until the end of their paths, where a peak of energy deposition occurs. This phenomenon is known as the Bragg peak [11]. A slowly increasing energy deposition with the depth, practically constant until near the end of the range, followed by a sharp increase of the dose, and then by a steep decrease. The position of the Bragg peak depends on particle energy - the greater the energy, the deeper the Bragg peak is located. By adjusting the energy of the incident beams which can change continuously the location of their maximum dose deposition [12]. Favorable dose distributions with a steep dose fall-off at the field borders and, thus, more precise dose localization can be achieved with these beams compared with photon beams. As a consequence, it seems likely that dose escalation can be performed without aggravating toxicity in surrounding normal tissues [13]. As show in figure (1-1):

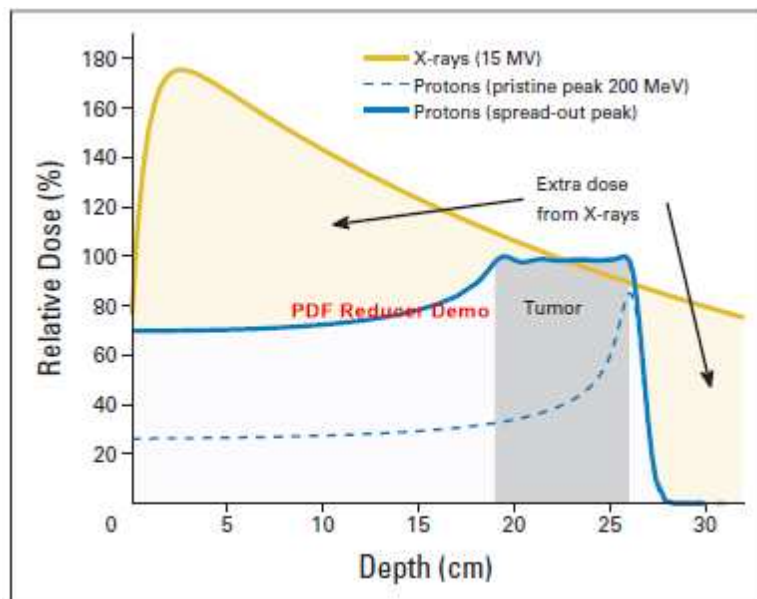


Fig (1-1): Comparison of relative depth dose distributions of photons versus protons [11].

1-4 Proton therapy

The history of proton therapy began in 1946 by Robert Wilson, he proposed to use accelerator produced beams of protons to treat deep seated tumors in humans and explained the biophysical rationale for proton therapy as well as the key engineering techniques of beam delivery, the first human was treated with proton beams was in 1954 at the Lawrence Berkeley Laboratory. In 1962, specialized radiosurgical proton treatments commenced at the Harvard Cyclotron Laboratory [14]. Proton therapy is one type of particle therapy. The main difference between protons and X-rays is the physical properties of the proton beam itself. X-rays are electromagnetic waves that have no mass or charge [15], it deposits dose in normal tissues beyond a tumor. In contrast, protons travel into the body and release the majority of their energy at the end of their path (called the Bragg peak) [15]. Beyond the proton range in a medium, virtually no dose is deposited. The finite range of protons in tissue can be used to spare dose to non-cancerous tissue distal to the tumor [16], Despite obstacles such as (cost, technical difficulty,.), much progress has been made in proton therapy, there are 16 proton therapy centers in operation in the United States and 46 centers worldwide [14].

1-5 Types of tissues

1-5-1 Skin tissue

The skin is the outer covering of the body protecting the body against pathogens, and excessive water loss, and other functions, consists of several layers, as show in figure 2 [17], consists from Water (65.3%), lipid (9.4%), protein (24.6%), [18] and some elements (H, C, N, O, Na, P, S, Cl, and K) as given in table (1-1) [19].

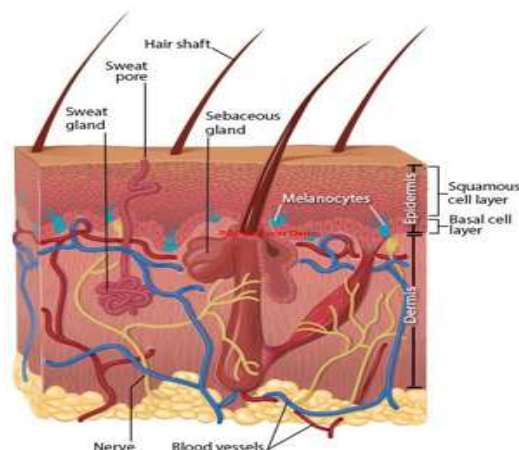


Fig (1-2) : Components of the Skin tissue [20].

1-5-2 Eye lens

The lens is part of the anterior segment of the eye. The lens of the eye focuses diminished, inverted images of near or distant objects on the retina, as show in figure 3 [21]. The composition of eye lens was taken to be (64.1%) water, (1.7-2.3 %) lipid, (33.6%) protein [18] and elements which are (H, C, N, O, Na, P, S, and Cl as given in table (1-1) [19].

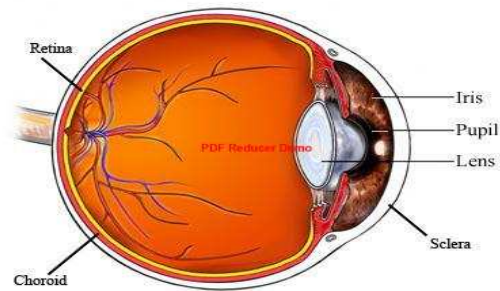


Fig (1-3): Eye human tissue [22].

1-5-3 Stomach tissue

The stomach is a hollow bag that initially stores ingested material. It is connected to the oesophagus, and is connected to the intestine, as show in figure 4 [23]. The composition of stomach was taken to be (water 75%, lipid 6.2% and protein17%) [18]. And the elements are (H, C, N, O, Na, P, S, K and Cl) as given in table (1-1) [19].

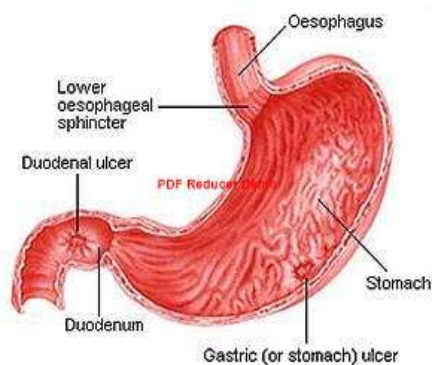


Fig (1-4): Part of the stomach [24].

1-5-4 *Pancreas tissue*

The pancreas is an organ that sits behind and to the right of the stomach, and is an important part of the digestive system. It plays a crucial role in the body's ability to process food, making it able to generate and use energy, as show in figure 5 [25], its composition was taken to be: water (71 %), protein (13.1%) and lipid (8%)[18], and consists from some elements(H, C, N, O, Na, P, S, Cl, and K) as given in table (1-1) [19].

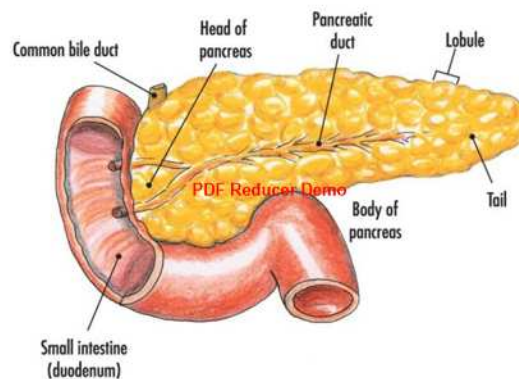


Fig (1-5) : Pancreas tissue [26].

1-5-5 *Liver tissue*

The liver is one of the most important solid organs in the human body, which is responsible for protein synthesis, detoxification, nutrient storage, and innate/adaptive immunity regulation, as show in figure 6 [27]. Liver consists of 75% water, 17 % protein, 6 % lipid, [28] and some other elements (H, C, N, O, Na, P, S, Cl, and K) as given in table (1-1) [19].



Fig (1-6) : Human liver anatomy [20].

1-5-6 Spleen tissue

Located in the abdomen, directly beneath the diaphragm, and connected to the stomach, the spleen is the body's largest filter of the blood, as show in figure 7 [29]. The spleen is made of three biological components (78.5%)water, (17.5%) protein, and (3%) lipid [28]. And other elements are (H, C, N, O, Na, P, S, Cl, and K) as given in table (1-1) [19].

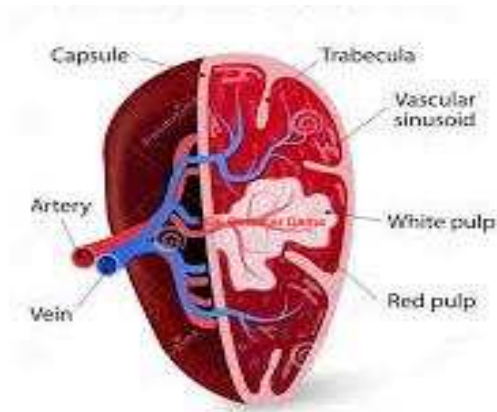


Fig (1-7) : Spleen tissue [22].

1-5-7 Blood tissue

A body fluid in humans and other animals that delivers necessary substances such as nutrients and oxygen to the cells and transports metabolic waste products away from those same cells, as show in figure 8 [30], and the blood composition was taken to be (79-80.8 %) water, (0.65%) lipid and (18.19%) protein [18]. The composition of blood was taken to be elements which are (H, C, N, O, Na, P, S, K, Cl and Fe) as given in table (1-1) [19].

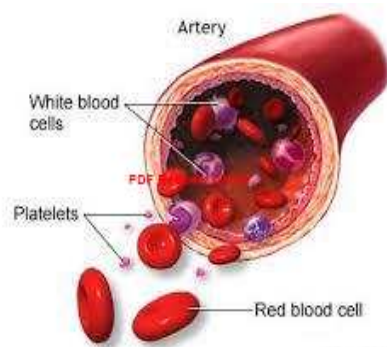


Fig (1-8): Blood tissue [31].

1-5- 8 Ovary tissue

The ovary is an ovum producing reproductive organ, found in pairs in the female as part of the female reproductive system, as show in figure 9 [32]. The composition of the ovary is for a nonpregnant woman, 78.5% water, 6% protein, 0.16% cholesterol, 0.03% ascorbic acid, and 0.012% inositol [28], and some elements are (H, C, N, O, Na, P, S, Cl, and K) as given in table (1-1) [19].

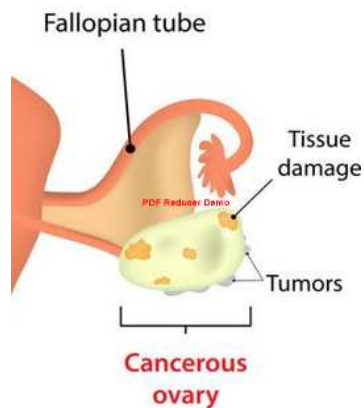


Fig (1-9): Ovary tissue [33].

1-5-9 Testis tissue

The testis are the most essential organs of the male reproductive system. They are the glands where sperm and testosterone are produced, as show in figure 10 [23]. The composition of testis was taken to be (82.7 %) water, (4.5%) lipid and (12.0%) protein [18] and some elements are (H, C, N, O, Na, P, S, K, and Cl) as given in table (1-1) [19].

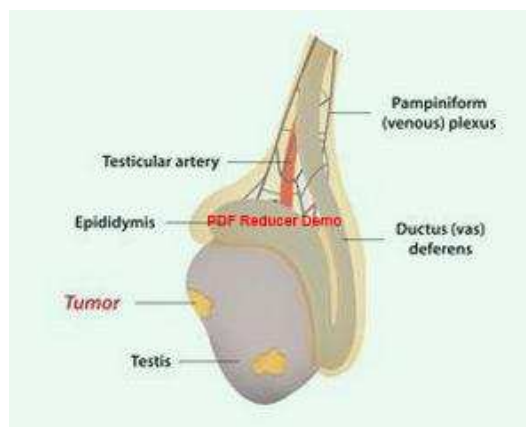


Fig (1-10) : Testis (testicular cancer) [34].

1-5- 10 Prostate tissue

It is a compound tubuloalveolar exocrine gland of the male reproductive system in most mammals. It differs considerably among species anatomically, chemically, and physiologically [35] prostate cancer affecting older men in developed countries and a significant cause of death for elderly men, as show in figure 11 [36] and the prostate composition was taken to be water (83.3%), lipid (1.2%), protein (15.0 %) [18] and some elements are (H, C, N, O, Na, P, S, K, and Cl as given in table (1-1) [19].

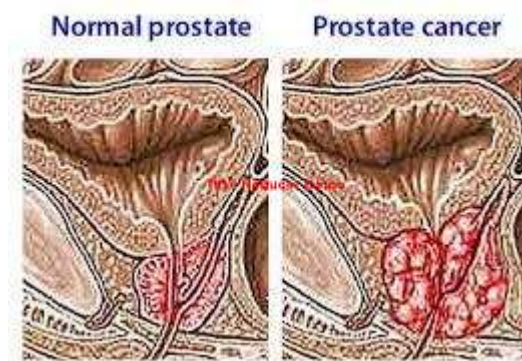


Fig (1-11) : Prostate tissue [37].

1-5- 11 Trachea tissue

The trachea can be defined as an elastic tube, which forms the continuation of the larynx and extends to the point at which it divides into the two main bronchi of the lungs, as show in figure 12 [23]. The composition of trachea was taken to be (60%) water [18] and elements are (H, C, N, O, Na, P, S, K and Cl as given in table (1-1) [19].

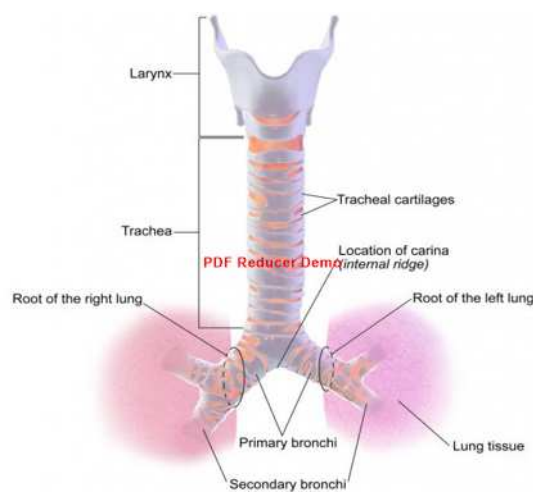


Fig (1-12): Trachea tissue [38].

1-5- 12 Mammary gland tissue

The mammary gland are structures derived from skin and are functionally related to the female sex organs. They develop during puberty under hormonal influence and are composed of glandular, adipose, and connective tissues, as show in figure 13 [39]. The composition of mammary gland (51.4%) water, (30.9%) lipid, (17.4%) protein [18] and elements which are (H, C, N, O, Na, P, S, and Cl as given in table (1-1) [19].

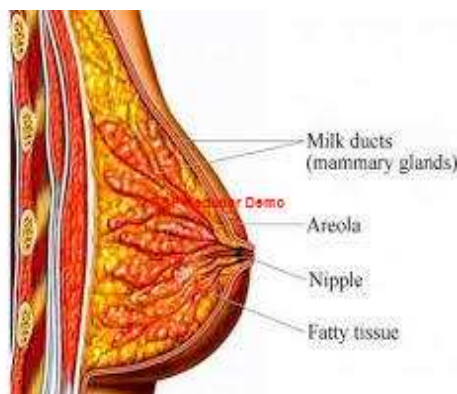


Fig (1-13) : Mammary gland tissue [40].

1-5-13 Thyroid tissue

The thyroid gland is an endocrine gland, consisting of two lobes connected by an isthmus. It is found at the front of the neck, below the Adam's apple. It secretes thyroid hormones, as show in figure 14 [39]. The composition of thyroid was taken to be (72-78%) water, (4.4%) lipid, (14%) protein [18] and elements which are (H, C, N, O, Na, P, S, Cl, K and I, as given in table (1-1) [19].

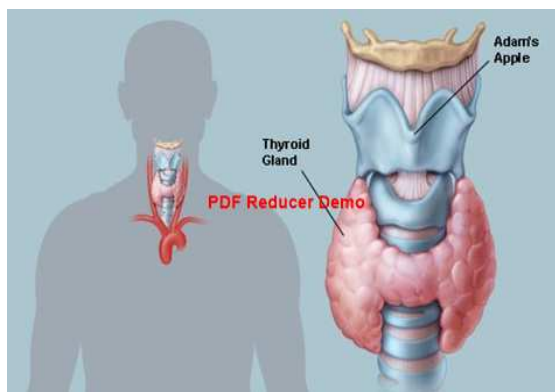


Fig (1-14) : Thyroid tissue [41].

Table (1-1): Chemical composition of various human tissues and fractional weight of the elements per tissue and density of tissues [19].

S.N	Human Tissue	Density (Kg m ⁻³)	Composition (element: fraction) by weight
1	Skin tissue	1090	H: 0.1, C: 0.204, N: 0.042, O: 0.645, Na: 0.002, P: 0.001, S: 0.002, Cl: 0.003, K: 0.001
2	Eye tissue	1070	H: 0.096, C: 0.195, N: 0.057, O: 0.646, Na: 0.001 P: 0.001, S: 0.003, Cl: 0.001
3	Stomach tissue	1050	H: 0.104, C: 0.139, N: 0.029, O: 0.721, Na: 0.001 P: 0.001, S: 0.002, Cl: 0.001, K: 0.002
4	Pancreas tissue	1040	H: 0.106, C: 0.169, N: 0.022, O: 0.694, Na: 0.002, P: 0.002, S: 0.001, Cl: 0.002, K: 0.002
5	Liver tissue	1060	H: 0.102, C: 0.139, N: 0.03, O: 0.716, Na: 0.002, P: 0.003, S: 0.003, Cl: 0.002, K: 0.003
6	Spleen tissue	1060	H: 0.103, C: 0.113, N: 0.032, O: 0.741, Na: 0.001, P: 0.003, S: 0.002, Cl: 0.002, K: 0.003
7	Blood tissue	1060	H: 0.102, C: 0.11, N: 0.033, O: 0.745, Na: 0.001, P: 0.001, S: 0.002, Cl: 0.003, K: 0.002, Fe: 0.001
8	Ovary tissue	1050	H: 0.105, C: 0.093, N: 0.024, O: 0.768, Na: 0.002, P: 0.002, S: 0.002, Cl: 0.002, K: 0.002
9	Testis tissue	1040	H: 0.106, C: 0.099, N: 0.02, O: 0.766, Na: 0.002 P: 0.001, S: 0.002, Cl: 0.002, K: 0.002
10	Prostate tissue	1040	H: 0.105, C: 0.089, N: 0.025, O: 0.774, Na: 0.002 P: 0.001, S: 0.002, K: 0.002
11	Trachea tissue	1060	H: 0.101, C: 0.139, N: 0.033, O: 0.713, Na: 0.001 P: 0.004, S: 0.004, Cl: 0.001, K: 0.004
12	Mammary gland tissue	990	H: 0.109, C: 0.506, N: 0.023, O: 0.358, Na: 0.001 P: 0.001, S: 0.001, Cl: 0.001
13	Thyroid tissue	1050	H: 0.104, C: 0.119, N: 0.024, O: 0.745, Na: 0.002 P: 0.001, S: 0.001, Cl: 0.002, K: 0.001, I: 0.001

1-6 Previous study

J. E. Turner, et al, [42] in (1964) reported that Monte Carlo technique has been used to obtain estimates of dose and dose equivalent in a homogeneous tissue slab irradiated by a broad beam of normally incident monoenergetic protons, and also for an isotropic flux of protons incident on a homogeneous parallel piped of tissue, in energies as high as 400 MeV. And calculate its stopping power, according to the formula of (Beth-Bloch (1932)) neglected density effect and shell correction. Also they pointed out the relationship between the stopping power and the relative biologic effects.

Young S. KIM, [43] in (1973) calculated the stopping power for some of biological materials (muscle, bone, ox lens, cat liver, standard man, rat fat, etc.) based on the Bethe-Bloch formula for heavy charged particles.

D. Bettega, C, et al, [44] in (1979) reported that the relative biological effectiveness (RBE) was determined for proton beams of 31, 12 and 8 MeV for Biological models (irradiating cultured human cells from the cyclotron beam pipe).

Bhaskar Mukherjee, [45] in (1983) studied the mass stopping power of protons from (0.5-200 MeV) in some biologically materials. By using Bethe-Bloch formula he stated that the stopping power of the protons is directly related to the linear energy transfer and must be well estimated in order to determine the proton dose distribution in the irradiated tissue accurately.

L. E. Porter, [46] gave in (1984) measurements of the stopping power of Al, Cu, Ag, and Au for protons, α particles, and Li ions.

E Waibel, and G Willems, [47] in (1987) studied stopping power data for protons in tissue equivalent gas (64.4% CH₄, +32.4% CO₂+3.2% N₂, partial pressures) were derived (i) from experimentally determined ranges and (ii) from differential ionization distributions. In energy range (1 - 100 KeV.) The results were compared with other data available. In general the experimental stopping power data tend to be higher values than calculated data for energies lower than 20keV; between 20 and 100keV agreed well within the stated uncertainties.

Nestor Azziz, et al, [48] developed in (1992) a new formalism for the calculation of the ion matter interaction phenomenon by incorporating the atomic electron shell structure. The concept of an "effective charge" in the context of the electron stopping power formalism is emphasized and extended.

T Hiraoka, et al, [49] (1994) measured the energy loss of 70 MeV protons in phantom materials, with a small uncertainty. A model with the assumption of a stochastic distribution of grains of material with different densities resulted in calculated Bragg curves.

N. Sakamoto, et al, [50] in (1996) reported that stopping powers of carbon (graphite) have been measured for (4-13 MeV) protons. Analyzed stopping powers with the usual Bethe-Bloch formula, they have extracted the mean excitation energy, I , of carbon atoms. To estimate the shell correction using both Bichsel's method and Bonderup's theory. The Barkas correction was evaluated by the theory of Ashley, Ritchie and Brandt. The I -values obtained are 79.6 eV for Bichsel's shell correction and 80.1 eV for Bonderup's shell correction.

J.F. Ziegler published report No. 49, [51] in (1999) in the international commission on radiation units and measurements (ICRU), stopping powers and ranges for protons and alpha particles. This report showed only limited comparisons to experimental data. Some of the stopping tabulations appear to have unusual variations for high energies (>1 MeV/nucleon) of the order of 2-4%, while the lower energies have possible errors of 10-20% for those targets which were not fitted with new data.

Raafat-Khalid, [52] in (2001) calculated mass stopping power for protons in fourteen biologic model (Tristearin $C_{57}H_{110}O_6$, rat fat, cat liver, water, ox lens, muscle A, muscle B, larvae "-1day", standard man, silk worm: pupae, hemoglobin A, cytochrome C, larvae "week", bone). Using the Bethe - Bluch equation for the energy range of protons (0.1-300 MeV) and noted the difference in mass stopping power in the models because of the different elements and their proportions in the composition and calculation of the factor correction density.

A. Akkerman, et al, [53] in (2001) reported that the stopping powers (SP) for 10 solid organic materials and water have been calculated in the range of proton energies 50–500 KeV.

Harald Paganetti, et al., [54] showed in (2002) that clinical proton beam therapy has been based on the use of a generic relative biological effective- ness (RBE) of 1.0 or 1.1.

Abebe Getachew, [10] in (2007) reported that an empirical formula based on Bohr's classical approach has been obtained to predict the stopping power for proton with energies (1-12MeV/amu) in elemental targets (AL, Cu, Pb, C, Be, Cd, Te and Cdte). The range formula is determined by directly integrating the stopping power formula of proton. His relations are also used to find the stopping power for compound targets by using the Bragg's additivity rule. The results are compared with experimental data and tabulated values of Bichsel and Sternheimer.

Marwan S. M. Alnimer and Zainab W. A. L, [55] in (2010) have been studied a theory to investigate the failures that can occur when applying the Bragg peak of a theoretical model of breast tumors in humans, using the SRIM-1998 and 2003 program to calculate the stopping power of hydrogen and carbon different energy in layers of skin and fat natural breast tissue with different densities. They found that the stopping

power of carbon ions is greater than the stopping power of hydrogen ions and proportional increased with tissue density and concluded that the typical Bragg's peak can be obtained and applied in the treatment of breast and taking into consideration the density or mass of the tumor, the location of the tumor in the natural tissue, nature of radioactive ions and energy.

Z. Francis, et al., [56] in (2011) calculated stopping power and ranges of electrons, protons, and alpha particles in liquid water, using the latest Geant4-DNA processes implemented in the Geant4 Monte Carlo simulation tool kit. Results show a good agreement between the analytical calculations obtained from the models, the Geant4-DNA Monte Carlo simulation predictions and the data published in the ICRU reports. Geant4-DNA processes apply in energy ranges: 0.025 eV–1 MeV for electrons, 100 eV–100 MeV for protons and 1 keV–400 MeV for alpha particles in liquid water.

Mohan Singh and Lakhwant Singh, [57] in (2011) calculated electronic stopping power of various organic compounds for proton (0.05-10 MeV) using different theoretical and semi-empirical formulations. Compared the stopping power values calculated using Ashley's dielectric model (ADM) and evaluation approach for optical energy loss function (OELF) with the values computed using the theoretical formulation CasP and semi-empirical approach SRIM. The merits and demerits of the adopted formulations are highlighted in this energy region. These types of stopping power analyses for proton will be helpful for scientific community to choose best formulation.

Zainab W Abdul Lateef, [58] in (2011) clarified the effect of proton beam radiation on the interferon (IFN- α , IFN- β , IFN- γ) and nucleotide, using (TRIM-SRIM) version 1998, and 2003 programs. A model of targeting certain interferon (IFN- α , IFN- β , IFN- γ) as well as the nucleotide pair was created. Each target was subjected to proton radiation of (H), (He), or (C) at different ranges of energy seeking for the Bragg's peak. She concludes that targeting of well precise located tumor with proton beam radiation therapy resulted in nucleotide damage of cancer cell without affecting the immune system in term of interferon surveillance.

Eko Sulistya, Kusminarto and Arief Hermanto [6] in (2012) calculated the stopping power and range of proton in the three types of body tissues which are skin, adipose tissue, and muscle. Range of proton as a function of proton energy in the 3 human tissues that have been studied can be calculated by computing the value of the stopping power of each element making up the tissue.

Ming Yang, et al., [59] in (2012) analyzed factors affecting proton stopping power ratio (SPR) estimations and range uncertainties in proton therapy planning using the standard stoichiometric calibration. The (SPR) uncertainties were grouped into five categories according to their origins, the impact of tissue composition variations on SPR estimation was assessed and the uncertainty estimates of each category were determined for high-density (bone), soft, and low-density (lung) tissues.

Khalid A. Ahmad and Ahmed J. Tahir, [60] in (2012) reported that the expressions of stopping parameters (i.e. Stopping number, energy loss cross section) and shell correction of swift proton in atomic target (Al) have been evaluated. There is target characterized as gas models as harmonic oscillator.

Zainab W. Abdul Lateef, [61] in (2012) using TRIM-SRIM the 1998 and 2003 versions to calculate the Bragg peak and calculate the effect of proton, helium and carbon ions against free radicals related to oxygen, nitrogen and halogen types. They concluded that such form of external beam irradiation is associated with direct scavenging effect on free radicals of whatever sources.

Hemalata Singh, et al., [62] in (2013) presented a simple method for the calculation of the mass stopping power (in MeV- cm²/g) of protons from (0.5 - 200) MeV energy range in biological human body substances such as water, bone, muscle and tissue. The proposed relations have been described in terms of energy of proton and mean ($\langle Z/A \rangle$) of atomic number (Z) and atomic weight (A).

Khansaa Nasir Aklo ,[63] in (2013) calculated the stopping power of the proton in the tissues of the human body (muscle, bone, brain, heart, kidney, lung, breast and soft tissue), in energy range from (1-10MeV) using the Bethe and Ziegler equation, SRIM and Pstar programs, by considering the tissue as composed of 9 elements with respect to fractional weight for every element.

Osamah. N. Oudah , [64] in (2013) calculated total stopping power of protons in the definite energy range (1 - 12 MeV) interacting with the elements (Be, C, Al, Cu, Cd, Te, and Pb), using the Bethe and Ziegler equations, PSTAR and SRIM programs. He found high stopping power in low energy and the increasing of value of stopping power is linear with the increase of atomic number Z, and he found that the stopping power values were different due to many reasons (The I value and shell correction, physical and chemical structure for some elements (gas or liquid or solid), and from the utilization of different theories in the calculation of the stopping power.

Alaa Mushatet Hammadi, [65] in (2013) reported that the dielectric formalism like Plasmon Pole Approximation (*PPA*) has been used to calculate the probability for an energetic proton and alpha particle to produce electronic excitations in liquid water and DNA. The effects of ionization fraction calculate the Partial Stopping Power Effective Charge (PSPEC) of (Au, C, Al, Cs), liquid water and DNA has been studied taking into consideration electronic excitation in the target.

Eko Sulistya, Kusminarto and Arief Hermanto, [5] in (2014) presented a numerical equation for mass stopping power of protons in four types of human body substance, i. e. water, bone, muscle and tissue, for energies (0.5-200) MeV. The equation was obtained by fitting the data values obtained from SRIM program and using the numerical equation, then the algorithm programming is expected to become easier and simpler.

Roaa Salam Kazim and Rashed Awaid Kazim ,[66] in (2014) showed a theoretical study was made to calculate electronic stopping power by using Bohr equation, Bethe equation and then calculated it by depending on close collisions and distant collisions and the equation which resulting from distant and close collisions for heavy charged particles (protons which interact with atomic targets (H, C, O, Si), in energy range(0.01-1000 Mev).

Iman Hammoud Abdullah, [67] in (2015) made a theoretical study to calculate the range of heavy charged particles (protons and alpha particles) on atomic targets (Lanthanum La, Samarium Sm, Alerdiom Er, Altantalm Ta, gold Au, Pb and uranium U) with atomic numbers (57,62,68,73,82,92) in range (0.3-100MeV) for protons, while Alpha is the range (1.6-100MeV), as well as for vehicles and the same as those charged particles when they pass in heavy vehicles (water, Almaalr and Kabton).

Rewaa Yaseen Taha, [68] in (2016) presented a theoretical study on the energy loss by using the dielectric function where the energy loss is lost count of charged particles (protons) interacting with the solid targets (Aluminum Al, Silicon Si and Tungsten W). Taking into account the distance between the proton and the surface of the targets. For this impact energy the main contribution to the energy loss is due to the excitation of (valence - band) electrons and the excitation of electrons (band – states) of the target's atoms, used mathematical appreciative methods in the calculation and some of the equation.

Kyle G. Reeves and Yosuke Kanai, [69] in (2017) presented a molecular level description of the electronic excitation dynamics in liquid water under proton irradiation via first-principles theory. Using non-equilibrium electron dynamics simulations based on their new large-scale real-time time-dependent density functional theory approach.

1-7 The aim of this study

- 1- Calculating total stopping power for proton with energy (1KeV-200MeV) in human tissues (skin, eye lens, stomach , pancreas, liver, spleen, blood, ovary, testis, prostate, trachea, mammary gland, and thyroid tissue), using the Bethe, Ziegler equation, Ziegler and Andreson (Vol.3) [100], SRIM and SRIM (dictionary) program, to determine the best value for stopping power in each tissues.
- 2- Calculating the range for proton in the same tissues and energy to know the best thickness to therapy each tissue.
- 3- Comparison our results of stopping power and range for the tissues under this study to determine which tissues can be treatment by using proton.
- 4- Comparison between the different methods which used in this study to determine the best method.

Chapter Two

Theory

2-1 Interactions of radiation with matter

Radiation is naturally present in our environment and artificially in hospitals, both types of radiation interact with the human body [70]. Ionizing radiation is divided into three groups:

1. Charged particles: p, α
2. Photons: gammas (γ) or x-rays
3. Neutrons (n)

The division into three groups is convenient because each group has its own characteristic properties and can be studied separately [71]. The charged particles are classified into two regimes

a-Light charged particles with atomic number ($z < 2$) like electrons and positrons.

b-Heavy charged particles with atomic number ($z \geq 2$) like protons, alpha particles and heavy ions [72].

There is a fundamental difference between the interaction of charged particle beams and photon beams with matter. Whenever a photon interacts with material, it is either absorbed or scattered and consequently removed from the beam. While a charged particle interacts with matter, it does not get removed from the beam except for the rare cases where it gets scattered to a very large angle, the net result of all interactions charged particles in the material is a reduction in energy of the particles as they pass through the medium [73]. A charged particle moving through a material interacts, primarily, through Coulomb forces, with the negative electrons and the positive nuclei that constitute the atoms of that material. As a result of these interactions, the charged particle loses energy continuously and finally stops after traversing a finite distance, called the range. The probability of a charged particle going through a piece of material without an interaction is zero. This fact is very important for the operation of charged particle detectors [71].

2-1-1 Proton interaction mechanisms

Several mechanisms by which a proton interacts with an atom or nucleus: Coulombic interactions with atomic electrons or with atomic nucleus, nuclear reactions, and Bremsstrahlung. To a first order approximation, protons continuously lose kinetic energy via frequent inelastic Coulombic interactions with atomic electrons. Most protons travel in a nearly straight line because the proton mass is 1832 times greater

than that of an electron. In contrast, a proton passing close to the atomic nucleus experiences a repulsive elastic Coulombic interaction which, owing to the large mass of the nucleus, deflects the proton from its original straight-line trajectory. Inelastic nuclear reactions between protons and the atomic nucleus are less frequent but, in terms of the fate of an individual proton, have a much more profound effect. In a nuclear reaction, the projectile proton enters the nucleus; the nucleus may emit a proton, deuteron, triton, or heavier ion or one or more neutrons. Finally, proton Bremsstrahlung is theoretically possible, but at therapeutic proton beam energies this effect is negligible [14].

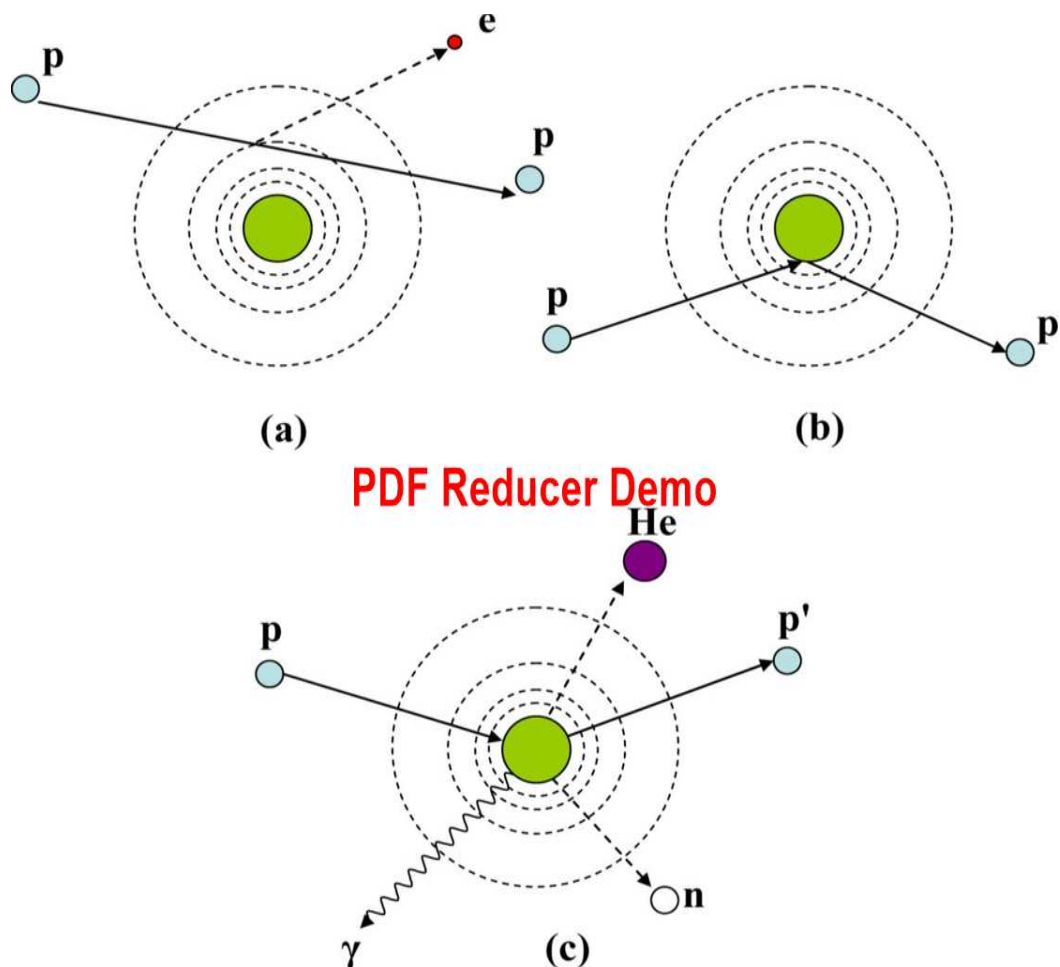


Fig : (2-1) Schematic illustration of proton interaction mechanisms: (a) energy loss via coulombic interactions, (b) deflection of proton trajectory by repulsive coulomb scattering with nucleus, (c) removal of primary proton and creation of secondary particles via non-elastic nuclear interaction. (p: proton, e: electron, n:neutron, He: α and γ : gamma rays) [14].

2-1-2 Interaction of proton with tissue

Tissues are made up of different types of molecules and contain inhomogeneities of various sizes and shapes. It is not only that those structures influence the range of the protons, but non-uniform multiple scattering takes on an important role. Neglecting this could result in local under or over dosage and in deformation of the distal end of the proton dose distribution, causing perhaps unintended irradiation of radiosensitive structures distal to the target volume [74].

The energy transferred to tissue by protons is inversely proportional to the proton velocity as protons lose their energy mainly in electromagnetic interactions with orbital electrons of atoms. The more the protons slow down, the higher the energy they transfer to tissue per track length, causing the maximum dose deposition at a certain depth in tissue. For a single proton, the peak is very sharp. For a proton beam, it is broadened into a peak of typically a few millimeters width because of the statistical distribution of the proton tracks [75].

2-2 Mechanisms of energy loss of charged particles in matter

Energy transfers to a molecule by a fast ion is frequently described in terms of the linear energy loss, or stopping power, of the target molecule (dE/dx) [76]. The greatest energy loss per unit path length of the particle occurs at ionization and excitation of atoms. The loss of kinetic energy in a nuclear encounter would be much larger. But such collisions are extremely rare compared to atomic encounters, roughly in proportion to the area of cross section of a nucleus compared to that of an atom, i.e., $10^{-24} \text{ cm}^2/10^{-16} \text{ cm}^2 = 10^{-8}$. Hence, they do not contribute appreciably to the overall energy loss. For kinetic energies larger than about M_0c^2 , where M_0 is the rest mass of the particle, energy loss by emission radiation called *bremsstrahlung* (decelerating radiation) becomes important, it is caused by the same mechanism as the emission of continuous x-rays. A crude idea of the important concepts of the energy loss process by collision (i.e., excitation and ionization of atoms) can be obtained by assuming that the charged particle is heavy and that it collides with a free electron. The loss of kinetic energy of the heavy particle must then be equal to the gain of kinetic energy of the electron. The latter can be estimated from the impact given to the electron as the charged particle passes by. If x, y coordinates are chosen as shown on Fig. (2-2), the impact equations for the electron are

$$\int F_x dt \approx 0 \dots\dots\dots(2-1)$$

$$\int F_y dt = p_e \dots\dots\dots(2-2)$$

Where :

$F = F_x + F_y =$ coulomb force exerted on the electron

t: time

P_e : momentum imparted to electron (only the y component is nonzero)

Equation (2-1) is a good approximation because the velocity of the heavy particle is practically unaffected by the encounter. If the impact parameter of the collision is b , the integral in eq. (2-2) can be estimated from the time of the impact

$$\Delta t \approx \frac{b}{v} \dots\dots\dots(2-3)$$

Where:

v : the speed of the heavy particle.

b : impact parameter of the collision.

And the average magnitude of F_y during that time

$$(F_y)_{ave} \approx \frac{ze^2}{b^2} \dots\dots\dots(2-4)$$

Where:

ze : the charge of the heavy particle. Hence from eq. (2-2)

$$p_e \approx \frac{ze^2}{bv} \dots\dots\dots(2-5)$$

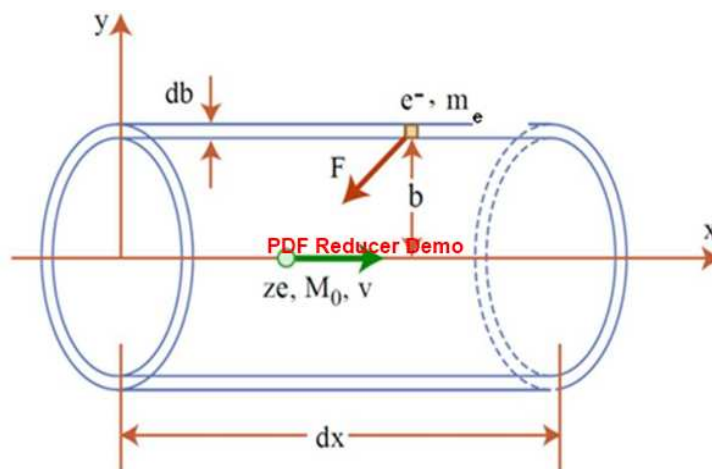


Fig (2.2) Encounter between a heavy charged particle of mass M_0 and a free electron of mass m_0 . The impact parameter b is indicated. [77].

A much cleaner estimate of the momentum imparted to the electron [eq.(2-5)] can be obtained by an application of Gauss' law of electrostatics

$$\int E.dS = 4\pi q \quad (\text{in electrostatic units}) \dots\dots\dots (2-6)$$

Where:

E: the electric field at the surface of any closed volume surrounding a charge

Q : The charge electric.

dS : an element of surface.

Applying this theorem in a system of reference in which the heavy particle is at rest to an infinite cylinder of radius b, as shown in Fig. (2-2), we find

$$\int \frac{F_v}{e} 2\pi b dx = 4\pi ze \dots\dots\dots (2-7)$$

Where:

b: Radius of cylinder

With respect to the heavy particle, the electron travels a distance

dx = v dt along the cylinder surface in a time dt so that

$$\int F_y dt = 2 \frac{ze^2}{bv} = p_e \dots\dots\dots (2-8)$$

in accordance with eq. (2-2). This yields the more correct estimate of p_e

$$p_e = 2 \frac{ze^2}{bv} \dots\dots\dots (2-9)$$

So that the kinetic energy gained by the electron (mass m_o) and lost by the heavy particle is

$$\frac{p_e^2}{2m_o} = \frac{2z^2 e^4}{m_o b^2 v^2} \dots\dots\dots (2-10)$$

If there are n atoms per unit volume, each with Z electrons, then in a path length dx there will be

$$n Z.2 \pi b db.dx \dots\dots\dots (2-11)$$

Electrons within a distance b to b +db from the path of the heavy particle. To each of these electrons, the particle loses an amount of energy given by expression (2-10) so that the total energy loss per unit path is

$$-\frac{dE}{dx} = \int_{b_{\min}}^{b_{\max}} nZ 2\pi b db \frac{2z^2 e^4}{m_o b^2 v^2} = \frac{4\pi e^4 z^2 nZ}{m_o v^2} \ln \frac{b_{\max}}{b_{\min}} \dots\dots\dots(2-12) .$$

This expression is approximate, because for nearly head on collisions eq. (2-10) is not valid. In reality, the electrons in the stopping material are not free but bound to atoms (or to the solid if the material is in solid form). Since each atom has electronic energy levels the particle cannot transfer any energy to the atom unless it excites the atom at least to its first excited state. In classical terms, we can argue that the time of impact [eq. (2-3)] must not be longer than the period of rotation of a typical electron in its orbit in order that energy will be transferred to the electron in the atom.

$$\Delta t_{\max} \approx \frac{1}{\nu} \dots\dots\dots (2-13)$$

Where:

ν : is the frequency of rotation.

Using Eq. (2-3) this gives

$$b_{\max} \approx \frac{v}{\nu} \dots\dots\dots (2-14)$$

Where:

b_{\max} : The maximum impact parameter .

The minimum impact parameter is limited by the uncertainty principle. If $\Delta p_x \Delta x \approx h$ (h =Planck's constant) is applied in the relative coordinate system of the electron and the particle, that

$$b_{\min} \approx \frac{h}{m_o v} \dots\dots\dots (2-15)$$

Where:

b_{\min} : The minimum impact parameter .

Therefore, obtain

$$-\frac{dE}{dx} \approx \frac{4\pi e^4 z^2 nZ}{m_o v^2} \ln \frac{2m_o v^2}{I_{ave}} \dots\dots\dots (2-16)$$

Where $h\nu$ has been replaced by a mean ionization and excitation potential I_{ave} of the atoms in the stopping material and a factor 2 has been added in the logarithm term in this equation are, as previously,

ze :charge of heavy particle

m_o : mass of electron

v :speed of heavy particle

nZ : number of electrons per unit volume in stopping material [77].

Eq. (2-16) describes the energy loss due to particle collisions in the non relativistic regime, one can include relativistic effects by replacing the logarithm by

$$\ln\left(\frac{2m_e v^2}{I}\right) - \ln\left[1 - \frac{v^2}{c^2}\right] - \frac{v^2}{c^2} \dots\dots\dots (2-17)$$

Eq.(2.16) is a relatively simple expression, yet one can gain much insight into the factors that govern the energy loss of a charged particle by collisions with the atomic electrons. In a collision with a nucleus, the stopping power would increase by a factor equals to atomic number Z [63]. Another useful observation is that (2.16) is independent of the mass of the incident charged particle. This means that no relativistic electrons and protons of the same velocity would lose energy at the same rate, or equivalently the stopping power of a proton at energy E is about the same as that of an electron at energy $\sim E/2000$. In this case of Bethe stopping powers, the reduced form of eq. (2.16) [63]. for protons, namely

$$-\frac{dE}{dx} (MeV / m) = 4\pi r_e^2 z_1^2 \frac{m_e c^2}{\beta^2} NZ_2 \left[\ln \frac{2mc^2}{I} \beta^2 - \ln(1 - \beta^2) - \beta^2 \right] . (2-18)$$

Where:

r_e : is classical electron radius= e^2/mc^2 .

Z_1 : Atomic number of the particle.

Z_2 : Atomic number of the target.

β : v/c

c : speed of light in vacuum,

N : number of atoms/ m^3 in the material which the particle moves which calculated from
 $N = \rho(N_A/A)$

N_A :Avogadro's number,

A : atomic weight.

It is more consistent results are recorded [71]. Experimentally, the energy loss is determined by the number of ion pairs formed along the path of the particle. By ion pair (positive and negative) constituents which result from an ionizing encounter. If on the average, an energy w has to be lost by the heavy particle in order to produce one ion pair, the number of ion pairs i per unit path is given by

$$-\frac{dE}{dx} = wi \quad \dots\dots\dots (2-19)$$

Where:

w : lost by the particle to produce one ion pair.

i : number of ion pairs per unit path of the particle.

The quantity w is the result of complicated processes: (1) there is atomic excitation as well as ionization, (2) an ejected electron can have sufficient energy eq. (2-10) to produce secondary ionization in turn. Empirically, in a given material, w is, fortuitously, practically independent of the kinetic energy or of the nature of the particle. For air, it has the value 35.0 eV for 5 keV electrons, 35.2 eV for 5.3-MeV alpha particles, and 33.3 eV for 340MeV protons, show in Fig (2-3a), (2-3b).

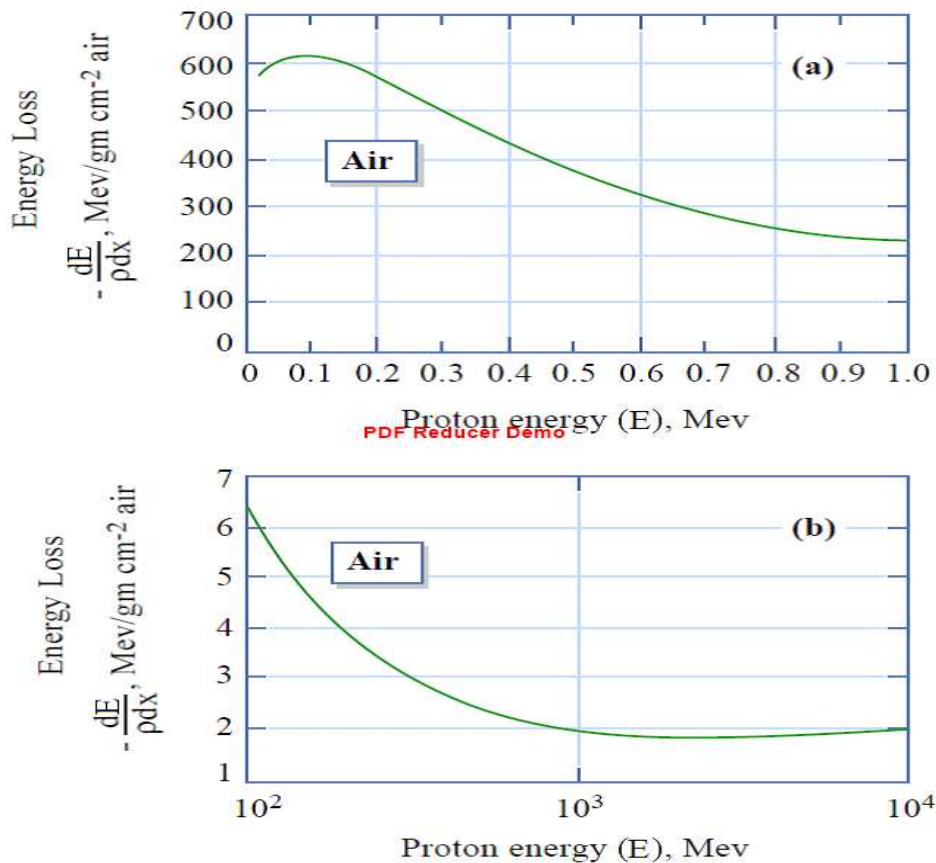


Fig (2-3a): The experimentally determined stopping power, $(- dE/dx)$, for protons in air, low energy region where the Bethe formula applies down to $E \sim 0.3$ MeV with $I \sim 80$ eV. Below this range charge loss to electron capture causes the stopper power to reach a peak and start to decrease, and Fig (2.3b): High-energy region where a broad minimum occurs at $E \sim 1500$ MeV [77].

This figure (Fig(2-3)), gives an experimentally determined energy loss curve for protons in air. Since the number of atoms per unit volume n is related to density of the material ρ , Avogadro's number N , and the atomic weight A [77].

$$\text{by } n = \frac{N\rho}{A} \dots\dots\dots (2-20)$$

2-2-1 Electronic stopping

Electronic stopping is a common term for the energy loss caused by all electronic processes. It originates from several different contributions depending on the type of the interaction. Ions moving faster than ~ 1 keV/amu lose kinetic energy mainly via electronic stopping. When an ion moves inside the material, it collides with the electrons of the material [78]. The energy loss to be primarily through inelastic collisions with electrons of the material [79]. (Electronic stopping) leads primarily to excitation and ionization of target atoms [80]. Ionization occurs when the electron

obtains enough energy to leave the atom and becomes a free particle with kinetic energy equal to

(KE) $e = (\text{energy given by particle}) - (\text{ionization potential})$ [71]. This is the principal mechanism for the energy loss of ions at high velocities, energy loss due to excitation and ionization is also called electronic energy loss, or inelastic energy loss [81]. A slow heavy particle, when passing through matter, will capture and lose electrons until its charge reaches a dynamic equilibrium state [82]. The possible phenomena contributing to the electronic stopping in the velocity region well below the light velocity are :

1. Momentum exchange in a collision between the ion and a free electron in the target material.
2. Ionization of the ion
3. The ion captures an electron.
4. Excitation of the ion.
5. Excitation of a target atom
6. Ionization of a target atom.
7. Collective effects such as the polarization or the plasmon excitation [70]. The relative significance of these processes depends primarily on the speed v and the atomic number Z_1 of the penetrating ion and to some extent on target parameters and projectile state [83].

2-2-2 Nuclear stopping

Nuclear collisions are the major mechanism for energy loss of projectiles at low velocities. Projectiles transfer their energies to the target nuclei by elastic collisions, and consequently the target atom recoils. Energy loss due to a nuclear collision is also called nuclear energy loss or elastic energy loss [81]. Interaction with the atomic nucleus contributes significantly to the energy loss, only for a relatively high particle energy, i.e. for about $E \geq 100$ MeV. Exotic processes like proton bremsstrahlung production begin to contribute significantly only in the GeV energy region. The elastic interaction of incoming protons with the atomic nucleus leads to an energy transfer to the nucleus and a change in flight direction of the protons, the interaction probability is very low, and it further decreases with increasing energy. Consequently, elastic nuclear interactions can be neglected for $E \geq 1$ MeV, i.e. they only play a small role toward the very end of the proton path. Inelastic nuclear interactions this type of interaction of the proton with the atomic nucleus leads to the excitation of the nucleus, to the formation of a compound nucleus or to a direct interaction between the incoming proton and individual components of the nucleus [74]. Nuclear energy loss can be ignored, especially for light ions at medium and high velocities [81].

2-2-3 Stopping power for a compound or a mixture

In case of a compound or a mixture of more than one element, we can use the so called Bragg-Kleeman rule to calculate the total mass stopping power

$$\left[\frac{1dE}{\rho dx}\right]_{total} = \sum_{i=1}^n \left[\frac{w_i}{\rho_i} \left(\frac{dE}{dx}\right)_i\right] \dots\dots\dots(2-21)$$

Where:

w_i is the fraction by mass of element i in the mixture.

ρ_i : its density of element i in the mixture.

The Bragg-Kleeman rule can also be applied to compute stopping power of a compound material using [73].

$$\left[\frac{dE}{dx}\right]_{total} = \sum_{i=1}^n w_i \left(\frac{dE}{dx}\right)_i \dots\dots\dots(2-22)$$

2-3 Bragg rule additivity

Bragg's rule of stopping power additivity can be expressed in terms of stopping cross sections as

$$\varepsilon(\text{compound}) = \sum_i n_i \varepsilon(i) \dots\dots\dots(2-23)$$

Where:

n_i is the number of atoms of element i in the molecule.

Similarly for the mean excitation energy [eq (1-5)]. Alternatively, it can be expressed in terms of mass stopping as eq (2-21) [84]. The accuracy of Bragg's rule is limited because the energy loss to the electrons in any material depends on the detailed orbital and excitation structure of the matter, and any differences between bonding in elemental materials and in compounds will cause Bragg's rule to become inaccurate. Bragg and Kleeman, in 1903, calculated the stopping contribution of hydrogen and carbon atoms in Hydrocarbon target gases using Bragg's rule, and detailed experimental studies of Bragg's rule started in the 1960's, and wide discrepancies were found from simple additivity of stopping powers [85]. The experimental tests of Bragg's rule may be classified into two general categories: physical-state effects (gas, liquid, or solid) and chemical-binding effects [65].

2-4 Mean ionization potential (I)

It is less amount of energy, enough to move the bond electron in the atom out of its orbit. A lot of researchers calculated the value (I) practically due to the difficulty calculated theoretically and adopted the compute on the analysis of the stopping power of high-energy protons. This factor can be determined by knowing the stopping power from Bethe formula. The value (I) depends mainly on the atomic or molecular properties and on the physical state of the absorbing medium. [52]. The value (I) can be represented by the following semi-empirical equation which gives good results:

$$I(\text{eV}) = (9.7 + 58.8Z^{-1.19}) Z \dots\dots\dots(2-24)$$

Where:

Z : atomic number for the target. [71].

In compound or mixture the value (I) can be obtained using (Bragg additivity rule) as follows:

$$\langle \ln I \rangle = \left(\sum_i \frac{W_i \times Z_i \times \ln I_i}{A_i} \right) / \langle Z / A \rangle \dots\dots\dots(2-25)$$

Where:

Z_i : atomic number for the element (i) in the compound.

I_i : mean ionization potential for element (i) in the compound.

A_i : mass number for the element (i) in the compound.

Z : atomic number for the target.

A : mass number for the target. [52].

The mean excitation energy, I , is a crucial parameter in the Bethe stopping power formula. Determination of the parameter relies on two sources :

1) Stopping power and range measurements.

2) Oscillator strength distribution (for gaseous media) and dielectric function (for condensed media) measurements or calculations [86]. The value of the mean excitation energy (I) depends on the details of the electronic structure of the medium, and it is especially sensitive to the arrangement of the valence electrons. Therefore, it is influenced by molecular binding and by the physical state of aggregation of the medium. The accurate theoretical prediction of (I) values is difficult, and its reliance is on experimental data which is unavoidable. Data in the form of experimental stopping power and range data in the energy region where the Bethe theory is applicable are rather abundant, especially for protons. Of particular importance are measurements at high energies (≥ 300 MeV) where the extraction of (I) values is simple and straightforward data are still relatively scarce and have become available in significant amounts only in recent years. Usually through application of an additivity rule. It has been known since the early work of Bragg and Kleeman that the stopping power of a

compound can be closely approximated by a weighted sum of the stopping powers for the atomic constituents. Within the framework of the Bethe theory, this additivity assumption is equivalent to assigning to a compound a mean excitation energy eq (2 - 25) [87].

For $Z = 1$ through 12, $I = 18, 42, 39, 64, 70, 78, 96, 117, 130, 132,$ and 140 eV, respectively. For Z greater than 12 used the Sternheimer formula (12) given by eq (2-24) [43].

2-5 Stopping power dependence on particle energy

2-5-1 At low energies:

The low energy region occurs when the incident particle velocity (V) is ($V < V_o Z_1^{2/3}$) Z_1 is the atomic number of ion and V_o represents the Bohr velocity ($v_o = 2.18 * 10^6$ m/s) and this is about the velocity of the conduction electrons in solid [88]. The Bethe formula begins to fail at low particle energies where charge exchange between the particle and absorber becomes important [89]. At low kinetic energies the velocity of the incident particle approaches that of the inner-shell electrons and thus they contribute less to stopping power. In addition, charge transfer (electron capture and loss) becomes important at low velocities and therefore the charge of the projectile becomes velocity dependent [90]. At the end of its track, the particle has accumulated Z electrons and becomes a neutral atom [89]. At much lower kinetic energies the loss of energy due to momentum transfer to the nuclei becomes important; therefore both nuclear and electronic stopping power should be considered [90].

2-5-2 At intermediate energies:

The intermediate energy region occurs when the velocity (V) of the incident particle is in the range ($2V_o Z_1 > V \geq V_o Z_1^{2/3}$); it includes the maximum stopping power [88]. The stopping power decreases with increasing particle speed V as $1/V^2$, due mainly to the decreasing collision times [43]. The energy loss by the particle is equal to the energy transfer to the electron in the atom and is proportional to the square of the momentum transfer, thus the rate of energy loss is inversely proportional to v^2 or E (particle energy) [10].

2-5-3 At high energies:

This region can occur at ($V \geq 2V_o Z_1$) [88]. The interaction time will be shorter at high energies, causing reduced momentum transfer and then reduced energy loss [91]. In the relativistic region ($V \sim c$), the factor $1/V^2$ becomes nearly constant, but there arises a

logarithmic increase in the stopping power due in part to the increase of the maximum energy transferred to atomic electrons in close collisions and in part due to the relativistic distortions of the Coulomb field of the incoming particle in distant collision [43]. This leads to higher energy loss at higher energies [10].

2-6 Range

Range is the distance traveled by the proton before stopping. Stopping power is inverted, the distance is obtained per unit of energy loss, but the range with energy (E_o) is calculated by integrating it to zero energy [6]

$$R(E_o) = \int_0^{E_o} (-dE / dx)^{-1} dE \dots\dots\dots (2-26)$$

The range depends upon the initial energy of the particle, its type and the material it traverses [92].

Range is distance, it measures in unit length meters (m), and in another common unit is Kg/m² or (g/cm²). The relationship between them is

$$R \text{ (Kg/m}^2\text{)} = (R \text{ (m)}) (\rho \text{ (Kg/m}^3\text{)}) \dots\dots\dots (2-27)$$

Where:

ρ : is the density of the material in which the particle travels [71].

If the number of charged particles N penetrating a substance is measured as a function of the depth x , the following curve results, in Fig (2-4):

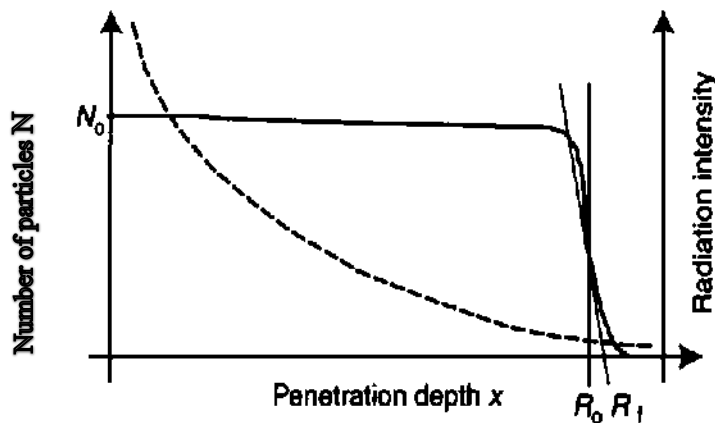


Fig. (2-4). Typical penetration curve for charged particles (solid line). The penetration depth x is in general presented in g/cm², i.e. Length x density N_0 : initial number of particles. R_0 : mean range and R_f : extrapolated range. For comparison a typical attenuation curve for electromagnetic radiation is added (dotted line). [74]

The above (solid) curve with its steep fall-off is typical for heavy charged particles characterized by an energy loss per interaction that is very small compared to the particle's energy. For electrons, losing more energy per collision, the distal falloff is much more gentle. If all protons would lose the same amount of energy per scattering event, all would display the same range, i.e. the penetration curve would be horizontal

with a perpendicular drop at its end. However, the interaction of charged particles with atoms and molecules is a statistical process. Consequently the energy loss for each individual particle varies to some degree, so the particle path length and range are characterized by straggling. If energy loss is dominated by the heavy particle-electron interaction the distal falloff is very steep (occurring within about 2% of the range for protons) and centred around R_0 . With increasing mass of the heavy particle, the curve's steepness increases but its tail becomes more pronounced. Range straggling is a measure of the uncertainty of the particle range. Under the reasonable assumption, that the difference $R_0 - R_f$ is approximately half the width of the Gaussian describing the range straggling, straggling can be calculated for p-e energy losses alone [74].

2-6-1 Range of proton

Charged particles, unlike photons and neutrons, can travel only a certain maximum distance in matter, called the range, before they are stopped, cause thousands of ionizations and excitations of the atoms along their path before they are slowed and become part of the ambient medium [93]. The path of most protons in matter is a nearly straight line. On average, the protons path length is very nearly equal to its projected path length and range. This simple but important fact renders many proton range calculations tractable with relatively simple numerical or analytical approaches [14]. The range $R(E)$ of a charged particle having kinetic energy E is the integral of the reciprocal of the negative stopping power from the initial kinetic energy to the final kinetic energy of a stopped particle ($E = 0$) written in terms of the stopping power as eq (2-27) [94]. Range is defined as the depth at which half of protons in the medium have come to rest. There are small variations in the energy loss of individual protons (an effect called range straggling). Consequently, the range is inherently an average quantity, defined for a beam and not for individual particles [14]. There exists a number of theoretical and semiempirical tabulations of range energy relations for heavy ions. Barkas and Berger (1967) use empirical proton range data between 1 and 8 MeV and calculate, with the use of the Bethe formula [95].

2-7 Niels Bohr formula

In 1913, Niels Bohr derived an explicit formula for the stopping power of heavy charged particles. Bohr calculated the energy loss of a heavy charged particle in a collision with an electron then averaged over all possible distances and energies. The nonrelativistic formula that Bohr obtained gave the correct physical features of stopping power. Bohr derived the formula based on the following assumptions:

- The particle move rapidly compared with the electron.
- For maximum energy transfer the collision is head on.
- The energy transferred is large compared with the binding energy of the electron.

- The electron is considered to be free and at rest and the collision is elastic.

The Bohr formula for heavier particle is given by:

$$-\frac{dE}{dx} = \frac{4\pi n z^2 k_o^2 e^4}{mv^2} \ln\left(\frac{2mv^2}{I}\right) \dots\dots\dots (2-28)$$

Where:

n : number of electrons per unit volume in the stopping material.

m : electron rest mass.

v : velocity of the particle.

Z : charge of the particle.

e : electron charge.

$$k_o = \frac{1}{4\pi\epsilon_o}$$

I : mean excitation energy of the medium and is normally treated as an experimentally determined parameter for each element [10].

2-8 Bethe theory

Using relativistic quantum mechanics, Bethe derived the expression for the stopping power of a uniform medium for a heavy charged particle (eq 2-18). As the (nonrelativistic) result:

$$\left(-\frac{dE}{dx} = \frac{4\pi k_o^2 z^2 e^4 n}{mv^2} \ln \frac{mv^2}{hf}\right) ,$$

is identical with the Bethe formula when $\beta \ll 1$, and write $V = \beta c$ and $hf = I/2$. Whereas the energy hf in the semi- classical theory has only a rather vague meaning, the mean excitation energy I is explicitly defined in the quantum theory in terms of the properties of the target atoms. The logarithmic term in Eq. (2.18) leads to an increase in stopping power at very high energies (as $\beta \rightarrow 1$). At low energies, the factor in front of the bracket in (2.18) increases as $\beta \rightarrow 0$ [96]. Bethe showed that the ratio of the energy loss by the particle to the target electrons was greater than the loss to the heavier target nuclei (less than 0.1%) of the energy loss of high velocity particles is to the target nuclei (ignoring nuclear reactions) [97]. The Bethe theory represents a standard framework for obtaining reasonably accurate values for light ions over a wide range of materials. The

only non-trivial parameter is the mean excitation energy of the material (I), which represents the main source of uncertainty in Bethe's formula at high energies [98].

2-9 Bethe – Bloch formula

Bloch evaluated the differences between the classical (Bohr) and quantum mechanical (Bethe) approaches for particles with velocities much larger than the target electrons. The original Bethe – Bloch relativistic stopping formula may be stated as:

$$-dE/dx = \frac{4\pi e^4 Z_1^2 Z_2}{m v^2} \left[\ln \frac{2m v^2}{I} - \ln(1 - \beta^2) - \beta^2 - \Psi(z_1) \right] \dots \dots \dots (2-29)$$

Where:

$$\beta = v/c$$

c : light velocity

$\psi (z_1)$: a small term which contains Bloch's error.

Z_1 : Atomic number for the particle.

Z_2 : Atomic number for the target.

Fano published various extensions of Bethe's and Bloch's work and described a relativistic version of Bethe – Bloch energy loss formula where two additional corrective terms are included, the shell correction term (C/z_2) and the density effect correction ($\delta/2$) [72]. Both of these corrections (shell-correction term at very low energies ($E \leq 10$ MeV/amu) and the density-effect correction at very high energies ($E \geq 2$ GeV/amu) depend on the nature of the absorbing material and the projectile velocity but are presumably independent of the projectile charge [99],

therefore eq (2-29) becomes:

$$-dE/dx = \frac{4\pi e^4 z_1^2 z_2}{m v^2} \left[\ln \frac{2m v^2}{I} - \ln(1 - \beta^2) - \beta^2 - \frac{C}{Z_2} - \frac{\delta}{2} \right] \dots \dots \dots (2-30)$$

Eq. (2-30) is usually simplified as

$$-dE/dx = \frac{4\pi r_o^2 m c^2 z_1^2 z_2}{B^2} \left[f(B) - \ln I - \frac{C}{z_2} - \frac{\delta}{2} \right] \dots \dots \dots (2-31)$$

$$f(B) = \ln[2m c^2 B^2 / (1 - B^2)] - B^2 \dots \dots \dots (2-32)$$

By making $k = 4 \pi r_o^2 m c^2$ the Bethe – Bloch stopping power formula is commonly expressed as [72]:

$$-dE / dx = \frac{k z_1^2 z_2}{B^2} [L_o(B) + z_1 L_1(B) + Z_1^2 L_2(B) + \dots] \dots\dots\dots (2-33) .$$

Where:

L_o : the Born correction.

L_1 , L_2 : Barkas and Bloch corrections.

The term in the brackets of eq. (2-33) is defined as the stopping number, $L(B)$ and this expansion will contain all the corrections to the basic two particle energy loss process, defined as: [97]

$$[L(B) = L_o(B) + z_1 L_1(B) + z_1^2 L_2(B) + \dots] \dots\dots\dots (2-34)$$

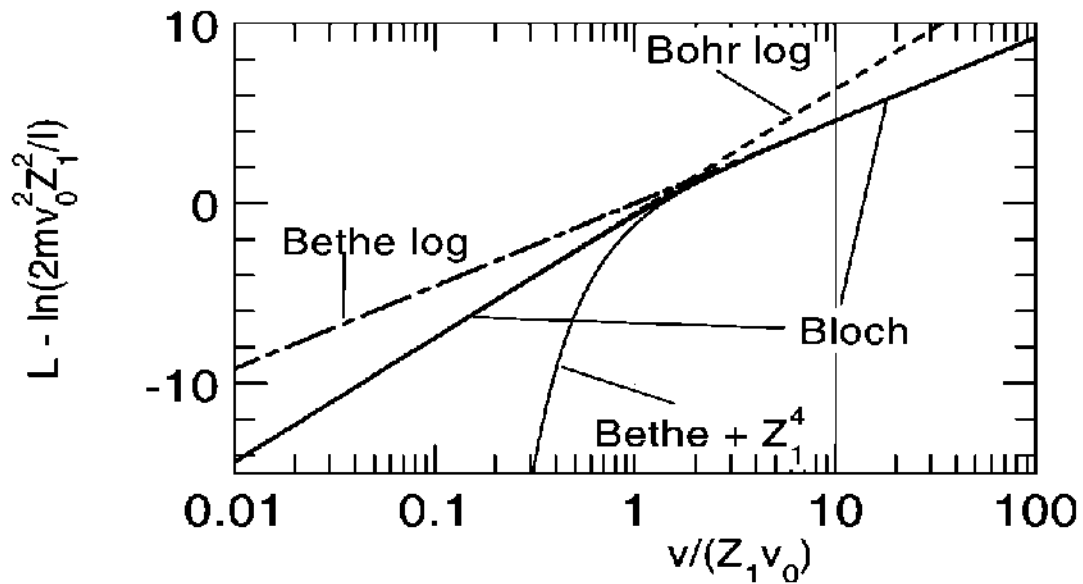


Fig (2-5). The stopping number according to Bloch (1933) (solid line) approaches the Bohr and Bethe logarithms at low and high projectile speed, respectively. Also included is a curve consisting of the Bethe logarithm and the Z_1^4 correction which often, erroneously, is called the Bloch correction. $V_o = c/137$ is the Bohr velocity [83].

In the simplest versions of Bethe and Bohr stopping theory, respectively. Fig. (2-5) shows the two expressions in a plot which, within the range of validity of the two schemes, is universally valid for all point charges Z_1 and all elemental materials with atomic number Z_2 . According to Bohr, the classical expression L_{Bohr} applies to the

regime $\kappa = 2Z_1 e^2 / \hbar.v > 1$, while L_{Bethe} , based on the Born approximation, has a complementary range of validity specified by $k/2 = Z_1 e^2 / \hbar.v < 1$. The curve labeled “Bloch” combines the two limits, the transition between which is seen to be rather abrupt. It is also shown that a curve labeled “Bethe + Z_1^4 ”, which approximates the Bloch curve in the region of small deviations from the Bethe logarithm, but which leads to absurd results at lower projectile speeds. The Z_1^4 term is often erroneously called Bloch correction [72].

2-10 Ziegler formula

Ziegler in his book attempts a nearly complete presentation of absolute experimental energy data. For hydrogen over the energy range 10 KeV<(E/amu)<20MeV. The extensive use of active computer programs have allowed a large variety of different fitting functions to be used, the data were finally fitted to simple analytical functions the parameters of which will be committed together with the experimental data for each element. An attempt has been made to calculate the fitting parameters to elements for which there is no experimental data. Finally the stopping powers were integrated to yield path length and projected range data for protons and Deuterons [100].

2-10-1 Review of theory:

At low energies, stopping power theory is mostly evaluated using the Thomas-Fermi statistical model of the atom. The electronic stopping is found to be proportional to projectile velocity, the specific dependence is given by: [100]

$$(-dE / dx)_e = z_1^{1/6} 8\pi e^2 a_o \frac{z_1 z_2}{(z_1^{2/3} + z_2^{2/3})^{3/2}} \frac{v}{v_o} \dots\dots\dots(2-35)$$

$$v < v_o z_1^{2/3}$$

The high-energy behavior of the stopping power is very well described by Bethe-formula

$$-dE/dx = \frac{4\pi e^4 Z_1^2 Z_2}{m v^2} \times [\ln \left(\frac{2mv^2}{I} \right) + \ln \left(\frac{1}{1-\beta^2} \right) - \beta^2 - \frac{c}{Z_2}] \dots\dots\dots(2-36)$$

I is the main parameter of the theory, the mean excitation potential, in I theoretically defined by the formula

$$\ln I = \sum_n f_n \ln E_n \dots\dots\dots(2-37)$$

Where:

E_n : possible energy transitions

f_n : corresponding oscillator strengths for the target atom.

Eq. (2-36) predicts the stopping power at high energies to be proportional to Z_1^2 . To bridge the gap between the high- and low-energy theories, interpolation formulas of different levels of complexity were proposed. Brice suggested

$$-dE/dx (E) = (Z_1+Z_2)(-dE/dx)_e (n) f (n) \dots\dots\dots(2-38)$$

Where:

$$n = \frac{E}{Z^2 M_1 E_1}$$

and

$$(-dE/dx)_e (n) = A[(30n^{\frac{5}{2}} + 53n^{\frac{3}{2}} + 21n^{\frac{1}{2}})/3(1 + n)^2] + (10n + 1) \arctan(n^{\frac{1}{2}}) \dots\dots\dots(2-39)$$

and

$$f (n) = [1 + (4Z^2 \acute{a}^2 n)^{n/2}]^{-1} \dots\dots\dots(2-40)$$

Here $A=1.22 \times 10^{-15}$ eV cm²/atom while Z, \acute{a} and n are fitting parameter. And $E_1 = 100$ KeV.

Varelas and Biersack proposed

$$(-dE/dx)^{-1} = \left((-dE/dx)_{LOW} \right)^{-1} + \left((-dE/dx)_{HIGH} \right)^{-1}$$

or

$$-dE/dx = (-dE/dx)_{LOW} (-dE/dx)_{HIGH} / ((-dE/dx)_{LOW} + (-dE/dx)_{HIGH}) \dots\dots(2-41)$$

Where :

$(-dE/dx)_{LOW}$: (Low Energy Stopping) is

$$(-dE/dx)_{LOW} = A_1 E^{\frac{1}{2}} \dots\dots\dots(2-42)$$

And

$(-dE/dx)_{HIGH}$ (High Energy Stopping) is

$$(-dE/dx)_{HIGH} = \left(\frac{A_2}{E}\right) \ln[1 + (A_3 / E) + (EA_4)] \dots\dots\dots (2-43)$$

Here $A_1, A_2,$ and A_3 are fitting constants and

$$A_4 = 4m/IM_1 \dots\dots\dots (2-44)$$

2-10-2 Fitting the high-energy region

The Bethe stopping power formula (2-36) was used as the theoretical basis in the high energy region. All stopping power data with $E/amu > 400$ KeV were considered in constructing the final fits. Note that both eq. (2-35) and eq. (2-36) depend on projectile velocity, but not on projectile mass. No theoretical predictions relate electronic energy loss to projectile mass. Hence, all data for protons, deuterons, and tritons have been reduced to a common energy scale by depicting them as a function of E/M_1 . One basic conclusion of Andreson and Ziegler study is that the entire experimental material considered does not give indication of any influence of projectile mass on stopping powers. Very little data scatter may be seen on the stopping graphs at high energies (due to the strong energy dependence of the stopping). However, this scatter may become evident using a procedure proposed by Bichsel. He proposed to invert eq. (2-36) to determine $\ln(I)$ plus C/Z_2 (mean ionization potential and shell-correction term) from experimental stopping powers. They have adopted basically the same approach but assumed values of the mean excitation potential I and extracted the experimental values of the shell-corrections C/Z_2 . These experimental shell corrections are shown on plots called "High Energy Stopping Power Evaluation" for elements with high energy data. All data points are shown, and the I -value used for the calculation of C/Z_2 is given. It is seen from eq. (2-36) that the transformation to C/Z_2 depends on energy [100]. For energies from 600-2000KeV, experimental data scatter more and there is less theoretical guidance concerning the shape of the shell corrections. Hence, it is not recommended to use the approach based on eq. (2-36) to obtain stopping powers below 600 KeV,. At 600 KeV the accuracy of the Bethe-fit is expected to be 3% or slightly worse depending on the amount and quality of experimental data for any specific element. A crucial test of their interpolation procedure is a comparison to high-precision relative measurements (where several targets are measured relative to each other, but no absolute measurements are made). In accordance with their accuracy claim, a 0.5% standard deviation has been assigned to their computed stopping powers. To allow easy computations of high-precision stopping cross sections (above 600 KeV) one may use the formula (which is a variation of eq. (2-36)):

$$-\frac{dE}{Ndx} = \frac{A}{\beta^2} [\ln B\beta^2 - \ln(1 - \beta^2) - \beta^2 - (a_0 + a_1 \ln E + a_2(\ln E)^2 + a_3(\ln E)^3 + a_4(\ln E)^4)] \dots\dots\dots (2-45)$$

Coefficients A and B are given on each graph of the shell correction for each element. Note that the first important term in the relativistic correction $(-\ln(1 - \beta^2) - \beta^2)$ is of the order of β^4 and hence only important at very high energies [100].

2-10-3 Fitting at lower energies

It is of basic physical interest to obtain the factors by which the Lindhard formula (eq. (2-35)) must be multiplied to give the best fit to the low energy experimental data. It turned out, however, that a velocity proportional stopping did not give the best fit to the low-energy data. Significantly lower χ^2 -values were found setting S proportional to $E^{0.45}$ (in comparison to factors of $E^{0.4}$, $E^{0.5}$, and $E^{0.58}$) in the low energy limit except for hydrogen and helium targets where no large difference was found. They decided to use.

$$(-dE/dx)_{LOW} = A_1 E^{0.45} \dots\dots\dots (2-46)$$

Instead of eq. (2-42), the overall fit to the data is better than with a velocity proportional stopping power. This may be due to a large weight of data for velocities higher than v_o (E higher than 25 KeV), but the somewhat lower E dependence seems also generally to fit the slope of the low-energy data better than a velocity-proportional term. Data for heavier projectiles do often show strong deviations from velocity proportionality [100].

2-10-4 Interpolation using 2-parameter fitting

In order to interpolate stopping to elements without experimental data, they attempted to find a 2 parameter fit (one parameter for low energies and one for high energies). They used the basic 4-parameter fit of eq.(2-43) and for A_4 they used:

$$A_4 = 4m_e/m_p I \dots\dots\dots (2-47)$$

Where m_e and m_p are the mass of the electron and proton. A new fit was made to all elements using this form for A_4 . For the targets used to test the fit, A_2 (eq.2-43) was found to decrease slowly with Z_2 . The variation of A_2 was now approximated

$$A_2 = (243 - 0.375 Z_2) Z_2 \dots\dots\dots (2-48)$$

With these smoothed A_2 coefficients, new optimal values of A_1 and A_3 were sought by the optimization program. The fits turned out to have a χ^2 virtually the same as for the original four-parameter fit. They briefly summarize the various fitting formulae which they combine in the Varelas-Biersack Formula

$$\left(-\frac{dE}{dx}\right)^{-1} = (-dE/dx)_{LOW}^{-1} + (-dE/dx)_{HIGH}^{-1} \dots\dots\dots (2-49)$$

These they call:

4-Parameter Fit

$$(-dE/dx)_{LOW} = A_1 E^{0.45} \dots\dots\dots (2-50)$$

$$(-dE/dx)_{HIGH} = (A_2/E) \ln[1 + (A_3/E) + A_4 E] \dots\dots\dots (2-51)$$

3-Parameter Fit

$$(-dE/dx)_{LOW} = A_1 E^{0.45} \dots\dots\dots(2-52)$$

$$(-dE/dx)_{HIGH} = (A_2/E) \ln[1 + (A_3/E) + (4 m_e E/m_p I)] \dots(2-53)$$

2-Parameter Fit

$$(-dE/dx)_{LOW} = A_1 E^{0.45} \dots\dots\dots (2-54)$$

$$(-\frac{dE}{dx})_{HIGH} = [(243 - 0.375Z_2)Z_2/E] \ln[1 + (A_2/E) + (4 m_e E/m_p I)] \dots\dots\dots(2-55).$$

A₁ is critical in attempting to interpolate stopping to unmeasured elements. The obvious basis for interpolation would be calculated for protons such as the ones Pietsch, Hauser, and Neuwirth have performed for lithium projectiles in various targets. However, the calculations show that this approach is not valid for hydrogen projectiles. In the absence of theoretical guidance. They note that the empirically determined values of A₁ showed a structure similar to the structure seen in the helium stopping power at 400 KeV in the semi-empirical tables of Ziegler and Chu. The parameter A₃ (eq. 2-43) and (2-51) was found by linear interpolation between experimentally determined values. It appears that the calculated stopping powers are very insensitive to the value of A₃. Finally small adjustments were made to A₂, for elements where considerable data exists and it was desired to make a very accurate fitted curve. The low-energy formula is simple and may easily be evaluated on a pocket calculator. That should not lead users into the temptation to use the formula for elements which have detailed experimental values at very high energies. The E⁻¹ dependence of eq. (2-43) does not asymptotically fit the β⁻² dependence of eq. (2-45). Hence, if high precision is needed, the high-energy formula (Bethe formula) must be used above 1 MeV. The fit is considered to be accurate to about 5% at 500 KeV. At lower energies the accuracy deteriorates. For elements where many experimental data exist, the accuracy is still approximately 10% at 10 KeV but some of the interpolated results may only be good to 20% [100].

As the equations :

(Energy: 1-10 KeV)

$$\text{Stopping} = A_1 E^{1/2} \quad \text{eV}/(10^{15} \text{ atoms/cm}^2) \dots\dots\dots(2-56).$$

(Energy: 10-999 KeV)

$$\text{Stopping}^{-1} = (S_{\text{LOW}})^{-1} + (S_{\text{HIGH}})^{-1} \quad \text{eV}/(10^{15} \text{ atoms/cm}^2) \dots\dots\dots(2-57).$$

$$S_{\text{LOW}} = A_2 E^{0.45}$$

$$S_{\text{HIGH}} = (A_3/E) \ln [1 + (A_4/E) + (A_5 E)]$$

(Energy: 1000 KeV-100000 KeV)

$$\text{Stopping} = (A_6/\beta^2) \left[\ln \left(\frac{A_7 \beta^2}{1 - \beta^2} \right) - \beta^2 - \sum_{i=0}^4 A_{i+8} (\ln E)^i \right] \quad \text{eV}/(10^{15} \text{ atoms/cm}^2) \dots\dots(2-$$

58)

2-11 SRIM programs

SRIM is a group of programs which calculate the stopping and range of ions (10 eV - 2 GeV /amu) into matter using a quantum mechanical treatment of ion-atom collisions (they always refer to the moving atom as an "ion" and all target atoms as "atoms"). During collisions, the ion and atom have a screened Coulomb collision, including exchange and correlation interactions between the overlapping electron shells. The ion also has long range interactions with target atoms creating electron excitations and plasmons within the target. These are described by including a description of the target's collective electronic structure and interatomic bond structure when the calculation is setup. The charge state of the ion within the target is described using the concept of effective charge, which includes a velocity dependent charge state and long range screening due to the collective electron sea of the target [101]. It has been continuously upgraded since its introduction in 1985. A recent textbook "SRIM – The Stopping and Range of Ions in Matter" describes in detail the fundamental physics of the software. Since this time, corrections have been made based on new experimental data. More than 700 scientific citations are made to SRIM every year. Major changes occur in SRIM about every six years. The last major changes were in 1995 and 1998 and 2003. In 1995 a complete overhaul was made of the stopping of relativistic light ions with energies above 1 MeV/u. In 1998, special attention was made to the Barkas Effect and the theoretical stopping of Li ions. In 2010, significant changes were made to correct the stopping of ions in compounds [85]. For SRIM-2013, several bugs corrected, including bugs in Compound Dictionary. No major changes [101]. The Core and Bond (CAB)

approach suggested that stopping powers in compounds can be predicted using the superposition of stopping by atomic “cores” and then adding the stopping corresponding to the bonding electrons. The core stopping would simply follow Bragg’s rule for the atoms of the compound, The chemical bonds of the compound would then contain the necessary stopping correction SRIM uses this CAB approach to generate corrections between Bragg’s rule and compounds containing the common elements in compounds: H, C, N, O, F, S and Cl. These light atoms have the largest bonding effect on stopping power. Heavier atoms are assumed not to contribute anomalously to stopping because of their bonds. Using SRIM, can be the option to use the compound dictionary which contains the chemical bonding information for about 150 common compounds. The compounds with available corrections are shown with a Star symbol, next to the name. When these compounds are selected, SRIM shows the chemical bonding diagram and calculates the best stopping correction. The correction is a variation from unity (1.0 = no correction). Some corrections are quite big: carbon atoms have almost a 4× change in stopping power from single bonds to triple bonds. This large change indicates the importance of making some sort of correction for the stopping of ions in compounds. The CAB corrections that SRIM uses have been extracted from the stopping of H, He, and Li ions in more than 100 compounds, from 162 experiments SRIM correctly predicts the stopping of H and He ions compounds with an accuracy of better than 2% at the peak of their stopping power curve, ~125 KeV/u [85].

Chapter Three

Data Redaction

&

Analysis

3-1 Stopping power calculation

The total mass stopping powers for proton interacting with thirteen organs of the human body are (skin, eye lens, stomach, pancreas, liver, spleen, blood, ovary, testis, prostate, trachea, mammary gland and thyroid) tissue, calculated in the energy region from 1 KeV to 200 MeV using the following methods:-

- 1) Bethe formula.
- 2) Ziegler formula.
- 3) Ziegler and Andreson (Vol.3), [100].
- 4) SRIM software (computer program).
- 5) SRIM software (computer program) dictionary.

3.2 Chemical compositions of the human tissues

Chemical compositions of human tissues are of importance in studying micro-dosimetric distributions in humans irradiated with radiation one may represent human tissues by their atomic compositions (% wt by elements). Chemical compositions of human tissues depend in general on breed, diet, age, sex, health, etc., and they may vary appreciably (5-10%) among individual human beings [28]. Each tissue consists of basic elements are H, C, O, N, and some other elements such as P, S, K, etc. Proton interacts with them, therefore the knowledge of the ratios of these elements is important to calculate the mass stopping power for proton in the tissues as well as the density of the tissue. These percentages and tissues density values are given in table (1-1).

3-3 Stopping power for proton interaction with tissues

a- Bethe formula

Stopping power is calculated for any element in biological model by Bethe formula using eq (2-16) in energy range (1-200) MeV in 5 intervals and it takes into account the ionization potential (I_{ave}), and atomic number (Z) for each element in model, we calculated according to eq.(2-24). Table (3.1) gives the ionization potential for each element considered in this study.

Table (3-1): Ionization potential and atomic numbers of elements considered for human tissue.

No.	Elements	Atomic number	Ionization potential (MeV)
1	Hydrogen (H)	1	6.8560×10^{-5}
2	Carbon (C)	6	1.0039×10^{-4}
3	Nitrogen (N)	7	1.0895×10^{-4}
4	Oxygen (O)	8	1.1769×10^{-4}
5	Sodium (Na)	11	1.4464×10^{-4}
6	Phosphorus (P)	15	1.8155×10^{-4}
7	Sulfur (S)	16	1.9088×10^{-4}
8	Chlorine (Cl)	17	2.0024×10^{-4}
9	Potassium (K)	19	2.1905×10^{-4}
10	Iron (Fe)	26	2.8542×10^{-4}
11	Iodine (I)	53	5.4493×10^{-4}

b- Ziegler formula

The total stopping power of proton interaction with chemical composition in any tissue calculated using eq (2-56), (2-57) and (2-58) in energy range from 0.001-100 MeV tabulated in table (3-3) where A1-A12 are fitting constant which are shown in table (3-2).

Table (3-2): Coefficient for stopping of hydrogen [100].

	H	C	N	O	Na	P	S	CL	K	Fe	I
A1	1.262	2.631	2.954	2.652	2.542	3.232	3.447	5.047	5.151	3.519	7.725
A2	1.440	2.989	3.350	3	2.869	3.647	3.891	5.714	5.833	3.963	8.716
A3	242.600	1445	1683	1920	2628	3561	3792	4023	4482	6065	1.18E+04
A4	1.20E+04	957.200	1900	2000	1854	1560	1219	878.600	545.700	1243	394.800
A5	0.116	0.028	0.025	0.022	0.015	0.013	0.012	0.012	0.011	0.008	0.004
A6	0.001	0.003	0.004	0.004	0.006	0.008	0.008	0.009	0.010	0.013	0.027
A7	5.44E+04	1.32E+04	1.18E+04	1.05E+04	6905	5942	5678	5524	5295	3650	2052
A8	-5.052	-4.380	-5.054	-6.734	-4.959	-6.527	-6.761	-6.994	-7.440	-9.809	-20.560
A9	2.049	2.044	2.325	3.019	2.073	2.616	2.694	2.773	2.923	3.763	7.627
A10	-0.304	-0.328	-0.371	-0.475	-0.305	-0.372	-0.381	-0.391	-0.409	-0.516	-1.019
A11	0.020	0.022	0.025	0.032	0.019	0.023	0.023	0.024	0.025	0.031	0.059
A12	-0.001	-0.001	-0.001	-0.001	-0.000	-0.001	-0.001	-0.001	-0.001	-0.001	-0.001

For energies 1-10KeV/amu use coeff.A1

For energies 10-999 KeV/amu use coeff A2 to A5.

For energies above 1 MeV/amu use coeff.A-6 to A12 (Bethe stopping).

c- Ziegler and Andreson (Vol.3) [100].

The total stopping power for proton interaction with chemical composition in any tissue calculated using Ziegler and Andreson (Vol.3) [100]. Where energy values and stopping values of proton with any element composition of tissue are found in book ref. [100].

d- SRIM program

The total stopping power of proton interaction with chemical composition in tissues organs selected here for energy range (10 KeV-200 MeV) in 1MeV interval is calculated by SRIM program.

e- SRIM dictionary program

The total stopping power of proton interaction with chemical composition in tissues organs selected here (skin, pancreas, spleen, blood, ovary, testis, prostate, trachea, mammary gland, thyroid) tissues, for energy range (10 KeV- 200 MeV) in 1MeV interval is calculated by SRIM program.

3-4 Stopping power for proton interaction with tissues

The Matlab programs have been used to calculate the stopping power of proton interact with (skin, eye lens, stomach, pancreas, liver, spleen, blood, ovary, testis, prostate, trachea, mammary gland and thyroid) tissue, using Bethe and Ziegler formula, Ziegler and Andreson (Vol.3) [100], SRIM and SRIM (dictionary) program. The results are shown in table (3-3) and average stopping power for all methods that have been used in the present work for tissues are shown from table (3-4) to (3- 16) respectively.

Table (3-3): The total stopping power for proton interacts with the composition of tissues.

Stopping power for proton interacts with the composition of tissues in (MeV-cm ² /g)											
Bethe formula											
E _P (MeV)	¹ ₁ H	¹² ₆ C	¹⁴ ₇ N	¹⁵ ₈ O	²² ₁₁ Na	³⁰ ₁₅ P	³² ₁₆ S	³⁵ ₁₇ Cl	³⁹ ₉ K	⁵⁶ ₂₆ Fe	¹²⁷ ₅₃ I
0.001	-	-	-	-	-	-	-	-	-	-	-
1	494.083	221.344	215.552	210.108	186.848	173.267	174.922	164.795	160.727	136.243	83.324
2	420.258	188.745	183.920	179.386	159.818	148.550	150.056	141.450	138.115	117.537	73.028
3	346.432	156.145	152.288	148.664	132.788	123.834	125.190	118.105	115.503	98.832	62.731
4	272.606	123.546	120.656	117.941	105.758	99.118	100.324	94.759	92.892	80.126	52.434
5	198.780	90.947	89.024	87.219	78.727	74.401	75.458	71.414	70.280	61.421	42.137
6	125.019	58.376	57.420	56.523	51.720	49.706	50.614	48.089	47.688	42.730	31.849
7	115.227	53.861	52.993	52.178	47.777	45.956	46.804	44.478	44.124	39.585	29.616
8	105.436	49.347	48.565	47.833	43.835	42.205	42.994	40.867	40.559	36.439	27.383
9	95.644	44.832	44.138	43.488	39.892	38.455	39.185	37.256	36.995	33.293	25.151
10	85.853	40.318	39.711	39.142	35.949	34.704	35.375	33.645	33.431	30.147	22.918
15	59.730	28.204	27.815	27.450	25.299	24.525	25.023	23.822	23.714	21.509	16.642
20	46.526	22.038	21.750	21.480	19.835	19.274	19.677	18.742	18.676	16.995	13.277
25	38.378	18.218	17.989	17.774	16.436	15.997	16.337	15.567	15.522	14.156	11.132
30	32.797	15.594	15.404	15.226	14.094	13.734	14.030	13.372	13.341	12.187	9.629
35	28.713	13.671	13.508	13.356	12.373	12.068	12.331	11.755	11.733	10.732	8.512
40	25.585	12.195	12.052	11.919	11.050	10.786	11.023	10.511	10.494	9.609	7.645
45	23.107	11.024	10.897	10.779	9.998	9.767	9.983	9.520	9.508	8.714	6.950
50	21.091	10.070	9.956	9.850	9.141	8.934	9.133	8.711	8.702	7.982	6.380
60	18.003	8.607	8.512	8.424	7.824	7.654	7.827	7.466	7.462	6.853	5.498
70	15.742	7.534	7.453	7.378	6.857	6.713	6.865	6.550	6.548	6.020	4.844
80	14.011	6.711	6.641	6.575	6.114	5.990	6.126	5.846	5.846	5.379	4.338
90	12.640	6.059	5.996	5.938	5.524	5.415	5.539	5.286	5.287	4.868	3.935
100	11.526	5.529	5.472	5.419	5.044	4.946	5.060	4.830	4.832	4.452	3.604
150	8.069	3.880	3.842	3.807	3.548	3.486	3.567	3.406	3.410	3.149	2.565
200	-	-	-	-	-	-	-	-	-	-	-

Table (3-3)..... cont..

Stopping power for proton interacts with the composition of tissues in (MeV-cm ² /g)											
Ziegler formula											
E _p (MeV)	¹ ₁ H	¹² ₆ C	¹⁴ ₇ N	¹⁵ ₈ O	²² ₁₁ Na	³⁰ ₁₅ P	³² ₁₆ S	³⁵ ₁₇ Cl	³⁹ ₉ K	⁵⁶ ₂₆ Fe	¹²⁷ ₅₃ I
0.001	754.115	131.933	127.024	99.835	66.597	62.848	64.746	85.743	79.350	37.953	36.664
1	679.281	229.815	224.360	213.698	176.577	168.498	169.874	165.051	161.971	130.216	88.931
2	408.763	146.986	142.738	137.649	117.488	112.854	114.555	108.763	109.014	90.491	59.581
3	293.023	108.898	106.081	102.724	88.464	85.366	86.780	82.476	82.733	69.788	47.419
4	230.781	87.495	85.394	82.911	71.797	69.499	70.716	67.253	67.504	57.515	39.942
5	197.505	75.641	73.898	71.849	62.402	60.512	61.603	58.607	58.847	50.407	35.442
6	164.245	63.793	62.407	60.792	53.012	51.529	52.493	49.965	50.194	43.301	30.944
7	146.482	57.266	56.057	54.656	47.758	46.479	47.365	45.095	45.312	39.226	28.265
8	128.726	50.742	49.711	48.523	42.507	41.430	42.237	40.226	40.433	35.152	25.587
9	117.572	46.563	45.637	44.575	39.108	38.153	38.906	37.059	37.257	32.472	23.780
10	106.424	42.387	41.566	40.630	35.712	34.877	35.576	33.895	34.084	29.795	21.974
15	82.487	33.170	32.557	31.865	28.108	27.505	28.071	26.755	26.916	23.654	17.673
20	58.546	23.952	23.547	23.099	20.502	20.132	20.565	19.614	19.747	17.512	13.371
25	49.824	20.492	20.155	19.784	17.598	17.300	17.677	16.864	16.983	15.104	11.612
30	41.102	17.031	16.762	16.469	14.695	14.469	14.790	14.114	14.218	12.696	9.853
35	36.514	15.183	14.948	14.692	13.131	12.938	13.228	12.625	12.721	11.381	8.871
40	31.926	13.336	13.134	12.916	11.566	11.408	11.666	11.137	11.223	10.065	7.890
45	29.525	12.356	12.171	11.971	10.730	10.588	10.829	10.338	10.420	9.354	7.349
50	27.123	11.376	11.208	11.027	9.895	9.767	9.991	9.539	9.616	8.642	6.809
60	22.319	9.417	9.283	9.138	8.223	8.127	8.316	7.942	8.008	7.220	5.728
70	19.807	8.381	8.263	8.136	7.332	7.251	7.421	7.088	7.147	6.454	5.137
80	17.294	7.344	7.243	7.134	6.441	6.375	6.525	6.233	6.287	5.687	4.546
90	15.739	6.698	6.607	6.509	5.883	5.825	5.963	5.697	5.746	5.204	4.169
100	14.184	6.052	5.971	5.883	5.325	5.275	5.401	5.160	5.206	4.721	3.793
150	-	-	-	-	-	-	-	-	-	-	-
200	-	-	-	-	-	-	-	-	-	-	-

Table (3-3)..... cont..

Stopping power for proton interacts with the composition of tissues in (MeV-cm ² /g)											
Ref. [100]											
E _p (MeV)	¹ ₁ H	¹² ₆ C	¹⁴ ₇ N	¹⁵ ₈ O	²² ₁₁ Na	³⁰ ₁₅ P	³² ₁₆ S	³⁵ ₁₇ Cl	³⁹ ₉ K	⁵⁶ ₂₆ Fe	¹²⁷ ₅₃ I
0.001	752.920	131.883	126.852	99.760	66.545	62.809	64.802	85.794	79.335	37.964	36.640
1	680.921	229.078	220.940	211.486	177.562	169.309	171.241	162.865	163.232	131.535	85.877
2	388.899	140.873	136.707	131.725	112.626	108.285	109.855	104.626	104.727	87.124	58.839
3	278.999	104.283	101.462	98.235	84.868	81.850	83.194	79.323	79.320	67.072	46.647
4	219.869	83.732	81.690	79.421	68.893	66.689	67.798	64.549	64.692	55.214	39.198
5	188.497	72.449	70.725	68.880	59.855	58.036	59.064	56.310	56.450	48.419	34.761
6	157.140	61.172	59.765	58.344	50.820	49.387	50.334	48.074	48.212	41.627	30.325
7	140.110	54.954	53.745	52.509	45.843	44.623	45.450	43.402	43.514	37.690	27.691
8	123.086	48.738	47.727	46.676	40.867	39.860	40.568	38.732	38.817	33.755	25.058
9	112.629	44.751	43.857	42.912	37.592	36.749	37.375	35.674	35.813	31.221	23.302
10	102.178	40.767	39.989	39.149	34.319	33.639	34.184	32.617	32.811	28.688	21.546
15	79.565	32.043	31.455	30.813	27.142	26.640	27.142	25.908	26.034	22.865	17.371
20	56.947	23.318	22.919	22.474	19.963	19.640	20.098	19.197	19.256	17.041	13.194
25	48.731	20.058	19.716	19.350	17.226	16.957	17.337	16.573	16.637	14.776	11.509
30	40.514	16.799	16.512	16.225	14.488	14.273	14.576	13.948	14.018	12.511	9.824
35	36.212	15.069	14.814	14.569	13.021	12.834	13.111	12.546	12.617	11.276	8.899
40	31.910	13.339	13.115	12.912	11.554	11.395	11.646	11.145	11.215	10.041	7.973
45	29.654	12.424	12.212	12.028	10.774	10.627	10.866	10.397	10.464	9.378	7.463
50	27.398	11.508	11.309	11.143	9.995	9.859	10.087	9.650	9.713	8.714	6.953
60	22.886	9.678	9.503	9.374	8.436	8.323	8.528	8.155	8.211	7.388	5.933
70	20.556	8.700	8.557	8.433	7.598	7.506	7.692	7.356	7.410	6.676	5.387
80	18.225	7.722	7.611	7.491	6.759	6.689	6.856	6.558	6.609	5.964	4.841
90	16.761	7.121	7.031	6.908	6.248	6.184	6.339	6.065	6.108	5.517	4.483
100	15.297	6.519	6.450	6.324	5.738	5.678	5.823	5.572	5.607	5.069	4.124
150	-	-	-	-	-	-	-	-	-	-	-
200	-	-	-	-	-	-	-	-	-	-	-

Table (3-3)..... cont..

Stopping power for proton interacts with the composition of tissues in (MeV-cm ² /g)											
SRIM program											
E _p (MeV)	¹ ₁ H	¹² ₆ C	¹⁴ ₇ N	¹⁵ ₈ O	²² ₁₁ Na	³⁰ ₁₅ P	³² ₁₆ S	³⁵ ₁₇ Cl	³⁹ ₉ K	⁵⁶ ₂₆ Fe	¹²⁷ ₅₃ I
0.001	-	-	-	-	-	-	-	-	-	-	-
1	637.712	230.323	207.676	202.467	178.830	172.432	174.434	156.968	168.329	132.037	80.657
2	403.829	142.036	139.436	134.736	113.234	109.735	110.838	108.533	106.834	87.303	59.916
3	286.090	105.233	103.633	100.333	85.140	82.710	83.682	82.078	80.689	67.167	47.530
4	223.762	84.520	83.260	80.780	69.117	67.236	68.108	66.715	65.696	55.323	39.877
5	185.038	71.117	70.076	68.096	58.603	57.073	57.875	56.622	55.833	47.400	34.635
6	158.421	61.654	60.773	59.123	51.121	49.830	50.562	49.430	48.790	41.668	30.783
7	138.908	54.582	53.821	52.411	45.479	44.369	45.050	44.008	43.478	37.316	27.812
8	123.997	49.090	48.419	47.179	41.067	40.097	40.728	39.766	39.317	33.875	25.431
9	112.188	44.678	44.078	42.988	37.506	36.646	37.236	36.345	35.955	31.073	23.480
10	102.581	41.057	40.517	39.526	34.575	33.804	34.355	33.524	33.174	28.752	21.839
15	72.721	29.594	29.224	28.573	25.182	24.682	25.112	24.481	24.271	21.230	16.437
20	56.997	23.421	23.150	22.650	20.059	19.699	20.060	19.539	19.399	17.068	13.366
25	47.208	19.539	19.319	18.918	16.807	16.527	16.838	16.397	16.287	14.386	11.365
30	40.513	16.857	16.667	16.337	14.546	14.316	14.597	14.206	14.126	12.515	9.939
35	35.618	14.876	14.716	14.426	12.876	12.685	12.936	12.585	12.515	11.115	8.873
40	31.885	13.366	13.216	12.966	11.585	11.425	11.655	11.335	11.275	10.034	8.041
45	28.932	12.155	12.035	11.805	10.564	10.424	10.635	10.344	10.294	9.173	7.373
50	26.540	11.175	11.065	10.865	9.729	9.603	9.796	9.528	9.486	8.465	6.823
60	22.887	9.679	9.582	9.411	8.444	8.342	8.513	8.278	8.245	7.374	5.969
70	20.225	8.581	8.497	8.349	7.502	7.416	7.569	7.360	7.334	6.569	5.336
80	18.203	7.742	7.669	7.537	6.780	6.706	6.846	6.656	6.634	5.949	4.847
90	16.612	7.079	7.014	6.895	6.208	6.142	6.271	6.097	6.078	5.457	4.457
100	15.321	6.540	6.481	6.373	5.743	5.684	5.805	5.643	5.627	5.057	4.137
150	11.367	4.882	4.843	4.767	4.307	4.267	4.360	4.237	4.228	3.810	3.141
200	9.335	4.024	3.996	3.935	3.561	3.530	3.607	3.508	3.502	3.159	2.618

Table (3-4) Stopping power for proton in skin tissues in (MeV-cm²/g).

Stopping power for proton in skin tissues in (MeV-cm ² /g).						
E _p (MeV)	Stopping power					Present work
	Bethe	Ziegler	Ref. [100]	SRIM	SRIM (dictionary)	S.P (P.W)
0.001	-	172.717	172.531	-	-	172.624
1	240.687	263.587	262.031	251.589	251.702	253.924
2	205.289	166.652	159.304	163.110	163.156	171.507
3	169.891	122.996	117.532	119.891	119.949	130.053
4	134.492	98.615	94.324	95.826	95.853	103.823
5	99.094	85.171	81.549	80.392	80.407	85.323
6	63.726	71.733	68.779	69.557	69.573	68.674
7	58.804	64.356	61.748	61.492	61.520	61.584
8	53.881	56.981	54.720	55.241	55.267	55.218
9	48.959	52.267	50.242	50.243	50.255	50.393
10	44.037	47.555	45.766	46.135	46.153	45.929
15	30.821	37.183	35.927	33.189	33.198	34.064
20	24.090	26.809	26.087	26.237	26.244	25.893
25	19.918	22.925	22.426	21.870	21.882	21.804
30	17.052	19.041	18.765	18.857	18.860	18.515
35	14.950	16.969	16.830	16.634	16.638	16.404
40	13.337	14.898	14.894	14.936	14.938	14.601
45	12.057	13.801	13.866	13.587	13.587	13.380
50	11.015	12.704	12.838	12.493	12.496	12.309
60	9.416	10.510	10.783	10.811	10.815	10.467
70	8.243	9.350	9.696	9.582	9.585	9.291
80	7.344	8.191	8.610	8.644	8.646	8.287
90	6.630	7.468	7.935	7.902	7.905	7.568
100	6.050	6.746	7.261	7.301	7.302	6.884
150	4.247	-	-	5.449	5.450	5.049
200	-	-	-	4.492	4.494	-

Table (3-5) Stopping power for proton in eye lens tissues in (MeV-cm²/g).

Stopping power for proton in eye lens tissues in (MeV-cm ² /g).					
E _p (MeV)	Stopping power				Present work
	Bethe	Ziegler	Ref.[100]	SRIM	S.P (P.W)
0.001	-	170.265	170.082	-	170.174
1	239.660	261.882	260.276	249.796	252.906
2	204.417	165.643	158.346	162.116	172.633
3	169.173	122.288	116.858	119.208	131.883
4	133.930	98.065	93.801	95.299	105.274
5	98.686	84.703	81.103	79.962	86.114
6	63.473	71.348	68.410	69.191	68.106
7	58.571	64.014	61.421	61.173	61.295
8	53.669	56.683	54.435	54.957	54.936
9	48.766	51.995	49.982	49.987	50.182
10	43.864	47.310	45.532	45.902	45.652
15	30.701	36.994	35.746	33.026	34.117
20	23.997	26.677	25.958	26.110	25.685
25	19.841	22.813	22.316	21.765	21.684
30	16.987	18.949	18.674	18.767	18.344
35	14.893	16.888	16.748	16.555	16.271
40	13.286	14.827	14.822	14.866	14.450
45	12.012	13.735	13.800	13.523	13.267
50	10.973	12.643	12.777	12.434	12.207
60	9.380	10.460	10.732	10.761	10.333
70	8.212	9.306	9.651	9.538	9.177
80	7.316	8.152	8.569	8.604	8.160
90	6.605	7.434	7.898	7.866	7.451
100	6.027	6.715	7.227	7.267	6.647
150	4.231	-	-	5.424	4.828
200	-	-	-	4.472	-

Table (3-6) Stopping power for proton in stomach tissues in (MeV-cm²/g).

Stopping power for proton in stomach tissues in (MeV-cm ² /g).					
E _p (MeV)	Stopping power				Present work
	Bethe	Ziegler	Ref.[100]	SRIM	S.P (P.W)
0.001	-	172.935	172.744	-	172.840
1	241.086	264.346	262.725	251.038	254.801
2	205.639	167.113	159.719	163.374	173.964
3	170.192	123.347	117.852	120.061	132.864
4	134.745	98.903	94.602	95.949	106.050
5	99.298	85.423	81.793	80.490	86.751
6	63.881	71.949	68.990	69.638	68.615
7	58.948	64.552	61.939	61.563	61.750
8	54.014	57.157	54.891	55.302	55.341
9	49.081	52.429	50.401	50.299	50.553
10	44.148	47.703	45.914	46.186	45.988
15	30.902	37.301	36.043	33.226	34.368
20	24.154	26.896	26.170	26.265	25.871
25	19.972	23.000	22.498	21.893	21.841
30	17.099	19.103	18.826	18.877	18.476
35	14.992	17.025	16.884	16.652	16.388
40	13.375	14.947	14.943	14.952	14.554
45	12.091	13.846	13.911	13.601	13.363
50	11.046	12.746	12.880	12.507	12.295
60	9.443	10.545	10.818	10.823	10.407
70	8.267	9.381	9.728	9.593	9.242
80	7.365	8.218	8.638	8.653	8.218
90	6.650	7.493	7.961	7.911	7.504
100	6.068	6.768	7.284	7.309	6.688
150	4.259	-	-	5.455	4.857
200	-	-	-	4.498	-

Table (3-7) Stopping power for proton in pancreas tissues in (MeV-cm²/g).

Stopping power for proton in pancreas tissues in (MeV-cm ² /g).						
E _p (MeV)	Stopping power					Present work
	Bethe	Ziegler	Ref. [100]	SRIM	SRIM dictionary	S.P (P.W)
0.001	-	174.967	174.776	-	-	174.871
1	241.883	265.599	264.041	253.130	253.307	255.596
2	206.311	167.849	160.426	164.372	164.457	172.688
3	170.739	123.853	118.339	120.766	120.849	130.911
4	135.167	99.291	94.970	96.501	96.554	104.497
5	99.595	85.750	82.104	80.947	80.988	85.877
6	64.053	72.215	69.244	70.030	70.074	69.123
7	59.106	64.787	62.163	61.906	61.951	61.982
8	54.158	57.360	55.084	55.609	55.648	55.572
9	49.211	52.613	50.576	50.576	50.605	50.716
10	44.263	47.869	46.071	46.439	46.473	46.223
15	30.980	37.427	36.164	33.405	33.419	34.279
20	24.214	26.983	26.255	26.406	26.424	26.056
25	20.021	23.073	22.570	22.009	22.022	21.939
30	17.141	19.163	18.885	18.977	18.980	18.629
35	15.028	17.078	16.937	16.739	16.749	16.506
40	13.407	14.993	14.989	15.030	15.038	14.691
45	12.120	13.889	13.954	13.672	13.677	13.462
50	11.073	12.784	12.920	12.572	12.576	12.385
60	9.465	10.576	10.851	10.879	10.885	10.531
70	8.286	9.409	9.757	9.642	9.648	9.348
80	7.382	8.242	8.664	8.698	8.702	8.337
90	6.665	7.515	7.984	7.952	7.956	7.614
100	6.082	6.788	7.305	7.346	7.350	6.926
150	4.269	-	-	5.483	5.485	5.079
200	-	-	-	4.520	4.523	-

Table (3-8) Stopping power for proton in liver tissues in (MeV-cm²/g).

Stopping power for proton in liver tissues in (MeV-cm ² /g).					
E _p (MeV)	Stopping power				Present work
	Bethe	Ziegler	Ref.[100]	SRIM	S.P (P.W)
0.001	-	171.477	171.289	-	171.383
1	240.297	263.154	261.540	250.475	253.869
2	204.972	166.425	159.068	163.014	173.373
3	169.647	122.865	117.395	119.831	132.436
4	134.322	98.529	94.246	95.783	105.720
5	98.998	85.105	81.490	80.361	86.489
6	63.703	71.688	68.740	69.533	68.416
7	58.784	64.320	61.718	61.474	61.574
8	53.866	56.955	54.698	55.226	55.186
9	48.947	52.245	50.225	50.232	50.412
10	44.028	47.538	45.755	46.127	45.862
15	30.820	37.174	35.921	33.188	34.275
20	24.091	26.808	26.084	26.238	25.805
25	19.921	22.925	22.425	21.872	21.785
30	17.055	19.042	18.766	18.860	18.431
35	14.953	16.971	16.831	16.637	16.348
40	13.341	14.900	14.896	14.939	14.519
45	12.061	13.803	13.868	13.590	13.330
50	11.018	12.706	12.840	12.496	12.265
60	9.419	10.512	10.785	10.814	10.383
70	8.246	9.353	9.698	9.585	9.221
80	7.346	8.193	8.612	8.647	8.200
90	6.633	7.471	7.937	7.905	7.487
100	6.053	6.748	7.262	7.304	6.678
150	4.249	-	-	5.452	4.850
200	-	-	-	4.495	-

Table (3-9) Stopping power for proton in spleen tissues in (MeV-cm²/g).

Stopping power for proton in spleen tissues in (MeV-cm ² /g).						
E _p (MeV)	Stopping power					Present work
	Bethe	Ziegler	Ref.[100]	SRIM	SRIM (dictionary)	S.P (P.W)
0.001	-	171.419	171.229	-	-	171.324
1	240.358	263.302	261.645	249.429	250.307	253.012
2	205.028	166.507	159.138	162.610	163.157	171.293
3	169.697	122.931	117.453	119.522	119.949	129.912
4	134.367	98.586	94.301	95.527	95.873	103.731
5	99.036	85.156	81.539	80.142	80.428	85.261
6	63.736	71.733	68.784	69.341	69.593	68.638
7	58.815	64.361	61.758	61.303	61.540	61.555
8	53.894	56.992	54.735	55.071	55.287	55.196
9	48.973	52.280	50.260	50.090	50.275	50.376
10	44.052	47.570	45.788	45.996	46.173	45.916
15	30.838	37.199	35.946	33.092	33.218	34.059
20	24.106	26.827	26.103	26.161	26.264	25.892
25	19.933	22.942	22.441	21.807	21.892	21.803
30	17.066	19.056	18.779	18.804	18.870	18.515
35	14.963	16.984	16.843	16.587	16.659	16.407
40	13.349	14.911	14.907	14.894	14.958	14.604
45	12.069	13.813	13.878	13.549	13.607	13.383
50	11.026	12.716	12.850	12.459	12.506	12.311
60	9.425	10.520	10.792	10.782	10.825	10.469
70	8.252	9.360	9.705	9.557	9.595	9.294
80	7.351	8.199	8.618	8.621	8.655	8.289
90	6.638	7.476	7.943	7.881	7.913	7.570
100	6.057	6.753	7.267	7.282	7.311	6.883
150	4.252	-	-	5.435	5.457	5.048
200	-	-	-	4.482	4.500	-

Table (3-10) Stopping power for proton in blood tissues in (MeV-cm²/g).

Stopping power for proton in blood tissues in (MeV-cm ² /g).						
E _p (MeV)	Stopping power					Present work
	Bethe	Ziegler	Ref.[100]	SRIM	SRIM (dictionary)	S.P (P.W)
0.001	-	170.714	170.525	-	-	170.620
1	240.050	262.809	261.137	248.773	249.908	252.539
2	204.766	166.215	158.861	162.239	162.956	171.012
3	169.483	122.727	117.259	119.260	119.849	129.718
4	134.200	98.428	94.151	95.322	95.783	103.577
5	98.916	85.022	81.412	79.972	80.358	85.136
6	63.663	71.623	68.679	69.195	69.533	68.539
7	58.748	64.263	61.665	61.175	61.480	61.466
8	53.833	56.907	54.654	54.957	55.237	55.118
9	48.918	52.202	50.186	49.987	50.235	50.306
10	44.003	47.500	45.721	45.901	46.133	45.852
15	30.803	37.146	35.894	33.025	33.188	34.011
20	24.079	26.790	26.066	26.108	26.244	25.857
25	19.911	22.910	22.410	21.763	21.872	21.773
30	17.047	19.030	18.753	18.766	18.860	18.491
35	14.947	16.961	16.820	16.554	16.639	16.384
40	13.335	14.891	14.887	14.864	14.938	14.583
45	12.056	13.795	13.860	13.522	13.597	13.366
50	11.014	12.699	12.832	12.434	12.496	12.295
60	9.415	10.506	10.778	10.760	10.815	10.455
70	8.243	9.347	9.692	9.538	9.587	9.281
80	7.344	8.189	8.607	8.604	8.648	8.278
90	6.631	7.467	7.932	7.866	7.907	7.560
100	6.051	6.745	7.258	7.267	7.305	6.874
150	4.247	-	-	5.425	5.452	5.041
200	-	-	-	4.473	4.496	-

Table (3-11) Stopping power for proton in ovary tissues in (MeV-cm²/g).

Stopping power for proton in ovary tissues in (MeV-cm ² /g).						
E _p (MeV)	Stopping power					Present work
	Bethe	Ziegler	Ref.[100]	SRIM	SRIM (dictionary)	S.P (P.W)
0.001	-	171.892	171.700	-	-	171.796
1	240.721	263.886	262.213	250.561	250.710	253.622
2	205.339	166.855	159.461	163.534	163.657	171.774
3	169.956	123.185	117.690	120.197	120.249	130.257
4	134.574	98.788	94.494	96.066	96.124	104.010
5	99.192	85.330	81.707	80.594	80.638	85.493
6	63.840	71.879	68.925	69.733	69.774	68.830
7	58.911	64.492	61.885	61.650	61.690	61.726
8	53.982	57.108	54.847	55.383	55.428	55.349
9	49.053	52.386	50.363	50.375	50.405	50.516
10	44.125	47.666	45.882	46.257	46.293	46.044
15	30.889	37.275	36.019	33.281	33.298	34.152
20	24.146	26.881	26.155	26.311	26.324	25.963
25	19.966	22.988	22.485	21.933	21.942	21.863
30	17.094	19.094	18.816	18.912	18.920	18.567
35	14.988	17.018	16.876	16.683	16.699	16.453
40	13.372	14.941	14.936	14.980	14.988	14.643
45	12.089	13.841	13.906	13.628	13.637	13.420
50	11.044	12.741	12.875	12.532	12.536	12.346
60	9.441	10.541	10.814	10.844	10.845	10.497
70	8.266	9.378	9.724	9.612	9.618	9.320
80	7.364	8.215	8.635	8.671	8.676	8.312
90	6.649	7.491	7.958	7.928	7.932	7.591
100	6.067	6.767	7.281	7.324	7.328	6.907
150	4.259	-	-	5.467	5.469	5.065
200	-	-	-	4.508	4.510	-

Table (3-12) Stopping power for proton in testis tissues in (MeV-cm²/g).

Stopping power for proton in testis tissues in (MeV-cm ² /g).						
E _p (MeV)	Stopping power					Present work
	Bethe	Ziegler	Ref. [100]	SRIM	SRIM dictionary	S.P (P.W)
0.001	-	172.667	172.475	-	-	172.571
1	241.087	264.451	262.793	250.522	251.309	254.036
2	205.648	167.187	159.777	163.422	163.857	171.983
3	170.209	123.416	117.910	120.091	120.450	130.417
4	134.770	98.967	94.664	95.970	96.274	104.130
5	99.331	85.482	81.851	80.508	80.758	85.586
6	63.922	72.003	69.044	69.653	69.874	68.899
7	58.987	64.602	61.990	61.577	61.780	61.787
8	54.052	57.203	54.939	55.315	55.498	55.401
9	49.116	52.473	50.446	50.311	50.475	50.564
10	44.181	47.745	45.956	46.197	46.353	46.086
15	30.927	37.335	36.077	33.235	33.339	34.182
20	24.175	26.923	26.195	26.273	26.364	25.986
25	19.990	23.023	22.520	21.900	21.972	21.881
30	17.115	19.123	18.845	18.883	18.940	18.581
35	15.006	17.043	16.902	16.657	16.719	16.465
40	13.388	14.963	14.959	14.957	15.008	14.655
45	12.103	13.861	13.926	13.606	13.657	13.431
50	11.057	12.760	12.894	12.512	12.546	12.354
60	9.452	10.556	10.829	10.827	10.865	10.506
70	8.275	9.392	9.738	9.597	9.630	9.326
80	7.372	8.227	8.647	8.657	8.686	8.318
90	6.657	7.502	7.969	7.914	7.941	7.597
100	6.074	6.776	7.292	7.312	7.337	6.908
150	4.264	-	-	5.458	5.476	5.066
200	-	-	-	4.500	4.516	-

Table (3-13) Stopping power for proton in prostate tissues in (MeV-cm²/g).

Stopping power for proton in prostate tissues in (MeV-cm ² /g).						
E _p (MeV)	Stopping power					Present work
	Bethe	Ziegler	Ref. [100]	SRIM	SRIM dictionary	S.P (P.W)
0.001	-	171.856	171.664	-	-	171.760
1	240.809	263.974	262.292	250.239	250.609	253.588
2	205.412	166.905	159.507	163.373	163.557	171.756
3	170.016	123.221	117.723	120.074	120.249	130.259
4	134.619	98.817	94.522	95.964	96.094	104.004
5	99.223	85.355	81.730	80.507	80.618	85.487
6	63.857	71.899	68.945	69.655	69.753	68.822
7	58.927	64.510	61.902	61.580	61.680	61.720
8	53.996	57.124	54.863	55.320	55.408	55.342
9	49.066	52.400	50.377	50.317	50.395	50.511
10	44.136	47.679	45.894	46.203	46.273	46.037
15	30.896	37.285	36.029	33.241	33.288	34.148
20	24.151	26.888	26.161	26.279	26.324	25.961
25	19.971	22.994	22.491	21.906	21.942	21.860
30	17.098	19.099	18.821	18.888	18.910	18.563
35	14.991	17.022	16.880	16.662	16.689	16.449
40	13.375	14.945	14.940	14.961	14.988	14.642
45	12.092	13.844	13.909	13.610	13.637	13.418
50	11.047	12.744	12.878	12.516	12.536	12.344
60	9.443	10.543	10.816	10.830	10.845	10.496
70	8.267	9.380	9.726	9.600	9.616	9.318
80	7.365	8.217	8.637	8.660	8.674	8.311
90	6.650	7.493	7.960	7.917	7.930	7.590
100	6.069	6.768	7.283	7.315	7.326	6.903
150	4.260	-	-	5.460	5.468	5.063
200	-	-	-	4.502	4.509	-

Table (3-14) Stopping power for proton in trachea tissues in (MeV-cm²/g).

Stopping power for proton in trachea tissues in (MeV-cm ² /g).						
E _p (MeV)	Stopping power					Present work
	Bethe	Ziegler	Ref.[100]	SRIM	SRIM (dictionary)	S.P (P.W)
0.001	-	170.859	170.672	-	-	170.765
1	239.977	262.665	261.051	249.202	250.105	252.604
2	204.701	166.142	158.800	162.194	162.756	170.923
3	169.425	122.666	117.206	119.230	119.649	129.637
4	134.150	98.374	94.099	95.302	95.663	103.518
5	98.874	84.974	81.365	79.957	80.257	85.086
6	63.629	71.580	68.636	69.183	69.453	68.497
7	58.716	64.224	61.626	61.165	61.410	61.428
8	53.803	56.871	54.618	54.948	55.167	55.082
9	48.891	52.169	50.152	49.979	50.175	50.273
10	43.978	47.469	45.689	45.894	46.083	45.823
15	30.785	37.121	35.870	33.020	33.148	33.989
20	24.064	26.771	26.048	26.105	26.214	25.841
25	19.899	22.894	22.394	21.761	21.852	21.760
30	17.036	19.017	18.740	18.764	18.840	18.479
35	14.937	16.949	16.808	16.552	16.618	16.373
40	13.326	14.880	14.876	14.863	14.928	14.575
45	12.048	13.785	13.850	13.521	13.577	13.356
50	11.007	12.690	12.823	12.433	12.476	12.286
60	9.409	10.499	10.771	10.759	10.805	10.449
70	8.237	9.341	9.686	9.536	9.577	9.275
80	7.339	8.183	8.601	8.603	8.638	8.273
90	6.626	7.461	7.927	7.865	7.898	7.555
100	6.046	6.740	7.253	7.266	7.296	6.870
150	4.244	-	-	5.424	5.446	5.038
200	-	-	-	4.472	4.491	-

Table (3-15) Stopping power for proton in mammary gland in (MeV-cm²/g).

Stopping power for proton in mammary gland in (MeV-cm ² /g).						
E _p (MeV)	Stopping power					Present work
	Bethe	Ziegler	Ref.[100]	SRIM	SRIM (dictionary)	S.P (P.W)
0.001	-	187.899	187.713	-	-	187.800
1	246.731	272.672	271.608	263.839	263.993	263.780
2	210.363	171.945	164.409	167.664	167.757	176.444
3	173.995	126.600	121.009	122.986	123.050	133.518
4	137.627	101.353	96.914	98.196	98.254	106.471
5	101.258	87.467	83.725	82.318	82.369	87.424
6	64.921	73.588	70.542	71.180	71.224	70.282
7	59.897	65.986	63.292	62.895	62.941	63.004
8	54.873	58.388	56.046	56.481	56.518	56.473
9	49.849	53.537	51.439	51.350	51.386	51.515
10	44.825	48.689	46.835	47.141	47.174	46.927
15	31.347	38.042	36.748	33.877	33.899	34.785
20	24.490	27.393	26.658	26.765	26.784	26.428
25	20.243	23.415	22.910	22.300	22.312	22.241
30	17.326	19.437	19.162	19.221	19.230	18.875
35	15.188	17.318	17.180	16.951	16.969	16.722
40	13.547	15.199	15.198	15.219	15.228	14.879
45	12.245	14.078	14.148	13.839	13.847	13.631
50	11.186	12.957	13.099	12.720	12.726	12.536
60	9.560	10.715	11.000	11.007	11.015	10.656
70	8.368	9.531	9.889	9.754	9.761	9.456
80	7.454	8.347	8.778	8.797	8.803	8.431
90	6.729	7.610	8.090	8.041	8.047	7.703
100	6.140	6.873	7.401	7.427	7.433	7.000
150	4.308	-	-	5.540	5.543	5.130
200	-	-	-	4.565	4.569	-

Table (3-16) Stopping power for proton in thyroid in (MeV-cm²/g).

Stopping power for proton in thyroid in (MeV-cm ² /g).						
E _p (MeV)	Stopping power					Present work
	Bethe	Ziegler	Ref.[100]	SRIM	SRIM (dictionary)	S.P (P.W)
0.001	-	172.102	171.911	-	-	172.007
1	240.724	263.855	262.206	250.820	251.207	253.767
2	205.336	166.825	159.441	163.456	163.657	171.748
3	169.948	123.153	117.665	120.140	120.249	130.233
4	134.561	98.757	94.465	96.021	96.133	103.988
5	99.173	85.301	81.679	80.556	80.648	85.472
6	63.816	71.852	68.899	69.699	69.783	68.810
7	58.889	64.466	61.860	61.619	61.700	61.707
8	53.961	57.084	54.824	55.355	55.427	55.330
9	49.034	52.363	50.340	50.349	50.405	50.498
10	44.106	47.645	45.860	46.233	46.293	46.027
15	30.874	37.257	36.001	33.263	33.298	34.139
20	24.134	26.867	26.141	26.297	26.324	25.953
25	19.956	22.975	22.474	21.920	21.942	21.853
30	17.085	19.084	18.806	18.901	18.920	18.559
35	14.980	17.008	16.867	16.673	16.689	16.443
40	13.364	14.932	14.928	14.971	14.988	14.637
45	12.082	13.833	13.898	13.620	13.637	13.414
50	11.038	12.733	12.868	12.524	12.536	12.340
60	9.436	10.535	10.808	10.838	10.845	10.492
70	8.261	9.373	9.719	9.606	9.616	9.315
80	7.359	8.210	8.630	8.665	8.674	8.308
90	6.645	7.486	7.953	7.922	7.930	7.587
100	6.064	6.762	7.277	7.319	7.326	6.903
150	4.256	-	-	5.464	5.468	5.063
200	-	-	-	4.505	4.509	-

3-5 Range calculation

The range for proton in thirteen biological organs of the human body, calculated by Matlab program in the computer in the energy region from 1 KeV to 200 MeV using the methods (eq (2-26), SRIM and SRIM (dictionary) program for (skin, eye lens, stomach, pancreas, liver, spleen, blood, ovary, testis, prostate, trachea, mammary gland, and thyroid) tissues, as shown in Fig from (3-1) to (3-26) .

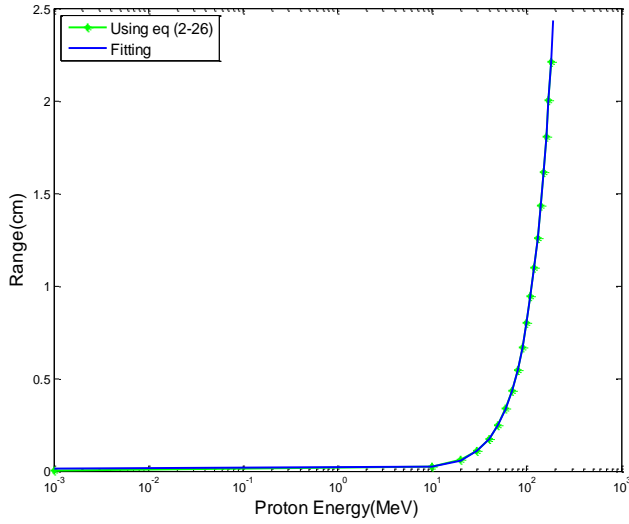


Fig (3-1): Range of proton in skin tissue

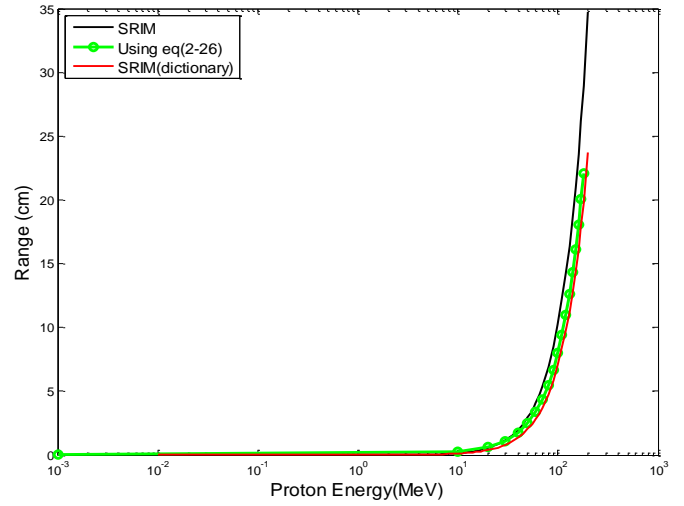


Fig (3-2): Range of proton in skin tissue in all methods.

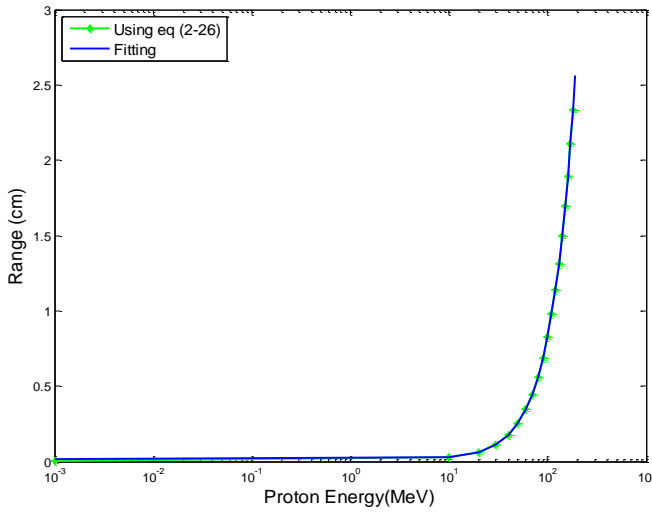


Fig (3-3): Range of proton in eye lens tissue

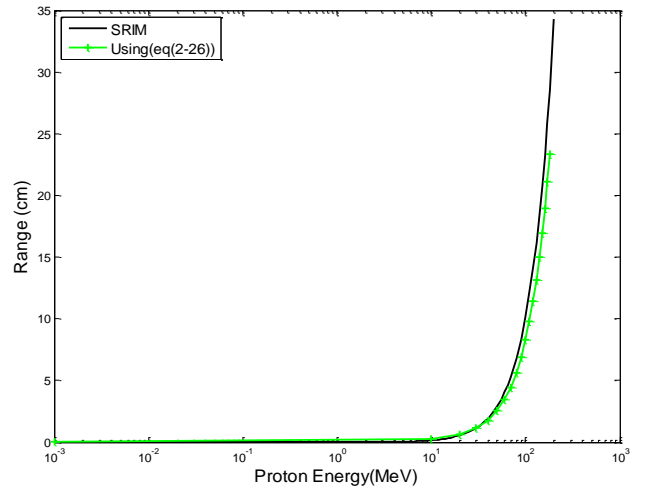


Fig (3-4): Range of proton in eye lens tissue in all methods.

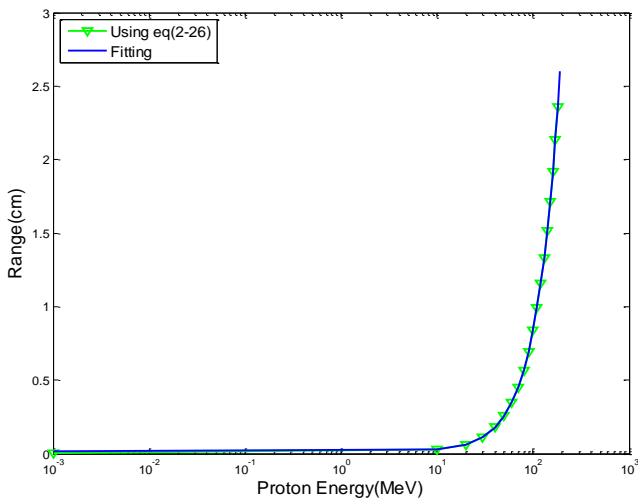


Fig (3-5): Range of proton in stomach tissue.

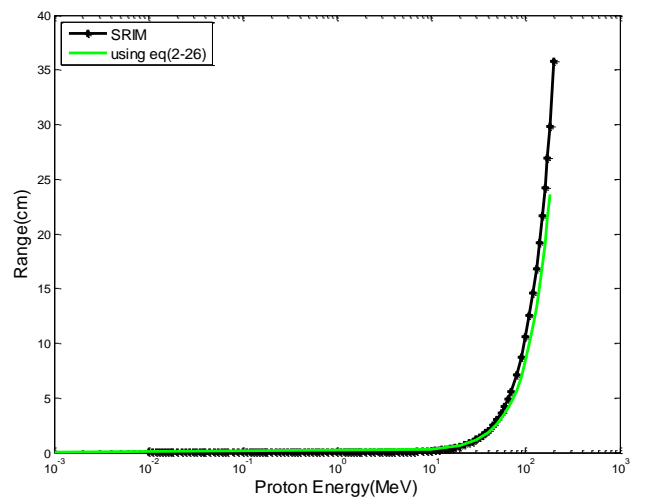


Fig (3-6): Range of proton in stomach tissue in all methods.

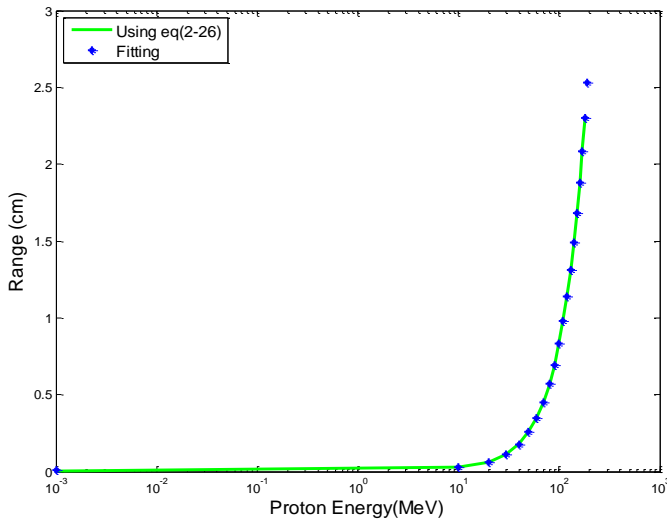


Fig (3-7): Range of proton in pancreas tissue.

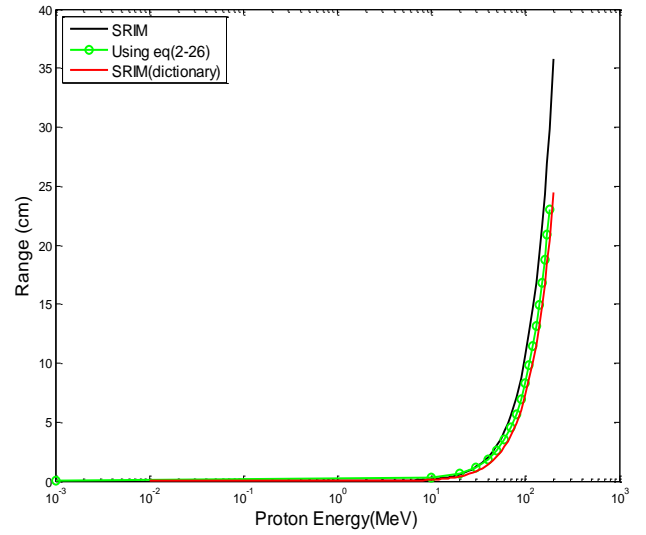


Fig (3-8): Range of proton in pancreas tissue in all methods.

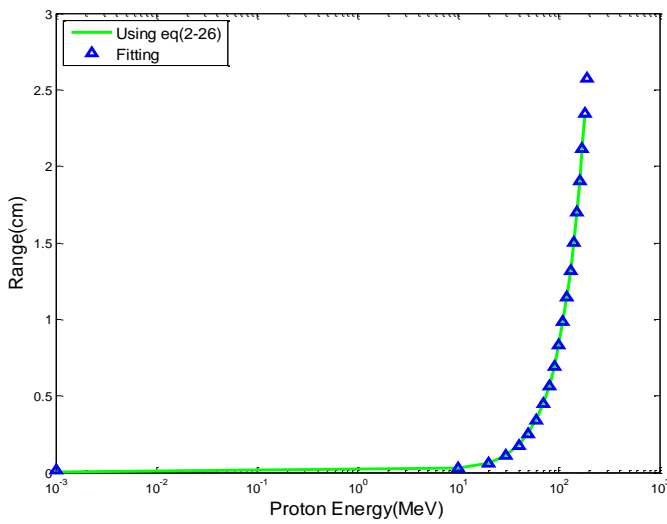


Fig (3-9): Range of proton in liver tissue

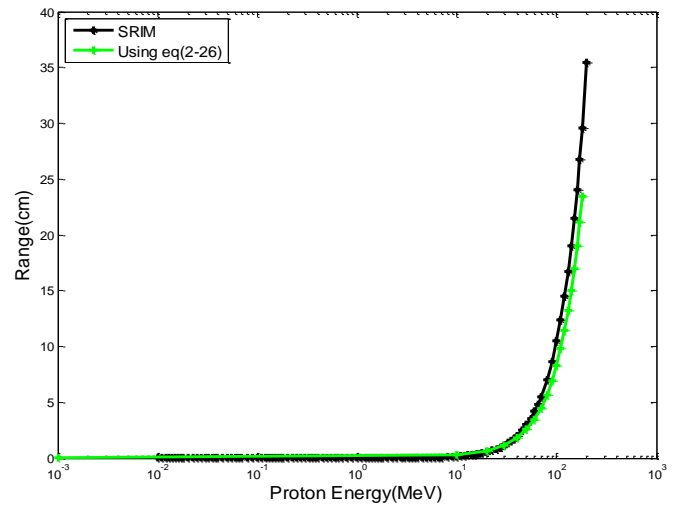


Fig (3-10): Range of proton in liver tissue in all methods.

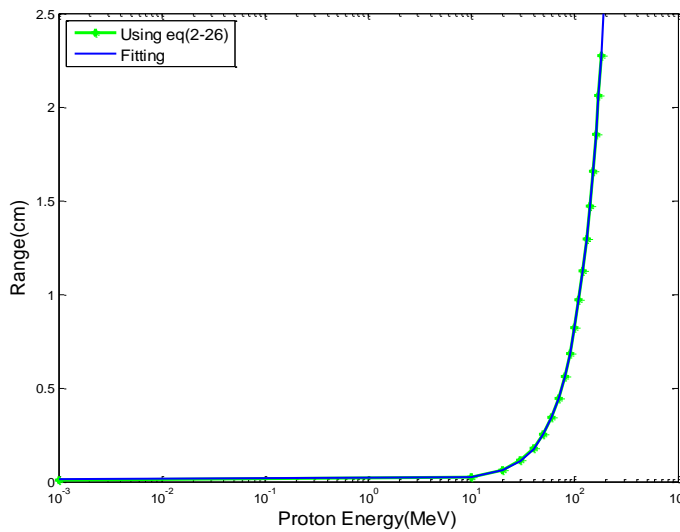


Fig (3-11): Range of proton in spleen tissue.

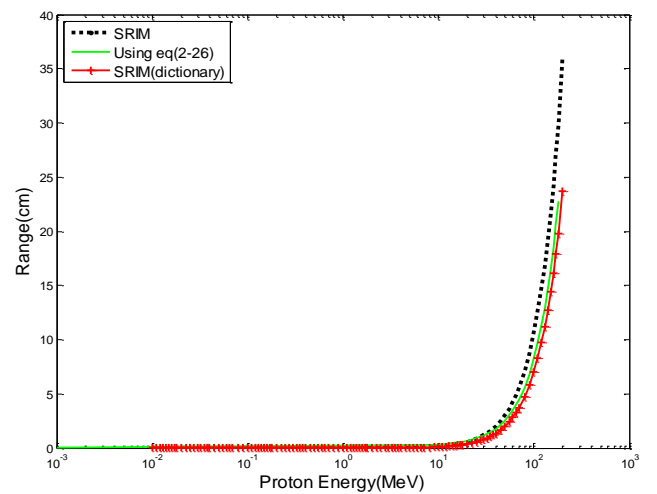


Fig (3-12): Range of proton in spleen tissue in all methods.

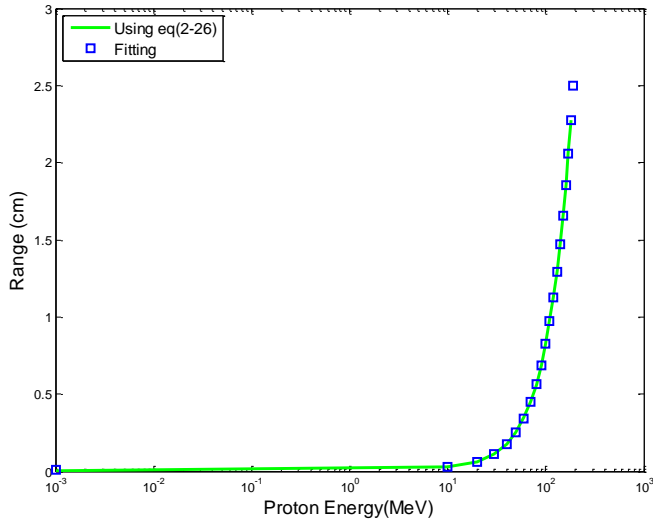


Fig (3-13): Range of proton in blood tissue.

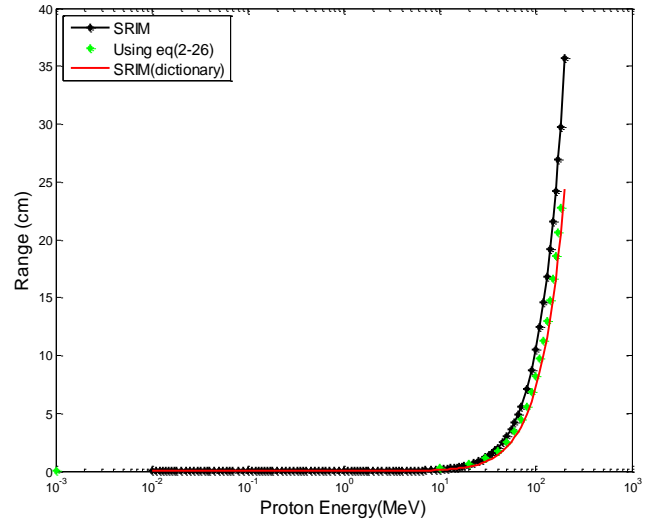


Fig (3-14): Range of proton in blood tissue

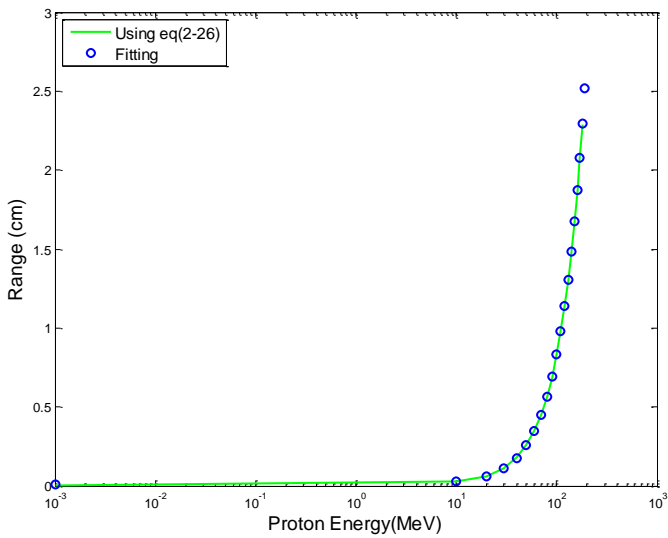


Fig (3-15): Range of proton in ovary tissue

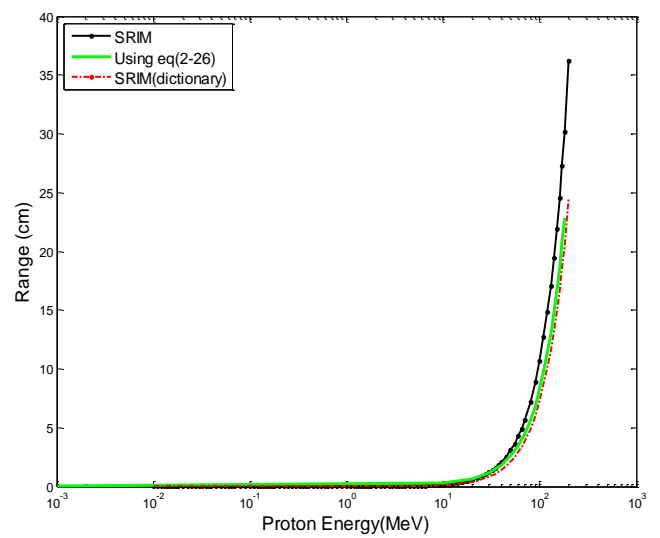


Fig (3-16): Range of proton in ovary tissue in all methods.

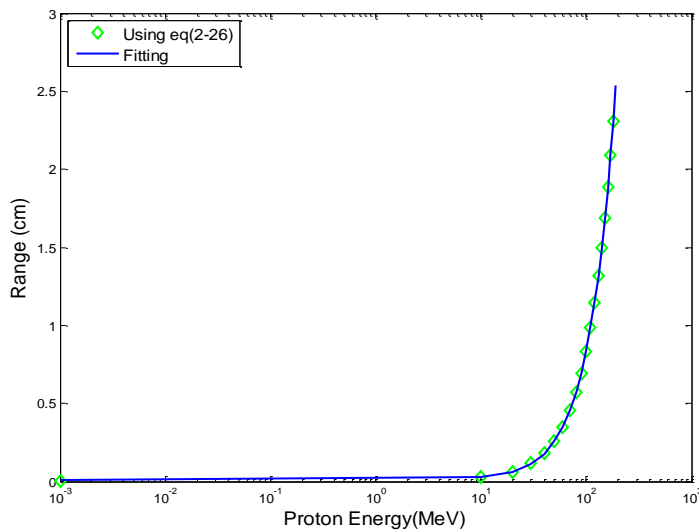


Fig (3-17): Range of proton in testis tissue.

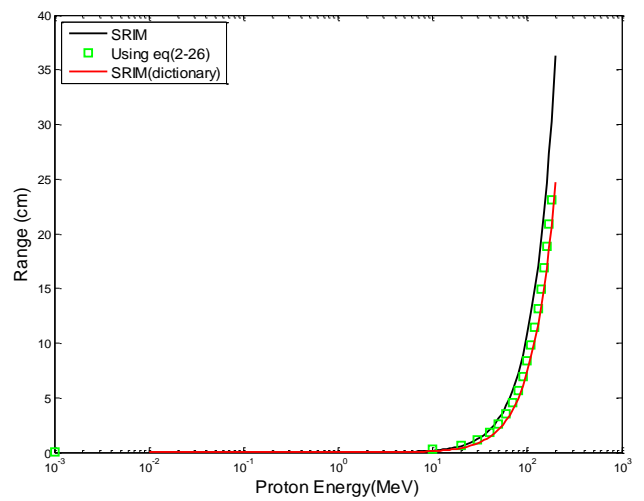


Fig (3-18): Range of proton in testis tissue in all methods.

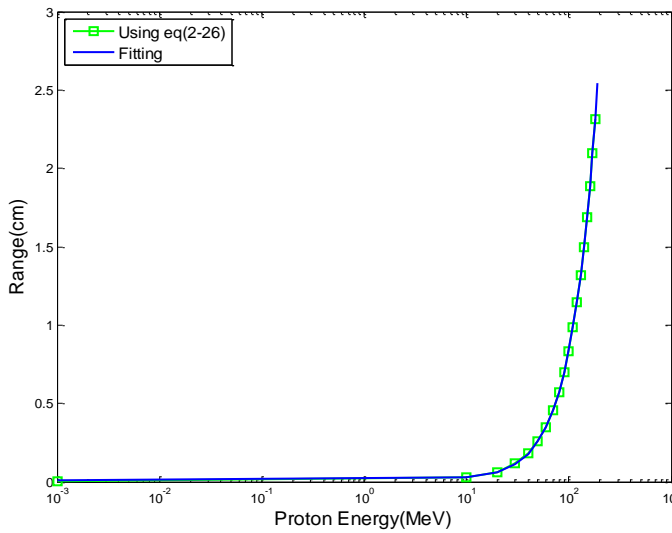


Fig (3-19): Range of proton in prostate tissue.

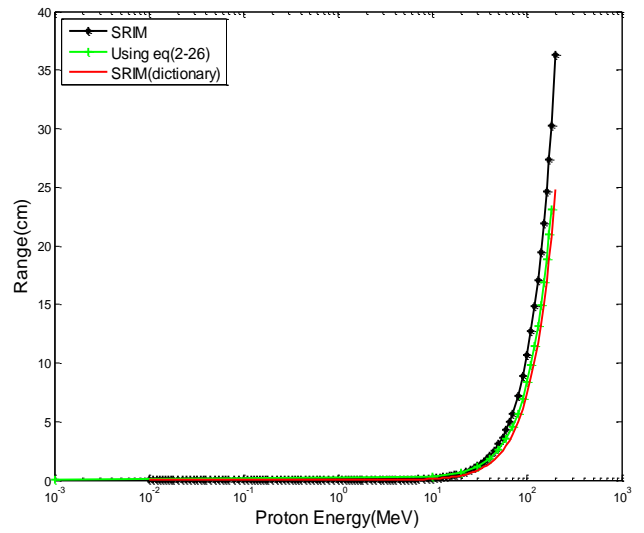


Fig (3-20): Range of proton in prostate tissue in all methods.

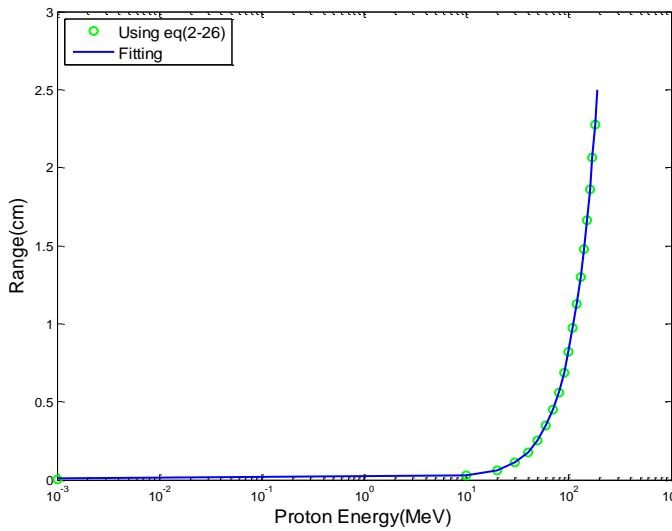


Fig (3-21): Range of proton in trachea tissue.

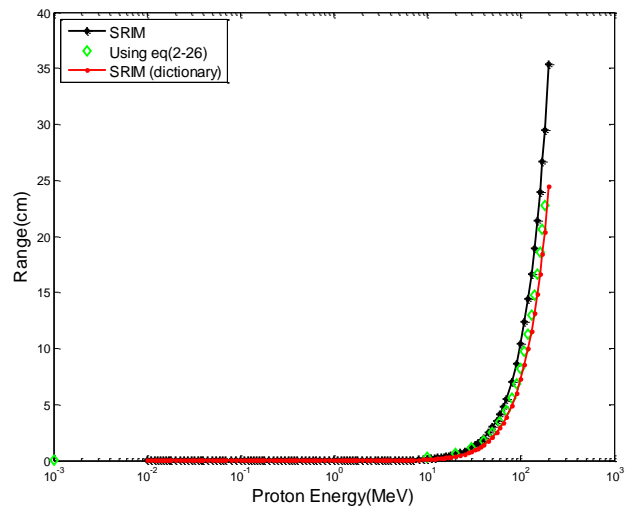


Fig (3-22): Range of proton in trachea tissue in all methods.

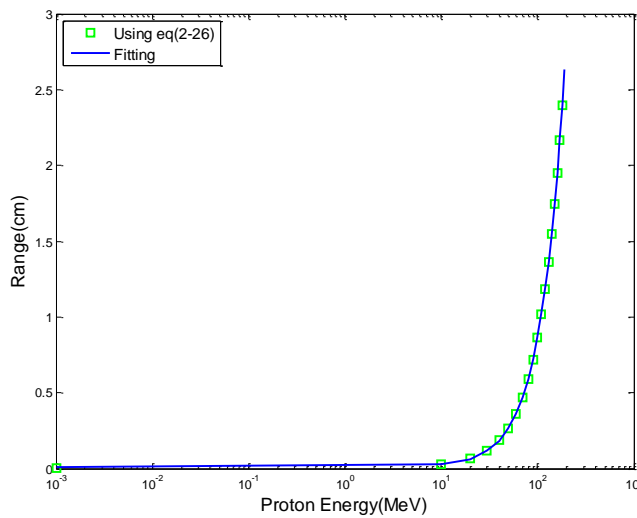


Fig (3-23): Range of proton in mammary gland tissue

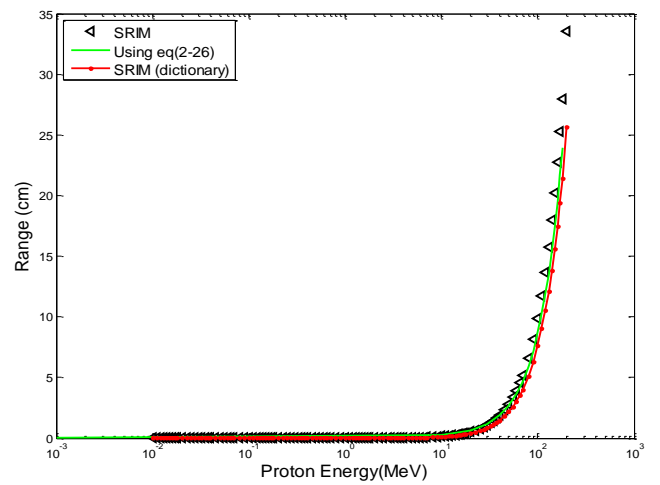


Fig (3-24): Range of proton in mammary gland tissue in all methods.

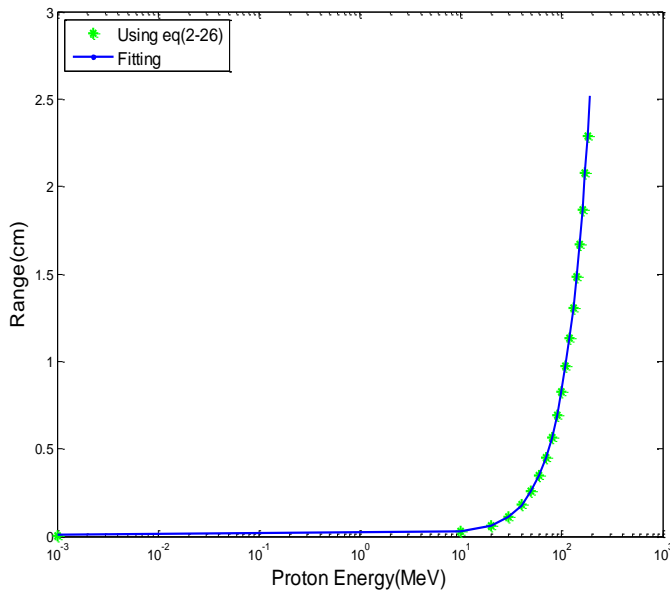


Fig (3-25): Range of proton in thyroid tissue.

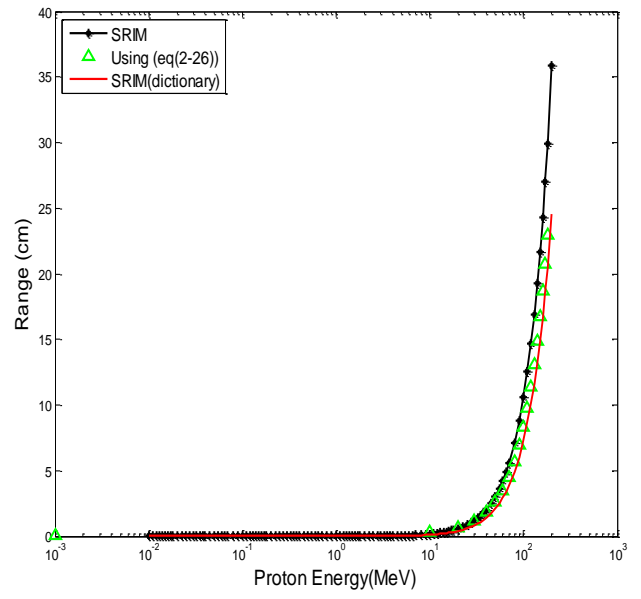


Fig (3-26): Range of proton in thyroid tissue in all methods.

Chapter Four

Result

&

Discussion

4-1 *Stopping power for tissues*

The stopping power for proton with each element in the tissues have been calculated using (Bethe and Ziegler equation, Ziegler and Andreson (Vol.3).[100], SRIM and SRIM dictionary program), then by considering the percentage values for each element which represented in table (1-1) and used equation (2-22) for compounds or mixture have calculated total stopping power.

a- Bethe formula

The stopping power of proton interaction with the chemical compositions existed in tissues using eq (2-16) were represented in table (3-3). The results of stopping powers calculated by Bethe equation are plotted from Fig. (4-1) to (4-61).

This figure shows a decrease in stopping power with increased energy of protons.

b- Ziegler formula

By using Ziegler equation (2-56),(2-57) and (2-58) the stopping power for proton interaction with chemical composition of tissues are tabulated in table (3-3). And the results are plotted from Fig. (4-2) to (4-62).

c- Ziegler and Andreson (Vol.3) [100].

By using Ziegler and Andreson (Vol.3) [100], the stopping power for proton interaction with chemical composition of the tissues are tabulated in table (3-3). And the results are plotted from Fig. (4-3) to (4-63).

d- SRIM and SRIM (dictionary) program

Using SRIM program the stopping power of proton interaction with the chemical compositions existed in the tissues are represented in table (3-3). The results are plotted from Fig. (4-4) to (4-64). The stopping power for proton in the tissues (as a compound) was calculated using SRIM (dictionary) program. Stopping power values were shown from table (3-4) to (3-17) and plotted from Fig (4-4) to (4-64).

e- Present work

The stopping power for proton interaction with the tissues using above methods and the average stopping power were calculated by methods which are tabulated from table (3-4) to (3-17) and plotted from Fig. (4-5) to (4-65).

Enlarging the scale for different regions from the Fig. (4-5) to (4-65) shows clearly the behavior of each individual curve as seen from Fig. (4.5a, b, c) to (4-65 a, b, c).

4-1-1 *Stopping power for skin tissue*

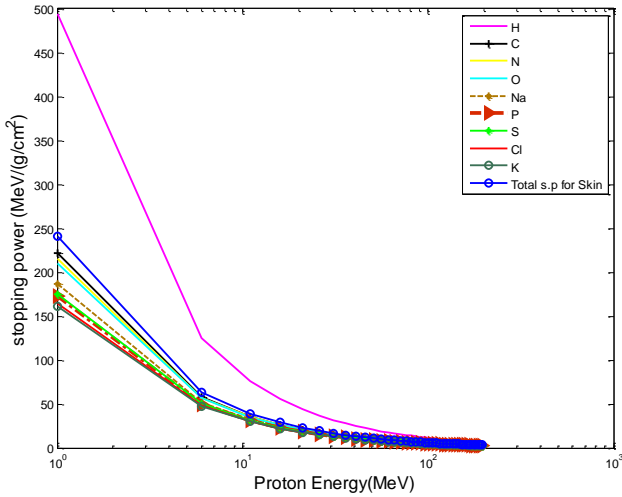


Fig (4-1): Stopping power for proton in elements Presented in skin tissue using Bethe equation.

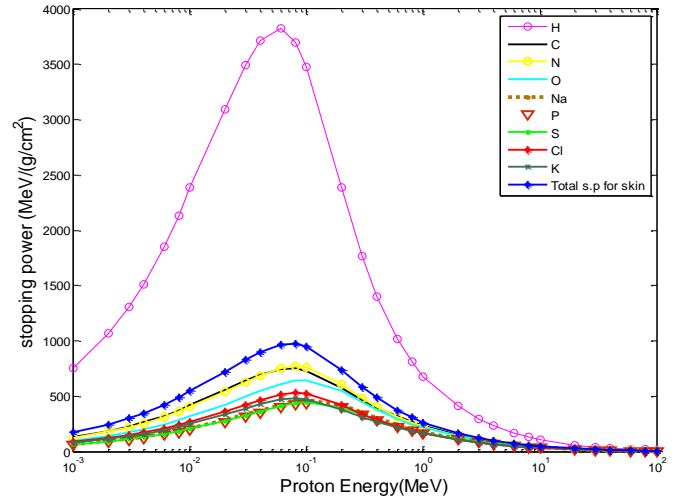


Fig.(4-2): Stopping power for proton in elements presented in skin tissue using Ziegler equation.

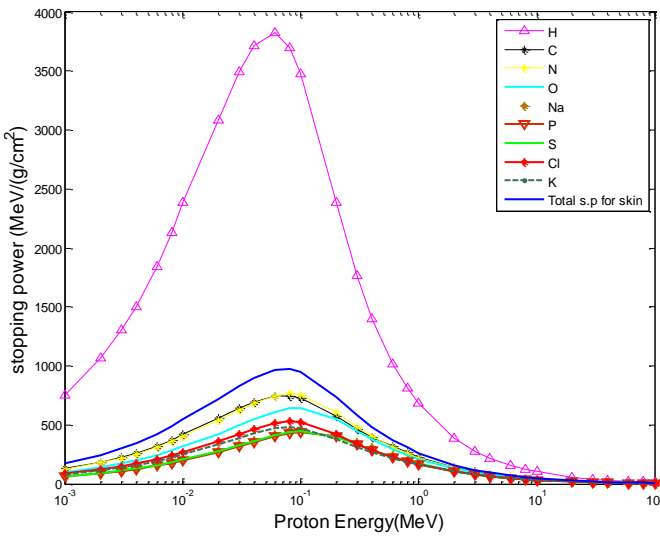


Fig (4-3): Stopping power for proton in elements presented in skin tissue using ref.[100]

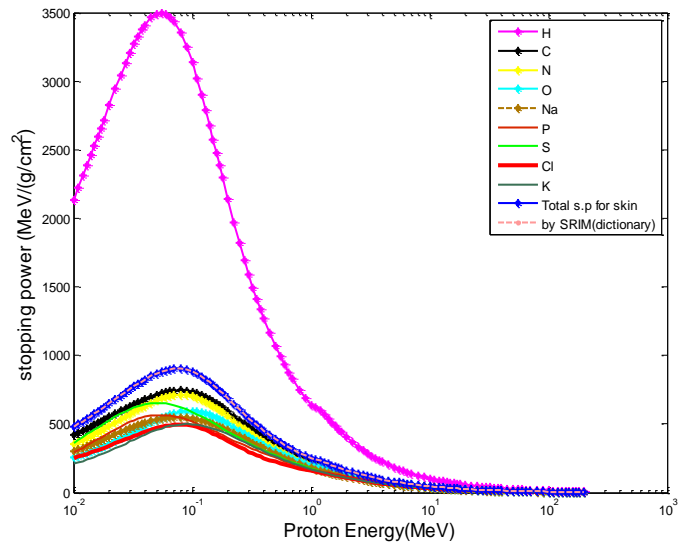


Fig (4-4): Stopping power for proton in elements presented in skin tissue using SRIM and SRIM dictionary.

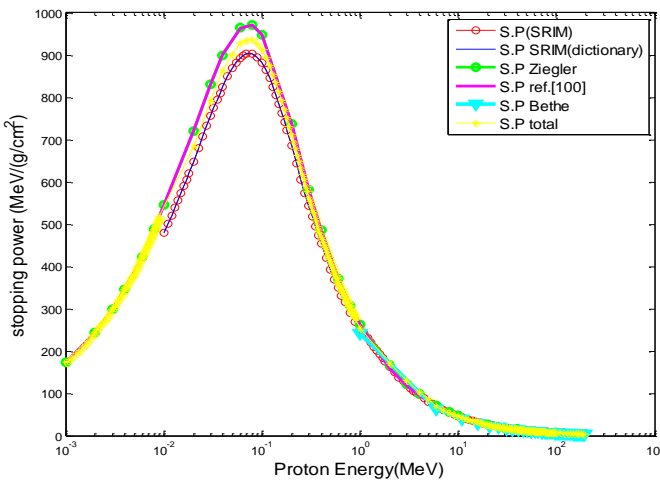


Fig. (4-5): Stopping power for skin tissue (present work).

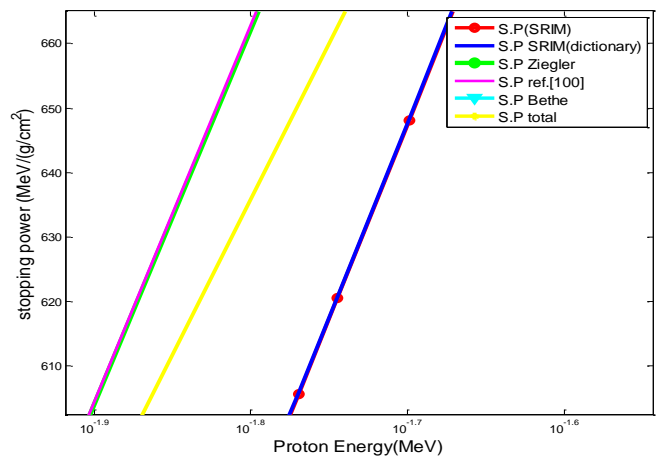


Fig. (4.5a): Stopping power for skin tissue from (10^{-1.9}-10^{-1.6} MeV) (present work).

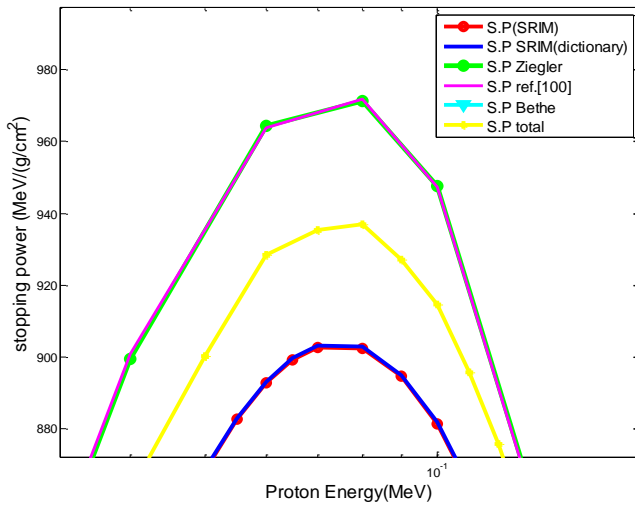


Fig. (4.5b): Stopping power for skin tissue from $(10^{-5}-10^{-1}$ MeV) (present work).

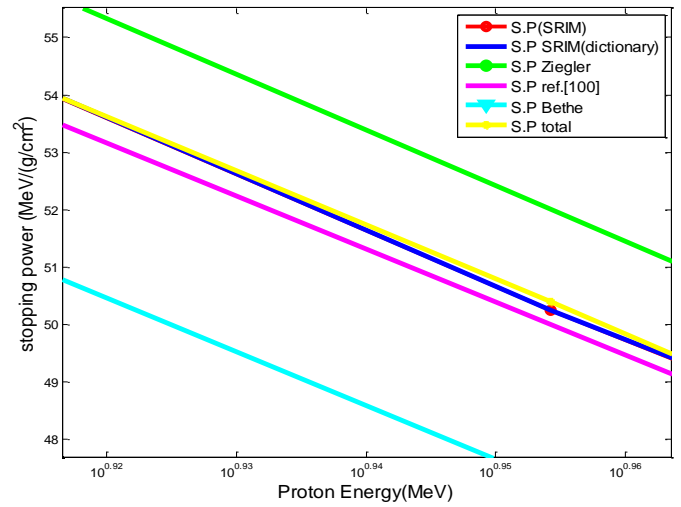


Fig. (4.5c): Stopping power for skin tissue from $(10^{0.92}-10^{0.96}$ MeV) (present work).

Discussion of skin tissue results:

- 1- In figures (4-1), (4-2), (4-3) and (4-4) the proton's stopping power is large for hydrogen because the atomic number of hydrogen ($Z=1$) is less than Z for other elements in skin tissue.
- 2- Using the above methods, stopping power were compatible with the low and high energy region and different at medium energy range.
- 3- Ziegler and Andreson (Vol.3) [100], is very well represented with SRIM and SRIM (dictionary) at high energy.
- 4- Ziegler equation is very well represented with Ziegler and Andreson (Vol.3) [100] at all energies
- 5- Bethe 's equation gives values of stopping power a little lower than other methods, especially at high energy.
- 6- At high energy ($>1\text{MeV}$) stopping power decreases with the increase of proton energy, i.e., it does not have enough time to collide, and at intermediate energy region, stopping power reaches the maximum value (more ionization and excitation), while at low energies ($E < 25\text{KeV}$) we observe the increase of the stopping power with the increase of the proton's energy.
- 7- From figure (4-5b) Ziegler and Andreson (Vol.3) [100] gives high value of stopping power ($971.7 \text{ MeV-cm}^2/\text{g}$) at energy (0.08) MeV.

8- The percentage deviation $[\frac{S_{cal} - S_{exp}}{S_{exp}}] * 100$ between the experimental and the calculated

stopping power values (using above methods), for skin tissue are shown in the following table, percentage deviation values convergent where deviation decreases as the energy of the proton increases (except Bethe). Bethe maximum deviation (18.889%), Ziegler maximum

deviation (5.738%) this leads that Ziegler gave better results from other methods, as shown in red color and minimum deviation is shown in green color in table (4-1).

Table (4-1): Percentage deviation (stopping power) in skin tissue in (MeV-cm²/g).

Stopping power in human tissues in (MeV-cm ² /g)											
E _p (MeV)	Skin tissue										S.P (P.W)
	Stopping power										
	Bethe	Error%	Ziegler	Error%	Ref. [100]	Error%	SRIM	Error%	SRIM dictio- nary	Error%	
0.001	-	-	172.717	-0.054	172.531	0.054	-	-	-	-	172.624
1	240.687	5.500	263.587	-3.666	262.031	-3.094	251.589	0.928	251.702	0.883	253.924
2	205.289	-16.456	166.652	2.913	159.304	7.660	163.110	5.148	163.156	5.119	171.507
3	169.891	-23.449	122.996	5.738	117.532	10.654	119.891	8.477	119.949	8.424	130.053
4	134.492	-22.804	98.615	5.281	94.324	10.070	95.826	8.345	95.853	8.314	103.823
5	99.094	-13.897	85.171	0.179	81.549	4.628	80.392	6.133	80.407	6.114	85.323
6	63.726	7.764	71.733	-4.264	68.779	-0.153	69.557	-1.269	69.573	-1.293	68.674
7	58.804	4.728	64.356	-4.307	61.748	-0.266	61.492	0.149	61.520	0.104	61.584
8	53.881	2.481	56.981	-3.095	54.720	0.911	55.241	-0.041	55.267	-0.089	55.218
9	48.959	2.929	52.267	-3.585	50.242	0.301	50.243	0.299	50.255	0.275	50.393
10	44.037	4.298	47.555	-3.418	45.766	0.356	46.135	-0.447	46.153	-0.485	45.929
15	30.821	10.523	37.183	-8.389	35.927	-5.187	33.189	2.634	33.198	2.607	34.064
20	24.090	7.488	26.809	-3.417	26.087	-0.741	26.237	-1.311	26.244	-1.336	25.893
25	19.918	9.469	22.925	-4.889	22.426	-2.773	21.870	-0.300	21.882	-0.354	21.804
30	17.052	8.580	19.041	-2.761	18.765	-1.334	18.857	-1.814	18.860	-1.828	18.515
35	14.950	9.726	16.969	-3.330	16.830	-2.527	16.634	-1.382	16.638	-1.407	16.404
40	13.337	9.470	14.898	-1.996	14.894	-1.969	14.936	-2.247	14.938	-2.256	14.601
45	12.057	10.965	13.801	-3.053	13.866	-3.509	13.587	-1.525	13.587	-1.525	13.380
50	11.015	11.748	12.704	-3.105	12.838	-4.122	12.493	-1.469	12.496	-1.496	12.309
60	9.416	11.161	10.510	-0.406	10.783	-2.932	10.811	-3.182	10.815	-3.220	10.467
70	8.243	12.715	9.350	-0.630	9.696	-4.179	9.582	-3.037	9.585	-3.060	9.291
80	7.344	12.843	8.191	1.173	8.610	-3.752	8.644	-4.129	8.646	-4.156	8.287
90	6.630	14.144	7.468	1.338	7.935	-4.626	7.902	-4.228	7.905	-4.255	7.568
100	6.050	13.786	6.746	2.053	7.261	-5.185	7.301	-5.702	7.302	-5.722	6.884
150	4.247	18.889	-	-	-	-	5.449	-7.348	5.450	-7.369	5.049
200	-	-	-	-	-	-	4.492	-	4.494	-	-

4-1-2 Stopping power for eye lens tissue

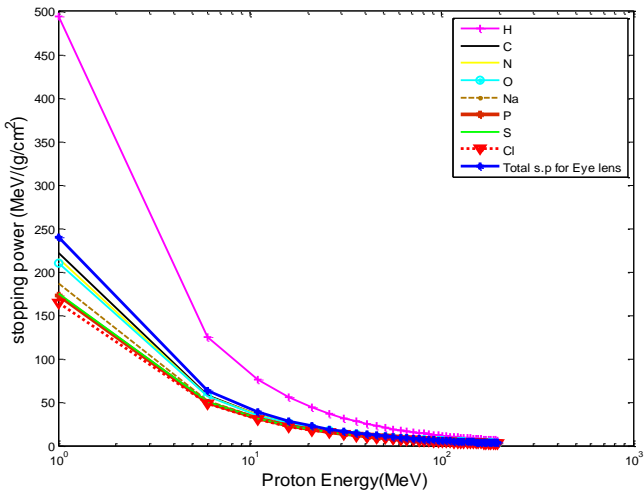


Fig. (4-6): Stopping power for proton in elements presented in eye lens tissue using Beth equation.

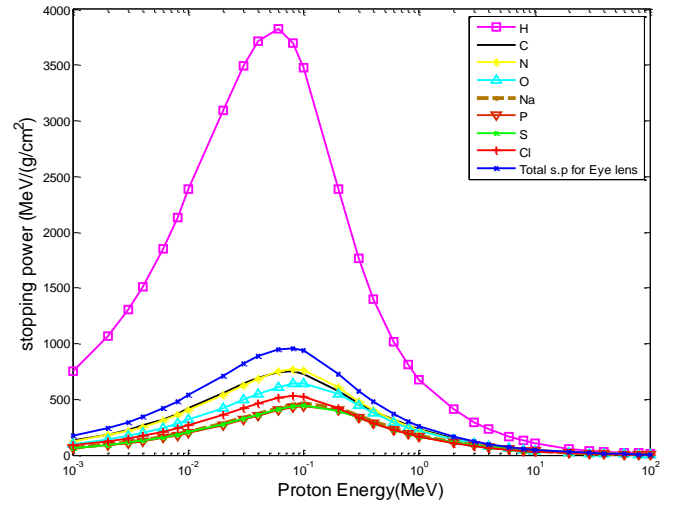


Fig. (4-7): Stopping power for proton in element presented in eye lens tissue using Ziegler equation.

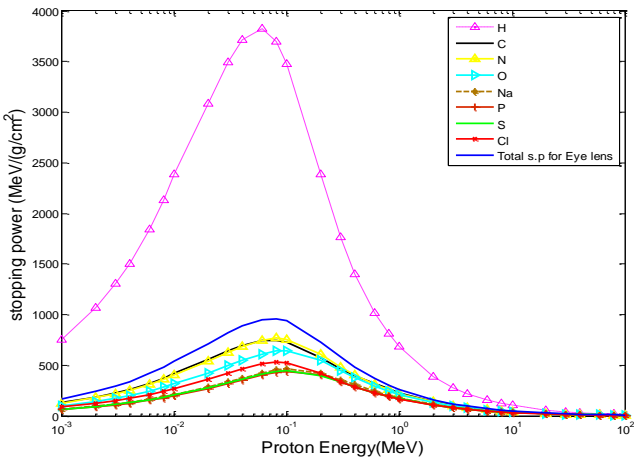


Fig. (4-8): Stopping power for proton in elements presented in eye lens tissue using ref. [100].

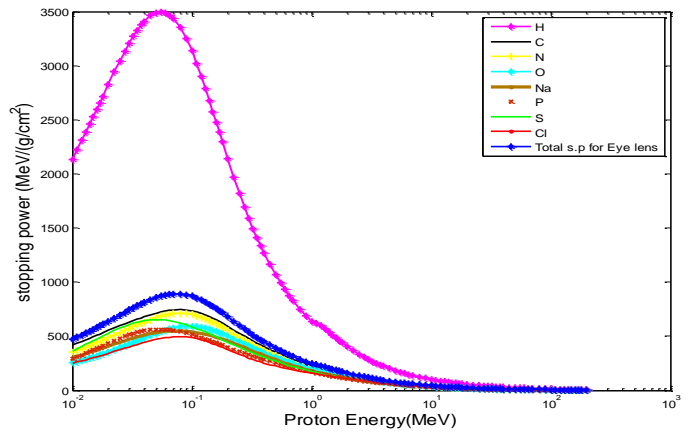


Fig. (4-9): Stopping power for proton in elements presented in eye lens tissue using SRIM program

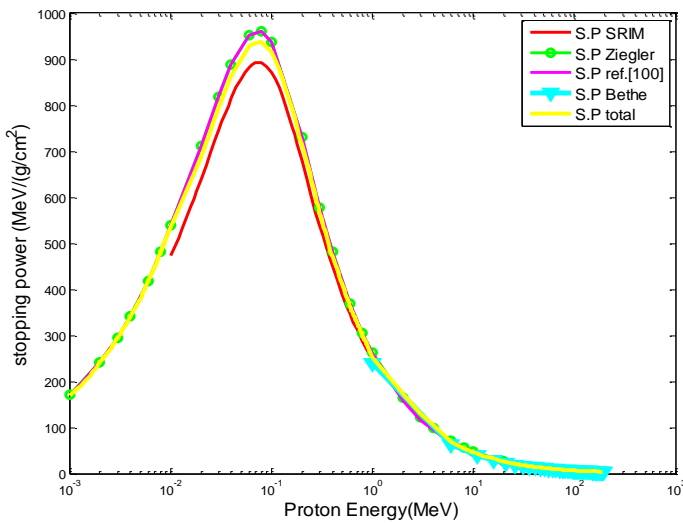


Fig. (4-10): Stopping power for eye lens tissue (present work).

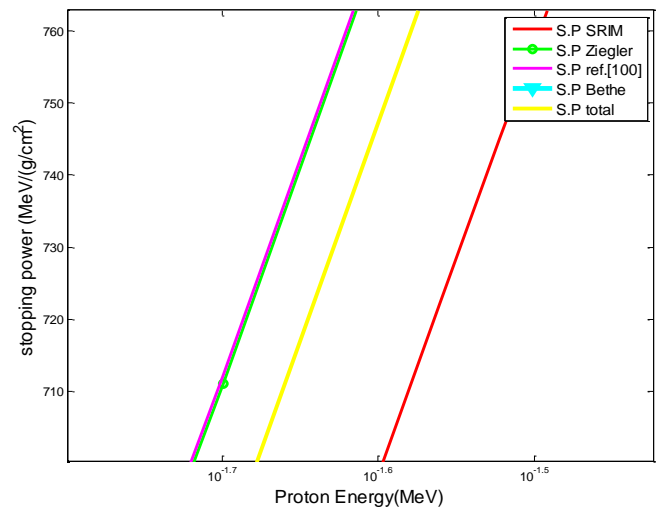


Fig. (4.10a): Stopping power for eye lens tissue from $10^{-1.7}$ - $10^{-1.5}$ MeV (present work).

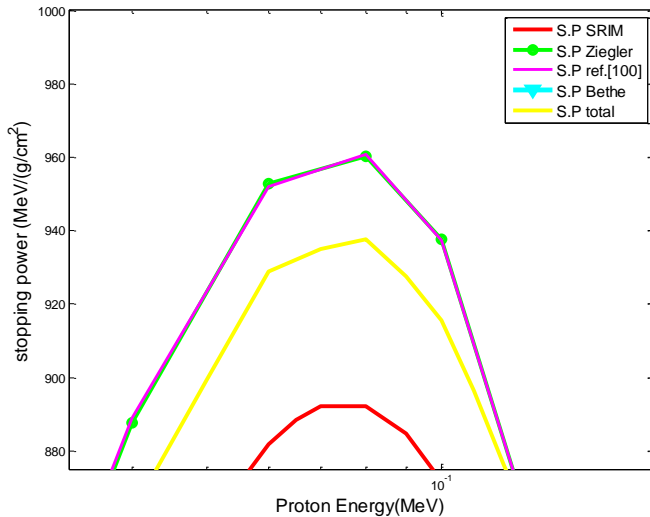


Fig. (4.10b): Stopping power for eye lens tissue from $(10^{-5}-10^{-1}$ MeV) (present work).

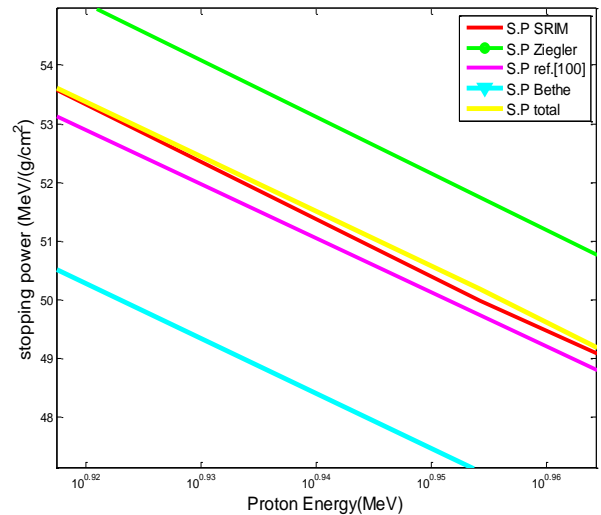


Fig. (4.10c): Stopping power for eye lens tissue from $(10^{0.92}-10^{0.96}$ MeV) (present work).

Discussion of eye lens tissue results:

- 1- In figures (4-6), (4-7), (4-8) and (4-9) the proton's stopping power is large for hydrogen because the atomic number of hydrogen ($Z=1$) is less than Z for other elements in eye lens tissue.
- 2- Using the above methods, stopping power were compatible with the low and high energy region and different at medium energy range.
- 3- Ziegler and Andreson (Vol.3) [100], is very well represented with SRIM program at high energy.
- 4- Ziegler equation is very well represented with Ziegler and Andreson (Vol.3) [100], at all energies
- 5- Bethe 's equation gives values of stopping power a little lower than other methods, especially at high energy.
- 6- At high energy (>1 MeV) stopping power decreases with the increase of proton energy, i.e., it does not have enough time to collide, and at intermediate energy region, stopping power reaches the maximum value (more ionization and excitation), while at low energies ($E < 25$ KeV) we observe the increase of the stopping power with the increase of the proton's energy.
- 7- From figure (4-10b) Ziegler and Andreson (Vol.3) [100], gives high value of stopping power ($960.8 \text{ MeV-cm}^2/\text{g}$) at energy (0.08) MeV.

- 8- The percentage deviation $\left[\frac{S_{cal} - S_{exp}}{S_{exp}} \right] * 100$ between the experimental and the calculated

stopping power values (using above methods) for eye lens tissue are shown in the following table, percentage deviation values convergent where deviation decreases as the energy of the proton increases (except Bethe). Bethe maximum deviation (14.109%), Ziegler maximum deviation (7.846%) this leads that Ziegler gave better results from other methods, as shown in red color and minimum deviation is shown in green color in table (4-2).

Table (4-2): Percentage deviation (stopping power) in eye lens tissue in (MeV-cm²/g).

Stopping power in human tissues in (MeV-cm ² /g)									
E _p (MeV)	Eye lens tissue								S.P (P.W)
	Stopping power								
	Bethe	Error%	Ziegler	Error%	Ref. [100]	Error%	SRIM	Error%	
0.001	-	-	170.265	-0.054	170.082	0.054	-	-	170.174
1	239.660	5.527	261.882	-3.427	260.276	-2.831	249.796	1.245	252.906
2	204.417	-15.548	165.643	4.220	158.346	9.023	162.116	6.488	172.633
3	169.173	-22.043	122.288	7.846	116.858	12.858	119.208	10.633	131.883
4	133.930	-21.396	98.065	7.351	93.801	12.232	95.299	10.467	105.274
5	98.686	-12.740	84.703	1.665	81.103	6.179	79.962	7.694	86.114
6	63.473	7.298	71.348	-4.544	68.410	-0.445	69.191	-1.568	68.106
7	58.571	4.650	64.014	-4.248	61.421	-0.206	61.173	0.199	61.295
8	53.669	2.361	56.683	-3.082	54.435	0.921	54.957	-0.039	54.936
9	48.766	2.904	51.995	-3.486	49.982	0.401	49.987	0.391	50.182
10	43.864	4.076	47.310	-3.504	45.532	0.264	45.902	-0.546	45.652
15	30.701	11.126	36.994	-7.779	35.746	-4.557	33.026	3.303	34.117
20	23.997	7.037	26.677	-3.717	25.958	-1.050	26.110	-1.627	25.685
25	19.841	9.285	22.813	-4.949	22.316	-2.833	21.765	-0.372	21.684
30	16.987	7.992	18.949	-3.191	18.674	-1.768	18.767	-2.254	18.344
35	14.893	9.253	16.888	-3.651	16.748	-2.849	16.555	-1.717	16.271
40	13.286	8.759	14.827	-2.539	14.822	-2.510	14.866	-2.794	14.450
45	12.012	10.455	13.735	-3.405	13.800	-3.858	13.523	-1.891	13.267
50	10.973	11.244	12.643	-3.452	12.777	-4.462	12.434	-1.828	12.207
60	9.380	10.161	10.460	-1.213	10.732	-3.714	10.761	-3.972	10.333
70	8.212	11.750	9.306	-1.393	9.651	-4.911	9.538	-3.787	9.177
80	7.316	11.544	8.152	0.097	8.569	-4.774	8.604	-5.155	8.160
90	6.605	12.799	7.434	0.231	7.898	-5.667	7.866	-5.278	7.451
100	6.027	10.285	6.715	-1.004	7.227	-8.026	7.267	-8.531	6.647
150	4.231	14.109	-	-	-	-	5.424	-11.004	4.828
200	-	-	-	-	-	-	4.472	-	-

4-1-3 Stopping power for stomach tissue

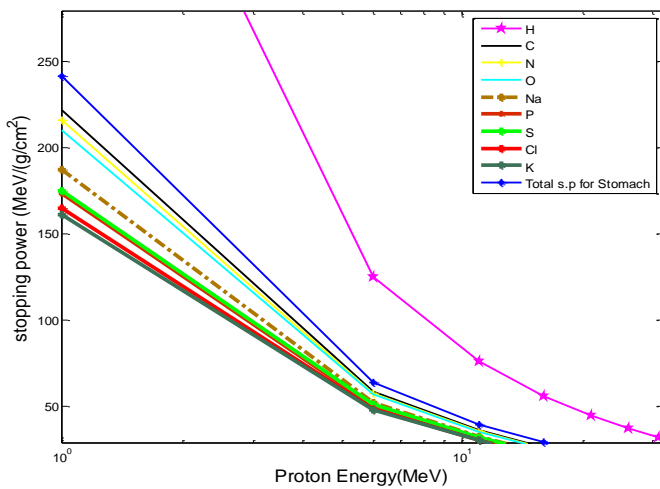


Fig. (4-11): Stopping power for proton in elements presented in stomach tissue using Bethe equation.

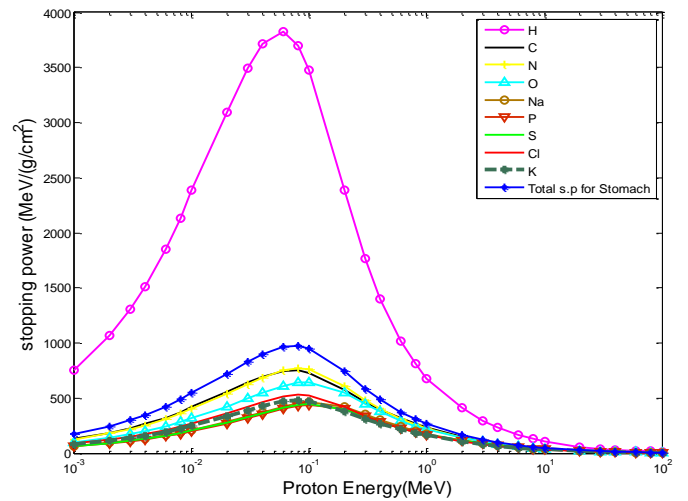


Fig. (4-12): Stopping power for proton in elements presented in stomach tissue using Ziegler equation.

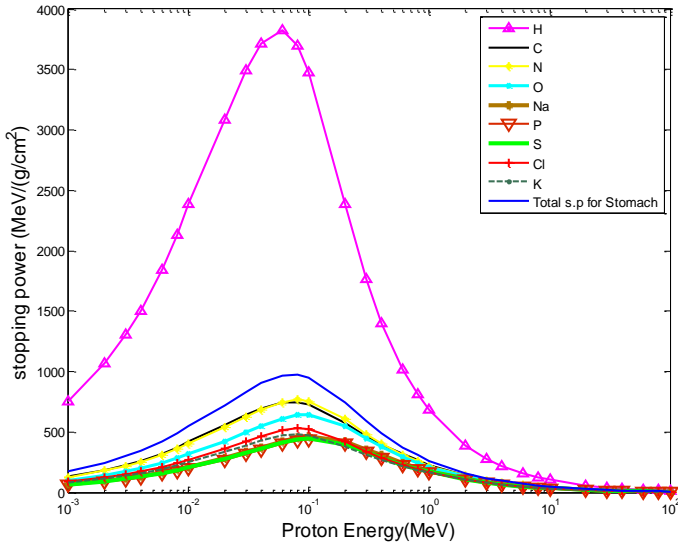


Fig.(4-13): Stopping power for proton in elements presented in stomach tissue using ref. [100].

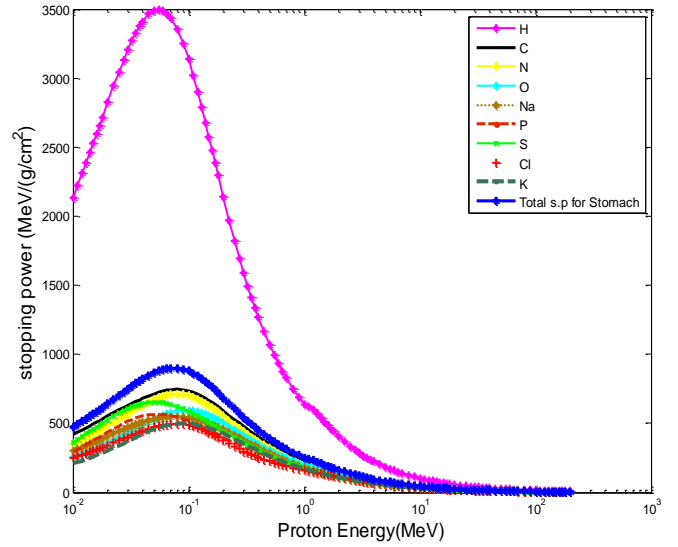


Fig. (4-14): Stopping power for proton in elements presented in stomach tissue using SRIM program.

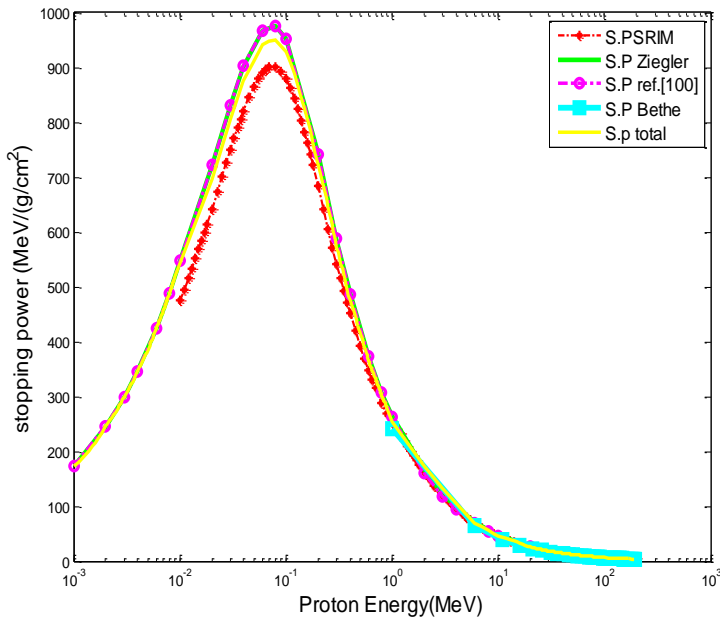


Fig. (4-15): Stopping power for stomach tissue (present work).

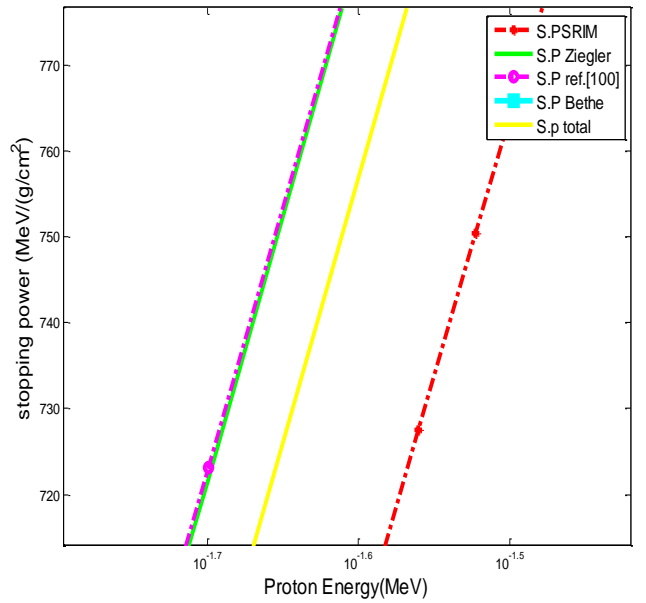


Fig. (4.15a): Stopping power for stomach tissue from $10^{-1.7}$ - $10^{-1.5}$ MeV (present work).

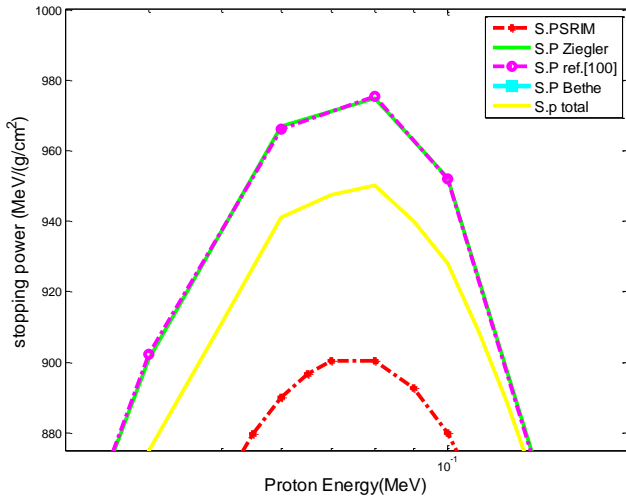


Fig. (4.15b): Stopping power for stomach tissue from $(10^{-5}-10^{-1} \text{MeV})$ (present work).

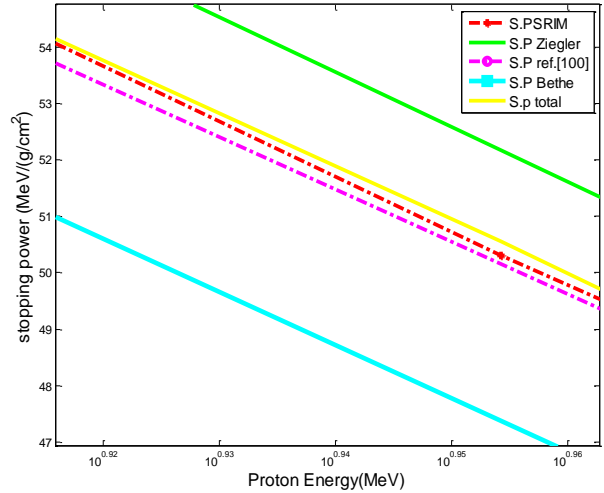


Fig. (4.15c): Stopping power for stomach tissue from $(10^{0.92}-10^{0.96} \text{MeV})$ (present work).

Discussion of stomach tissue results:

- 1- In figures (4-11), (4-12), (4-13) and (4-14) the proton's stopping power is large for hydrogen because the atomic number of hydrogen ($Z=1$) is less than Z for other elements in stomach tissue.
- 2- Using the above methods, stopping power were compatible with the low and high energy region and different at medium energy range.
- 3- Ziegler and Andreson (Vol.3) [100], is very well represented with SRIM program at high energy.
- 4- Ziegler equation is very well represented with Ziegler and Andreson (Vol.3) [100], at all energies
- 5- Bethe 's equation gives values of stopping power a little lower than other methods, especially at high energy.
- 6- At high energy ($>1\text{MeV}$) stopping power decreases with the increase of proton energy, i.e., it does not have enough time to collide, and at intermediate energy region, stopping power reaches the maximum value (more ionization and excitation), while at low energies ($E < 25\text{KeV}$) we observe the increase of the stopping power with the increase of the proton's energy.
- 7- From figure (4-15b) Ziegler and Andreson (Vol.3) [100], gives high value of stopping power ($975.5 \text{ MeV}\cdot\text{cm}^2/\text{g}$) at energy (0.08) MeV.

8- The percentage deviation $[\frac{S_{cal} - S_{exp}}{S_{exp}}] * 100$ between the experimental and the calculated stopping power values (using above methods) for stomach tissue are shown in the following table, percentage deviation values convergent where deviation decreases as the energy of the proton increases (except Bethe). Bethe maximum deviation (14.043%), Ziegler maximum deviation (7.716%) this leads that Ziegler gave better results from other methods, as shown in red color and minimum deviation is shown in green color in table (4-3).

Table (4-3): Percentage deviation (stopping power) in stomach tissue in (MeV-cm²/g).

Stopping power in human tissues in (MeV-cm ² /g)									
E _p (MeV)	Stomach tissue								S.P (P.W)
	Stopping power								
	Bethe	Error%	Ziegler	Error%	Ref. [100]	Error%	SRIM	Error%	
0.001	-	-	172.935	-0.055	172.744	0.055	-	-	172.840
1	241.086	5.689	264.346	-3.611	262.725	-3.016	251.038	1.499	254.801
2	205.639	-15.403	167.113	4.100	159.719	8.919	163.374	6.482	173.964
3	170.192	-21.933	123.347	7.716	117.852	12.738	120.061	10.664	132.864
4	134.745	-21.296	98.903	7.226	94.602	12.102	95.949	10.528	106.050
5	99.298	-12.635	85.423	1.555	81.793	6.062	80.490	7.779	86.751
6	63.881	7.411	71.949	-4.635	68.990	-0.544	69.638	-1.469	68.615
7	58.948	4.755	64.552	-4.340	61.939	-0.305	61.563	0.305	61.750
8	54.014	2.456	57.157	-3.177	54.891	0.820	55.302	0.071	55.341
9	49.081	2.998	52.429	-3.579	50.401	0.300	50.299	0.504	50.553
10	44.148	4.167	47.703	-3.596	45.914	0.161	46.186	-0.429	45.988
15	30.902	11.216	37.301	-7.863	36.043	-4.648	33.226	3.437	34.368
20	24.154	7.109	26.896	-3.810	26.170	-1.140	26.265	-1.500	25.871
25	19.972	9.355	23.000	-5.039	22.498	-2.920	21.893	-0.239	21.841
30	17.099	8.054	19.103	-3.283	18.826	-1.856	18.877	-2.123	18.476
35	14.992	9.315	17.025	-3.741	16.884	-2.938	16.652	-1.582	16.388
40	13.375	8.817	14.947	-2.629	14.943	-2.601	14.952	-2.659	14.554
45	12.091	10.513	13.846	-3.493	13.911	-3.945	13.601	-1.754	13.363
50	11.046	11.303	12.746	-3.538	12.880	-4.546	12.507	-1.694	12.295
60	9.443	10.210	10.545	-1.305	10.818	-3.798	10.823	-3.840	10.407
70	8.267	11.798	9.381	-1.484	9.728	-4.994	9.593	-3.654	9.242
80	7.365	11.589	8.218	0.006	8.638	-4.857	8.653	-5.024	8.218
90	6.650	12.843	7.493	0.140	7.961	-5.743	7.911	-5.149	7.504
100	6.068	10.224	6.768	-1.183	7.284	-8.176	7.309	-8.489	6.688
150	4.259	14.043	-	-	-	-	5.455	-10.964	4.857
200	-	-	-	-	-	-	4.498	-	-

4-1-4 Stopping power for pancreas tissue

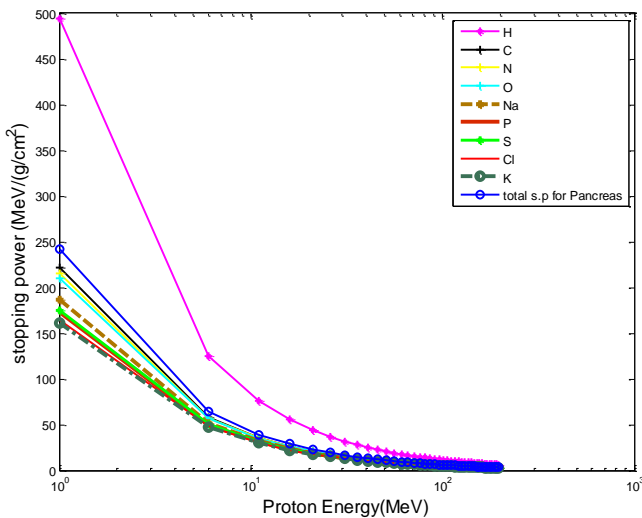


Fig. (4-16): Stopping power for proton in elements presented in pancreas tissue using Bethe equation

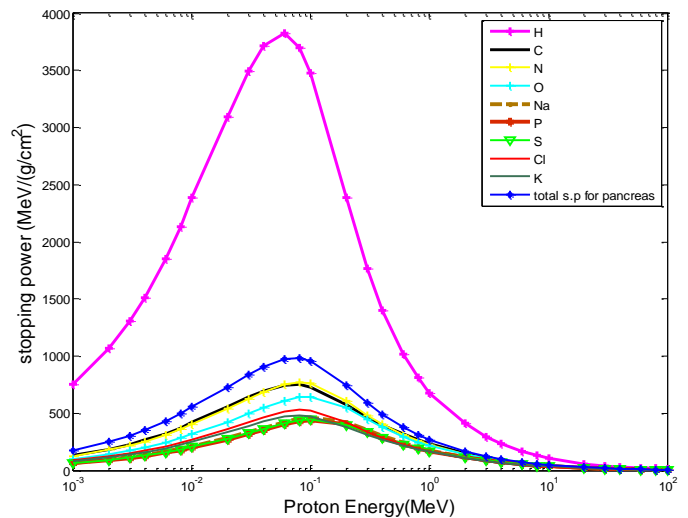


Fig.(4-17): Stopping power for proton in elements presented in pancreas tissue using Ziegler equation.

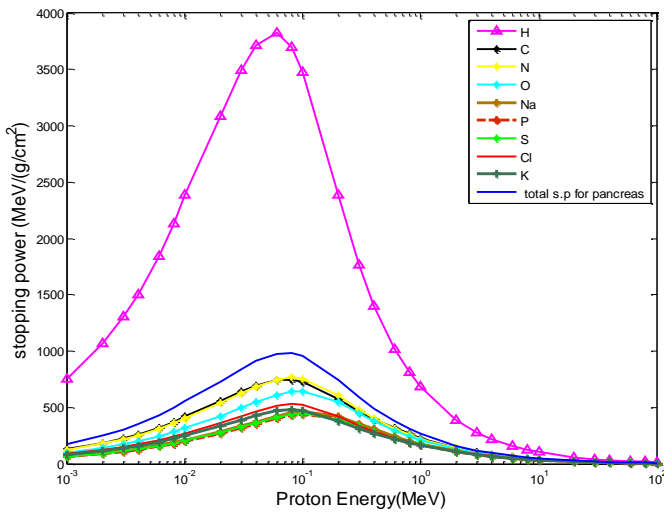


Fig. (4-18): Stopping power for proton in elements presented in pancreas tissue using ref. [100].

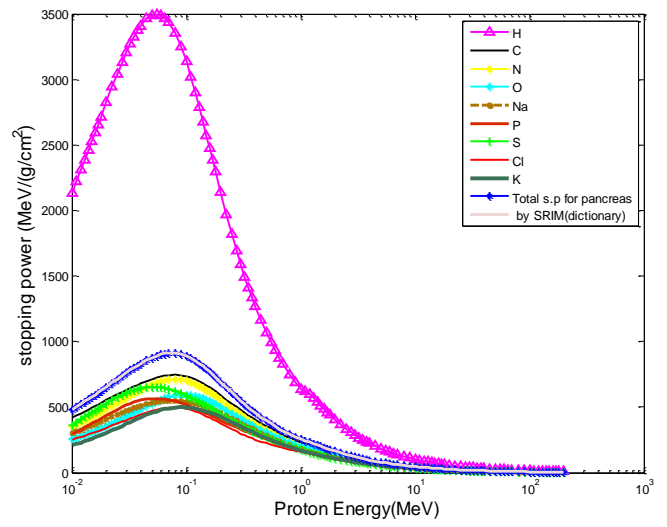


Fig (4-19) Stopping power for proton in elements presented in pancreas tissue using SRIM and SRIM (dictionary) program.

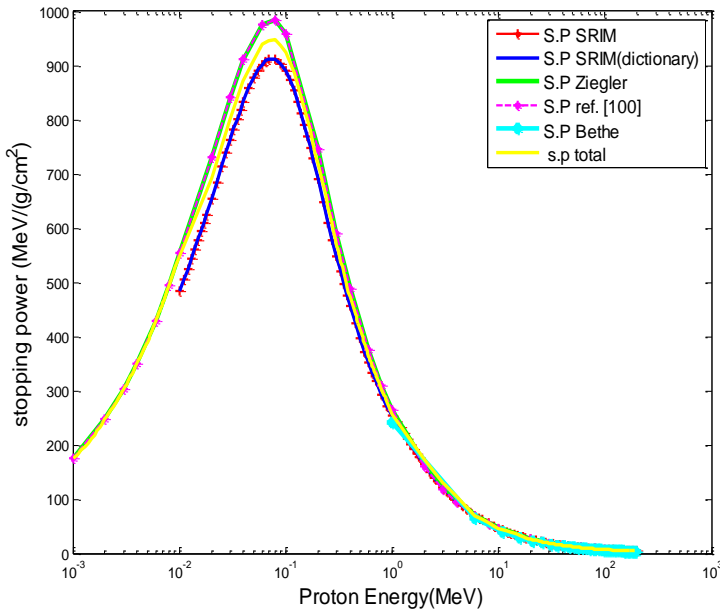


Fig. (4-20): Stopping power for pancreas tissue (present work)

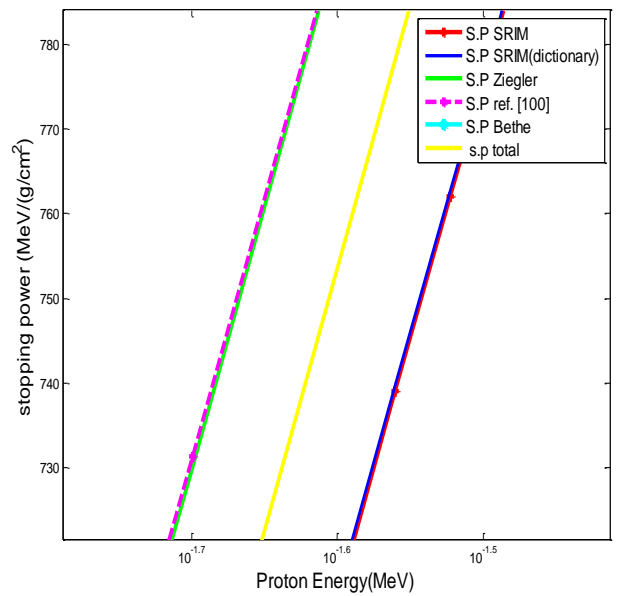


Fig.(4.20a): Stopping power for pancreas tissue from (10^{-1.7}-10^{-1.5} MeV) (present work).

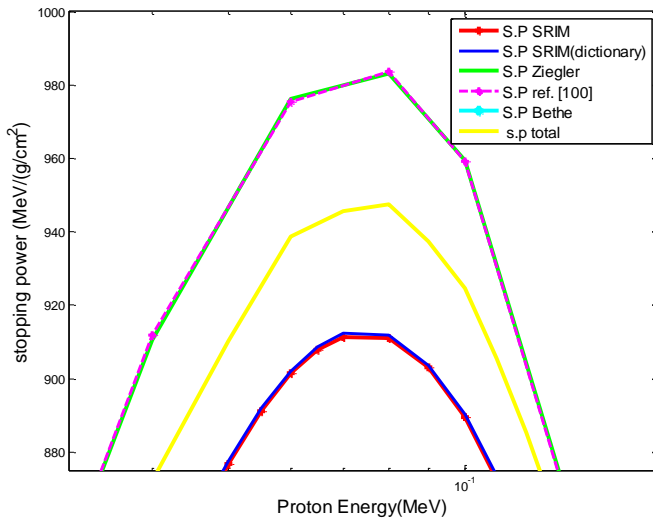


Fig. (4.20b): Stopping power for pancreas tissue from (10^{-5} - 10^{-1} MeV) (present work).

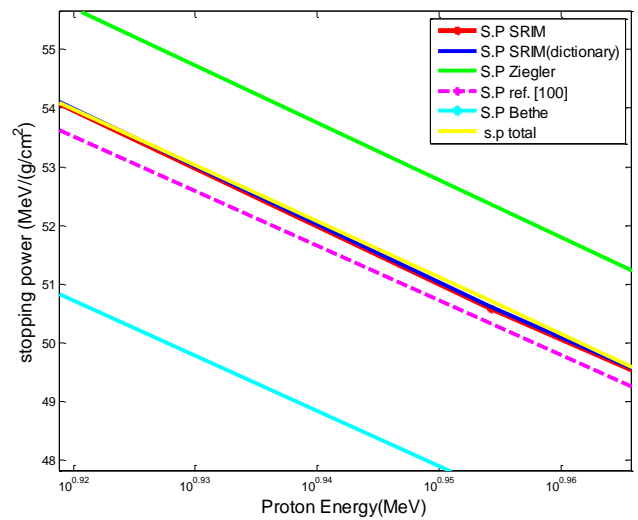


Fig. (4.20c): Stopping power for pancreas tissue from ($10^{0.92}$ - $10^{0.96}$ MeV) (present work).

Discussion of pancreas tissue results:

- 1- In figures (4-16), (4-17), (4-18) and (4-19) the proton's stopping power is large for hydrogen because the atomic number of hydrogen ($Z=1$) is less than Z for other elements in pancreas tissue.
- 2- Using the above methods, stopping power were compatible with the low and high energy region and different at medium energy range.
- 3- Ziegler and Andreson (Vol.3) [100], is very well represented with SRIM and SRIM (dictionary) program at high energy.
- 4- Ziegler equation is very well represented with Ziegler and Andreson (Vol.3) [100], at all energies
- 5- Bethe 's equation gives values of stopping power a little lower than other methods, especially at high energy.
- 6- At high energy (>1 MeV) stopping power decreases with the increase of proton energy, i.e., it does not have enough time to collide, and at intermediate energy region, stopping power reaches the maximum value (more ionization and excitation), while at low energies ($E < 25$ KeV) we observe the increase of the stopping power with the increase of the proton's energy.
- 7- From figure (4-20b) Ziegler and Andreson (Vol.3) [100], gives high value of stopping power ($983.6 \text{ MeV-cm}^2/\text{g}$) at energy (0.08) MeV.

- 8- The percentage deviation $[\frac{S_{cal} - S_{exp}}{S_{exp}}] * 100$ between the experimental and the calculated

stopping power values (using above methods) for pancreas tissue are shown in the following table, percentage deviation values convergent where deviation decreases as the energy of the proton increases (except Bethe). Bethe maximum deviation (18.980%), Ziegler maximum deviation (5.698%) this leads that Ziegler gave better results from other methods, as shown in red color and minimum deviation is shown in green color in table (4-4).

Table (4-4): Percentage deviation (stopping power) in pancreas tissue in (MeV-cm²/g).

Stopping power in human tissues in (Mev-cm ² /g)											
E _p (MeV)	Pancreas tissue										S.P (P.W)
	Stopping power										
	Bethe	Error%	Ziegler	Error%	Ref. [100]	Error%	SRIM	Error%	SRIM dictio- nary	Error%	
0.001	-	-	174.967	-0.055	174.776	0.055	-	-	-	-	174.871
1	241.883	5.669	265.599	-3.766	264.041	-3.198	253.130	0.974	253.307	0.904	255.596
2	206.311	-16.297	167.849	2.883	160.426	7.644	164.372	5.059	164.457	5.005	172.688
3	170.739	-23.327	123.853	5.698	118.339	10.624	120.766	8.401	120.849	8.326	130.911
4	135.167	-22.690	99.291	5.243	94.970	10.032	96.501	8.286	96.554	8.227	104.497
5	99.595	-13.773	85.750	0.148	82.104	4.596	80.947	6.090	80.988	6.037	85.877
6	64.053	7.916	72.215	-4.282	69.244	-0.174	70.030	-1.294	70.074	-1.356	69.123
7	59.106	4.867	64.787	-4.329	62.163	-0.290	61.906	0.124	61.951	0.051	61.982
8	54.158	2.610	57.360	-3.118	55.084	0.885	55.609	-0.066	55.648	-0.136	55.572
9	49.211	3.059	52.613	-3.606	50.576	0.277	50.576	0.278	50.605	0.219	50.716
10	44.263	4.427	47.869	-3.438	46.071	0.331	46.439	-0.466	46.473	-0.538	46.223
15	30.980	10.649	37.427	-8.411	36.164	-5.212	33.405	2.616	33.419	2.574	34.279
20	24.214	7.607	26.983	-3.433	26.255	-0.755	26.406	-1.323	26.424	-1.392	26.056
25	20.021	9.578	23.073	-4.914	22.570	-2.795	22.009	-0.320	22.022	-0.375	21.939
30	17.141	8.684	19.163	-2.786	18.885	-1.356	18.977	-1.833	18.980	-1.849	18.629
35	15.028	9.836	17.078	-3.347	16.937	-2.543	16.739	-1.394	16.749	-1.448	16.506
40	13.407	9.580	14.993	-2.010	14.989	-1.984	15.030	-2.256	15.038	-2.304	14.691
45	12.120	11.073	13.889	-3.068	13.954	-3.524	13.672	-1.535	13.677	-1.568	13.462
50	11.073	11.852	12.784	-3.125	12.920	-4.139	12.572	-1.486	12.576	-1.522	12.385
60	9.465	11.262	10.576	-0.424	10.851	-2.945	10.879	-3.196	10.885	-3.253	10.531
70	8.286	12.820	9.409	-0.643	9.757	-4.189	9.642	-3.047	9.648	-3.100	9.348
80	7.382	12.944	8.242	1.159	8.664	-3.764	8.698	-4.143	8.702	-4.190	8.337
90	6.665	14.241	7.515	1.321	7.984	-4.635	7.952	-4.242	7.956	-4.290	7.614
100	6.082	13.881	6.788	2.035	7.305	-5.191	7.346	-5.719	7.350	-5.771	6.926
150	4.269	18.980	-	-	-	-	5.483	-7.368	5.485	-7.405	5.079
200	-	-	-	-	-	-	4.520	-	4.523	-	-

4-1-5 Stopping power for liver tissue

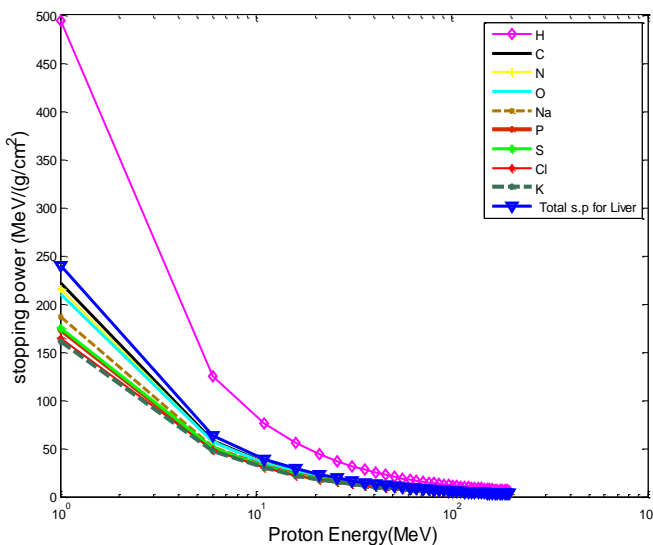


Fig. (4-21): Stopping power for proton in elements presented in liver tissue using Bethe equation.

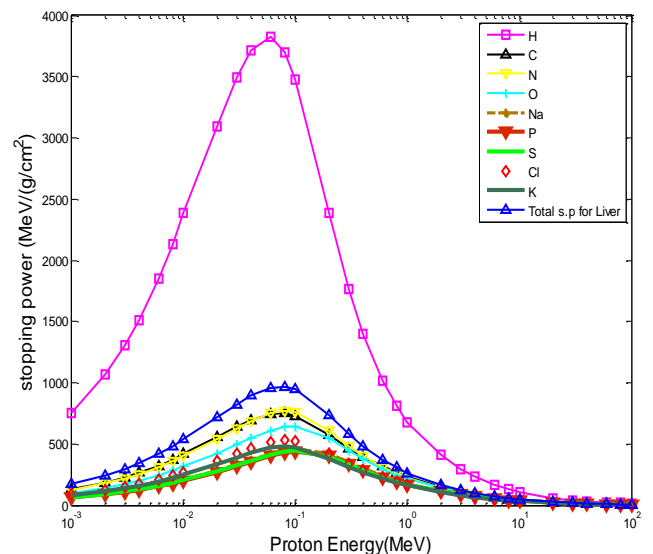


Fig. (4-22): Stopping power for proton in elements presented in liver tissue using Ziegler equation.

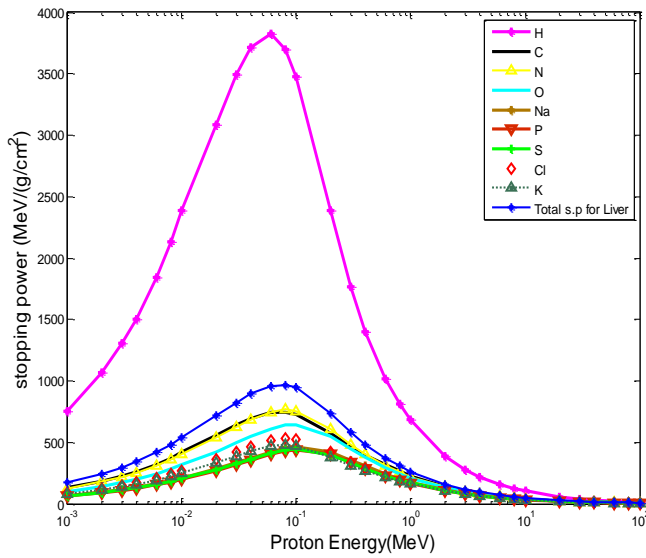


Fig. (4-23): Stopping power for proton in elements presented in liver tissue using ref. [100]

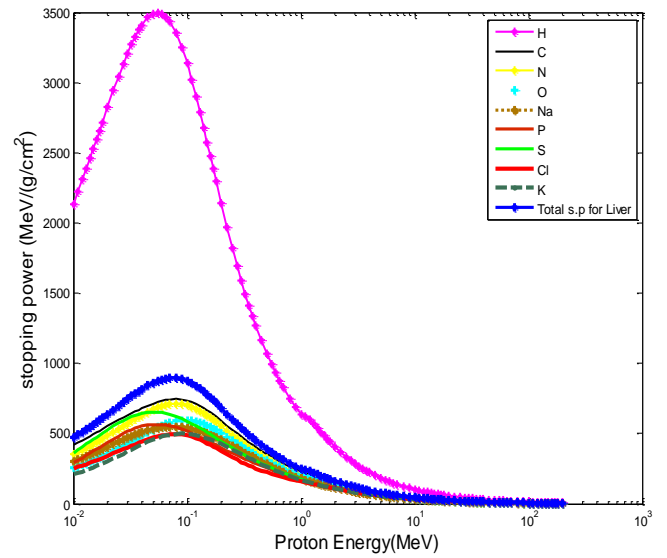


Fig. (4-24): Stopping power for proton in elements presented in liver tissue using SRIM program.

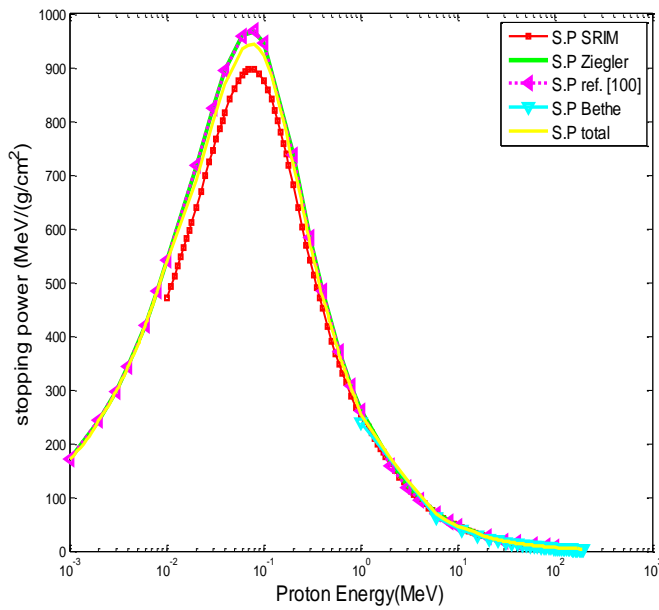


Fig. (4-25): Stopping power for liver tissue (present work)

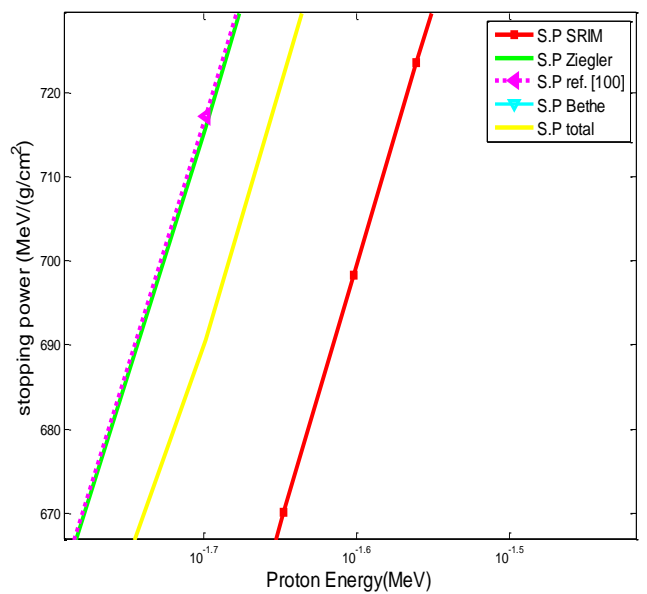


Fig. (4.25a): Stopping power for liver tissue from $(10^{-1.7}-10^{-1.5}\text{MeV})$ (present work).

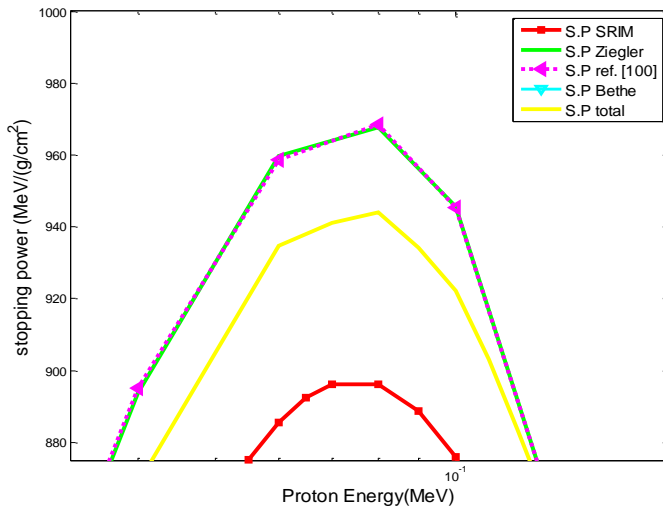


Fig. (4.25b): Stopping power for liver tissue from $(10^{-5}-10^{-1}\text{MeV})$ (present work).

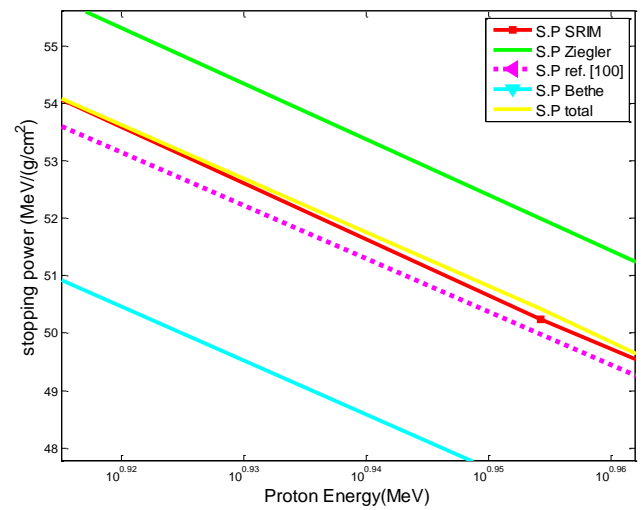


Fig. (4.25c): Stopping power for liver tissue from $(10^{0.92}-10^{0.96}\text{MeV})$ (present work).

Discussion of liver tissue results:

- 1- In figures (4-21), (4-22), (4-23) and (4-24) the proton's stopping power is large for hydrogen because the atomic number of hydrogen ($Z=1$) is less than Z for other elements in liver tissue.
- 2- Using the above methods, stopping power were compatible with the low and high energy region and different at medium energy range.
- 3- Ziegler and Andreson (Vol.3) [100], is very well represented with SRIM program at high energy.
- 4- Ziegler equation is very well represented with Ziegler and Andreson (Vol.3) [100], at all energies
- 5- Bethe 's equation gives values of stopping power a little lower than other methods, especially at high energy.
- 6- At high energy ($>1\text{MeV}$) stopping power decreases with the increase of proton energy, i.e., it does not have enough time to collide, and at intermediate energy region, stopping power reaches the maximum value (more ionization and excitation), while at low energies ($E < 25\text{KeV}$) we observe the increase of the stopping power with the increase of the proton's energy.
- 7- From figure (4-25b) Ziegler and Andreson (Vol.3) [100], gives high value of stopping power ($968.4 \text{ MeV-cm}^2/\text{g}$) at energy (0.08) MeV.

- 8- The percentage deviation $[\frac{S_{cal} - S_{exp}}{S_{exp}}] * 100$ between the experimental and the calculated stopping power values (using above methods) for liver tissue are shown in the following table, percentage deviation values convergent where deviation decreases as the energy of the proton increases (except Bethe). Bethe maximum deviation (14.160%), Ziegler maximum

deviation (7.790%) this leads that Ziegler gave better results from other methods, as shown in red color and minimum deviation is shown in green color in table (4-5).

Table (4-5): Percentage deviation (stopping power) in liver tissue in (MeV-cm²/g).

Stopping power in human tissues in (MeV-cm ² /g)									
E _p (MeV)	Liver tissue								S.P (P.W)
	Stopping power								
	Bethe	Error%	Ziegler	Error%	Ref. [100]	Error%	SRIM	Error%	
0.001	-	-	171.477	-0.055	171.289	0.055	-	-	171.383
1	240.297	5.648	263.154	-3.528	261.540	-2.933	250.475	1.355	253.869
2	204.972	-15.416	166.425	4.175	159.068	8.993	163.014	6.355	173.373
3	169.647	-21.935	122.865	7.790	117.395	12.812	119.831	10.519	132.436
4	134.322	-21.294	98.529	7.299	94.246	12.175	95.783	10.375	105.720
5	98.998	-12.636	85.105	1.626	81.490	6.134	80.361	7.625	86.489
6	63.703	7.398	71.688	-4.564	68.740	-0.471	69.533	-1.606	68.416
7	58.784	4.746	64.320	-4.269	61.718	-0.233	61.474	0.163	61.574
8	53.866	2.452	56.955	-3.105	54.698	0.892	55.226	-0.072	55.186
9	48.947	2.994	52.245	-3.508	50.225	0.372	50.232	0.359	50.412
10	44.028	4.165	47.538	-3.525	45.755	0.234	46.127	-0.574	45.862
15	30.820	11.213	37.174	-7.797	35.921	-4.580	33.188	3.277	34.275
20	24.091	7.116	26.808	-3.739	26.084	-1.069	26.238	-1.650	25.805
25	19.921	9.362	22.925	-4.971	22.425	-2.851	21.872	-0.394	21.785
30	17.055	8.066	19.042	-3.212	18.766	-1.785	18.860	-2.275	18.431
35	14.953	9.326	16.971	-3.672	16.831	-2.867	16.637	-1.736	16.348
40	13.341	8.831	14.900	-2.559	14.896	-2.531	14.939	-2.812	14.519
45	12.061	10.528	13.803	-3.425	13.868	-3.876	13.590	-1.910	13.330
50	11.018	11.318	12.706	-3.469	12.840	-4.477	12.496	-1.849	12.265
60	9.419	10.228	10.512	-1.234	10.785	-3.729	10.814	-3.992	10.383
70	8.246	11.819	9.353	-1.411	9.698	-4.925	9.585	-3.806	9.221
80	7.346	11.613	8.193	0.079	8.612	-4.787	8.647	-5.173	8.200
90	6.633	12.866	7.471	0.213	7.937	-5.675	7.905	-5.299	7.487
100	6.053	10.334	6.748	-1.036	7.262	-8.040	7.304	-8.563	6.678
150	4.249	14.160	-	-	-	-	5.452	-11.037	4.850
200	-	-	-	-	-	-	4.495	-	-

4-1-6 Stopping power for spleen tissue

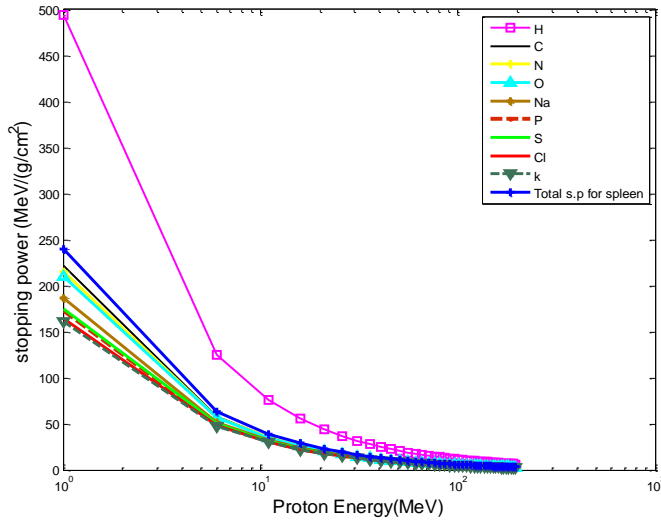


Fig. (4-26): Stopping power for proton in elements presented in spleen tissue using Bethe equation.

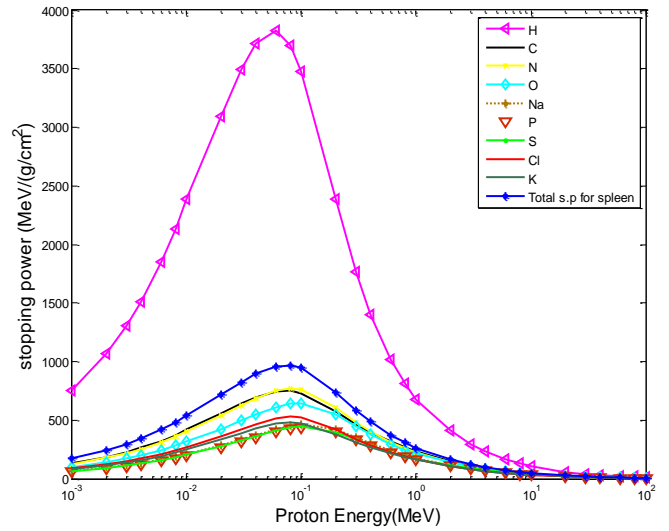


Fig. (4-27): Stopping power for proton in elements presented in spleen tissue using Ziegler equation.

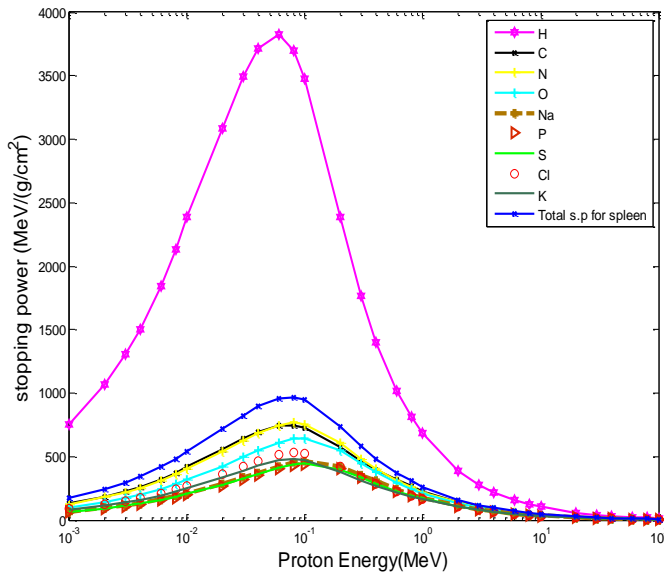


Fig. (4-28): Stopping power for proton in elements presented in spleen tissue using ref. [100].

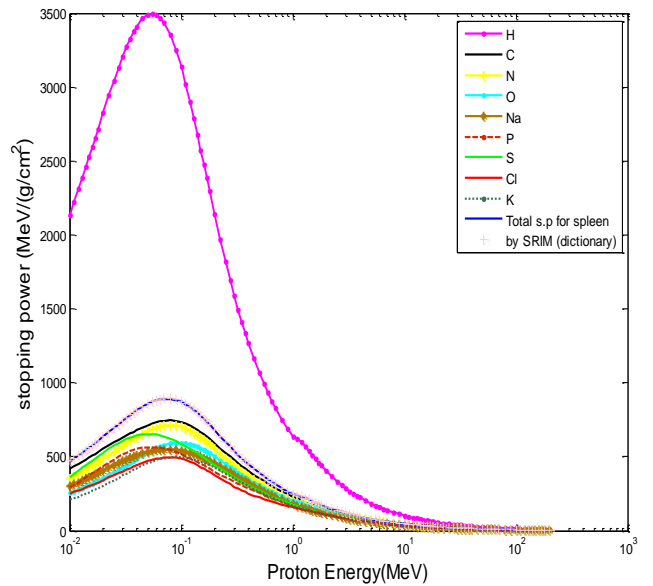


Fig. (4-29): Stopping power for proton in elements presented in spleen tissue using SRIM and SRIM (dictionary) program.

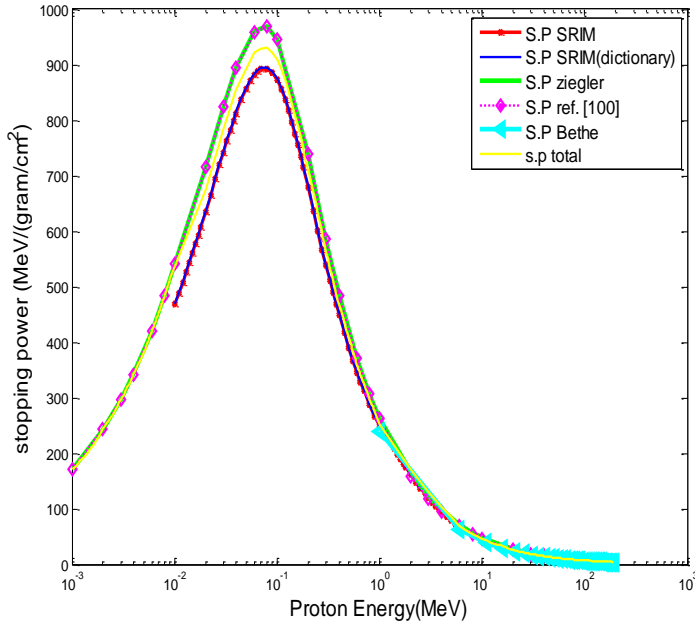


Fig. (4-30): Stopping power for spleen tissue (present work).

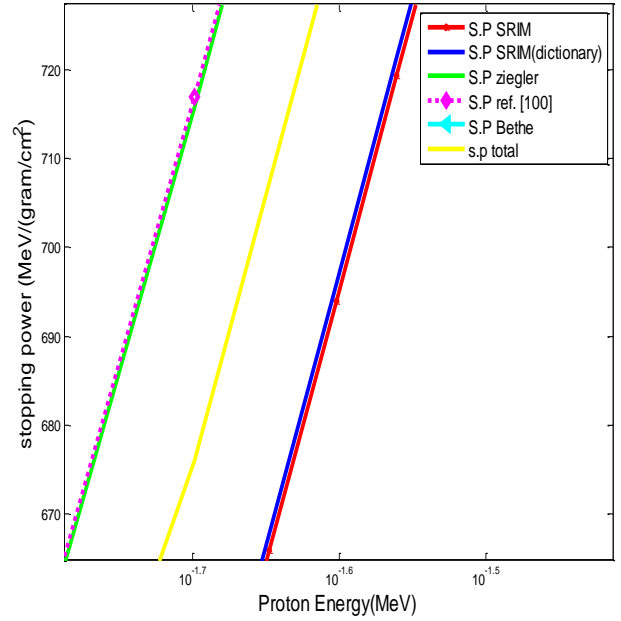


Fig. (4.30a): Stopping power for spleen tissue from (10^{-1.7}-10^{-1.5}MeV) (present work).

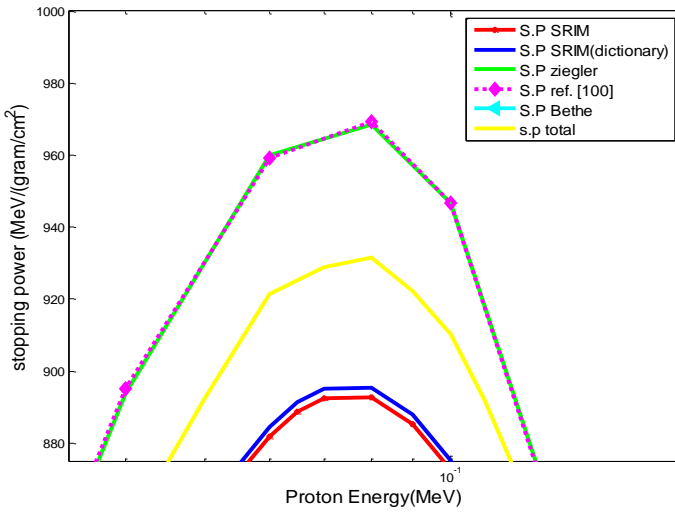


Fig. (4.30b): Stopping power for spleen tissue from (10⁻⁵-10⁻¹MeV) (present work).

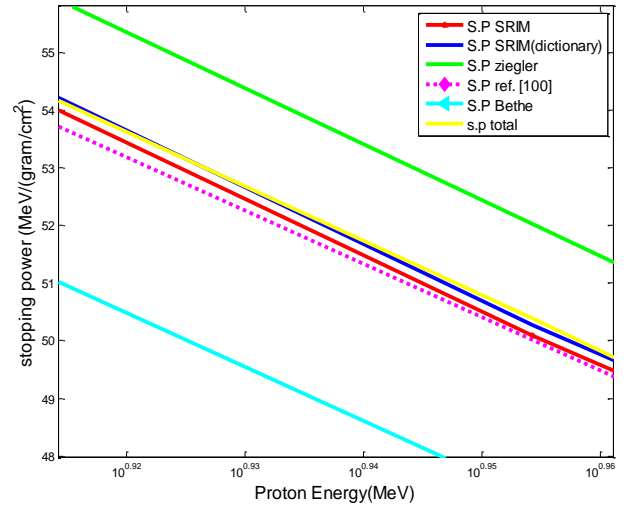


Fig. (4.30c): Stopping power for spleen tissue from (10^{0.92}-10^{0.96}MeV) (present work).

Discussion of spleen tissue results:

- 1- In figures (4-26), (4-27), (4-28) and (4-29) the proton's stopping power is large for hydrogen because the atomic number of hydrogen ($Z=1$) is less than Z for other elements in spleen tissue.
- 2- Using the above methods, stopping power were compatible with the low and high energy region and different at medium energy range.

- 3- Ziegler and Andreson (Vol.3) [100], are very well represented with SRIM and SRIM (dictionary) program at high energy.
- 4- Ziegler equation is very well represented with Ziegler and Andreson (Vol.3) [100], at all energies
- 5- Bethe 's equation gives values of stopping power a little lower than other methods, especially at high energy.
- 6- At high energy (>1MeV) stopping power decreases with the increase of proton energy, i.e., it does not have enough time to collide, and at intermediate energy region, stopping power reaches the maximum value (more ionization and excitation), while at low energies ($E < 25\text{KeV}$) we observe the increase of the stopping power with the increase of the proton's energy.
- 7- From figure (4-30b) Ziegler and Andreson (Vol.3) [100], gives high value of stopping power ($969.4 \text{ MeV-cm}^2/\text{g}$) at energy (0.08) MeV.
- 8- The percentage deviation $[\frac{S_{cal} - S_{exp}}{S_{exp}}]*100$ between the experimental and the calculated

stopping power values (using above methods) for spleen tissue are shown in the following table, percentage deviation values convergent where deviation decreases as the energy of the proton increases (except Bethe). Bethe maximum deviation (18.732%), Ziegler maximum deviation (5.679%) this leads that Ziegler gave better results from other methods, as shown in red color and minimum deviation is shown in green color in table (4-6).

Table (4-6): Percentage deviation (stopping power) in spleen tissue in (MeV-cm²/g).

Stopping power in human tissues in (MeV-cm ² /g)											
E _p (MeV)	Spleen tissue										S.P (P.W)
	Stopping power										
	Bethe	Error%	Ziegler	Error%	Ref. [100]	Error%	SRIM	Error%	SRIM dictionary	Error%	
0.001	-	-	171.419	-0.055	171.229	0.056	-	-	-	-	171.324
1	240.358	5.265	263.302	-3.908	261.645	-3.299	249.429	1.437	250.307	1.081	253.012
2	205.028	-16.454	166.507	2.874	159.138	7.638	162.610	5.340	163.157	4.987	171.293
3	169.697	-23.445	122.931	5.679	117.453	10.608	119.522	8.693	119.949	8.307	129.912
4	134.367	-22.800	98.586	5.219	94.301	10.000	95.527	8.588	95.873	8.196	103.731
5	99.036	-13.910	85.156	0.123	81.539	4.564	80.142	6.387	80.428	6.009	85.261
6	63.736	7.691	71.733	-4.315	68.784	-0.213	69.341	-1.014	69.593	-1.373	68.638
7	58.815	4.659	64.361	-4.359	61.758	-0.328	61.303	0.412	61.540	0.025	61.555
8	53.894	2.416	56.992	-3.151	54.735	0.842	55.071	0.227	55.287	-0.165	55.196
9	48.973	2.864	52.280	-3.642	50.260	0.230	50.090	0.570	50.275	0.200	50.376
10	44.052	4.230	47.570	-3.477	45.788	0.280	45.996	-0.174	46.173	-0.558	45.916
15	30.838	10.445	37.199	-8.443	35.946	-5.250	33.092	2.922	33.218	2.530	34.059
20	24.106	7.411	26.827	-3.485	26.103	-0.806	26.161	-1.029	26.264	-1.417	25.892
25	19.933	9.381	22.942	-4.964	22.441	-2.843	21.807	-0.020	21.892	-0.406	21.803
30	17.066	8.492	19.056	-2.841	18.779	-1.406	18.804	-1.535	18.870	-1.881	18.515
35	14.963	9.651	16.984	-3.396	16.843	-2.587	16.587	-1.086	16.659	-1.510	16.407
40	13.349	9.398	14.911	-2.062	14.907	-2.032	14.894	-1.949	14.958	-2.365	14.604
45	12.069	10.894	13.813	-3.114	13.878	-3.565	13.549	-1.225	13.607	-1.643	13.383
50	11.026	11.661	12.716	-3.181	12.850	-4.189	12.459	-1.188	12.506	-1.558	12.311
60	9.425	11.072	10.520	-0.487	10.792	-2.997	10.782	-2.900	10.825	-3.291	10.469
70	8.252	12.628	9.360	-0.707	9.705	-4.242	9.557	-2.752	9.595	-3.137	9.294
80	7.351	12.753	8.199	1.093	8.618	-3.820	8.621	-3.849	8.655	-4.231	8.289
90	6.638	14.049	7.476	1.255	7.943	-4.691	7.881	-3.950	7.913	-4.329	7.570
100	6.057	13.642	6.753	1.924	7.267	-5.287	7.282	-5.471	7.311	-5.854	6.883
150	4.252	18.732	-	-	-	-	5.435	-7.126	5.457	-7.498	5.048
200	-	-	-	-	-	-	4.482	-	4.500	-	-

4-1-7 Stopping power for blood tissue

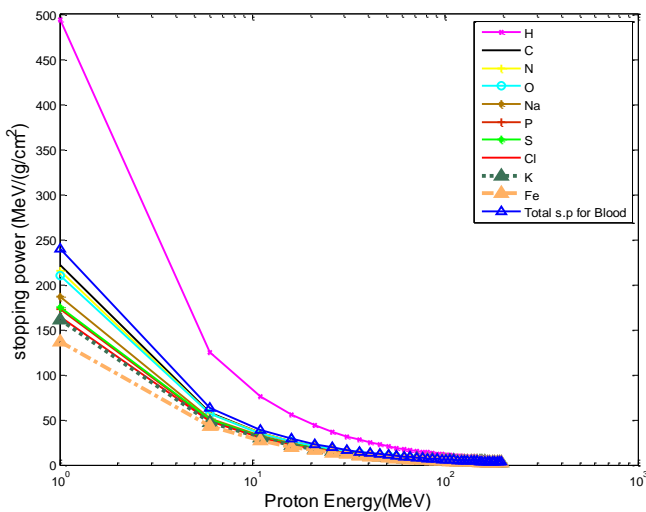


Fig. (4-31): Stopping power for proton in elements presented in blood tissue using Bethe equation.

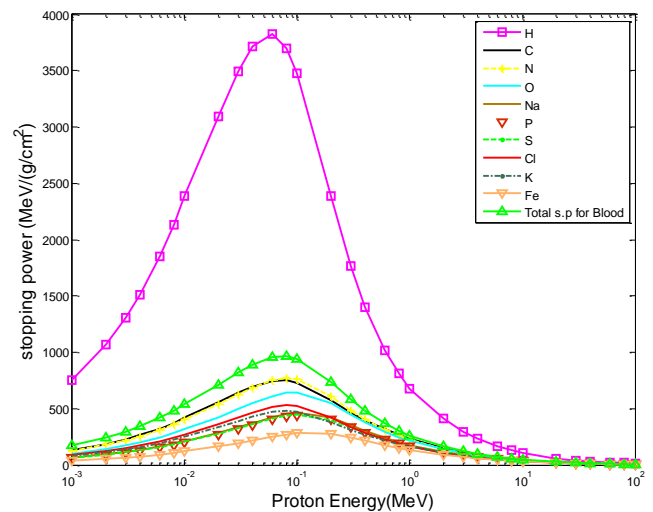


Fig. (4-32): Stopping power for proton in elements presented in blood tissue using Ziegler equation.

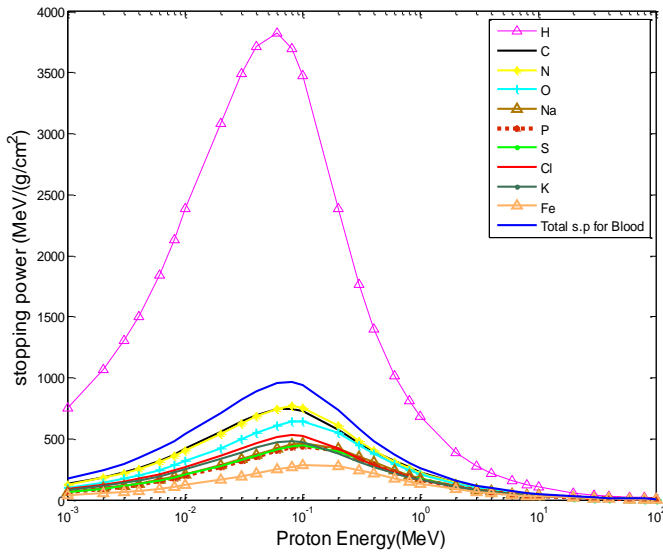


Fig. (4-33): Stopping power for proton in elements presented in blood tissue using ref. [100]

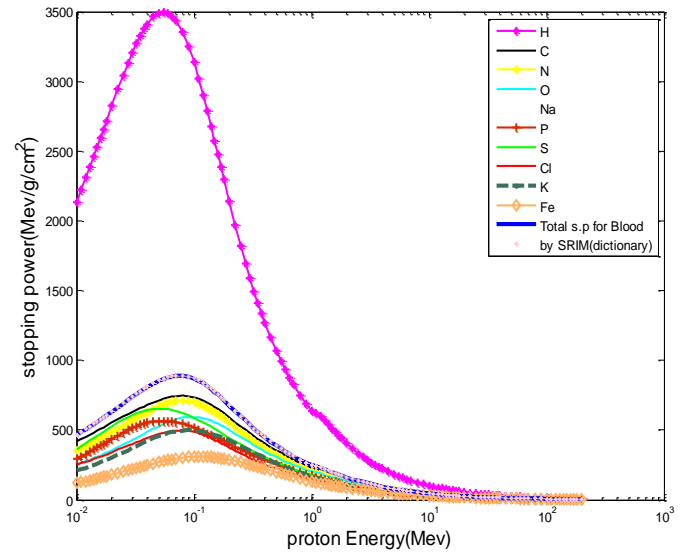


Fig. (4-34): Stopping power for proton in elements presented in blood tissue using SRIM and SRIM (dictionary).

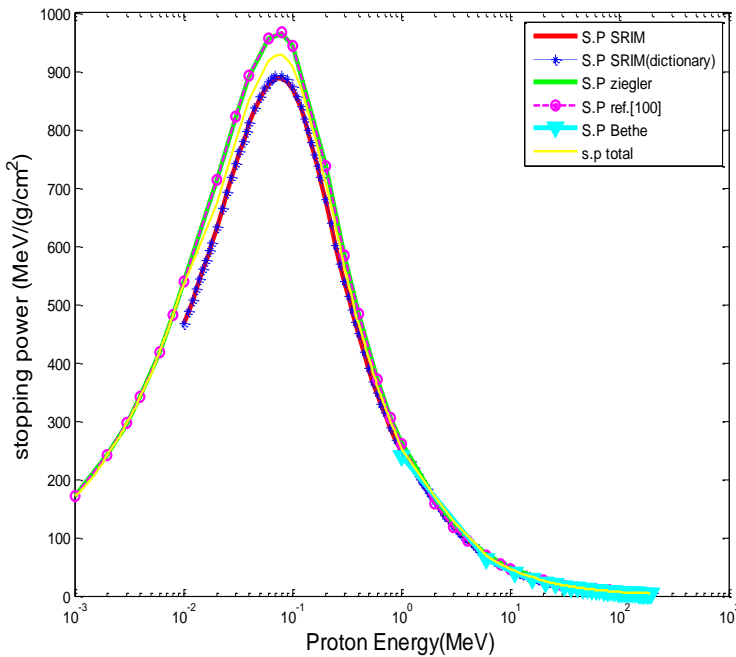


Fig. (4-35): Stopping power for blood tissue (present work).

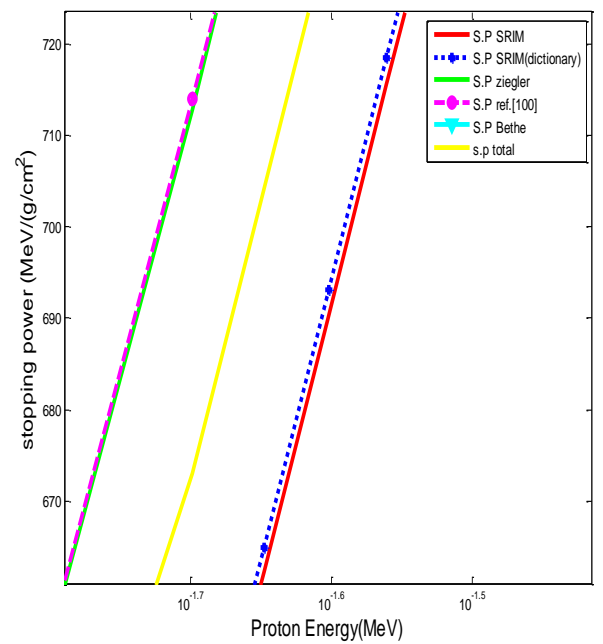


Fig. (4.35a): Stopping power for blood tissue from $10^{-1.7}$ - $10^{-1.5}$ MeV (present work).

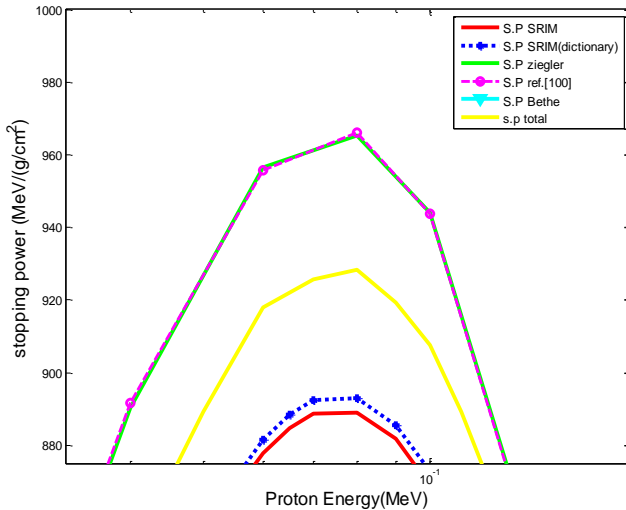


Fig. (4.35b): Stopping power for blood tissue from (10^{-5} - 10^{-1} MeV) (present work).

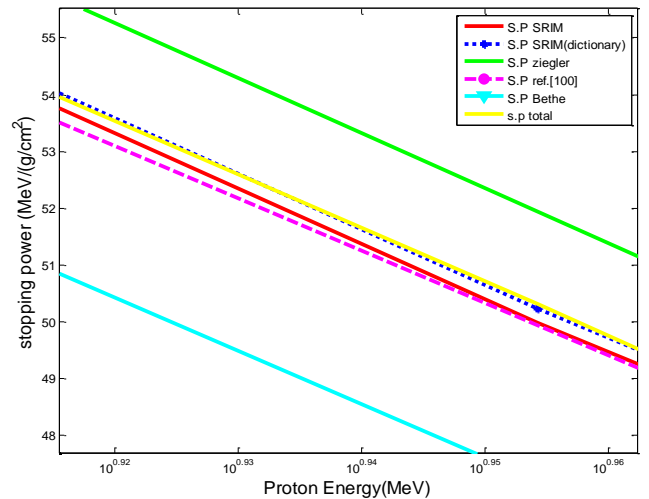


Fig. (4.35c): Stopping power for blood tissue from ($10^{0.91}$ - $10^{0.95}$ MeV) (present work).

Discussion of blood tissue results:

- 1- In figures (4-31), (4-32), (4-33) and (4-34) the proton's stopping power is large for hydrogen because the atomic number of hydrogen ($Z=1$) is less than Z for other elements in blood tissue.
- 2- Using the above methods, stopping power were compatible with the low and high energy region and different at medium energy range.
- 3- Ziegler and Andreson (Vol.3) [100], are very well represented with SRIM and SRIM (dictionary) program at high energy.
- 4- Ziegler equation is very well represented with Ziegler and Andreson (Vol.3) [100], at all energies
- 5- Bethe 's equation gives values of stopping power a little lower than other methods, especially at high energy.
- 6- At high energy (>1 MeV) stopping power decreases with the increase of proton energy, i.e., it does not have enough time to collide, and at intermediate energy region, stopping power reaches the maximum value (more ionization and excitation), while at low energies ($E < 25$ KeV) we observe the increase of the stopping power with the increase of the proton's energy.
- 7- From figure (4-35b) Ziegler and Andreson (Vol.3) [100], gives high value of stopping power ($966.2 \text{ MeV-cm}^2/\text{g}$) at energy (0.08) MeV.

- 8- The percentage deviation $\left[\frac{S_{cal} - S_{exp}}{S_{exp}} \right] * 100$ between the experimental and the calculated

stopping power values (using above methods) for blood tissue are shown in the following table, percentage deviation values convergent where deviation decreases as the energy of the proton increases (except Bethe). Bethe maximum deviation (18.700%), Ziegler maximum deviation (5.696%) this leads that Ziegler gave better results from other methods, as shown in red color and minimum deviation is shown in green color in table (4-7).

Table (4-7): Percentage deviation (stopping power) in blood tissue in (MeV-cm²/g)

Stopping power in human tissues in (MeV-cm ² /g)											
E _p (MeV)	Blood tissue										S.P (P.W)
	Stopping power										
	Bethe	Error%	Ziegler	Error%	Ref. [100]	Error%	SRIM	Error%	SRIM dictio- nary	Error%	
0.001	-	-	170.714	-0.055	170.525	0.056	-	-	-	-	170.620
1	240.050	5.203	262.809	-3.908	261.137	-3.292	248.773	1.514	249.908	1.053	252.539
2	204.766	-16.484	166.215	2.886	158.861	7.649	162.239	5.408	162.956	4.944	171.012
3	169.483	-23.463	122.727	5.696	117.259	10.625	119.260	8.769	119.849	8.234	129.718
4	134.200	-22.819	98.428	5.232	94.151	10.012	95.322	8.661	95.783	8.137	103.577
5	98.916	-13.931	85.022	0.134	81.412	4.575	79.972	6.458	80.358	5.947	85.136
6	63.663	7.659	71.623	-4.306	68.679	-0.204	69.195	-0.949	69.533	-1.430	68.539
7	58.748	4.627	64.263	-4.352	61.665	-0.323	61.175	0.476	61.480	-0.022	61.466
8	53.833	2.386	56.907	-3.144	54.654	0.848	54.957	0.293	55.237	-0.217	55.118
9	48.918	2.837	52.202	-3.633	50.186	0.238	49.987	0.638	50.235	0.141	50.306
10	44.003	4.201	47.500	-3.471	45.721	0.286	45.901	-0.107	46.133	-0.610	45.852
15	30.803	10.414	37.146	-8.439	35.894	-5.246	33.025	2.988	33.188	2.480	34.011
20	24.079	7.385	26.790	-3.480	26.066	-0.801	26.108	-0.961	26.244	-1.474	25.857
25	19.911	9.352	22.910	-4.962	22.410	-2.840	21.763	0.046	21.872	-0.450	21.773
30	17.047	8.471	19.030	-2.833	18.753	-1.397	18.766	-1.463	18.860	-1.954	18.491
35	14.947	9.616	16.961	-3.400	16.820	-2.592	16.554	-1.027	16.639	-1.530	16.384
40	13.335	9.359	14.891	-2.071	14.887	-2.041	14.864	-1.893	14.938	-2.375	14.583
45	12.056	10.869	13.795	-3.111	13.860	-3.562	13.522	-1.157	13.597	-1.698	13.366
50	11.014	11.635	12.699	-3.178	12.832	-4.186	12.434	-1.120	12.496	-1.609	12.295
60	9.415	11.044	10.506	-0.488	10.778	-2.998	10.760	-2.836	10.815	-3.331	10.455
70	8.243	12.600	9.347	-0.707	9.692	-4.242	9.538	-2.687	9.587	-3.184	9.281
80	7.344	12.727	8.189	1.093	8.607	-3.818	8.604	-3.783	8.648	-4.277	8.278
90	6.631	14.023	7.467	1.256	7.932	-4.690	7.866	-3.884	7.907	-4.379	7.560
100	6.051	13.615	6.745	1.923	7.258	-5.287	7.267	-5.407	7.305	-5.899	6.874
150	4.247	18.700	-	-	-	-	5.425	-7.068	5.452	-7.536	5.041
200	-	-	-	-	-	-	4.473	-	4.496	-	-

4-1-8 Stopping power for ovary tissue

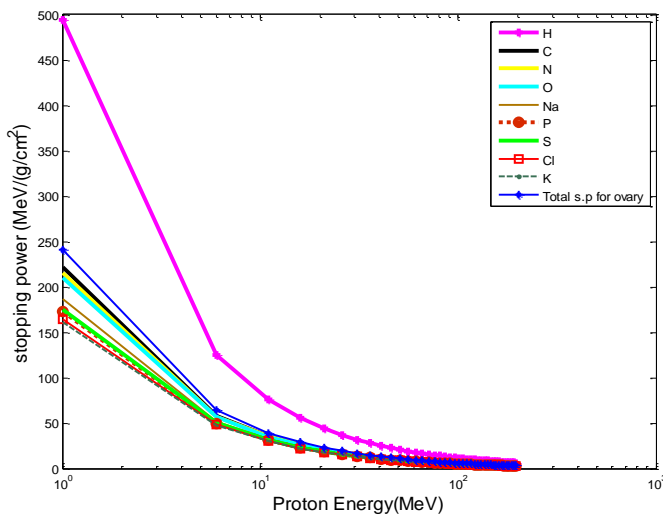


Fig. (4-36): Stopping power for proton in elements presented in ovary tissue using Bethe equation.

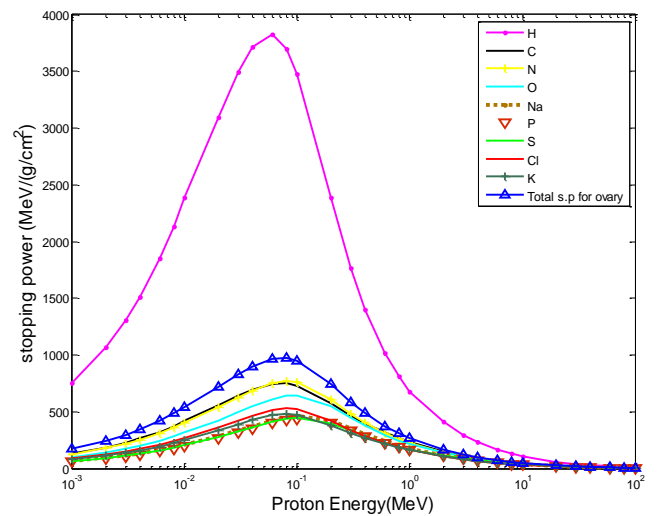


Fig. (4-37): Stopping power for proton in elements presented in ovary tissue using Ziegler equation.

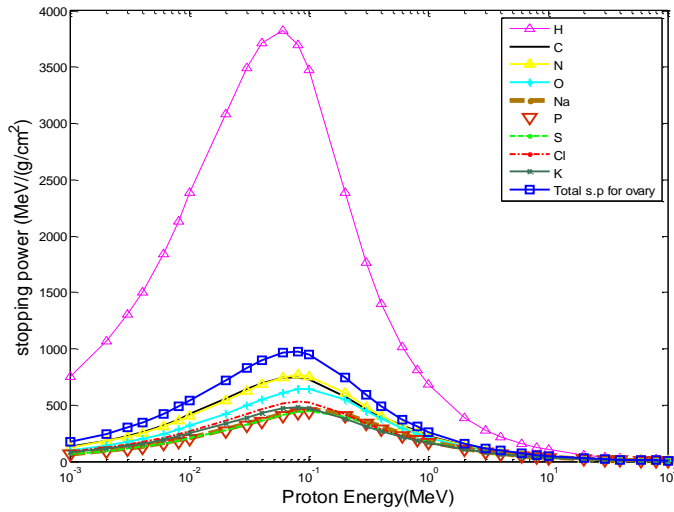


Fig. (4-38): Stopping power for proton in elements presented in ovary tissue using ref. [100].

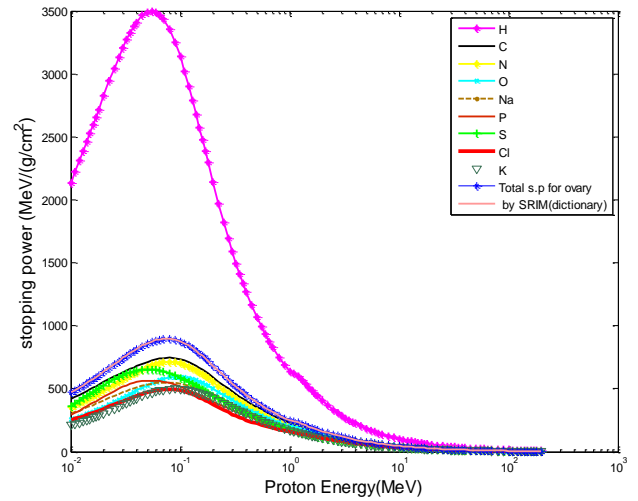


Fig. (4-39): Stopping power for proton in elements presented in ovary tissue using SRIM and SRIM (dictionary).

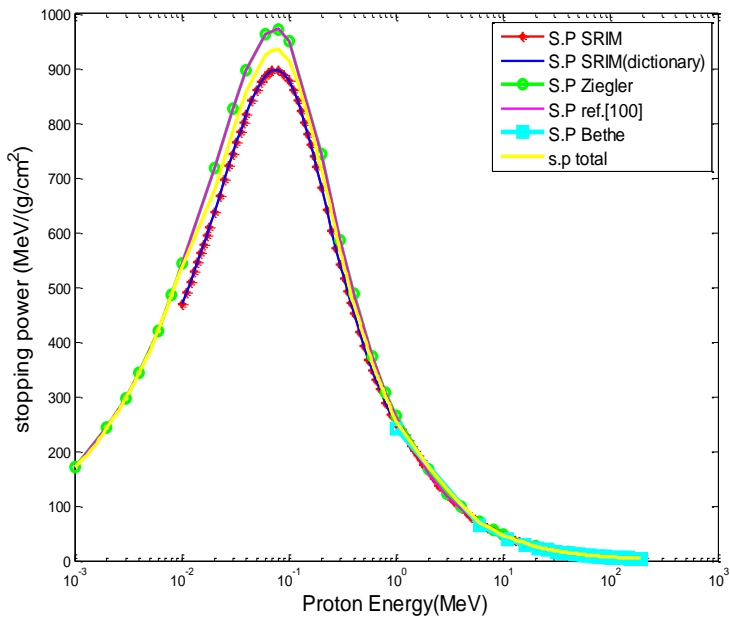


Fig. (4-40): Stopping power for ovary tissue (present work).

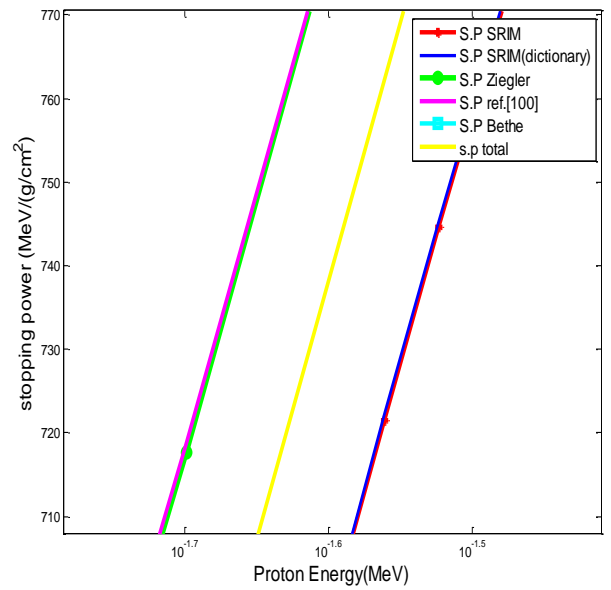


Fig. (4.40a): Stopping power for ovary tissue from (10^{-1.7}-10^{-1.5}MeV) (present work).

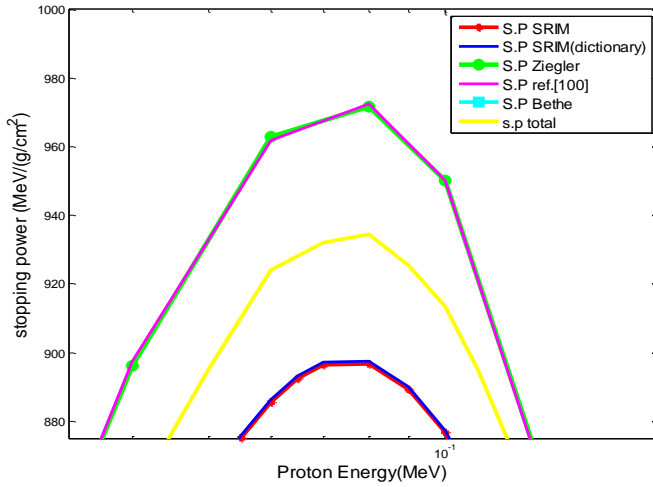


Fig. (4.40b): Stopping power for ovary tissue from $(10^{-5}-10^{-1}\text{MeV})$ (present work).

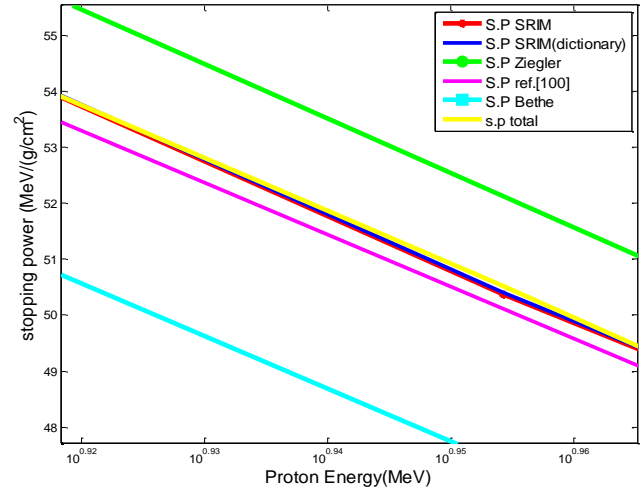


Fig. (4.40c): Stopping power for ovary tissue from $(10^{0.92}-10^{0.96}\text{MeV})$ (present work).

Discussion of ovary tissue results:

- 1- In figures (4-36), (4-37), (4-38) and (4-39) the proton's stopping power is large for hydrogen because the atomic number of hydrogen ($Z=1$) is less than Z for other elements in ovary tissue.
- 2- Using the above methods, stopping power were compatible with the low and high energy region and different at medium energy range.
- 3- Ziegler and Andreson (Vol.3) [100], are very well represented with SRIM and SRIM (dictionary) program at high energy.
- 4- Ziegler equation is very well represented with Ziegler and Andreson (Vol.3) [100], at all energies
- 5- Bethe 's equation gives values of stopping power a little lower than other methods, especially at high energy.
- 6- At high energy ($>1\text{MeV}$) stopping power decreases with the increase of proton energy, i.e., it does not have enough time to collide, and at intermediate energy region, stopping power reaches the maximum value (more ionization and excitation), while at low energies ($E < 25\text{KeV}$) we observe the increase of the stopping power with the increase of the proton's energy.
- 7- From figure (4-40b) Ziegler and Andreson (Vol.3) [100], gives high value of stopping power ($972.5 \text{ MeV}\cdot\text{cm}^2/\text{g}$) at energy (0.08) MeV.

- 8- The percentage deviation $\left[\frac{S_{cal} - S_{exp}}{S_{exp}} \right] * 100$ between the experimental and the calculated

stopping power values (using above methods) for ovary tissue are shown in the following table, percentage deviation values convergent where deviation decreases as the energy of the proton increases (except Bethe). Bethe maximum deviation (18.933%), Ziegler maximum

deviation (5.742%) this leads that Ziegler gave better results from other methods, as shown in red color and minimum deviation is shown in green color in table (4-8).

Table (4-8): Percentage deviation (stopping power) in ovary tissue in (MeV-cm²/g).

Stopping power in human tissues in (MeV-cm ² /g)											
E _p (MeV)	Ovary tissue										S.P (P.W)
	Stopping power										
	Bethe	Error%	Ziegler	Error%	Ref. [100]	Error%	SRIM	Error%	SRIM dictio- nary	Error%	
0.001	-	-	171.892	-0.056	171.700	0.056	-	-	-	-	171.796
1	240.721	5.359	263.886	-3.890	262.213	-3.277	250.561	1.222	250.710	1.162	253.622
2	205.339	-16.346	166.855	2.948	159.461	7.721	163.534	5.039	163.657	4.960	171.774
3	169.956	-23.358	123.185	5.742	117.690	10.679	120.197	8.370	120.249	8.323	130.257
4	134.574	-22.712	98.788	5.286	94.494	10.070	96.066	8.269	96.124	8.204	104.010
5	99.192	-13.811	85.330	0.190	81.707	4.633	80.594	6.078	80.638	6.020	85.493
6	63.840	7.817	71.879	-4.241	68.925	-0.138	69.733	-1.294	69.774	-1.352	68.830
7	58.911	4.778	64.492	-4.289	61.885	-0.257	61.650	0.123	61.690	0.057	61.726
8	53.982	2.533	57.108	-3.079	54.847	0.916	55.383	-0.060	55.428	-0.141	55.349
9	49.053	2.982	52.386	-3.568	50.363	0.304	50.375	0.281	50.405	0.221	50.516
10	44.125	4.351	47.666	-3.402	45.882	0.355	46.257	-0.459	46.293	-0.537	46.044
15	30.889	10.566	37.275	-8.376	36.019	-5.183	33.281	2.618	33.298	2.564	34.152
20	24.146	7.528	26.881	-3.414	26.155	-0.731	26.311	-1.323	26.324	-1.371	25.963
25	19.966	9.499	22.988	-4.894	22.485	-2.769	21.933	-0.320	21.942	-0.360	21.863
30	17.094	8.618	19.094	-2.760	18.816	-1.322	18.912	-1.823	18.920	-1.863	18.567
35	14.988	9.773	17.018	-3.320	16.876	-2.510	16.683	-1.381	16.699	-1.472	16.453
40	13.372	9.511	14.941	-1.992	14.936	-1.962	14.980	-2.248	14.988	-2.297	14.643
45	12.089	11.012	13.841	-3.041	13.906	-3.492	13.628	-1.526	13.637	-1.590	13.420
50	11.044	11.785	12.741	-3.103	12.875	-4.111	12.532	-1.485	12.536	-1.520	12.346
60	9.441	11.184	10.541	-0.417	10.814	-2.926	10.844	-3.203	10.845	-3.210	10.497
70	8.266	12.752	9.378	-0.626	9.724	-4.162	9.612	-3.045	9.618	-3.099	9.320
80	7.364	12.879	8.215	1.178	8.635	-3.737	8.671	-4.138	8.676	-4.193	8.312
90	6.649	14.175	7.491	1.340	7.958	-4.608	7.928	-4.240	7.932	-4.289	7.591
100	6.067	13.835	6.767	2.069	7.281	-5.146	7.324	-5.702	7.328	-5.754	6.907
150	4.259	18.933	-	-	-	-	5.467	-7.358	5.469	-7.389	5.065
200	-	-	-	-	-	-	4.508	-	4.510	-	-

4-1-9 Stopping power for testis tissue

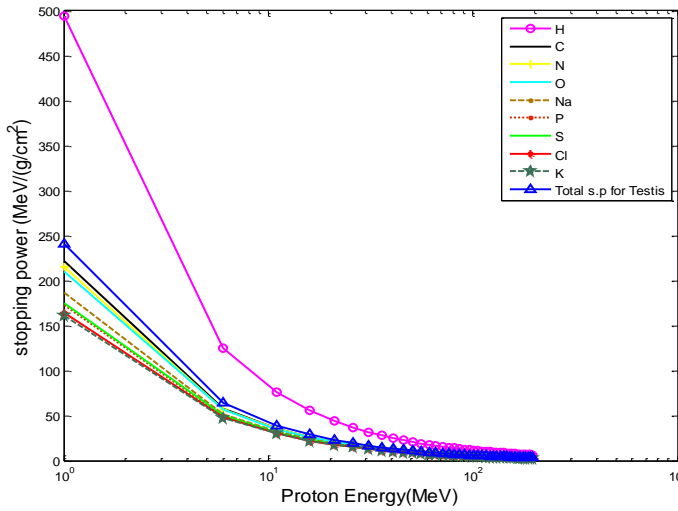


Fig. (4-41): Stopping power for proton in elements presented in testis tissue using Bethe equation.

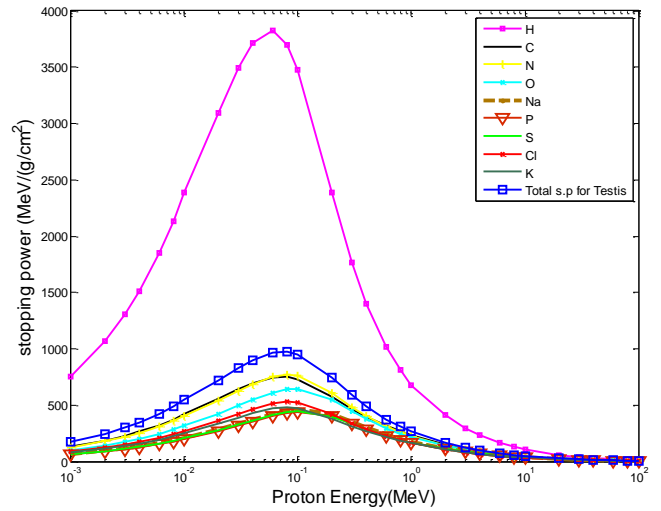


Fig. (4-42): Stopping power for proton in elements presented in testis tissue using Ziegler equation.

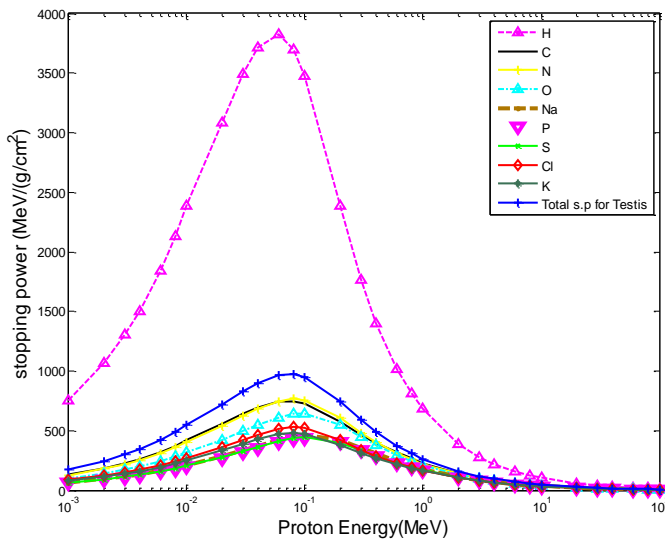


Fig. (4-43): Stopping power for proton in elements presented in testis tissue using ref. [100].

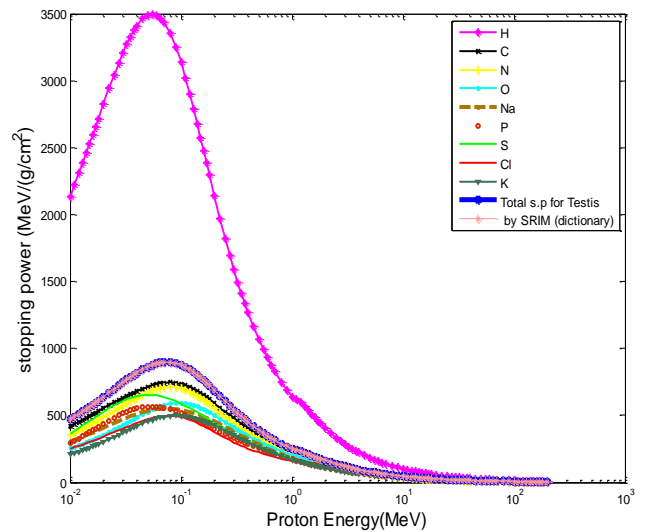


Fig. (4-44): Stopping power for proton in elements presented in testis tissue using SRIM and SRIM (dictionary).

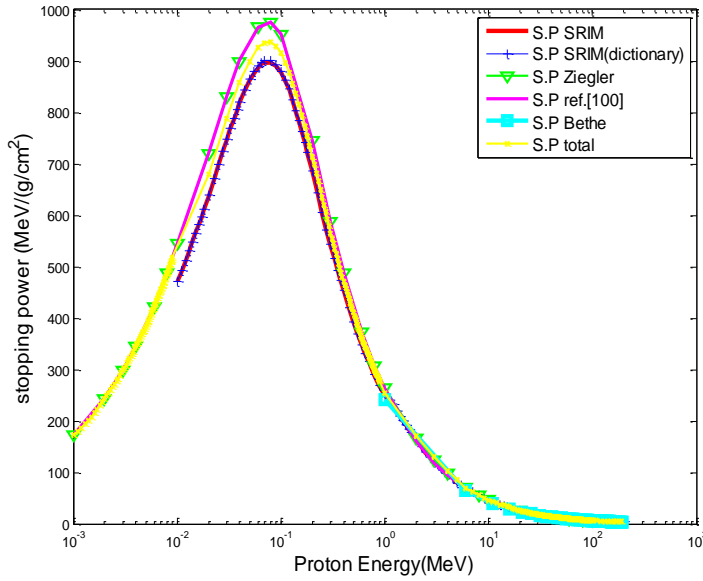


Fig. (4-45): Stopping power for testis tissue (present work).

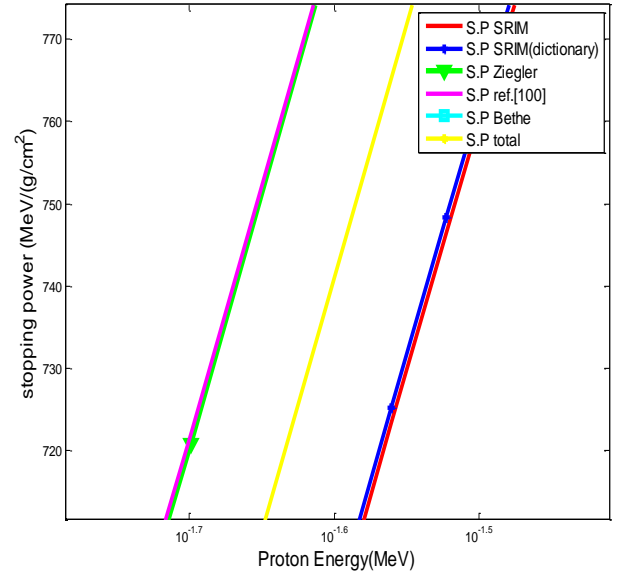


Fig. (4.45a): Stopping power for testis tissue from $(10^{-1.7}-10^{-1.5})$ MeV (present work).

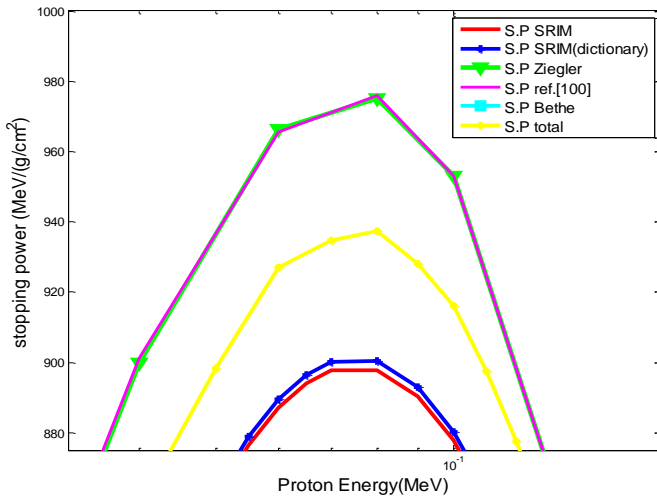


Fig. (4.45b): Stopping power for testis tissue from $(10^{-5}-10^{-1})$ MeV (present work).

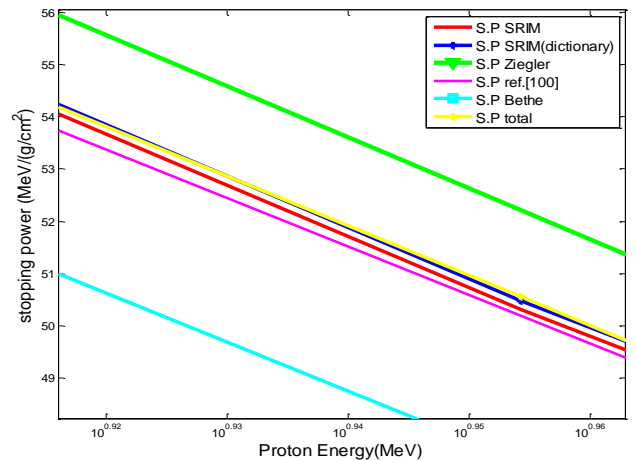


Fig. (4.45c): Stopping power for testis tissue from $(10^{0.92}-10^{0.96})$ MeV (present work).

Discussion of testis tissue results:

- 1- In figures (4-41), (4-42), (4-43), and (4-44) the proton's stopping power is large for hydrogen because the atomic number of hydrogen ($Z=1$) is less than Z for other elements in testis tissue.
- 2- Using the above methods, stopping power were compatible with the low and high energy region and different at medium energy range.
- 3- Ziegler and Andreson (Vol.3) [100], are very well represented with SRIM and SRIM (dictionary) program at high energy.
- 4- Ziegler equation is very well represented with Ziegler and Andreson (Vol.3) [100], at all energies

- 5- Bethe 's equation gives values of stopping power a little lower than other methods, especially at high energy.
- 6- At high energy (>1MeV) stopping power decreases with the increase of proton energy, i.e., it does not have enough time to collide, and at intermediate energy region, stopping power reaches the maximum value (more ionization and excitation), while at low energies ($E < 25\text{KeV}$) we observe the increase of the stopping power with the increase of the proton's energy.
- 7- From figure (4-45b) Ziegler and Andreson (Vol.3) [100], gives high value of stopping power ($975.9 \text{ MeV-cm}^2/\text{g}$) at energy (0.08) MeV.
- 8- The percentage deviation $[\frac{S_{cal} - S_{exp}}{S_{exp}}]*100$ between the experimental and the calculated

stopping power values (using above methods) for testis tissue are shown in the following table, percentage deviation values convergent where deviation decreases as the energy of the proton increases (except Bethe). Bethe maximum deviation (18.815%), Ziegler maximum deviation (5.673%) this leads that Ziegler gave better results from other methods, as shown in red color and minimum deviation is shown in green color in table (4-9).

Table (4-9): Percentage deviation (stopping power) in testis tissue in ($\text{MeV-cm}^2/\text{g}$).

Stopping power in human tissues in ($\text{MeV-cm}^2/\text{g}$)											
E_p (MeV)	Testis tissue										S.P (P.W)
	Stopping power										
	Bethe	Error%	Ziegler	Error%	Ref. [100]	Error%	SRIM	Error%	SRIM dictio- nary	Error%	
0.001	-	-	172.667	-0.056	172.475	0.056	-	-	-	-	172.571
1	241.087	5.371	264.451	-3.938	262.793	-3.332	250.522	1.403	251.309	1.085	254.036
2	205.648	-16.370	167.187	2.869	159.777	7.640	163.422	5.239	163.857	4.959	171.983
3	170.209	-23.378	123.416	5.673	117.910	10.607	120.091	8.598	120.450	8.275	130.417
4	134.770	-22.736	98.967	5.217	94.664	9.999	95.970	8.502	96.274	8.160	104.130
5	99.331	-13.837	85.482	0.122	81.851	4.563	80.508	6.308	80.758	5.979	85.586
6	63.922	7.786	72.003	-4.310	69.044	-0.209	69.653	-1.082	69.874	-1.394	68.899
7	58.987	4.747	64.602	-4.357	61.990	-0.327	61.577	0.342	61.780	0.011	61.787
8	54.052	2.497	57.203	-3.151	54.939	0.842	55.315	0.156	55.498	-0.174	55.401
9	49.116	2.949	52.473	-3.637	50.446	0.234	50.311	0.503	50.475	0.177	50.564
10	44.181	4.314	47.745	-3.473	45.956	0.283	46.197	-0.240	46.353	-0.576	46.086
15	30.927	10.526	37.335	-8.443	36.077	-5.251	33.235	2.850	33.339	2.531	34.182
20	24.175	7.491	26.923	-3.479	26.195	-0.798	26.273	-1.094	26.364	-1.434	25.986
25	19.990	9.458	23.023	-4.960	22.520	-2.837	21.900	-0.088	21.972	-0.413	21.881
30	17.115	8.568	19.123	-2.834	18.845	-1.398	18.883	-1.600	18.940	-1.893	18.581
35	15.006	9.726	17.043	-3.390	16.902	-2.581	16.657	-1.153	16.719	-1.515	16.465
40	13.388	9.466	14.963	-2.061	14.959	-2.032	14.957	-2.020	15.008	-2.352	14.655
45	12.103	10.970	13.861	-3.107	13.926	-3.558	13.606	-1.290	13.657	-1.655	13.431
50	11.057	11.726	12.760	-3.182	12.894	-4.190	12.512	-1.263	12.546	-1.534	12.354
60	9.452	11.148	10.556	-0.477	10.829	-2.985	10.827	-2.963	10.865	-3.306	10.506
70	8.275	12.701	9.392	-0.697	9.738	-4.232	9.597	-2.817	9.630	-3.150	9.326
80	7.372	12.825	8.227	1.102	8.647	-3.809	8.657	-3.913	8.686	-4.238	8.318
90	6.657	14.120	7.502	1.264	7.969	-4.679	7.914	-4.016	7.941	-4.333	7.597
100	6.074	13.722	6.776	1.942	7.292	-5.262	7.312	-5.527	7.337	-5.854	6.908
150	4.264	18.815	-	-	-	-	5.458	-7.182	5.476	-7.492	5.066
200	-	-	-	-	-	-	4.500	-	4.516	-	-

4-1-10 Stopping power for prostate tissue

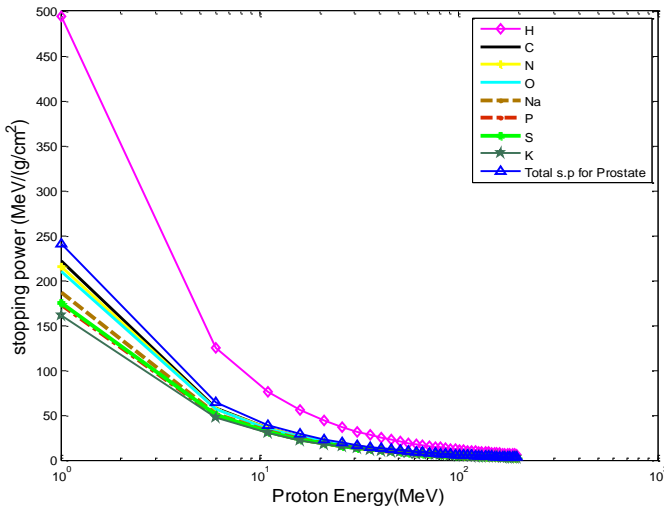


Fig. (4-46): Stopping power for proton in elements presented in prostate tissue using Bethe equation.

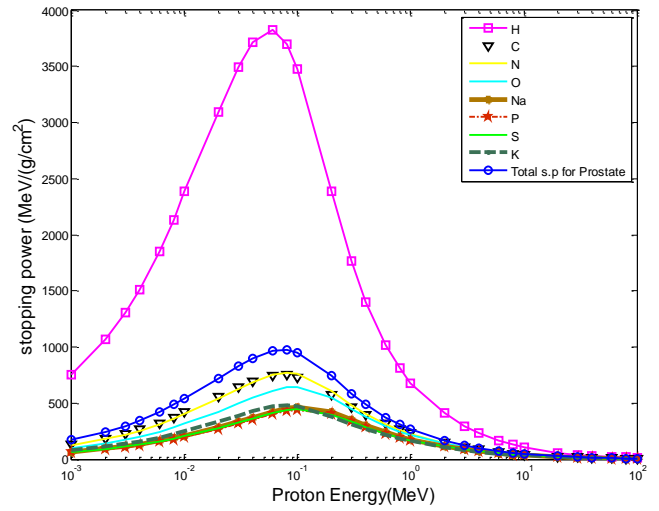


Fig. (4-47): Stopping power for proton in elements presented in prostate tissue using Ziegler equation.

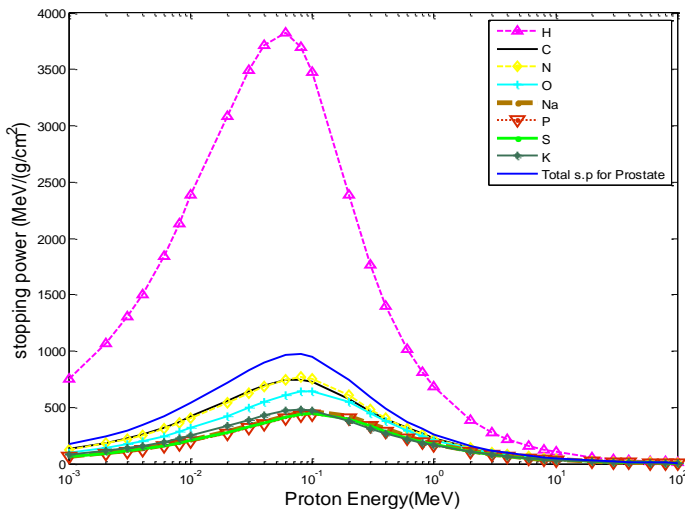


Fig. (4-48): Stopping power for proton in elements presented in prostate tissue using ref. [100].

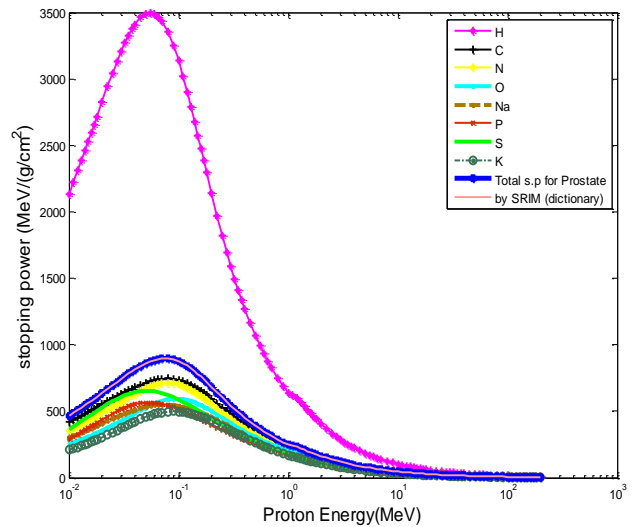


Fig. (4-49): Stopping power for proton in elements presented in prostate tissue using SRIM and SRIM (dictionary).

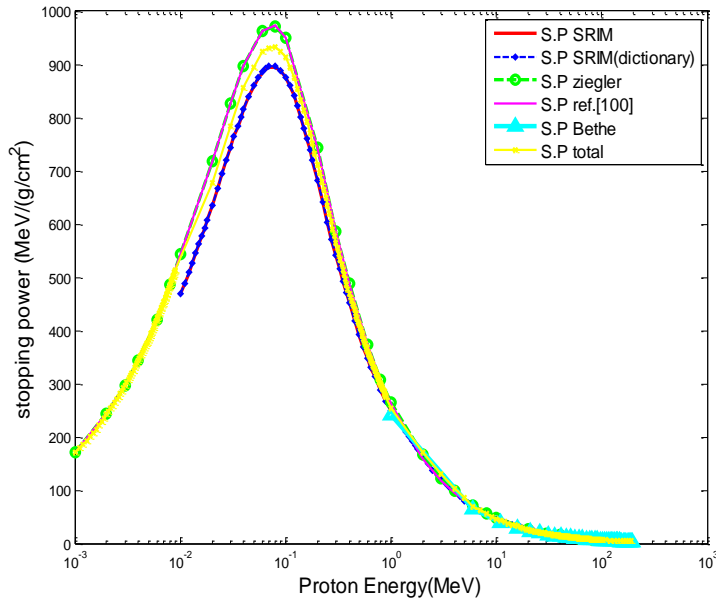


Fig. (4-50): Stopping power for prostate tissue (present work).

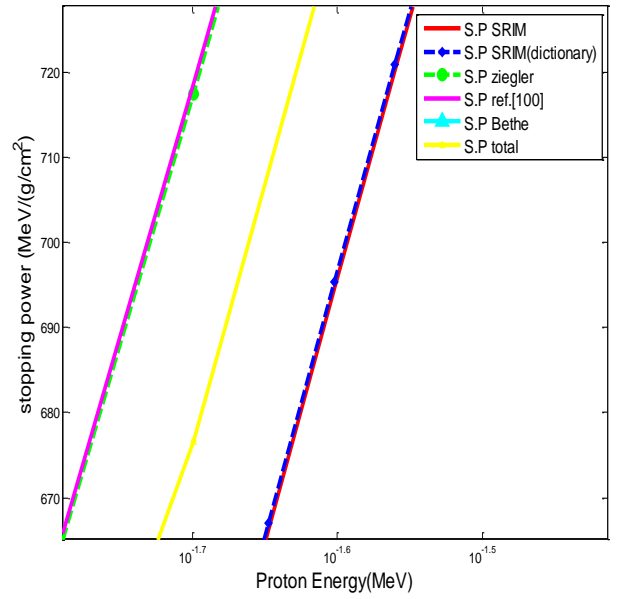


Fig. (4.50a): Stopping power for prostate tissue from $(10^{-1.7}-10^{-1.5} \text{MeV})$ (present work).

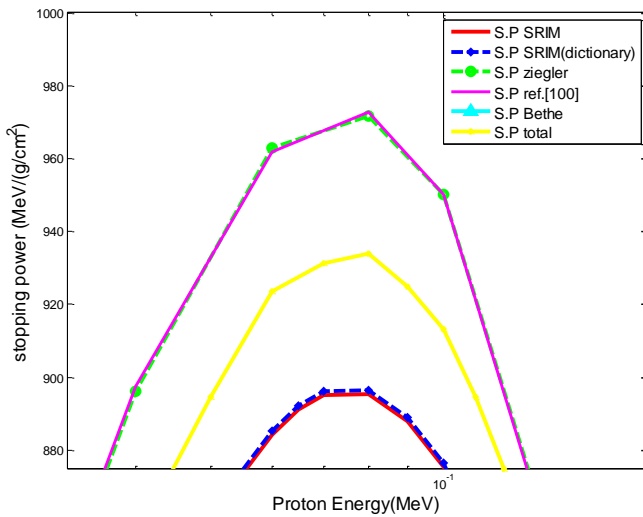


Fig. (4.50b): Stopping power for prostate tissue from $(10^{-5}-10^{-1} \text{MeV})$ (present work).

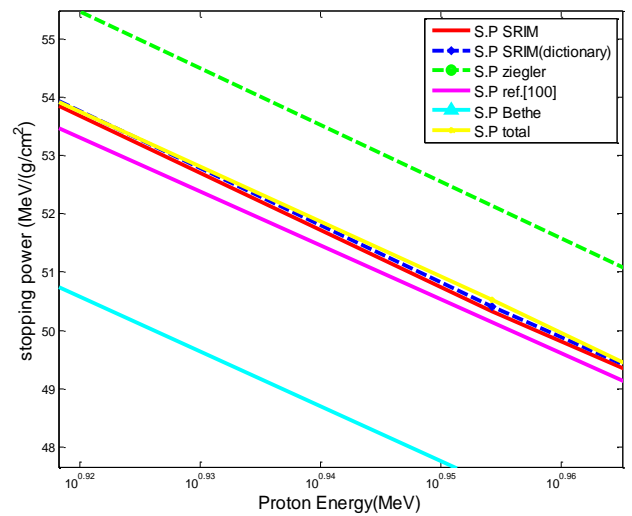


Fig. (4.50c): Stopping power for prostate tissue from $(10^{0.92}-10^{0.96} \text{MeV})$ (present work).

Discussion of prostate tissue results:

- 1- In figures (4-46), (4-47), (4-48) and (4-49) the proton's stopping power is large for hydrogen because the atomic number of hydrogen ($Z=1$) is less than Z for other elements in prostate tissue.
- 2- Using the above methods, stopping power were compatible with the low and high energy region and different at medium energy range.

- 3- Ziegler and Andreson (Vol.3) [100], are very well represented with SRIM and SRIM (dictionary) program at high energy.
- 4- Ziegler equation is very well represented with Ziegler and Andreson (Vol.3) [100], at all energies.
- 5- Bethe 's equation gives values of stopping power a little lower than other methods, especially at high energy.
- 6- At high energy (>1MeV) stopping power decreases with the increase of proton energy, i.e., it does not have enough time to collide, and at intermediate energy region, stopping power reaches the maximum value (more ionization and excitation), while at low energies ($E < 25\text{KeV}$) we observe the increase of the stopping power with the increase of the proton's energy.
- 7- From figure (4-50b) Ziegler and Andreson (Vol.3) [100], gives high value of stopping power ($972.6 \text{ MeV-cm}^2/\text{g}$) at energy (0.08) MeV.
- 8- The percentage deviation $[\frac{S_{cal} - S_{exp}}{S_{exp}}]*100$ between the experimental and the calculated stopping power values (using above methods) for Prostate tissue are shown in the following table, percentage deviation values convergent where deviation decreases as the energy of the proton increases (except Bethe). Bethe maximum deviation (18.849%), Ziegler maximum deviation (5.711%) this leads that Ziegler gave better results from other methods, as shown in red color and minimum deviation is shown in green color in table (4-10).

Table (4-10): Percentage deviation (stopping power) in prostate tissue in (MeV-cm²/g).

E _p (MeV)	Stopping power in human tissues in (MeV-cm ² /g)										S.P (P.W)
	Prostate tissue										
	Stopping power										
	Bethe	Error %	Ziegler	Error %	Ref. [100]	Error %	SRIM	Error %	SRIM (dictionary)	Error %	
0.001	-	-	171.856	-0.056	171.664	0.056	-	-	-	-	171.760
1	240.809	5.307	263.974	-3.935	262.292	-3.318	250.239	1.339	250.609	1.189	253.588
2	205.412	-16.385	166.905	2.906	159.507	7.679	163.373	5.131	163.557	5.013	171.756
3	170.016	-23.385	123.221	5.711	117.723	10.648	120.074	8.482	120.249	8.324	130.259
4	134.619	-22.742	98.817	5.249	94.522	10.031	95.964	8.378	96.094	8.232	104.004
5	99.223	-13.844	85.355	0.155	81.730	4.596	80.507	6.186	80.618	6.040	85.487
6	63.857	7.776	71.899	-4.280	68.945	-0.178	69.655	-1.196	69.753	-1.335	68.822
7	58.927	4.741	64.510	-4.325	61.902	-0.295	61.580	0.227	61.680	0.064	61.720
8	53.996	2.492	57.124	-3.119	54.863	0.874	55.320	0.040	55.408	-0.118	55.342
9	49.066	2.945	52.400	-3.605	50.377	0.265	50.317	0.386	50.395	0.230	50.511
10	44.136	4.308	47.679	-3.444	45.894	0.311	46.203	-0.359	46.273	-0.510	46.037
15	30.896	10.524	37.285	-8.413	36.029	-5.221	33.241	2.727	33.288	2.582	34.148
20	24.151	7.492	26.888	-3.448	26.161	-0.766	26.279	-1.212	26.324	-1.381	25.961
25	19.971	9.462	22.994	-4.928	22.491	-2.803	21.906	-0.206	21.942	-0.370	21.860
30	17.098	8.569	19.099	-2.806	18.821	-1.367	18.888	-1.721	18.910	-1.833	18.563
35	14.991	9.722	17.022	-3.366	16.880	-2.556	16.662	-1.280	16.689	-1.436	16.449
40	13.375	9.472	14.945	-2.028	14.940	-1.997	14.961	-2.136	14.988	-2.309	14.642
45	12.092	10.974	13.844	-3.076	13.909	-3.527	13.610	-1.411	13.637	-1.602	13.418
50	11.047	11.746	12.744	-3.138	12.878	-4.146	12.516	-1.371	12.536	-1.532	12.344
60	9.443	11.145	10.543	-0.453	10.816	-2.961	10.830	-3.090	10.845	-3.224	10.496
70	8.267	12.707	9.380	-0.666	9.726	-4.200	9.600	-2.937	9.616	-3.096	9.318
80	7.365	12.833	8.217	1.137	8.637	-3.776	8.660	-4.030	8.674	-4.1895	8.311
90	6.650	14.129	7.493	1.299	7.960	-4.646	7.917	-4.133	7.930	-4.2839	7.590
100	6.069	13.753	6.768	1.996	7.283	-5.214	7.315	-5.626	7.326	-5.776	6.903
150	4.260	18.849	-	-	-	-	5.460	-7.280	5.468	-7.417	5.063
200	-	-	-	-	-	-	4.502	-	4.509	-	-

4-1-11 Stopping power for trachea tissue

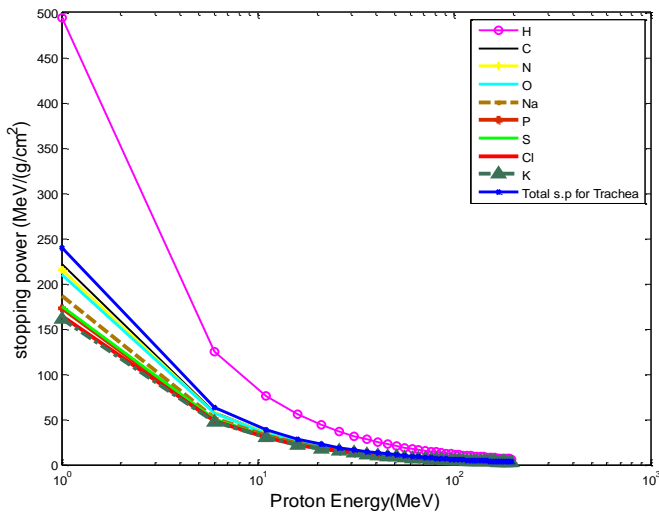


Fig. (4-51): Stopping power for proton in elements presented in trachea tissue using Bethe equation.

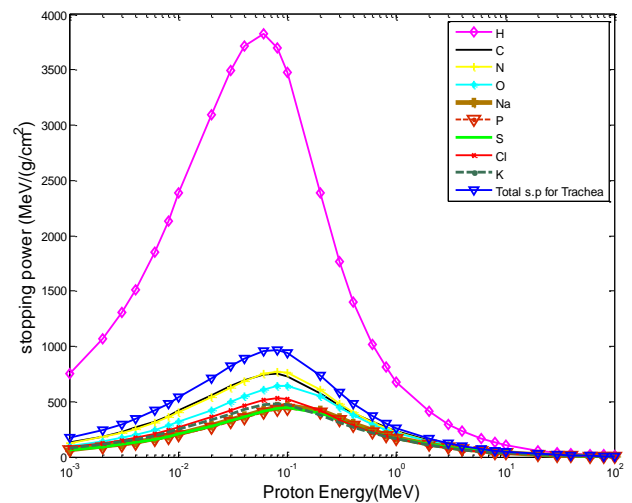


Fig. (4-52): Stopping power for proton in elements presented in trachea tissue using Ziegler equation.

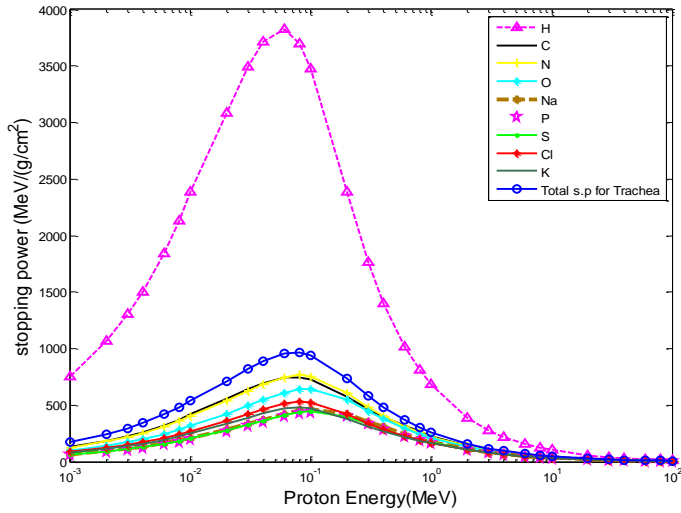


Fig. (4-53): Stopping power for proton in elements presented in trachea tissue using ref. [100].

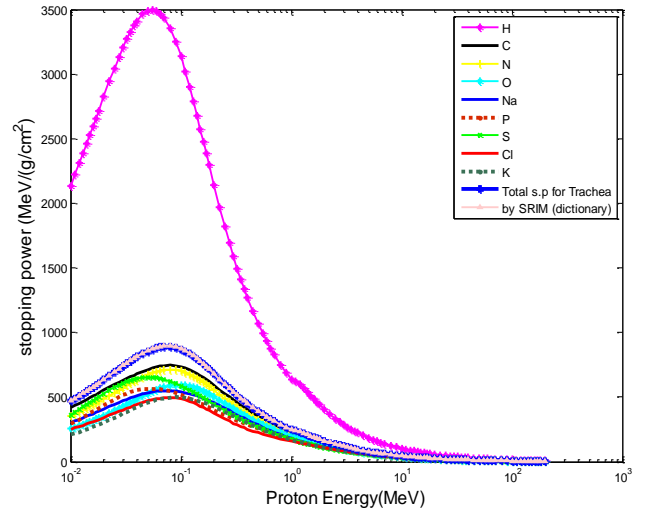


Fig.(4-54): Stopping power for proton in elements presented in trachea tissue using SRIM and SRIM (dictionary).

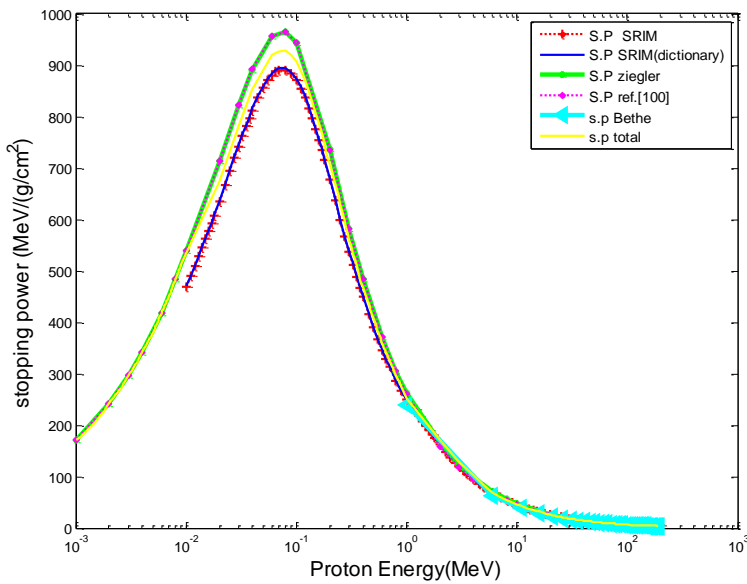


Fig (4-55): Stopping power for trachea tissue (present work).

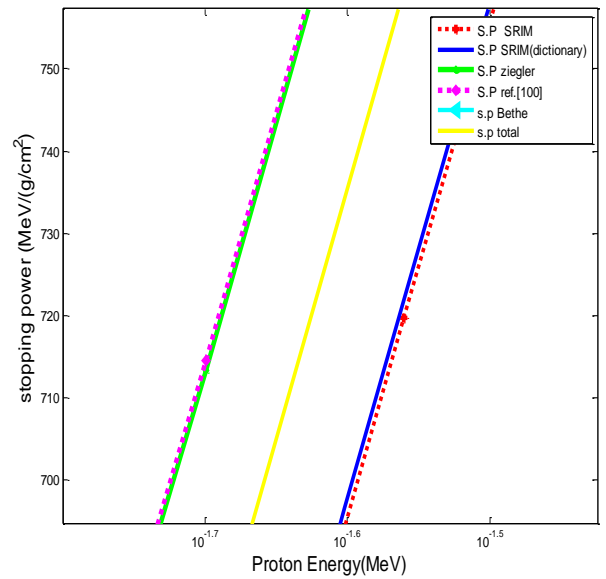


Fig. (4.55a): Stopping power for trachea tissue from (10^{-1.7}-10^{-1.5} MeV) (present work).

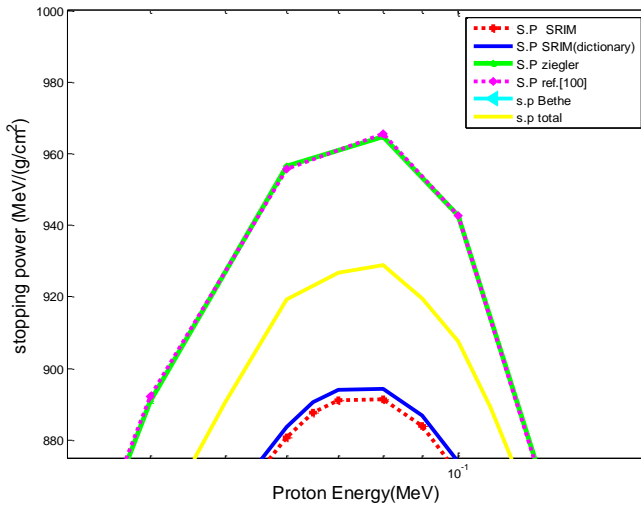


Fig. (4.55b): Stopping power for trachea tissue from $(10^{-5}-10^{-1}\text{MeV})$ (present work).

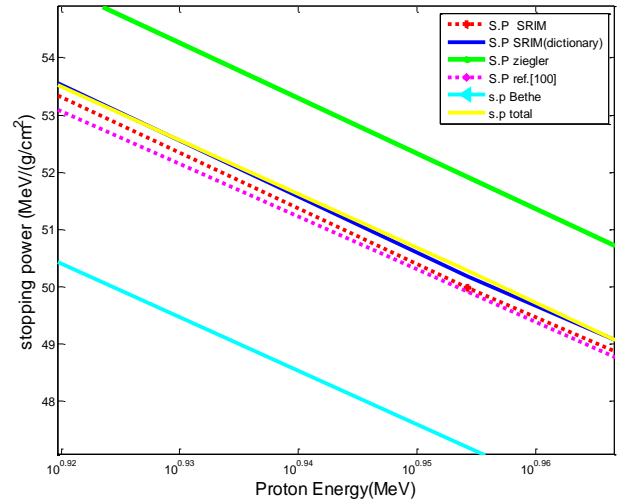


Fig. (4.55c): Stopping power for trachea tissue from $(10^{0.92}-10^{0.96}\text{MeV})$ (present work).

Discussion of trachea tissue results:

- 1- In figures (4-51), (4-52), (4-53) and (4-54) the proton's stopping power is large for hydrogen because the atomic number of hydrogen ($Z=1$) is less than Z for other elements in trachea tissue.
- 2- Using the above methods, stopping power were compatible with the low and high energy region and different at medium energy range.
- 3- Ziegler and Andreson (Vol.3) [100], are very well represented with SRIM and SRIM (dictionary) program at high energy.
- 4- Ziegler equation is very well represented with Ziegler and Andreson (Vol.3) [100], at all energies
- 5- Bethe 's equation gives values of stopping power a little lower than other methods, especially at high energy.
- 6- At high energy ($>1\text{MeV}$) stopping power decreases with the increase of proton energy, i.e., it does not have enough time to collide, and at intermediate energy region, stopping power reaches the maximum value (more ionization and excitation), while at low energies ($E < 25\text{KeV}$) we observe the increase of the stopping power with the increase of the proton's energy.
- 7- From figure (4-55b) Ziegler and Andreson (Vol.3) [100], gives high value of stopping power ($965.5\text{MeV}\cdot\text{cm}^2/\text{g}$) at energy (0.08) MeV.

8- The percentage deviation $[\frac{S_{cal} - S_{exp}}{S_{exp}}] * 100$ between the experimental and the calculated

stopping power values (using above methods) for trachea tissue are shown in the following table, percentage deviation values convergent where deviation decreases as the energy of the proton increases (except Bethe). Bethe maximum deviation (18.706%), Ziegler maximum

deviation (5.683%) this leads that Ziegler gave better results from other methods, as shown in red color and minimum deviation is shown in green color in table (4-11).

Table (4-11): Percentage deviation (stopping power) in trachea tissue in (MeV-cm²/g).

Stopping power in human tissues in (MeV-cm ² /g)											
E _p (MeV)	Trachea tissue										S.P (P.W)
	Stopping power										
	Bethe	Error %	Ziegler	Error %	Ref. [100]	Error %	SRIM	Error %	SRIM dictionary	Error %	
0.001	-	-	170.859	-0.055	170.672	0.055	-	-	-	-	170.765
1	239.977	5.262	262.665	-3.830	261.051	-3.236	249.202	1.365	250.105	0.999	252.604
2	204.701	-16.501	166.142	2.878	158.800	7.635	162.194	5.382	162.756	5.018	170.923
3	169.425	-23.484	122.666	5.683	117.206	10.606	119.230	8.728	119.649	8.348	129.637
4	134.150	-22.834	98.374	5.229	94.099	10.010	95.302	8.621	95.663	8.211	103.518
5	98.874	-13.945	84.974	0.132	81.365	4.574	79.957	6.414	80.257	6.016	85.086
6	63.629	7.650	71.580	-4.307	68.636	-0.204	69.183	-0.993	69.453	-1.377	68.497
7	58.716	4.619	64.224	-4.353	61.626	-0.321	61.165	0.430	61.410	0.030	61.428
8	53.803	2.376	56.871	-3.146	54.618	0.849	54.948	0.243	55.167	-0.155	55.082
9	48.891	2.828	52.169	-3.634	50.152	0.241	49.979	0.588	50.175	0.196	50.273
10	43.978	4.195	47.469	-3.469	45.689	0.292	45.894	-0.156	46.083	-0.565	45.823
15	30.785	10.407	37.121	-8.438	35.870	-5.244	33.020	2.934	33.148	2.536	33.989
20	24.064	7.381	26.771	-3.475	26.048	-0.798	26.105	-1.013	26.214	-1.425	25.841
25	19.899	9.353	22.894	-4.953	22.394	-2.834	21.761	-0.004	21.852	-0.420	21.760
30	17.036	8.470	19.017	-2.825	18.740	-1.393	18.764	-1.515	18.840	-1.913	18.479
35	14.937	9.612	16.949	-3.397	16.808	-2.590	16.552	-1.083	16.618	-1.478	16.373
40	13.326	9.367	14.880	-2.056	14.876	-2.026	14.863	-1.938	14.928	-2.365	14.575
45	12.048	10.859	13.785	-3.112	13.850	-3.565	13.521	-1.218	13.577	-1.626	13.356
50	11.007	11.621	12.690	-3.183	12.823	-4.193	12.433	-1.183	12.476	-1.527	12.286
60	9.409	11.048	10.499	-0.477	10.771	-2.991	10.759	-2.885	10.805	-3.301	10.449
70	8.237	12.603	9.341	-0.699	9.686	-4.236	9.536	-2.738	9.577	-3.145	9.275
80	7.339	12.726	8.183	1.099	8.601	-3.815	8.603	-3.836	8.638	-4.231	8.273
90	6.626	14.023	7.461	1.263	7.927	-4.688	7.865	-3.937	7.898	-4.334	7.555
100	6.046	13.615	6.740	1.927	7.253	-5.287	7.266	-5.459	7.296	-5.847	6.870
150	4.244	18.706	-	-	-	-	5.424	-7.113	5.446	-7.493	5.038
200	-	-	-	-	-	-	4.472	-	4.491	-	-

4-1-12 Stopping power for mammary gland tissue

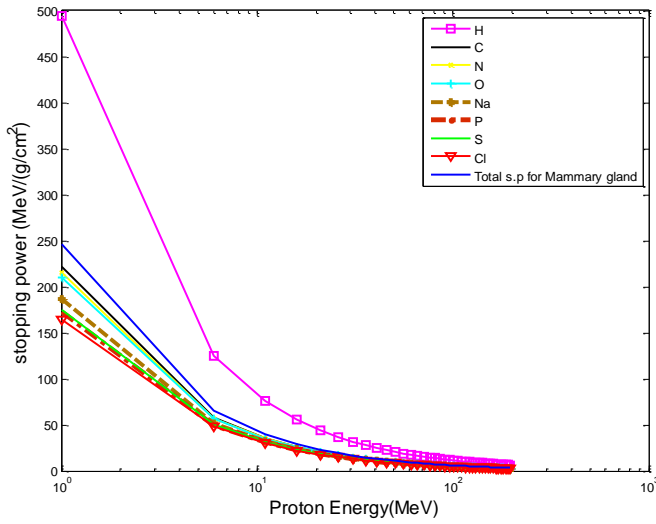


Fig. (4-56): Stopping power for proton in elements presented in mammary gland tissue using Bethe equation.

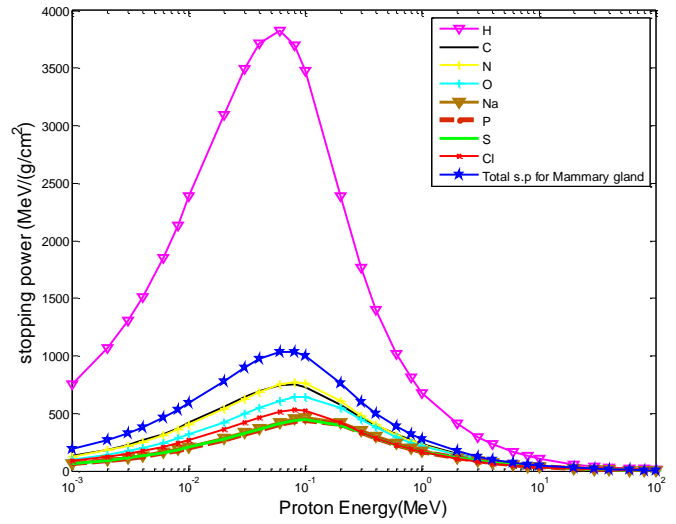


Fig.(4-57): Stopping power for proton in elements presented in mammary gland tissue using Ziegler equation.

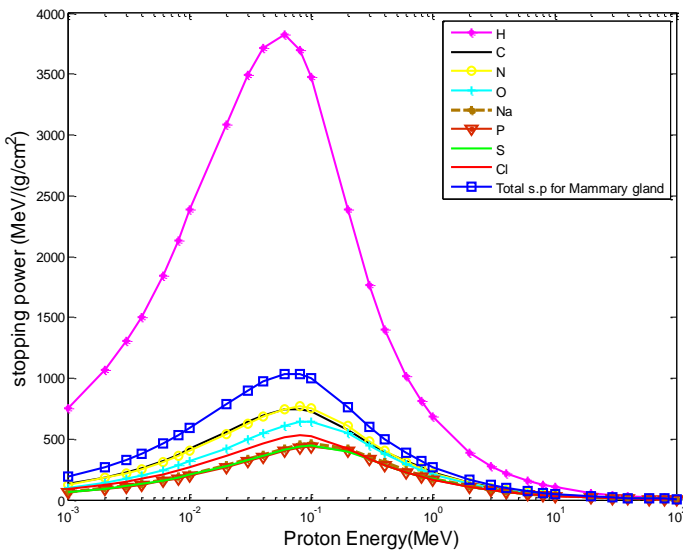


Fig. (4-58): Stopping power for proton in elements presented in mammary gland tissue using ref. [100].

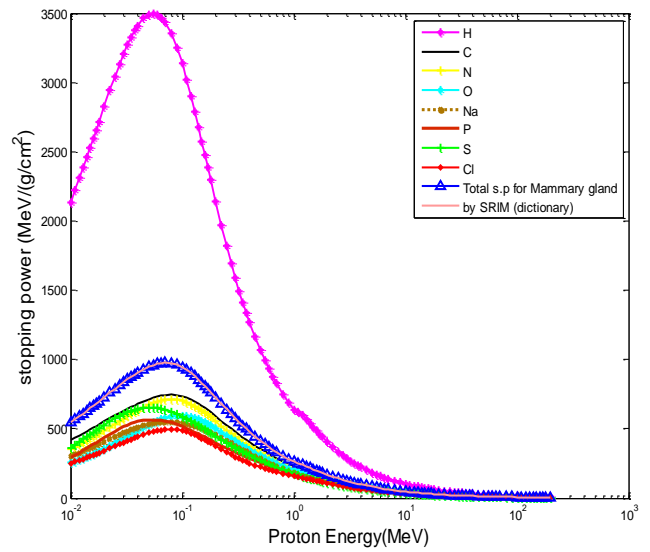


Fig. (4-59): Stopping power for proton in elements presented in mammary gland tissue using SRIM and SRIM (dictionary) program.

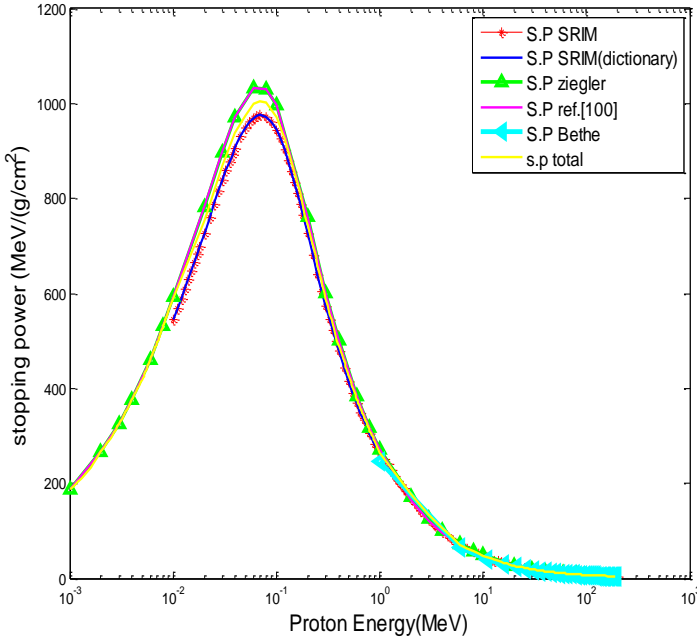


Fig. (4-60): Stopping power for mammary gland tissue (present work).

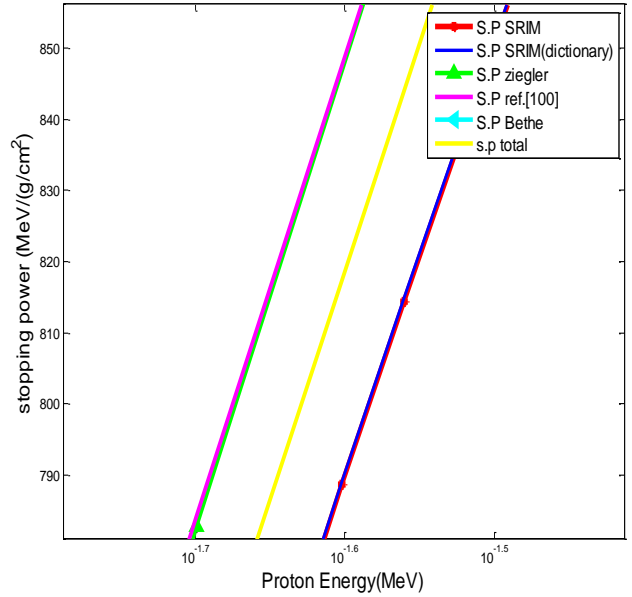


Fig. (4.60a): Stopping power for mammary gland tissue from $10^{-1.7}$ - $10^{-1.5}$ MeV (present work).

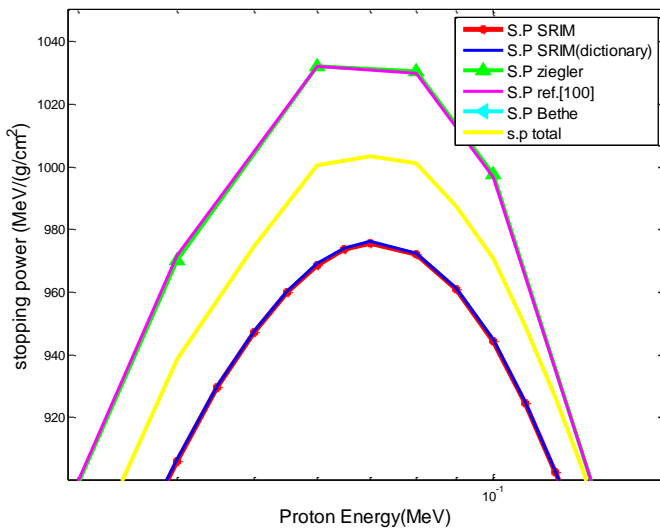


Fig. (4.60b): Stopping power for mammary gland tissue from $10^{-1.5}$ - 10^{-1} MeV (present work).

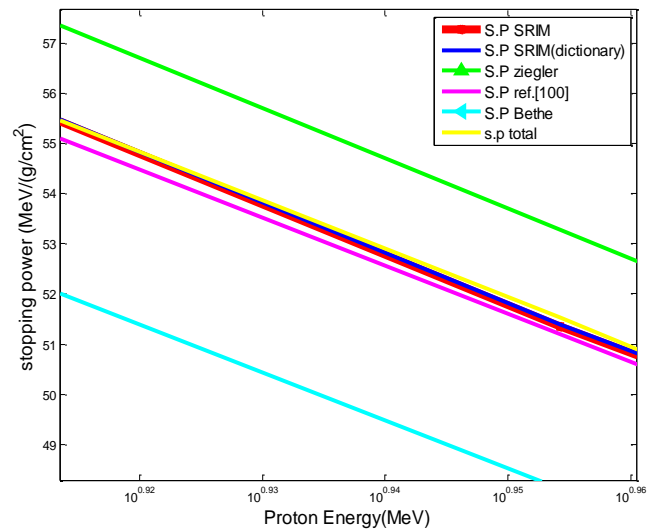


Fig. (4.60c): Stopping power for mammary gland tissue from $10^{0.92}$ - $10^{0.96}$ MeV (present work).

Discussion of mammary gland tissue results:

- 1- In figures (4-56), (4-57), (4-58) and (4-59) the proton's stopping power is large for hydrogen because the atomic number of hydrogen ($Z=1$) is less than Z for other elements in mammary gland tissue.

- 2- Using the above methods, stopping power were compatible with the low and high energy region and different at medium energy range.
- 3- Ziegler and Andreson (Vol.3) [100], are very well represented with SRIM and SRIM (dictionary) program at high energy.
- 4- Ziegler equation is very well represented with Ziegler and Andreson (Vol.3) [100], at all energies
- 5- Bethe 's equation gives values of stopping power a little lower than other methods, especially at high energy.
- 6- At high energy (>1MeV) stopping power decreases with the increase of proton energy, i.e., it does not have enough time to collide, and at intermediate energy region, stopping power reaches the maximum value (more ionization and excitation), while at low energies (E <25KeV) we observe the increase of the stopping power with the increase of the proton's energy.
- 7- From figure (4-60b) Ziegler and Andreson (Vol.3) [100], gives high value of stopping power (1032.2MeV-cm²/g) at energy (0.06) and stopping power for Ziegler at energy (0.06) MeV is (1032.1 MeV).

- 8- The percentage deviation $\left[\frac{S_{cal} - S_{exp}}{S_{exp}} \right] * 100$ between the experimental and the calculated

stopping power values (using above methods) for mammary gland tissue are shown in the following table, percentage deviation values convergent where deviation decreases as the energy of the proton increases (except Bethe). Bethe maximum deviation (19.093%), Ziegler maximum deviation (5.465%) this leads that Ziegler gave better results from other methods, as shown in red color and minimum deviation is shown in green color in table (4-12).

Table (4-12): Percentage deviation (stopping power) in mammary gland tissue in (MeV-cm²/g).

Stopping power in human tissues in (MeV-cm ² /g)											
E _p (MeV)	Mammary gland tissue										S.P (P.W)
	Stopping power										
	Bethe	Error%	Ziegler	Error%	Ref. [100]	Error%	SRIM	Error%	SRIM dictionary	Error%	
0.001	-	-	187.899	-0.053	187.713	0.047	-	-	-	-	187.800
1	246.731	6.910	272.672	-3.261	271.608	-2.882	263.839	-0.023	263.993	-0.081	263.780
2	210.363	-16.124	171.945	2.617	164.409	7.320	167.664	5.237	167.757	5.178	176.444
3	173.995	-23.263	126.600	5.465	121.009	10.338	122.986	8.564	123.050	8.507	133.518
4	137.627	-22.638	101.353	5.049	96.914	9.861	98.196	8.427	98.254	8.362	106.471
5	101.258	-13.663	87.467	-0.050	83.725	4.418	82.318	6.203	82.369	6.137	87.424
6	64.921	8.258	73.588	-4.492	70.542	-0.367	71.180	-1.261	71.224	-1.322	70.282
7	59.897	5.186	65.986	-4.520	63.292	-0.456	62.895	0.172	62.941	0.100	63.004
8	54.873	2.915	58.388	-3.280	56.046	0.762	56.481	-0.015	56.518	-0.081	56.473
9	49.849	3.343	53.537	-3.777	51.439	0.148	51.350	0.321	51.386	0.252	51.515
10	44.825	4.690	48.689	-3.620	46.835	0.196	47.141	-0.454	47.174	-0.523	46.927
15	31.347	10.966	38.042	-8.563	36.748	-5.341	33.877	2.678	33.899	2.613	34.785
20	24.490	7.912	27.393	-3.523	26.658	-0.863	26.765	-1.258	26.784	-1.331	26.428
25	20.243	9.870	23.415	-5.015	22.910	-2.920	22.300	-0.263	22.312	-0.318	22.241
30	17.326	8.943	19.437	-2.890	19.162	-1.495	19.221	-1.799	19.230	-1.844	18.875
35	15.188	10.100	17.318	-3.446	17.180	-2.667	16.951	-1.356	16.969	-1.457	16.722
40	13.547	9.830	15.199	-2.110	15.198	-2.098	15.219	-2.234	15.228	-2.292	14.879
45	12.245	11.318	14.078	-3.177	14.148	-3.653	13.839	-1.499	13.847	-1.558	13.631
50	11.186	12.077	12.957	-3.248	13.099	-4.291	12.720	-1.446	12.726	-1.492	12.536
60	9.560	11.471	10.715	-0.549	11.000	-3.119	11.007	-3.185	11.015	-3.258	10.656
70	8.368	13.011	9.531	-0.786	9.889	-4.372	9.754	-3.048	9.761	-3.117	9.456
80	7.454	13.106	8.347	0.998	8.778	-3.958	8.797	-4.160	8.803	-4.232	8.431
90	6.729	14.477	7.610	1.223	8.090	-4.775	8.041	-4.196	8.047	-4.266	7.703
100	6.140	14.014	6.873	1.849	7.401	-5.421	7.427	-5.753	7.433	-5.828	7.000
150	4.308	19.093	-	-	-	-	5.540	-7.394	5.543	-7.450	5.130
200	-	-	-	-	-	-	4.565	-	4.569	-	-

4-1-13 Stopping power for thyroid tissue

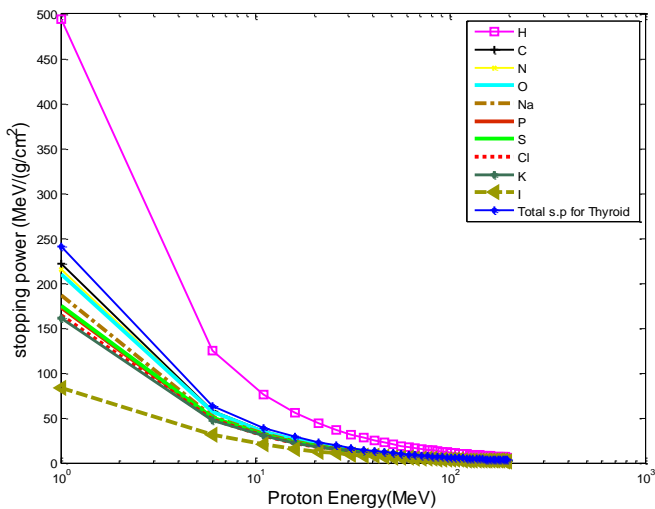


Fig. (4-61): Stopping power for proton in elements presented in thyroid tissue using Bethe equation.

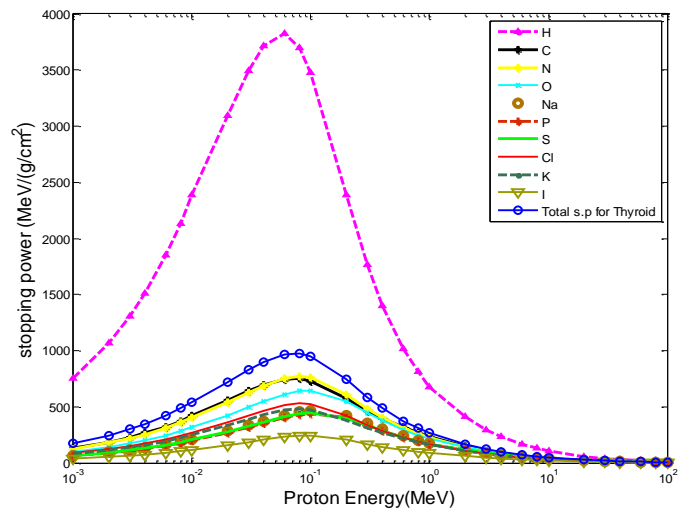


Fig. (4-62): Stopping power for proton in elements presented in thyroid tissue using Ziegler equation.

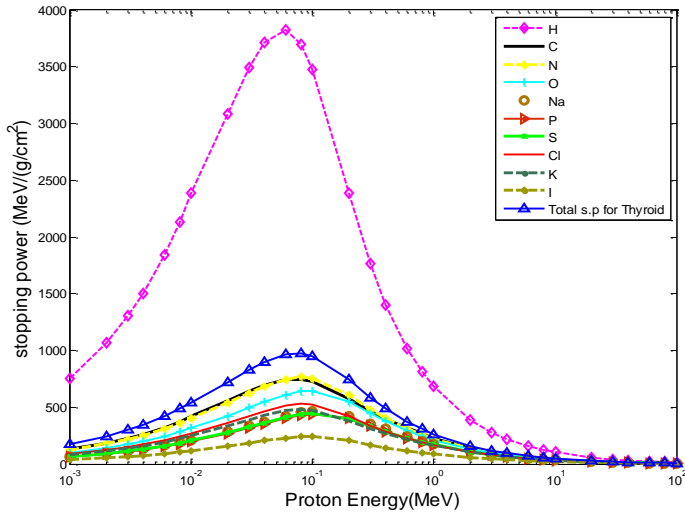


Fig. (4-63): Stopping power for proton in elements presented in thyroid tissue using ref. [100].

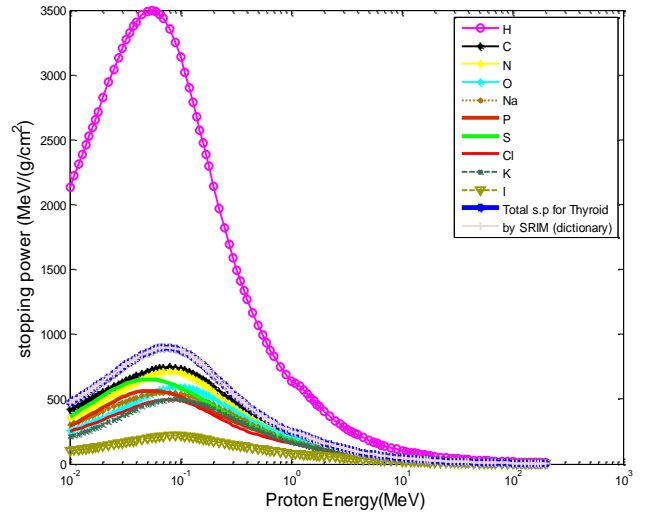


Fig. (4-64): Stopping power for proton in elements presented in thyroid tissue using SRIM and SRIM (dictionary).

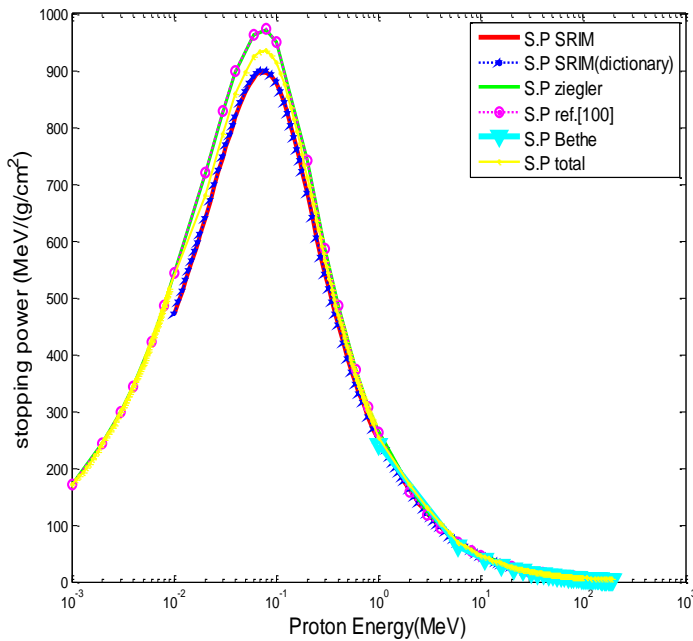


Fig. (4-65): Stopping power for thyroid tissue (present work).

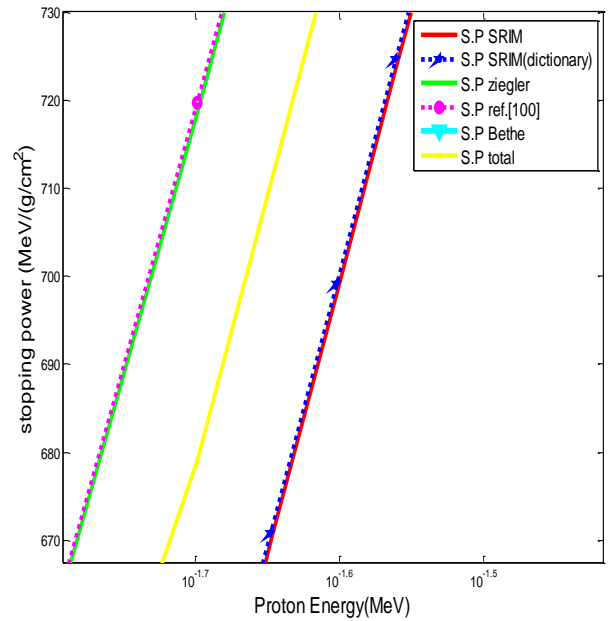


Fig. (4.65a): Stopping power for thyroid tissue from (10^{-1.7}-10^{-1.5} MeV) (present work).

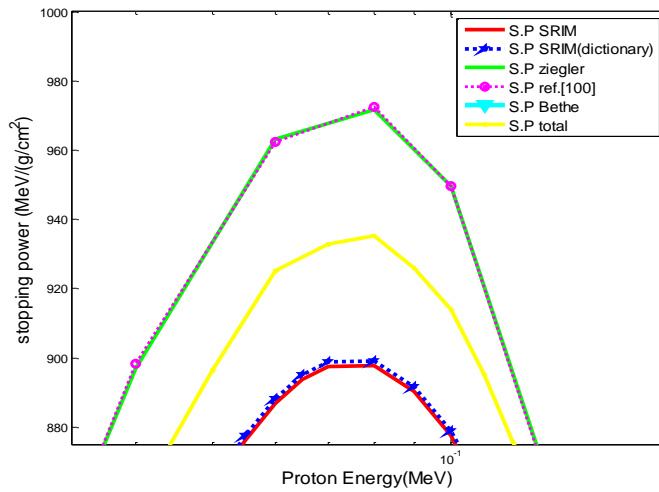


Fig. (4.65b): Stopping power for thyroid tissue from (10^{-5} - 10^{-1} MeV) (present work).

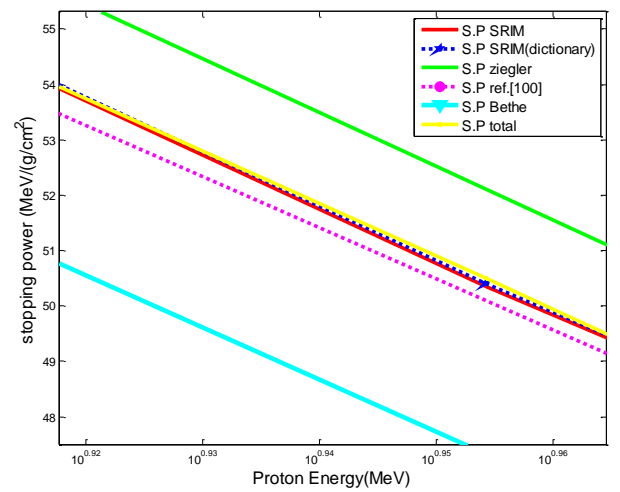


Fig. (4.65c): Stopping power for thyroid tissue from ($10^{0.92}$ - $10^{0.96}$ MeV) (present work).

Discussion of thyroid tissue results:

- 1- In figures (4-61), (4-62), (4-63) and (4-64) the proton's stopping power is large for hydrogen because the atomic number of hydrogen ($Z=1$) is less than Z for other elements in thyroid tissue. And less value of stopping power is for iodine due to atomic number of it is large ($Z=53$).
- 2- Using the above methods, stopping power were compatible with the low and high energy region and different at medium energy range.
- 3- Ziegler and Andreson (Vol.3) [100], are very well represented with SRIM and SRIM (dictionary) program at high energy.
- 4- Ziegler equation is very well represented with Ziegler and Andreson (Vol.3) [100], at all energies
- 5- Bethe 's equation gives values of stopping power a little lower than other methods, especially at high energy.
- 6- At high energy (>1 MeV) stopping power decreases with the increase of proton energy, i.e., it does not have enough time to collide, and at intermediate energy region, stopping power reaches the maximum value (more ionization and excitation), while at low energies ($E < 25$ KeV) we observe the increase of the stopping power with the increase of the proton's energy.
- 7- From figure (4-65b) Ziegler and Andreson (Vol.3) [100], gives high value of stopping power ($972.4 \text{ MeV}\cdot\text{cm}^2/\text{g}$) at energy (0.08) and stopping power for Ziegler at energy (0.08) MeV is ($971.6 \text{ MeV}\cdot\text{cm}^2/\text{g}$).

8-The percentage deviation $\left[\frac{S_{cal} - S_{exp}}{S_{exp}} \right] * 100$ between the experimental and the calculated stopping power values (using above methods) for thyroid tissue are shown in the following

table, percentage deviation values convergent where deviation decreases as the energy of the proton increases (except Bethe). Bethe maximum deviation (18.949%), Ziegler maximum deviation (5.749%) this leads that Ziegler gave better results from other methods, as shown in red color, and minimum deviation is shown in green color in table (4-13).

Table (4-13): Percentage deviation (stopping power) in thyroid tissue in (MeV-cm²/g).

Stopping power in human tissues in (MeV-cm ² /g)											
E _P (MeV)	Thyroid tissue										S.P (P.W)
	Stopping power										
	Bethe	Error%	Ziegler	Error%	Ref. [100]	Error%	SRIM	Error%	SRIM dictio- Nary	Error%	
0.001	-	-	172.102	-0.055	171.911	0.055	-	-	-	-	172.007
1	240.724	5.418	263.855	-3.824	262.206	-3.219	250.820	1.175	251.207	1.019	253.767
2	205.336	-16.358	166.825	2.951	159.441	7.719	163.456	5.073	163.657	4.944	171.748
3	169.948	-23.369	123.153	5.749	117.665	10.681	120.140	8.401	120.249	8.303	130.233
4	134.561	-22.720	98.757	5.297	94.465	10.081	96.021	8.298	96.133	8.171	103.988
5	99.173	-13.816	85.301	0.200	81.679	4.644	80.556	6.102	80.648	5.982	85.472
6	63.816	7.826	71.852	-4.233	68.899	-0.129	69.699	-1.275	69.783	-1.395	68.810
7	58.889	4.786	64.466	-4.280	61.860	-0.247	61.619	0.142	61.700	0.011	61.707
8	53.961	2.537	57.084	-3.072	54.824	0.924	55.355	-0.045	55.427	-0.175	55.330
9	49.034	2.987	52.363	-3.561	50.340	0.314	50.349	0.296	50.405	0.185	50.498
10	44.106	4.356	47.645	-3.395	45.860	0.366	46.233	-0.445	46.293	-0.574	46.027
15	30.874	10.574	37.257	-8.369	36.001	-5.174	33.263	2.633	33.298	2.524	34.139
20	24.134	7.536	26.867	-3.403	26.141	-0.722	26.297	-1.309	26.324	-1.412	25.953
25	19.956	9.509	22.975	-4.883	22.474	-2.760	21.920	-0.305	21.942	-0.402	21.853
30	17.085	8.627	19.084	-2.748	18.806	-1.313	18.901	-1.809	18.920	-1.907	18.559
35	14.980	9.769	17.008	-3.320	16.867	-2.512	16.673	-1.379	16.689	-1.469	16.443
40	13.364	9.520	14.932	-1.980	14.928	-1.951	14.971	-2.235	14.988	-2.341	14.637
45	12.082	11.022	13.833	-3.029	13.898	-3.483	13.620	-1.510	13.637	-1.635	13.414
50	11.038	11.795	12.733	-3.091	12.868	-4.103	12.524	-1.469	12.536	-1.566	12.340
60	9.436	11.195	10.535	-0.403	10.808	-2.918	10.838	-3.188	10.845	-3.256	10.492
70	8.261	12.759	9.373	-0.617	9.719	-4.156	9.606	-3.034	9.616	-3.128	9.315
80	7.359	12.887	8.210	1.188	8.630	-3.731	8.665	-4.127	8.674	-4.222	8.308
90	6.645	14.182	7.486	1.349	7.953	-4.603	7.922	-4.230	7.930	-4.317	7.587
100	6.064	13.845	6.762	2.082	7.277	-5.138	7.319	-5.688	7.326	-5.775	6.903
150	4.256	18.949	-	-	-	-	5.464	-7.340	5.468	-7.417	5.063
200	-	-	-	-	-	-	4.505	-	4.509	-	-

4-2 The range calculation

Using the computer programs in Matlab to calculate the range of proton in the each tissue using (SRIM, SRIM (dictionary) program and by integral total stopping power [eq (2-26)], the curves in any tissue where compatible and have the same behavior. Range increase with increase proton energy inside the organ, range depends on the stopping power value and density of organ. We have concluded the semi-empirical formula for range of proton in each tissue, this formula have fitting constant different for every single tissue, as following:

4-2-1 In skin tissue

The results are plotted in Fig. (3-1) and (3-2), and the semi-empirical formula for range of proton in skin tissue is :

$$f(x) = a \cdot x^b + c \dots\dots\dots (4-1)$$

Where a, b and c are fitting constant, in skin tissue these constants are:

$$a = 0.0002569, \quad b = 1.744, \quad c = 0.01074.$$

4-2-2 In eye lens tissue

The results are plotted in Fig. (3-3) and (3-4), and the semi-empirical formula for range of proton in eye lens tissue is:

$$f(x) = a \cdot x^b + c \dots\dots\dots (4-2)$$

Where a, b and c are fitting constant, in eye lens tissue these constants are:

$$a = 0.0002301, \quad b=1.775, \quad c=0.01315.$$

4-2-3 In stomach tissue

The results are plotted in Fig. (3-5) and (3-6), and the semi-empirical formula for range of proton in stomach tissue is:

$$f(x) = a \cdot x^b + c \dots\dots\dots (4-3)$$

Where a, b and c are fitting constant, in stomach tissue these constants are:

$$a = 0.0002321, \quad b = 1.776, \quad c = 0.01325.$$

4-2-4 In pancreas tissue

The results are plotted in Fig. (3-7) and (3-8), and the semi-empirical formula for range of proton in pancreas tissue is:

$$f(x) = a \cdot x^b + c \dots\dots\dots (4-4)$$

Where a, b and c are fitting constant, in pancreas tissue these constants are:

$$a=0.0002674, \quad b= 1.744, \quad c= 0.01116.$$

4-2-5 In liver tissue

The results are plotted in Fig. (3-9) and (3-10), and the semi-empirical formula for range of proton in liver tissue is:

$$f(x) = a \cdot x^b + c \dots\dots\dots (4-5)$$

Where a, b and c are fitting constant, in liver tissue these constants are:

a= 0.0002313, b= 1.775, c= 0.01316.

4-2-6 In spleen tissue

The results are plotted in Fig. (3-11) and (3-12), and the semi-empirical formula for range of proton in spleen tissue is:

$$f(x) = a*x^b+c \dots\dots\dots (4-6)$$

Where a, b and c are fitting constant, in spleen tissue these constants are:

a= 0.0002637, b= 1.744, c= 0.01113.

4-2-7 In blood tissue

The results are plotted in Fig. (3-13) and (3-14), and the semi-empirical formula for range of proton in blood tissue is:

$$f(x) = a*x^b+c \dots\dots\dots (4-7)$$

Where a, b and c are fitting constant, in blood tissue these constants are:

a= 0.0002642, b=1.744, c=0.01114.

4-2-8 In ovary tissue

The results are plotted in Fig. (3-15) and (3-16), and the semi-empirical formula for range of proton in ovary tissue is:

$$f(x) = a*x^b+c \dots\dots\dots (4-8)$$

Where a, b and c are fitting constant, in ovary tissue these constants are:

a= 0.0002663, b= 1.744, c= 0.01113.

4-2-9 In testis tissue

The results are plotted in Fig. (3-17) and (3-18), and the semi-empirical formula for range of proton in testis tissue is:

$$f(x) = a*x^b+c \dots\dots\dots (4-9)$$

Where a, b and c are fitting constant, in testis tissue these constants are:

a= 0.0002679, b=1.744, c=0.01126.

4-2-10 In prostate tissue

The results are plotted in Fig. (3-19) and (3-20), and the semi-empirical formula for range of proton in prostate tissue is:

$$f(x) = a*x^b+c \dots\dots\dots (4-10)$$

Where a, b and c are fitting constant, in prostate tissue these constants are:

a= 0.0002685, b=1.744, c= 0.01128.

4-2-11 In trachea tissue

The results are plotted in Fig. (3-21) and (3-22), and the semi-empirical formula for range of proton in trachea tissue is:

$$f(x) = a \cdot x^b + c \dots\dots\dots (4-11)$$

Where a, b and c are fitting constant, in trachea tissue these constants are:
 a= 0.0002643, b= 1.744, c= 0.01115.

4-2-12 In mammary gland tissue

The results are plotted in Fig. (3-23) and (3-24), and the semi-empirical formula for range of proton in mammary gland tissue is:

$$f(x) = a \cdot x^b + c \dots\dots\dots (4-12)$$

Where a, b and c are fitting constant, in mammary gland tissue these constants are:
 a= 0.0002753, b= 1.746, c= 0.01123.

4-2-13 In thyroid tissue

The results are plotted in Fig. (3-25) and (3-26), and the semi-empirical formula for range of proton in thyroid tissue is:

$$f(x) = a \cdot x^b + c \dots\dots\dots (4-13)$$

Where a, b and c are fitting constant, in thyroid tissue these constants are:
 a= 0.0002663, b= 1.744, c= 0.01113.

Chapter Five

Conclusion



Future work

5-1 Conclusion

Calculation of the loss of proton energy in the tissue at high accuracy is necessary for the radiation treatment of cancer from their values and the values of the depth of the proton can be drawn data to obtain the curve of (Bragg peak), which corresponds to the location of the tumor in the tissue. We note from the previous figures that all the curves, stopping power of the proton calculated using the previous methods in each tissue have the same behavior (except Bethe), where starting increases with the increase of energy of proton until it reaches the maximum amount in specific energy then begins to decrease with the increase of the proton energy. The maximum value of the stopping power in (MeV-cm²/g) does not often appear in the tables because of the interpolation, so we will mention it as following:

5-1-1 For skin tissue:

Bethe equation, maximum stopping power is 240.7225 (MeV-cm²/g) at 1 MeV proton energy.

Ziegler equation, maximum stopping power is 971.1933 (MeV-cm²/g) at 0.08 MeV proton energy.

Ziegler and Andreson (Vol.3) [100], maximum stopping power is 971.6868 (MeV-cm²/g) at 0.08 MeV proton energy.

SRIM program, maximum stopping power is 902.7460 (MeV-cm²/g) at 0.07 MeV proton energy.

SRIM (dictionary) program, maximum stopping power is 903.2210 (MeV-cm²/g) at 0.07 MeV proton energy.

Total stopping power (P.W) is 937.0337 (MeV-cm²/g) at 0.08 MeV proton energy. **At range** 0.0107 cm.

5-1- 2 For eye lens tissue:

Bethe equation, maximum stopping power is 239.6950 (MeV-cm²/g) at 1 MeV proton energy.

Ziegler equation, maximum stopping power is 960.2577 (MeV-cm²/g) at 0.08 MeV proton energy.

Ziegler and Andreson (Vol.3) [100], maximum stopping power is 960.7992 (MeV-cm²/g) at 0.08 MeV proton energy.

SRIM program, maximum stopping power is 892.1453 (MeV-cm²/g) at 0.08 MeV proton energy.

Total stopping power (P.W) is 937.7341 (MeV-cm²/g) at 0.08 MeV proton energy. **At range** 0.0132 cm.

5-1- 3 For stomach tissue:

Bethe equation, maximum stopping power is 241.1218 (MeV-cm²/g) at 1 MeV proton energy.

Ziegler equation, maximum stopping power is 974.8024 (MeV-cm²/g) at 0.08 MeV proton energy.

Ziegler and Andreson (Vol.3) [100], maximum stopping power is 975.5166 (MeV-cm²/g) at 0.08 MeV proton energy.

SRIM program, maximum stopping power is 900.3535 (MeV-cm²/g) at 0.07 MeV proton energy.

Total stopping power (P.W) is 950.2180 (MeV-cm²/g) at 0.08 MeV proton energy. **At range** 0.0133 cm.

5-1- 4 For pancreas tissue:

Bethe equation, maximum stopping power is 241.9186 (MeV-cm²/g) at 1 MeV proton energy.

Ziegler equation, maximum stopping power is 483.0350 (MeV-cm²/g) at 0.08 MeV proton energy.

Ziegler and Andreson (Vol.3) [100], maximum stopping power is 983.6359 (MeV-cm²/g) at 0.08 MeV proton energy.

SRIM program, maximum stopping power is 911.4170 (MeV-cm²/g) at 0.07 MeV proton energy.

SRIM (dictionary) program, maximum stopping power is 912.2530 (MeV-cm²/g) at 0.07 MeV proton energy.

Total stopping power (P.W) is 947.3557 (MeV-cm²/g) at 0.08 MeV proton energy. **At range** 0.0112 cm.

5-1-5 For liver tissue:

Bethe equation, maximum stopping power is 240.3324 (MeV-cm²/g) at 1 MeV proton energy.

Ziegler equation, maximum stopping power is 967.7319 (MeV-cm²/g) at 0.08 MeV proton energy.

Ziegler and Andreson (Vol.3) [100], maximum stopping power is 968.4407 (MeV-cm²/g) at 0.08 MeV proton energy.

SRIM program, maximum stopping power is 896.1404 (MeV-cm²/g)

at 0.08 MeV proton energy.

Total stopping power (P.W) is 944.1043 (MeV-cm²/g) at 0.08 MeV proton energy. **At range** 0.0132 cm.

5-1-6 For spleen tissue:

Bethe equation, maximum stopping power is 240.3935 (MeV-cm²/g) at 1 MeV proton energy.

Ziegler equation, maximum stopping power is 968.5599 (MeV-cm²/g) at 0.08 MeV proton energy.

Ziegler and Andreson (Vol.3) [100], maximum stopping power is 969.3628 (MeV-cm²/g) at 0.08 MeV proton energy.

SRIM program, maximum stopping power is 892.5877 (MeV-cm²/g) at 0.08 MeV proton energy.

SRIM (dictionary) program, maximum stopping power is 895.2320 (MeV-cm²/g) at 0.08 MeV proton energy.

Total stopping power (P.W) is 931.4356 (MeV-cm²/g) at 0.08 MeV proton energy. **At range** 0.0111cm.

5-1-7 For blood tissue:

Bethe equation, maximum stopping power is 240.0851 (MeV-cm²/g) at 1 MeV proton energy.

Ziegler equation, maximum stopping power is 965.4019 (MeV-cm²/g) at 0.08 MeV proton energy.

Ziegler and Andreson (Vol.3) [100], maximum stopping power is 966.2174 (MeV-cm²/g) at 0.08 MeV proton energy.

SRIM program, maximum stopping power is 888.9760 (MeV-cm²/g) at 0.08 MeV proton energy.

SRIM (dictionary) program, maximum stopping power is 892.8280 (MeV-cm²/g) at 0.08 MeV proton energy.

Total stopping power (P.W) is 928.3558 (MeV-cm²/g) at 0.08 MeV proton energy. **At range** 0.0111 cm.

5-1-8 For ovary tissue:

Bethe equation, maximum stopping power is 240.7562 (MeV-cm²/g) at 1 MeV proton energy.

Ziegler equation, maximum stopping power is 971.6150 (MeV-cm²/g) at 0.08 MeV proton energy.

Ziegler and Andreson (Vol.3) [100], maximum stopping power is 972.4849 (MeV-cm²/g) at 0.08 MeV proton energy.

SRIM program, maximum stopping power is 896.5818 (MeV-cm²/g) at 0.08 MeV proton energy.

SRIM (dictionary) program, maximum stopping power is 897.4420 (MeV-cm²/g) at 0.08 MeV proton energy.

Total stopping power (P.W) is 934.5309 (MeV-cm²/g) at 0.08 MeV proton energy. **At range** 0.0111 cm.

5-1-9 For testis tissue:

Bethe equation, maximum stopping power is 241.1227 (MeV-cm²/g) at 1 MeV proton energy.

Ziegler equation, maximum stopping power is 975.0336 (MeV-cm²/g) at 0.08 MeV proton energy.

Ziegler and Andreson (Vol.3) [100], maximum stopping power is 975.8802 (MeV-cm²/g) at 0.08 MeV proton energy.

SRIM program, maximum stopping power is 897.8551 (MeV-cm²/g) at 0.08 MeV proton energy.

SRIM (dictionary) program, maximum stopping power is 900.3470 (MeV-cm²/g) at 0.08 MeV proton energy.

Total stopping power (P.W) is 937.2790 (MeV-cm²/g) at 0.08 MeV proton energy. **At range** 0.0113 cm.

5-1-10 For prostate tissue:

Bethe equation, maximum stopping power is 240.8442 (MeV-cm²/g) at 1 MeV proton energy.

Ziegler equation, maximum stopping power is 971.7324 (MeV-cm²/g) at 0.08 MeV proton energy.

Ziegler and Andreson (Vol.3) [100], maximum stopping power is 972.6212 (MeV-cm²/g) at 0.08 MeV proton energy.

SRIM program, maximum stopping power is 895.3115 (MeV-cm²/g) at 0.08 MeV proton energy.

SRIM (dictionary) program, maximum stopping power is 896.4410 (MeV-cm²/g) at 0.08 MeV proton energy.

Total stopping power (P.W) is 934.0265 (MeV-cm²/g) at 0.08 MeV proton energy. **At range** 0.0113 cm.

5-1-11 For trachea tissue:

Bethe equation, maximum stopping power is 240.0118 (MeV-cm²/g) at 1 MeV proton energy.

Ziegler equation, maximum stopping power is 964.7825 (MeV-cm²/g) at 0.08 MeV proton energy.

Ziegler and Andreson (Vol.3) [100], maximum stopping power is 965.4922 (MeV-cm²/g) at 0.08 MeV proton energy.

SRIM program, maximum stopping power is 891.2827 (MeV-cm²/g) at 0.08 MeV proton energy.

SRIM (dictionary) program, maximum stopping power is 894.2230 (MeV-cm²/g) at 0.08 MeV proton energy.

Total stopping power (P.W) is 928.9451 (MeV-cm²/g) at 0.08 MeV proton energy. **At range** 0.0112 cm.

5-1-12 For mammary gland tissue:

Bethe equation, maximum stopping power is 246.7676 (MeV-cm²/g) at 1 MeV proton energy.

Ziegler equation, maximum stopping power is 1.0321×10^3 (MeV-cm²/g) at 0.06 MeV proton energy.

Ziegler and Andreson (Vol.3) [100], maximum stopping power is 1.0322×10^3 (MeV-cm²/g) at 0.06 MeV proton energy.

SRIM program, maximum stopping power is 975.7762 (MeV-cm²/g) at 0.07 MeV proton energy.

SRIM (dictionary) program, maximum stopping power is 976.1990 (MeV-cm²/g) at 0.07 MeV proton energy.

Total stopping power (P.W) is 1003.6 (MeV-cm²/g) at 0.07 MeV proton energy.

At range 0.0112 cm.

5-1-13 For thyroid tissue:

Bethe equation, maximum stopping power is 240.7590 (MeV-cm²/g) at 1 MeV proton energy.

Ziegler equation, maximum stopping power is 971.6122 (MeV-cm²/g) at 0.08 MeV proton energy.

Ziegler and Andreson (Vol.3) [100], maximum stopping power is 972.3921 (MeV-cm²/g) at 0.08 MeV proton energy.

SRIM program, maximum stopping power is 897.6310 (MeV-cm²/g) at 0.08 MeV proton energy.

SRIM (dictionary) program, maximum stopping power is 899.0400 at 0.08 MeV proton energy.

Total stopping power (P.W) is 935.1688 (MeV-cm²/g) at 0.08 MeV proton energy.

At range 0.0111 cm.

The stopping power of each tissue is different from the one tissues to other for several reasons, including the difference in the components of the tissue and its percentage, the effect density of the organ, and the effect of the values (*I*) on the values of the stopping power, especially for the Bethe, where we notice from the tables of the percentage deviation for all tissues that Bethe have higher percentage deviation at high energy due to uncertainty of (*I*). The results of the calculation of stopping power in the SRIM program is not exactly the same as (dictionary) using a Bragg addition rule, because the excitation energy of the compound is higher than the excitation energy of a single atom. We notice from the above values, mammary gland tissue have higher stopping power because the number of its elements is low and it's the hydrogen ratio is high. But blood, tissue has less stopping power. The largest proton range is also in mammary gland tissue (2.3939 at 180MeV) because mammary gland is less dense than the remaining tissue density. We conclude from the fitting of equations (2-26), semi-empirical equation (power 2) for proton range in each tissue, as following:

Table (5-1): Semi-empirical equation for human tissues.

No.	Human tissue	Semi-empirical equation	
1	Skin	$R = aE^b + c,$	$a=0.0002569, b=1.744, c=0.01074.$
2	Eye lens	$R = aE^b + c,$	$a=0.0002301, b=1.775, c=0.01315.$
3	Stomach	$R = aE^b + c,$	$a=0.0002321, b=1.776, c=0.01325.$
4	Pancreas	$R = aE^b + c,$	$a=0.0002674, b=1.744, c=0.01116.$
5	Liver	$R = aE^b + c,$	$a=0.0002313, b=1.775, c=0.01316.$
6	Spleen	$R = aE^b + c,$	$a=0.0002637, b=1.744, c=0.01113.$
7	Blood	$R = aE^b + c,$	$a=0.0002642, b=1.744, c=0.01114.$
8	Ovary	$R = aE^b + c,$	$a=0.0002663, b=1.744, c=0.01113.$
9	Testis	$R = aE^b + c,$	$a=0.0002679, b=1.744, c=0.01126.$
10	Prostate	$R = aE^b + c$	$a=0.0002685, b=1.744, c=0.01128.$
11	Trachea	$R = aE^b + c,$	$a=0.0002643, b=1.744, c=0.01115.$
12	Mammary gland	$R = aE^b + c,$	$a=0.0002753, b=1.746, c=0.01123.$
13	Thyroid	$R = aE^b + c,$	$a=0.0002663, b=1.744, c=0.01113.$

By comparing the results of range for skin tissue with result from ref. [6] we find a very good agreement between them as shown in figure (5-1).

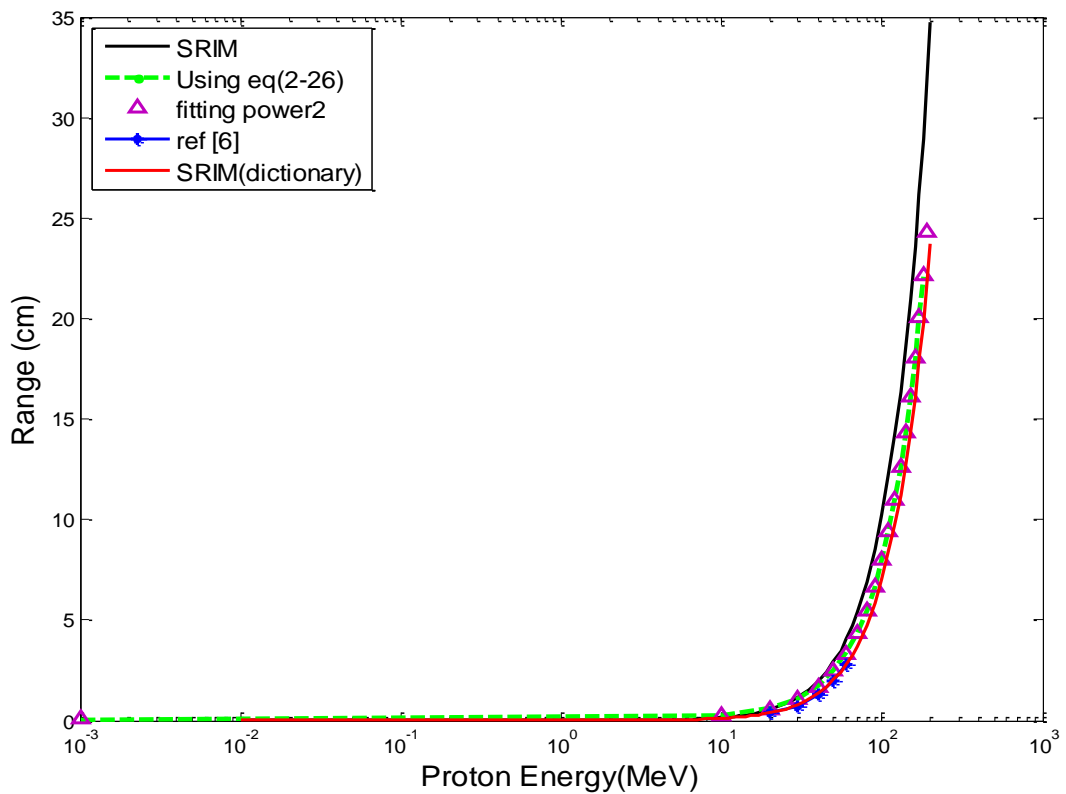


Fig. (5-1): Range of proton in skin tissue.

5-2 Future work

- 1- Calculation of the stopping power of the proton in tissues using new methods as Fermi-Dirac method and casp program.
- 2- The range of proton in the tissue can be calculated using the semi-empirical equation to a different range of proton energy.
- 3- Study of the effect of some factors on the stopping power and range, such as active charge and the effect of Parkes.
- 4 - Using proton instead of x-rays in destroying tumor specially the mammary gland tissue.

REFERENCES

PDF Reducer Demo

References

References

- [1] Hans B. "Tumor therapy with heavy charged particles" Division of radiation medicine, paul scherrer institute, proceeding 495, 444 (1999).
- [2] M. R. Nchodu "Determination of energy spectra of proton therapy beam", Ph.D. Thesis, University of Cape Town, of Physics faculty of science, (2002).
- [3] Sayyed B. J., and et al., RPOR-373; No. of pages 9, (2014).
- [4] Yang, G. V., and et al., Physics in medicine and biology, 55,1343-1362. (10 February 2010).
- [5] Eko S., K. and Arief H. "Numerical equation for the mass stopping power of proton in human body substances" International conference on physics (ICP 2014), Atlantis Press.
- [6] Eko S., K. and Arief H., "Stopping power and range of proton in medium; a study for proton radiotherapy" ICP, ISBN: 979-95620-2-3, (2012).
- [7] Mohammed A. A., "Production of some diagnostic and therapeutic radionuclide", Ph.D, Thesis, college of education pure science Ibn AL- Haitham, university of Baghdad, (2008).
- [8] Zainab W. A." Energy loss of hydrogen dicluster ions in DNA and liquid water" Ph.D, Thesis college of science, Al Mustansiriyah university, (2016).
- [9] Raafat A.H. M. "Neutron yield estimation for some medium isotopes nuclei due to proton, alpha and neutron reactions for energy range (10- 50) MeV" Ph., Thesis, college of education for pure science Ibn Al- Haitham university of Baghdad (2015).
- [10] Abebe G., " Stopping power and range of protons of various energies in different materials", M. Sc thesis, Addis Ababa, Ethiopia (2007).
- [11] Timur M. and Anthony L. Z. "Promise and pit falls of heavy particle therapy" Journal of clinical oncology Vol.32 N.26, (2014).
- [12] Ligia S.and Gheorghe C."Heavy ions straggling in biological matter" O. P. B. Sci. Bull, series A.Vol.71, Iss.3, (2009).
- [13] Daniela S.E. and Hirohiko T. "Particle radiation therapy using proton and heavier ion beams" Journal of clinical oncology Vol.25. No.8, (2007)
- [14] Wayne D N. and Rui Z." The physics of proton therapy" Phys Med Biol. 60 (8): R155–R209, (2015).

References

- [15] WWW.Oncolink.org@2017 Trustees of the university of Pennsylvania
- [16] Jason E. Matney "Investigation of respiratory motion management techniques for proton and photon radiotherapy of lung cancer" M.S.Ph.D. Thesis, university of Texas MD Anderson cancer center, faculty of the university of texas health science center at Houston, (2013).
- [17] Ehrhardt p., Johanna M. Brandner and Jens-M. J." The skin:an indispensable barrier" (2008).
- [18] Francis A. Duck "Physical properties of tissues" London San Diego New York, Boston, Sydney, Tokyo, Toronto (1990) by Academic press Limited.
- [19] ICRU, Vol.49, (1993).
- [20] Russ F.F. Knapp " Radiopharmaceutcals for therapy" isotope production and applications division bhabha atomic research centre Mumbai landia (2016).
- [21] Walls C. J.and Cantab. M.A. "Human biology" Second edition, London, (1976).
- [22] Stephanie M. and Eric W. "Anatomy coloring book" New York (2017).
- [23] Valentin J. "Basic anatomical and physiological data for use in radiological protection: Reference values" the International commission on radiological protection, ICRP publication 89, (2001).
- [24] Harold E. " Clinical anatomy" USA (2006).
- [25] NHS. Retrieved "Cancer of the pancreas" (2014).
- [26] Lionel B.et al " The facts on file illustrated guide to the human body: Digestive system" copyright (2005). The diagram group.
- [27] Jiaxiao and George L. T., "The antioxidant, anti-in flammatory, and antiapoplotic effects of wolfberry in fatty liver" January (2015).
- [28] Kim Y. S, human tissues: Chemical composition and photon dosimetry data. Radial. Res.57, 38-45 (1974).
- [29] Reina E.and Mebiusand G. K., Vol.5, (2005).
- [30] "Definition of blood". Retrieved (2017).
- [31] Mader S.S: Human reproductive biology, WCB, dubunque, (1992).
- [32] Anju R.S and Radhakrishnan B. "Detection of ovary cystusing kirsch templatc" International journal of engineering researchard general science, Vol.3 Issue 4, part2, (2015).

References

- [33] Richard E. J. and Kristin H.L. "Human reproductive biology" USA (2008).
- [34] Anne M. R. Agurand and Dalley "Atlas of anatomy" USA (2009).
- [35] Kanya K., Durga and Ramakrishna B." Tran srectal vitrasoun guided needle core biopsy of prostatic lesions" International journal of health sciences and research Vol.4; Issue:3, (2014)
- [36] Tsukise. A and Yamada K."Complex carbohydrates in the secretory epithelium of the goat prostate" The Histochemical journal. 16 (3) (1984).
- [37] Frank H. and Netter. M.D " Atlas of human anatomy" USA (2014).
- [38] *Blausen.com staff (2014). "Medical gallery of Blausen Medical 2014". WikiJournal of Medicine 1 (2). DOI:10.15347/wjm/2014.010. ISSN 2002-4436.*
- [39] Faller. A. and Schuenke M." The human body : an introduction to structure and function " Thieme stuttgart. New York (2004).
- [40] Moores" Clinical anatomy " china (2014).
- [41] Joseph and Museoline " Kinesiology: The skeletal system and muscle function" china (2011).
- [42] Turner J.E., et al., " Calculation of radiation dose from protons to 400 MeV " Vol 10, pp. 783-808. , Northern Ireland, (1964).
- [43] Young S. Kim,"Density effect in dE /dx of fast charged particles traversing various biological materials" physics department, ohio state university, Columbus,ohio 43210, radiat. Res. 56, 21-27, (1973).
- [44] Bettega D., et al., "Relative Biological effectiveness for protons of energies up to 31 MeV", Radiat. Res.77, 85-97 (1979).
- [45] Bhaskar M. " Mass stopping powers of protons up to 200 MeV in some biologically important materials" Nuclear instruments and methods 211, 235-237(1983).
- [46] Porter L. E. and Bryan S. R.,"Bethe-Bloch stopping power parameters for Al, Cu, and Ag extracted from recent accurate measurements", radiat. Res. 97, 25-35 (1948)
- [47] Waibel E. and Willems. G," Stopping power and ranges of low-energy protons in tissue-equivalent gas", Phys. Med. Biol., Vol. 32, No 3, 365-370, (1987) .

References

- [48] Nestor A., et al., "Stopping power and the concept of effective ion charge at low energies" radiation research 132, 277-281 (1992).
- [49] T Hiraoka, et al., "Energy loss of 70 MeV protons in tissue-substitute materials" Phys, Med, Biol. 39, 983-991(1994).
- [50] N. Sakamoto, H. Ogawa and N. Shiomi-Tsuda, " Stopping powers of carbon for protons from 4 to 13 MeV" Nuclear instruments and methods in physics research B115, 84-87, (1996).
- [51] J. F. Ziegler, " Comments on ICRU report No.49: Stopping powers and ranges for protons and alpha particles", radiation research 152, 219-222 (1999).
- [52] Raafat K., "Calculation mass stopping power of biological models for protons" , M.Sc. Thesis, college of education, university of Baghdad, (2001).
- [53] A. Akkerman, et al., " Calculation of proton stopping power in the region of its maximum value for several organic materials and water", radiation physics and chemistry 61, 333-335, (2001).
- [54] Harald P., et al., "Relative biological effectiveness (RBE) Values for proton beam therapy" Int J. Radiation oncology Biol. Phys., Vol. 53, No. 2, pp. 407-421, (2002).
- [55] Marwan S.M., Al-Nimer and Zainab W. A. L. " The limitations and pitfalls in clinical implications of Bragg's Peak: A theoretical SRIM-TRIM model of human breast tumor" Al-Mustansiriya J. Sci. Vol.21 No.5, (2010).
- [56] Z. Francis, et al., " Stopping power and ranges of electrons, protons and alpha particles in liquid water using the Geant4-DNA package", nuclear instruments and methods in physics research B 269, 2307–2311, (2011).
- [57] Mohan S. and Lakhwant S. " Electronic stopping power of various organic compounds for proton (0.05-10 MeV): A comparative study" Materials physics and mechanics 12, 43-57, (2011).
- [58] Zainab W. A. L., " Proton beam radiation targeted nucleotides with negligible effect on interferon", Iraqi J MED SCI, Vol.9 (2) (2011).
- [59] Yang M., et al., " Comprehensive analysis of proton range uncertainties related to patient stopping-power-ratio estimation using the stoichiometric calibration" Phys. Med. Biol. **57** , 4095–4115, (2012).
- [60] Khalid A. Ahmad and Ahmed J. Tahir, " Electronic stopping parameters of swift proton in Al using harmonic oscillator model: environmental pollution of space protons", Al - Mustansiriyah J. Sci. Vol. 32, No 8, (2012).

References

- [61] Zainab W. A. L. , " Proton, helium and carbon radiation beam targeting reactive oxygen, nitrogen and halogenated species in TRIM-SRIM model" journal of Al-Nahrain university Vol.15 (1), pp. 65-72, (2012).
- [62] Hemalata S., S. K. Rathi and A. S. Verma, " Stopping powers of protons in biological human body substances", Universal journal of medical science 22, (2013). 1(2): 17-
- [63] Khansaa N. A., " Energy loss of protons in human tissues using model simulations", M. Sc Thesis, college of education/Ibn AL- Haitham university of Baghdad, (2013).
- [64] Osamah. N. Oudah, " Stopping power for protons on some materials (AL, Cu, Pb ,C, Be, Cd, and Te) for energy range 1- 12MeV", M.Sc Thesis, college of education for pure science Ibn Al- Haitham-university of Baghdad, (2013).
- [65] Alaa M. H., " Energy loss of protons beam in liquid water and DNA", M.Sc Thesis , college of science Al- Mustansiriyah university, (2013).
- [66] Roaa S. K. and Rashed A. K., " Accumulation of near and far collisions in calculating the stopping power of heavy charged particles", Journal of Babylon university/pure and applied sciences No. (3), Vol.22, (2014)
- [67] Eman H. A., " Study the range of heavy charged particles of certain elements and compounds in the energy range (0.3-100MeV)", Journal of the university of Babylon / pure and applied sciences / Issue (3), Vol. 23, (2015).
- [68] Rewaa Y. T., " Study of energy loss of reactant protons with solid materials" Al - Mustansiriyah J. Sci. Vol. 27, No 3, (2016).
- [69] Kyle G. R. and Yosuke K., " Electronic excitation dynamics in liquid water under proton irradiation", Scientific reports / department of chemistry, university of north Carolina at Chapel Hill, Chapel Hill, north Carolina 27599, USA, (2017).
- [70] M. O. El-Ghossain "Calculations of stopping power, and range of ions radiation (alpha particles) interaction with different materials and human body parts". International journal of physics, Vol.5, No3, (2017).
- [71] Nicholas Tsoulfanidis, Measurement and detection of radiation. Library of congress cataloging in publication data. (1972).
- [72] Rasha S. A. "Heavy swift ion-impact and Bohr theory"M.Sc.Thesis,college of science Al- Mustansiriyah university, (2008).

References

- [73] Syed N. A. "Physics and engineering of radiation detection" USA (2007).
- [74] Hans B. and Berend J. Smit " Proton therapy and radiosurgery " Verlag Berlin Heidelberg New York (2000).
- [75] Harald P. " Proton therapy physics" by Taylor and Francis, New York (2012).
- [76] John R. Sabin, Jens O. and Stephan P.A.Sauer "Amino Acid mean excitation energies and directional dependencies from core and bond calculations" American institute of physics, (2008).
- [77] Walter E. Meyerhof " Elements of nuclear physics" United States of American, (1967).
- [78] Jarkko P. "Stopping power for ions and clusters in crystalline solids" university of Helsinki report series in physics, (2003).
- [79] Darden powers " Influence of molecular structure on stopping power of chemical species for He⁺ ions from a low energy particle accelerator" Baylor university, Waco, Texas, Vol.13, No.12 (1980).
- [80] Helmut P. " Nuclear stopping power and its impact on the determination of electronic stopping power". Application of accelerators in research and industry, AIP conf.Proc.1525,30g-313 (2013).
- [81] Patrick R. "Atomic physics accelerators" Kansas, Vol.17,(1980).
- [82] "Atomic and molecular data for radiotherapy and radiation research" IAEA Vienna-TECDOC-799, ISSN 1011-4289 (1995).
- [83] Peter S. " Charge-dependent electronic stopping of swift nonrelativistic heavy ions" Physical review A, Vol.56, No5, (1997).
- [84] D. I. Thwaites " Departures from Bragg's rule of stopping power additivity for ions in dosimetric and related materials". Nuclear instruments and methods in physics research B69, 53-63, (1992).
- [85] James F. Ziegler, M.D. Ziegler and J.P. Biersack "SRIM – the stopping and range of ions in matter (2010)" Nuclear instruments and methods in physics research B 268, 1818-1823, (2010).
- [86] C. J. Tung and D. E. Watt " Mean excitation energy and electronic stopping power of solids" Radiation effects, Vol.90, pp. 177-190, (1985).
- [87] Stephen M. S. and Martin J. B. " Evaluation of the collision stopping power of elements and compounds for electrons and positrons" Int. J. Appl Radiat

References

- . Isot. Vol. 33, pp. 1189-1218, (1982).
- [88] Hamza A. Mezher "Calculation of cross section for reactions induced proton with Molybdenum to product technetium isotopes". Journal of Kerbala university, Vol.14 No.2 scientific, (2016).
- [89] Glenn F. Knoll "Radiation detection and measurement" USA, (1999).
- [90] Efsthios K. "The mean excitation energy for stopping I, the Bragg rule, and chemical and phase effects. Application of a statistical treatment to the determination of I for chemically bound particles" Chem. Rev. 84,561-576,(1984)
- [91] Alexandru Csete "Experimental investigations of the energy loss of slow protons and antiprotons in matter" M. Sc. Thesis, institute of physics and astronomy, university of Aarhus, (2002).
- [92] Abothur. G. Mohammed, Rashid. A. Kadhum, Hussan. M. Almoswi "Calculation of proton range in some organic compounds energies (10-900) KeV" International journal of science and research (IJSR), Vol.3 Issue 10, (2014).
- [93] J. Kenneth S. and Richard E. Faw "Fundamentals of nuclear science and engineering" United States of America, (2002).
- [94] J.J. Bevelacqua "Systematics of heavy ion radiotherapy" radiation protection management, Vol. 22, No. 6, (2005).
- [95] Steven P. Ahlen "Theoretical and experimental aspects of the energy loss of relativistic heavily ionizing particles" reviews of modern physics, Vol.52, No.1,(1980)
- [96] James E. Turner" Atoms, radiation, and radiation protection" USA, (2007).
- [97] J. F. Ziegler "The stopping of energetic light ions in elemental matter". J. Apply. Phys/Rev. Appl. Phys., 85, 1249-1272, (1999).
- [98] D Emfietzoglou, et al., "A dielectric response study of the electronic stopping power of liquid water for energetic protons and a new $I -$ Value for water" phys, Med, Biol. 54, 3451-3472, (2009).
- [99] Steven P. Ahlen "Calculation of the relativistic Bloch correction to stopping power physical review A, Vol.25, No.4, (1982).
- [100] Anderson H. H. And Ziegler J. F., "Hydrogen stopping power and range in all elements" Vol. 3, IBM - research, yorktown heights, New York, 10598 USA. (1977).
- [101] J. F. Ziegler, M. D. Ziegler, J. P. Biersack (SRIM.com). SRIM (2013).

الخلاصة

من التطورات الحديثة الطبية هو استخدام اشعاع البروتون في معالجة الاورام ،حيث يعتبر شعاع البروتون فريدا في المعالجة لانه يودع طاقته بعمق محدد داخل النسيج. لذلك من اجل السيطرة على قتل الخلايا السرطانية في الانسجة يجب تقديم وصف دقيق لفقدان طاقة الايون ومداه داخل النسيج. تم في هذه الدراسة حساب قدرة الايقاف والمدى للبروتون في ثلاثة عشر نسيج من انسجة جسم الانسان وهم نسيج (الجلد ،عدسة العين، المعدة، البنكرياس، الكبد، الطحال، الدم، المبيض، الخصية ،البروستات ،القنطرة الهوائية ،الغدة اللبنية ،الغدة الدرقية) باستخدام معادلتى (Bethe) و(Ziegler) وبيانات Andreson و Ziegler (Vol.3) وبرنامج SRIM وايضا استخدام SRIM (قاموس) وبمدى طاقة من (1KeV-200MeV) ومن خلال استخدام برنامج الماتلاب تم الحصول على الحسابات العددية لقدرة الايقاف والمدى لكل نسيج حيث اظهرت النتائج تباين قيم قدرة الايقاف والمدى للبروتون في كل نسيج عن الانسجة الاخرى وذلك باختلاف العناصر المكونة للنسيج ونسبها كذلك تباين قيم قدرة الايقاف للنسيج الواحد حسب الطريقة المستخدمة للحساب.

استنتجنا بان اكبر مقدار للطاقة المفقودة للبروتون هي طاقة (0.07MeV) يكون في نسيج الغدة اللبنية . و اكبر مدى للبروتون يكون في هذا النسيج ايضا (2.3939 cm عند طاقة 180MeV) لان كثافة الغدة اللبنية اقل من كثافة الانسجة الباقية. كذلك استخرجنا صيغة تجريبية لقياس المدى يمكن استخدامها لايجاد مدى البروتون في النسيج وذلك بمعرفة طاقة البروتون، التي تساعد المختصين في تحديد عمق الورم والطاقة اللازمة لمعالجته دون احداث ضرر في الانسجة المحيطة بالورم واسلافها.



جمهورية العراق
وزارة التعليم العالي والبحث العلمي
جامعة بغداد
كلية التربية للعلوم الصرفة ابن الهيثم

حساب مدى و قدرة الايقاف للبروتون المتفاعل مع المواد البيولوجية

رسالة مقدمة

الى مجلس كلية التربية للعلوم الصرفة- ابن الهيثم- جامعة بغداد
كجزء من متطلبات نيل درجة ماجستير علوم في الفيزياء

من قبل

شيماء محسن هادي

بكالوريوس (2006)

بإشراف

أ. د. بشائر محمد سعيد